Mechanisms of Central Nervous System Disease in Childhood Acute Lymphoblastic Leukaemia

Dr Yasar Mehmood Yousafzai

MBBS, PGDip.

Submitted in fulfilment of the requirements for the degree of Doctor of Philosophy

Institute of Infection, Immunity and Inflammation,

College of Medical, Veterinary and Life Sciences,

University of Glasgow

January, 2015

Abstract

Acute lymphoblastic leukaemia (ALL) is the commonest childhood malignancy. Once a universally fatal disease, modern therapy has achieved excellent outcome and the majority of children achieve long term cure. Yet relapse remains a challenge. One of the major hurdles in achieving complete cure is the relapse of ALL at extramedullary sites such as the central nervous system (CNS). Despite significant advances in understanding leukaemia biology, most predictors of leukaemic behaviour are accurate for the bone marrow disease only. The precise timing, frequency and properties of CNS infiltrating leukaemic cells are not elucidated. Therefore, the broad aim of this thesis is to develop a better understanding of the mechanisms of leukaemic entry and infiltration patterns of leukaemic cells in the CNS. In order to address the frequency and pattern of CNS infiltration, a xenograft model using primary leukaemic cells from children with B-cell precursor (BCP) ALL in NOD/Scid IL2Rγ null (NSG) mice was established. The majority of samples from children with and without overt CNS disease were able to infiltrate the CNS in NSG mice. CNS infiltration was seen in mice engrafted with small numbers of cells and distinct immunophenotypic subpopulations. The leukaemic samples followed a distinct and reproducible pattern of CNS infiltration with leukaemic infiltrates in the meninges while sparing the CNS parenchyma.

To investigate whether a distinct set of leukocyte trafficking molecules provided tissue specificity for entering the CNS, leukaemic cells retrieved from the bone marrow and the CNS were assessed for expression levels of selected chemokine receptors and P-selectin glycoprotein ligand-1 (PSGL1). Additionally, chemotaxis assays were utilized to investigate the function of the chemokine receptor CXCR4. Despite surface expression of chemokine receptors on leukaemic cells and presence of chemokines in the CNS, no evidence for positive selection of a high-expressing subpopulation was seen. Overall, it appears that, unlike the bone marrow, chemokine receptors do not direct leukaemic cell trafficking to the CNS.

To investigate the published observation that interleukin-15 (IL-15) expression in leukaemic samples correlates with the risk of CNS disease, the effects of IL-15 stimulation on BCP-ALL cells were assessed. IL-15 and IL-15 receptor subunits were noted to be expressed at mRNA level in samples from BCP-ALL patient and cell lines. Exogenous IL-15 stimulated leukaemic cell proliferation and upregulated genes associated with migration and invasion in SD1 cells. A higher proliferative advantage was observed at low-serum conditions which mimics conditions found in the CNS. Therefore a plausible mechanistic

link was established for the association of CNS disease with high IL-15 expression levels.

In cerebrospinal fluid (CSF) samples from patients, quantitative PCR (qPCR) was utilized to detect submicroscopic levels of CNS disease. In approximately 40% patients, qPCR using patient specific primers tested positive for the presence of leukaemic DNA. Therefore this test is much more sensitive than conventional diagnostic techniques which only detect CNS disease in 2-5% of patients. CSF supernatants were also tested to assess whether the levels of chemokines could be used to diagnose patients with qPCR positive disease. Although differences in the levels of chemokines between qPCR positive and negative patients were noted, the values are not sufficiently discriminatory to be clinically useful.

In conclusion, CNS entry appears to be a much more frequent property of leukaemic cell than previously appreciated. Leukocyte trafficking molecules do not appear to play an instructive role in the CNS entry and therefore, it is unlikely that expression levels of leukocyte trafficking molecules or the levels of chemokines in the CSF will be useful biomarkers of CNS disease. In addition, CNS disease appears to be present at diagnosis in at least 40% of patients. Therefore, attempts at blocking leukaemic entry into the CNS are unlikely to be therapeutically useful. Instead, analysing and targeting factors that allow long-term survival of leukaemic cells in the CNS may be a better strategy to eradicate CNS disease and prevent leukaemic relapse.

Abstract **1**
List of Tables **9**
List of Figures **10**
Publication arising from this work **12**
Acknowledgments **13**
Author's declaration **14**
Definitions/Abbreviations **15**
Chapter1: Introduction **18**
1.1 Epidemiology and aetiology 19
1.2 Pathogenesis 20
1.2.1 Chromosomal translocations in ALL 20
1.2.2 Leukaemia as an evolutionary process 23
1.2.3 Clonal evolution in ALL 24
1.3 Prognostic factors in ALL 25
1.3.1 Patient characteristics 25
1.3.2 Immunophenotype 26
1.3.3 Cytogenetic characteristics 27
1.3.4 Risk assignment 31
1.3.5 Response to treatment 32
1.3.6 Extramedullary disease (excluding CNS) 36
1.3.7 CNS disease 37
1.4 ALL treatment 42
1.5 Current clinical challenges 46
1.6 Extramedullary dissemination in ALL – cell entry 47
1.6.1 Physiological leukocyte trafficking 48
1.6.2 Leukocyte trafficking molecules in site-specific trafficking 57
1.6.3 Leukocyte trafficking into the CNS 58
1.6.4 Malignant cell trafficking 61
1.6.5 Chemokine receptors and extramedullary dissemination in ALL 63
1.6.6 CXCR4 in ALL 63
1.6.7 CXCR7 in ALL 65
1.6.8 BCR/ABL1 and leukaemic trafficking in ALL 65
1.6.9 Chemokine receptors and CNS entry 67
1.6.10 CNS entry - alternative mechanisms 68
1.7 Extramedullary dissemination in ALL – microenvironmental niche 69
1.7.1 CNS stromal support 69
1.7.2 Chemotherapy penetration in the CNS 70
1.7.3 Immune surveillance 71
1.7.4 Host factors – IL-15 and IL-15 receptor 72

1.8 Study aims 74
Chapter 2: Materials and methods 76
2.1 General equipment and reagents 76
2.1.1 Plastics 76
2.1.2 General reagents 76
2.2 Cell culture methods 77
2.2.1 Cell lines 78
2.2.2 Thawing of cells from frozen stocks 78
2.2.3 Cell counting 78
2.2.4 Maintenance of cell lines in culture 79
2.2.5 Passage of cell lines 79
2.2.6 Cryopreservation of cells 79
2.3 Patient Methods 80
2.3.1 Ethics approval 80
2.3.2 Collection of human CSF 80
2.3.3 Processing of CSF 80
2.3.4 Blood collection 80
2.4 Animal methods 81
2.4.1 Mice 81
2.4.2 Intra-femoral injections of primary cells 81
2.4.3 Intravenous injections of cell lines 81
2.4.4 Monitoring of engraftment 82
2.4.5 Tail vein blood sampling of xenograft mice 82
2.4.6 Culling and dissection 82
2.4.7 *In vitro* imaging of xenografts injected with $REH^{GFP\text{-}Luciferase}$ cells 83
2.5 Cell based assays 83
2.5.1 Flow cytometry 83
2.5.2 General equipment, materials and solutions 84
2.5.3 Analysis of surface receptor expression 86
2.5.4 Chemotaxis assay 86
2.5.5 Chemokine receptor internalization and recycling assay 87
2.5.6 Chemokine competition assay 87
2.5.7 Analysis of cellular proliferation using cytoplasmic dye Celltrace Violet 88
2.6 Molecular biology methods: DNA 89
2.6.1 DNA extraction using Trizol 89
2.6.2 DNA extraction from CSF using QIAmp DNA micro kit 89
2.6.3 DNA extraction from blood, cultured cells and bone marrow samples using Qiagen blood DNA mini kit 90
2.6.4 DNA concentration and cleanup 90

2.6.5 DNA quantification by spectrophotometric method 90
2.7 Molecular biology: RNA 91
2.7.1 RNA extraction from cells 91
2.7.2 cDNA synthesis 91
2.8 Molecular biology: SYBR Green qPCR 92
2.8.1 Primer design 92
2.8.2 Generation of standards 95
2.8.3 TOPO cloning of vectors 96
2.8.4 SYBR Green qPCR 97
2.8.5 Analysis of SYBR Green qPCR assay 98
2.8.6 Normalization of qPCR data 98
2.9 Molecular biology: TaqMan qPCR 99
2.9.1 TaqMan qPCR for relative gene expression 99
2.9.2 TaqMan qPCR for Albumin gene 99
2.10 Cytology methods 100
2.10.1 Cytospin preparation 100
2.10.2 Blood smear preparation 101
2.10.3 Giemsa staining 101
2.10.4 Immunofluorescence staining 101
2.11 Histology methods 102
2.11.1 Tissue fixation, embedding and cutting 102
2.11.2 Haemotoxylin and Eosin staining 102
2.11.3 Immunohistochemistry 102
2.12 Molecular biology: Protein 104
2.12.1 Western blotting 104
2.12.2 ELISA 106
2.12.3 Luminex multiplex protein detection assay 107
2.13 Statistical analysis 108
Chapter 3: Investigating frequency and patterns of central nervous system infiltration in xenograft models of acute lymphoblastic leukaemia 109
3.1 Introduction and aims 109
3.1.1 Selecting an appropriate model 110
3.1.2 Selecting leukaemic samples for xenograft experiments 112
3.1.3 Other factors influencing xenograft models 113
3.2 Development of a xenograft model of extramedullary disease 115
3.2.1 Primary leukaemic cells 115
3.2.2 Mice 115
3.2.3 Flow cytometry for identification of leukaemic cells 116
3.2.4 Determining engraftment at early and late time points 117

3.2.5 Monitoring for engraftment....117
3.2.6 Analysis of bone marrow engraftment upon cull....118
3.2.7 Analysis of extramedullary infiltration (excluding the CNS)....121
3.3 Analysis of CNS infiltration....127
3.3.1 Comparison of IV vs IF route of transplant....127
3.3.2 Frequency of infiltration in the CNS....128
3.3.3 Pattern of leukaemic infiltration in the CNS....130
3.3.4 Validation using independent cohort of primary xenografts....132
3.3.5 Analysis of CNS leukaemia in mice engrafted with limiting numbers of leukaemic cells....134
3.3.6 Analysis of CNS leukaemia in mice engrafted with immunophenotypically sorted cells....135
3.3.7 Analysing CNS-specific tropism with serial transplants....137
3.4 Discussion....140
Chapter 4: Investigating leukocyte trafficking molecules in association with central nervous system disease in acute lymphoblastic leukaemia....144
4.1 Introduction and aims....144
4.2 Differential CNS homing and chemokine receptor expression in BCP-ALL cell lines 147
4.2.1 Validation of surface expression using flow cytometry....150
4.2.2 Functional analysis using chemotaxis assays....152
4.2.3 CXCL12 mediated chemotaxis in primagraft cells....154
4.3 Analysing expression levels of selected leukocyte trafficking molecules in cells from the CNS and the bone marrow....156
4.3.1 Retrieval of cells from the CNS compartment....156
4.3.2 Expression of selected leukocyte trafficking molecules on primagraft samples retrieved from the bone marrow....157
4.3.3 Comparing bone marrow- and CNS- retrieved leukaemic cells for expression of selected leukocyte trafficking molecules....157
4.4 Investigating the dysfunctional CXCR4-CXCL12 axis in SD1 cells....161
4.4.1 Functional assays of CXCR4....162
4.4.2 Analysing the effect of CXCR7 on CXCL12 mediated chemotaxis....166
4.4.3 Analysing the effect of CXCR7 blockade on CXCL12 mediated chemotaxis 170
4.4.4 Does inhibiting BCR/ABL tyrosine kinase restore CXCL12 mediated chemotaxis?....172
4.4.5 Investigating key CXCL12-activated signalling pathways....177
4.5 Discussion....180
Chapter 5: Investigating interleukin-15 mediated proliferative advantage in B- cell precursor acute lymphoblastic leukaemia cells....185
5.1 Introduction and aims....185
5.2 Expression patterns of IL-15 and IL-15 receptors in BCP-ALL....187

5.2.1 ALL cells express differential levels of IL-15 mRNA.....188
5.2.2 ALL cells differentially express IL-15 receptor sub-units.....190
5.2.3 Association of IL-15/IL-15 receptor expression with CNS disease in xenograft models 192
5.2.4 Detecting IL-15 in CSF samples from BCP-ALL patients 194
5.3 Investigating mechanisms of the association of IL-15 with the CNS disease.....195
5.3.1 Analysing effect of exogenous IL-15 on growth of BCP-ALL cells 195
5.3.2 Determining the role of endogenous IL-15 on growth by IL-15Rα blockade 197
5.3.3 Determining IL-15 mediated growth advantage under serum depletion 198
5.3.4 IL-15 mediated growth is a result of increased proliferation.....199
5.3.5 Investigating the effects of IL-15 - induced signalling on the growth of SD1 cells 201
5.3.6 Regulation of genes associated with leukaemic dissemination following exposure to IL-15 202
5.4 Discussion 205
Chapter 6: Investigating novel biomarkers to improve diagnostic accuracy of central nervous system disease in childhood acute lymphoblastic leukaemia.....208
6.1 Introduction and aims.....208
6.2 Study design 210
6.2.1 Ethics.....210
6.2.2 Study population 210
6.2.3 Inclusion criteria.....210
6.2.4 Exclusion criteria 210
6.2.5 Patient selection and enrolment 210
6.2.6 Treatment protocols 211
6.2.7 Data collection 211
6.2.8 Initial sample processing.....211
6.2.9 Detection of leukaemic DNA.....212
6.3 Method optimization 213
6.3.1 Optimization of DNA quantification 213
6.3.2 Optimization of DNA extraction.....215
6.3.3 Effect of storage and shipment on DNA yield.....217
6.3.4 Optimization of patient specific (ASO) primers and probes.....218
6.4 Detection of CNS disease by PCR 219
6.4.1 Clinical and demographic features of recruited patients.....220
6.4.2 Frequency of CSF qPCR positivity at diagnosis.....220
6.4.3 Frequency of qPCR positivity during treatment 223
6.4.4 Analysing chemokines as novel biomarkers for CNS disease.....224
6.5 Discussion 230

Chapter 7: General discussion and conclusions 234

7.1 Summary of findings 234

7.2 How do these finding extend current knowledge on CNS involvement in leukaemia? 235

7.2.2 Clinical implications of the findings 242

7.3 Future directions 244

7.3.1 Leukaemia-host microenvironment factors may play a dominant role in determining the risk of CNS relapse disease 244

7.3.2 Investigating the biomarkers for CNS disease 245

7.3.3 Clonal origins of CNS infiltrating cells 246

7.4 Overall conclusions 246

Appendix: Interleukin-15 enhances cellular proliferation and upregulates CNS homing molecules in pre-B acute lymphoblastic leukaemia 247

List of References 248

List of Tables

Table 1-1 Diagnostic criteria for CNS disease....38
Table 1-2 Chemokine receptor nomenclature....53
Table 2-1 Plastic lab-ware used in this thesis....76
Table 2-2 Composition of solutions....77
Table 2-3 Clinical and immunophenotypic characteristics of the cell lines....78
Table 2-4 Antibodies, fluorescent conjugated and native chemokines and reagents for FCM....85
Table 2-5 Criteria for optimal primer design....92
Table 2-6 Primer details for PCR, SYBR Green qPCR and TaqMan qPCR.....94
Table 2-7 PCR cycling conditions for generating standards....95
Table 2-8 Calculation for SYBR Green qPCR mastermix....97
Table 2-9 Temperature conditions for SYBRGreen qPCR assay....97
Table 2-10 Calculation of TaqMan qPCR mastermix for Albumin gene....100
Table 2-11 Temperature conditions for TaqMan qPCR assay for Albumin gene....100
Table 2-12 Antibodies and reagents for western blotting....104
Table 3-1 Analysis of engraftment at early and late time point....117
Table 3-2 Clinical and laboratory features of patients....119
Table 3-3 Association of successful engraftment with clinical feature....120
Table 3-4 Details of individual xenograft experiments....121
Table 3-5 Comparison of IV vs IF route of transplant.....128
Table 3-6 Analysis of CNS infiltration in primary xenografts....129
Table 3-7 Clinical characteristics and CNS engraftment....133
Table 4-1: Clinical and cytogenetic features of BCP-ALL cell lines....147
Table 4-2 FCM analysis of primagraft cells for selected trafficking molecules....157
Table 4-3: Correlation of chemotaxis with signalling molecules....179
Table 5-1: Clinical features of patients....187
Table 5-2: Individual results of IL-15 and IL-15 receptor expression data in 4 cell lines, 13 primary samples and 5 primagraft samples.....191
Table 6-1 Demographic and clinical features of recruited patients in comparison with SJCRH and BFM trial cohorts....220
Table 6-2 Comparison between CSF qPCR+ve and qPCR –ve patients....221
Table 6-3 Raw data of individual patients....225

List of Figures

Figure 1-1 Common genetic rearrangements with chromosomal translocation 20
Figure 1-2 Clonal evolution and heterogeneity in ALL.....24
Figure 1-3 Philadelphia chromosome and BCR-ABL1 variants.....30
Figure 1-4 Principle of MRD monitoring 33
Figure 1-5 Simplified model of (a) B- cell development stages and corresponding BCP-ALL types and (b) V(D)J and VJ rearrangement.....34
Figure 1-6 Possible mechanisms of leukaemic entry into extramedullary tissues.....48
Figure 1-7 Leukocyte migration across the endothelium into the tissue 50
Figure 1-8: Illustration of a typical and an atypical chemokine receptor 56
Figure 1-9: Routes of leukocyte entry into the CNS.....61
Figure 1-10 Possible modes of IL-15/IL-15 receptor signalling.....73
Figure 3-1 Scheme of transplantation experiments.....115
Figure 3-2 Monitoring for engraftment.....116
Figure 3-3 Kinetics of engraftment.....118
Figure 3-4 Pattern of leukaemic infiltration in the liver 122
Figure 3-5 Correlation of BM engraftment with splenic infiltration 123
Figure 3-6 Pattern of leukaemic infiltration in the kidneys 124
Figure 3-7 Histological sections of gonads showing patterns of leukaemic infiltration....125
Figure 3-8 Histological sections of nodules showing patterns of leukaemic infiltration in skeletal muscle and uterus.....126
Figure 3-9 Pattern of CNS infiltration in NSG mice in the independent cohort of samples 132
Figure 3-10 Frequency of CNS infiltrating leukaemic cells using limiting dilution experiments 135
Figure 3-11 Frequency of CNS infiltrating leukaemic cells in various immunophenotypic subpopulations 136
Figure 3-12 Experimental scheme for analysing CNS-specific tropism of $REH^{Luc\text{-}GFP}$ cells 138
Figure 3-13 Analysis of CNS tropism of CNS- and BM-isolated cells using *in vivo* bioluminescence.....139
Figure 4-1: The potential utility for identifying mechanism of CNS entry of leukaemic cells. 145
Figure 4-2: Time to hind-limb paralysis and expression of leukocyte trafficking molecules. 149
Figure 4-3: Chemokine receptor and PSGL1 expression in BCP-ALL cell lines 151
Figure 4-4: CXCL12-mediated chemotaxis in BCP-ALL cell lines.....153
Figure 4-5 CXCL12 mediated chemotaxis in primagraft cells 155
Figure 4-6 Comparison of expression of chemokine receptors and PSGL1 in primagraft cells retrieved from the BM and the CNS compartments. 158
Figure 4-7 Effect of AMD3100 on REH engraftment in NSG mice. 160
Figure 4-8: Effect of CXCR4 blockade on CXCL12 mediated chemotaxis.....162
Figure 4-9: Dose-dependent binding of $CXCL12^{AF647}$ in SD1 and Sup B15 163
Figure 4-10 CXCR4 internalisation in response to CXCL12 stimulation: 164
Figure 4-11: Time-dependent restoration of surface CXCR4 following CXCL12-mediated internalization.....165
Figure 4-12: Comparison between CXCR7 mRNA in SD1 and Sup B15.....166
Figure 4-13: CXCR7 protein expression in SD1 & Sup B15 167
Figure 4-14: CXCR7/CXCR4 co-expression in SD1 and Sup B15.....169
Figure 4-15: CXCL12-CXCL11 competition assay 170
Figure 4-16: Effect of CXCR7 blockade on CXCL12-mediated chemotaxis in SD1. 171
Figure 4-17: BCR-ABL1 expression in SD1 and Sup B15 173

Figure 4-18 Effect of BCR-ABL inhibition on CXCR4 expression and function. 175
Figure 4-19: Downstream signalling pathways activated by CXCL12 in cell lines 178
Figure 5-1: IL-15 mRNA expression in BCP-ALL cells 189
Figure 5-2 IL-15 receptor subunit mRNA expression in BCP-ALL cells 191
Figure 5-3: Relative expression levels of IL-15 receptor subunits in BCP-ALL cell lines. 193
Figure 5-4: ELISA detection of IL-15 levels in CSF supernatants from patients with CNS disease. 194
Figure 5-5 Effect of exogenous IL-15 on growth of BCP-ALL cell lines 196
Figure 5-6: Growth of BCP-ALL cell lines following blockade of IL-15 Rα. 197
Figure 5-7: Growth of IL-15 treated SD1 cells under low serum conditions: 198
Figure 5-8: Effect of IL-15 treatment on apoptosis and cell proliferation: 200
Figure 5-9: Effect of inhibition of downstream signalling pathways on IL-15 mediated growth. 201
Figure 5-10: qPCR analysis of metastasis-associated genes identified by RT^2 profiler array 203
Figure 5-11: qPCR and FCM analysis of IL-15 treated SD1 cells. 204
Figure 6-1: Envisaged potential for using more sensitive methods for the diagnosis of CNS disease in ALL. 209
Figure 6-2 Scheme for patient recruitment and sample analysis 212
Figure 6-3: Optimization of DNA quantification 214
Figure 6-4: Optimization of DNA extraction methods 216
Figure 6-5: Effect of storage and shipping on CSF DNA yield 218
Figure 6-6: Flow chart for patient recruitment and analysis 219
Figure 6-7 CSF qPCR detection by PCR 222
Figure 6-8 CSF qPCR positivity during induction chemotherapy 223
Figure 6-9 Levels of chemokines in CSF qPCR +ve and CSF qPCR –ve patients 227
Figure 6-10 ROC analysis for diagnostic accuracy of chemokine levels to predict CSF qPCR positivity 229
Figure 7-1 IL-15 stimulation may provide survival advantage to leukaemic cells in the CNS but less so in the bone marrow 241

Publication arising from this work

Williams, M. T., Yousafzai, Y., Cox, C., Blair, A., Carmody, R., Sai, S., Chapman, K. E., McAndrew, R., Thomas, A., Spence, A., Gibson, B., Graham, G. J. & Halsey, C. 2014. Interleukin-15 enhances cellular proliferation and upregulates CNS homing molecules in pre-B acute lymphoblastic leukemia. Blood, 123, 3116-27.

Acknowledgments

I am grateful to the Khyber Medical University and Yorkhill Children's Charity for the generous funding of this research project. I would like to thank my supervisors Dr Chris Halsey and Professor Gerard Graham for their close supervision, mentorship and guidance during this PhD project. Chris has always been there for discussions on research projects, providing useful feedback on the thesis, and keeping me on track. Thanks to my assessors Professor Rob Nibbs and Professor Hugh Willison for assessing my progress during the PhD. Many thanks to all the members of the chemokine research group, especially to Dr Mark Williams for teaching most of the laboratory techniques, Dr Clive McKimmie for his guidance on qPCR, Dr Alasdair Fraser for his help in flow cytometry and Dr Ruaidhri Carmody for his guidance in western blotting experiments.

In connection to the work presented in this thesis, I gratefully acknowledge the contribution of our collaborators who shared their valuable resources such as cell lines, primary samples and mouse brains. Research staff Alison, Wendy and Saeeda provided invaluable help in obtaining clinical information and patient recruitment. Members of the UK MRD laboratory including Sandra, Linda and Amanda provided patient specific reagents. I am grateful to all the patients and their parents who agreed to participate in the research presented in this thesis.

Author’s declaration

I declare that, except where explicit reference is made to the contribution of others, that this thesis is the result of my own work and has not been submitted for any other degree at the University of Glasgow or any other institution.

Signature:…….

Printed name: Yasar Mehmood Yousafzai

Definitions/Abbreviations

ACKR	Atypical chemokine receptor
ALL	Acute lymphoblastic leukaemia
AML	Acute myeloid leukaemia
APC	Allophycocyanin
BBB	Blood-brain barrier
BCP	B-cell precursor
BCR	B-cell receptor
BCSFB	Blood-CSF barrier
BM	Bone marrow
BP	Base pair
BSA	Bovine serum albumin
CALLA	Common ALL antigen
CAN	Copy number alteration
CCG	Children's Cancer group
CD	Cluster of differentiation
cDNA	complementary DNA
CML	Chronic myeloid leukaemia
CNS	Central nervous system
CPE	Choroid plexus epithelium
cRNA	Carrier RNA
CSC	Cancer stem cell
CTV	CellTrace violet
Ct	Cycle threshold
DAB	3. 3'-diaminobenzidine
DARC	Duffy antigen /receptor for chemokines
DAPI	4' , 6-diamidino-2-phenylindole
ddH2O	distilled, deionized water
DMSO	Dimethylsulfozide
DNA	deoxyribonucleic acid
EAE	Experimental autoimmune encephalitis
EDTA	Ethylenediaminetetraacetic acid
ETP	Early T-cell precursor
EFS	Event free survival
ELISA	Enzyme linked immunosorbent assay
ERK	Extracellular signal-regulated kinase
EtOH	Ethanol
FACS	Fluorescence activated cell sorting
FBC	Full blood count
FCM	flow cytometry
FCS	Foetal calf serum
FISH	Fluorescence *in site* hybridisation
FITC	Fluorescein isothiocyanate
FSC	Forward Scatter
GAPDH	Glyceraldehyde 3-phosphate
GAG	Glycosaminoglycan

GFP	Green fluorescent protein
GPCR	G-protein coupled receptor
HH	High hyperdiploid
HSC	Haematopoietic stem cells
HSCT	Haematopoietic stem cell transplant
HSPC	Haematopoietic stem and progenitor cell
I.P	Intraperitoneal
ICAM	Intracellular adhesion molecule
id	Identity
IF	Intrafemoral
Ig	Immunoglobulin
IgH	Immunoglobulin heavy
IL-15	Interleukin-15
IL-15R	IL-15 receptor
IV	Intravenous
JAK	Janus activated kinase
kDa	KiloDalton
KO	knock-out
LPS	Lipopolysacchride
Luc	Luciferase
LSC	Leukaemia stem cell
mAB	monoclonal antibody
MAPK	Mitogen-activated protein kinase
m-BCR	Minor-breakpoint cluster region
MFI	Mean fluorescence intensity
MMP	Matrix metalloproteinase
MNC	mononuclear cell
MRD	Minimal residual disease
MRI	Magnetic resonance imaging
mRNA	Messenger RNA
MS	multiple sclerosis
NBF	Neutral buffered saline
NCI	National Cancer Institute
NK	Natural killer (cell)
NOD	Non-obese diabetic
NOG	NOD/Shi-scid IL-2R$\gamma^{-/-}$
NSG	NOD/LtSz-Scis IL-2R$\gamma^{-/-}$
PBMC	Peripheral blood mononuclear cells
PBS	Phosphate buffered saline
PCR	Polymerase chain reaction
PE	Phycoerythrin
PE-Cy7	PE with cyanine 7 conjugate
PFA	Paraformaldehyde
Ph	Philadelphia chromosome
g	gravitational force
qPCR	quantitative Polymerase chain reaction
RBC	Red blood cell
RBC	Red blood cell
RFS	Relapse free survival

RPM	Revolutions per minute
RPMI	Roswell park memorial institute media
RQ	Relative quantitative
S.c.	Subcutaneous
SCF	Stem cell factor
SD	Standard deviation
SDS PAGE	Sodium dodecyl sulphate polyacrylamide gel electrophoresis
SEM	Standard error of the mean
SSC	Side scatter
STAT	Signal Trunsducer and Activator of Transcription
T_{CM}	Central memory T cell
TBP	TATA binding protein
TdT	Terminal deoxynucleotidyl transferase
TBS-Tween	Tris-buffered sodium Tween
TE	Tris-EDTA
TLDA	TaqMan low density array
TPMT	Thiopurine S-methyltransferase
TRITC	Tetramethyl rhodamine isothiocyante
UV	Ultra violet
V	Volts
VCAM	Vascular-associated adhesion molecule
WCC	White cell count
WHIM	Warts, Hypogammaglobulinemia, Infections, and Myelokathexis
WT	Wild type
µg	microgram
µl	microliter

1 Introduction

The first descriptions of signs that can be retrospectively interpreted as cancer date as far back as 3000 BC. Ancient Egyptian writings say about the disease, ‘There is no treatment’ (Cancer.gov). For several centuries after recognising solid cancers, physicians remained unaware of a similar pathology of the blood. Even long after the discovery of the microscope and identification of the white blood cells, haematological pathologies were considered mostly as pus and inflammation. It was only in the early 19th century, when European physicians identified patients with uncommon alteration of the blood - findings then interpreted as inflammation. David Craigie, a physician at the Royal Infirmary of Edinburgh began to question interpretation of such peculiar findings on a patient admitted and later died in his ward in 1841. Three years later, when he admitted another such patient, he had no doubt that the patient would meet a similar fate. A young Pathologist John Hughes Bennet who performed autopsy on this patients and published the findings, concluded that the alteration of blood was independent of inflammation and that the pathology involved the whole blood system. Shortly after, Rudolf Wirchow described the case of a woman with distended abdomen and increased circulating white blood cells – findings that can be interpreted in retrospect as chronic leukaemia. Wirchow called it ‘Weisses Blut (White blood) and later used the term ‘Leukhemia’ (Piller, 2001).

Currently, leukaemia comprises a diverse and heterogenous group of malignant proliferations of blood cells. Leukaemia can arise from lymphoid or myeloid haematopoietic precursors and can present in an acute or chronic form. Over the past few decades, the world has seen great improvements in the diagnosis and success of treatment in leukaemic patients. Not only has the treatment of certain leukaemias been a success story, this group of disorders has been on the frontier of scientific discovery and therapeutic advancements in the field of cancer. The current classification of leukaemias incorporates immunology, cytogenetics and molecular genetics for the diagnosis and management (Swerdlow et al., 2008).

This thesis focuses on childhood Acute Lymphoblastic Leukaemia (ALL) that arises within the haematopoietic precursors of B- and T- cell origin. In this PhD project, I have investigated aspects of leukaemic cell dissemination to extramedullary sites with a particular emphasis on the CNS. Therefore, this chapter begins with an overview of relevant biological and clinical aspects of ALL followed by a discussion on possible mechanisms of extramedullary dissemination of ALL and how this is relevant to the current clinical problems, followed by aims of the study.

1.1 Epidemiology and aetiology

Despite being a rare disease, ALL is the commonest childhood malignancy accounting for 75-80% cases of leukaemia and 25% of all malignancies of children (NationalCancerInstitute, 2014). The incidence of ALL in under-developed countries, and poor socioeconomic groups is lower than developed countries. Small differences in prognosis are observed between different races, although the reasons for such differences are poorly understood. In the United Kingdom (UK), approximately 300 children are diagnosed with ALL each year. The peak incidence of ALL is seen at 2-3 years of age and decreases sharply afterwards. This disease is slightly more common in boys than in girls with a ratio of 1.3:1 (CancerResearchUK, 2014). Fortunately, recent decades have seen a decrease in mortality from ALL – with a 5 year overall survival now above 90% (Hunger et al., 2012). However, prognosis in relapsed cases is still poor and the majority of children with relapse die due to treatment failure or therapy related complications (Roy et al., 2005). Overall, leukaemia account for 30% of cancer related deaths in children (CancerResearchUK, 2014).

What exactly causes leukaemia is not known. There are, however, a few predisposing inherited conditions, and acquired risk factors associated with a higher incidence of ALL. Disorders associated with chromosomal aneuploidy or instability such as Down syndrome, ataxia telengectasia and Bloom syndrome are more commonly associated with ALL. Similarly, exposure to mutagens such as ionizing radiation, Benzene or chemotherapy has been implicated. However, the majority of cases occur sporadically (Pui et al., 2008). Epidemiologic data point to infections as causal exposure for the development of ALL (Kinlen, 1995, Kinlen, 1988, Greaves, 2006). Germline single nucleotide polymorphisms (SNPs) in patients with ALL and control populations have implicated ARID5B and IKZF1 (Trevino et al., 2009) and IL-15 genes (Lin et al., 2010) in leukaemia. The mechanistic link between these SNPs and ALL is still unclear.

1.2 Pathogenesis

1.2.1 Chromosomal translocations in ALL

The majority of leukaemias contain a variety of genetic changes such as deletions and point mutations. However, chromosomal numerical or structural abnormalities such as translocations are characteristic of ALL. Chromosomal translocations result from breakage of double-stranded DNA followed by their recombination resulting in a fusion gene, loss of function or an altered functioning gene. For example, translocation between chromosome 9 and 22 (t(9;22)) where the fusion gene 'BCR-ABL1' encodes for a novel chimeric oncoprotein. This aberrant protein is associated with constitutively active tyrosine kinase. Translocations may also result in an intact gene being placed next regulatory elements of another gene on the partner chromosome resulting in dysregulated expression of normal proteins. Such translocations result in an aberrant function of a normal protein. For instance, t(1;14)(p34;q11) involves coding regions of the transcription factor TAL1/SCL being placed adjacent to constitutively active T-cell receptor α/β region (Figure 1-1). In a similar manner, chromosomal inversion can place a transcription factor besides a regulatory gene and result in aberrant gene expression. However, chromosomal translocations may not always be enough to initiate overt leukaemia and the fact that many ALL cases lack recurring chromosomal alterations, required high resolution screening of the leukaemic genomic and genetic make-up.

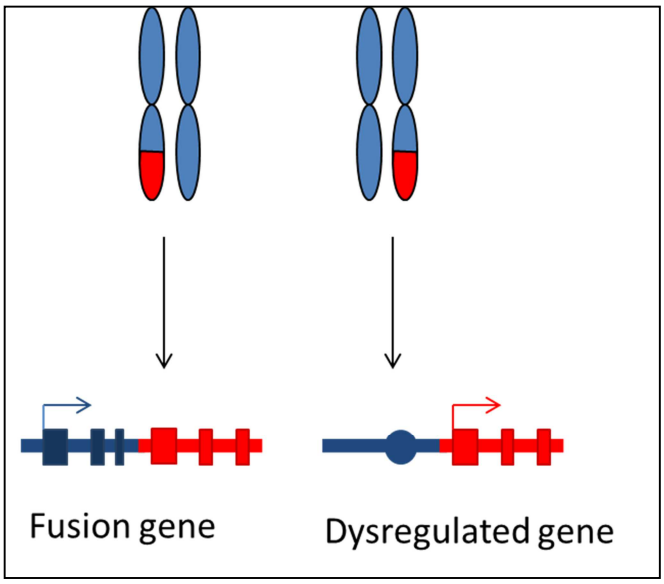

Figure 1-1 Common genetic rearrangements with chromosomal translocation

1.2.1.1 The multi-step pathogenesis of leukaemia

The incidence of leukaemia in monozygotic twins has long been observed. It was also realized that the concordance of leukaemia is identical twins varied with age. For instance, the concordance of neonatal leukaemia in identical twins in nearly 100% while in childhood age group this drops down to nearly 10%. Molecular genetic analyses have identified that the leukaemic cells in the twins share clonal origins. This implies that the mutation arise in a progenitor cell in one twin and its daughter cells spread to the other twin through trans-placental circulation (Greaves et al., 2003). Further evidence came from the retrospective studies analysing archival material from children with leukaemia. Strikingly, many children with ALL were found to have the characteristic translocation present in their post-natal Guthrie card blood samples. The latency period between birth and leukaemia implied that further post-natal events are necessary for transformation from a mutant progenitor cell to the heterogeneous population of leukaemic cells numbering in order of 10^{12}. This latent period is generally translocation-specific. For instance, MLL-rearrangements have a very short latency period to overt clinical disease whereas TEL-AML1 have longer latency and lower transformation rate (Greaves and Wiemels, 2003). These findings suggest that some leukaemic subtypes need accumulation of more secondary hits than others. The evidence for this multi-step model further cemented with the identification of leukaemia-associated translocation (TEL-AML1) in a high frequency of samples from normal children (approximately 1%). This implies that TEL-AML1 translocation is not sufficient to cause overt leukaemia and further mutations are necessary for frank disease (Mori et al., 2002).

Studies on genetically engineered mice have not only validated the multiple-hit hypothesis, but also shed light on the behaviour of pre-leukaemic clones – at least in TEL-AML1 subtype. Transplantation of TEL-AML1 transfected bone marrow cells into immunodeficient mice resulted in increased self-renewal capacity and relative accumulation of early B cell progenitors compromising the differentiated populations (Tsuzuki et al., 2004). However, this translocation was not sufficient to cause leukaemia in mice even till the age of 1 year (Fischer et al., 2005). When additional mutations are accrued, the mice quickly develop acute leukaemia (Bernardin et al., 2002).

It is not exactly known as to how the haematopoietic precursors acquire the first and second hit. It is hypothesised that the prenatal immune system is prone to chromosomal translocations due to rapid expansion and genetic rearrangements needed for normal B- and T- cell development. Once generated, the mutant clone will undergo limited

expansion. During the post natal life, this clone will normally be cleared from the body, unless a second mutation is acquired. Epidemiologic data points to an increased incidence of leukaemia in children unexposed to normal infectious agents during early life and it is suggested that immune system may need such exposures for normal development. Exposure to infection at a later-than-usual stage results in abnormal immune responses which may lead to acquisition of further hits (Greaves, 2006). This 'delayed-infection' hypothesis presents plausible explanations to the observed peak incidence seen in leukaemia (2-5 years of age), the latency period after the first hit (months to years), and the rare transformation of pre-leukaemic clones to overt leukaemia (1%). However, *in utero* acquisition of pre-leukaemic clone has been identified in only a subset of childhood ALL. It is not known if other subtypes of leukaemia, especially those at a later age acquire the pre-leukaemic clone *in utero*, or are a result of sporadic post-natal incidence. It is likely that other mechanisms of leukaemogenesis co-exist.

1.2.1.2 Additional genomic abnormalities in ALL

Cytogenetic abnormalities such as rearrangements and aneuploidy are insufficient to explain the myriad of cellular abnormalities found in leukaemia. Genome-wide association studies to determine copy number alterations (CNAs) and loss of heterozygosity (LOH) performed using single nucleotide polymorphism (SNP) arrays in ALL have opened up new avenues for new classification and therapeutic strategies. In 2007, Mullighan et al. analysed 242 children with ALL using SNP arrays and reported several novel genetic alterations in different leukaemic subsets. Notably, patients with MLL-rearrangements had approximately one abnormality while TEL-AML1 leukaemia had an average of 6 abnormalities. This could explain for the high concordance and short latency in MLL-rearranged ALL while a low concordance and long latency in TEL-AML1 leukaemia. Furthermore, the researchers identified more than 50 recurrent genetic abnormalities that involved genes with potential role in lymphoid development and leukaemogenesis. For instance, EBF1, PAX5 *and* IKZF1 play important roles in B- cell development and differentiation (Mullighan et al., 2007). The same group later identified IKZF1 deletion in 76.2% paediatric BCR-ABL1 cases (Mullighan et al., 2008a).

These observations were followed by *in vivo* studies to explore their role in leukaemogenesis. In once such study, transgenic mice carrying BCR-ABL1 mutation were crossed with mice carrying mutant IKZF1 allele with impaired functions. These mice experienced leukaemia with a significantly shorter latency compared to mice carrying BCR-ABL1 alone. Furthermore, comparative genomic hybridization analysis (CGH) of

leukaemic cells from these mice exhibited fewer additional chromosomal abnormalities. This implies that impaired IKAROS, a transcription factor encoded by IKZF1, shortens leukaemia latency by bypassing the requirement for additional pro-oncogenic hits in BCR-ABL1 positive leukaemias (Virely et al., 2010). In fact, IKZF1 deletions have been described in other subtypes of ALL and are reported to have poor prognostic outcome (Mullighan et al., 2009b).

Not only these novel genetic mutations expanded our understanding of the pathogenesis of ALL, but also led to therapeutic decision making. SNP analysis of a large cohort of childhood ALL cases identified mutations in CRLF2 in high proportion in a cohort of childhood ALL and Down syndrome associated ALL. These mutations are associated with activating mutations in the Janus-kinase (JAK) family genes or JAK/STAT signalling pathways (Mullighan et al., 2009a). Such patients are likely candidates for the newly developed inhibitor Ruxolinib. Phase I studies are underway studying the patients with relapsed or refractory disease (ClinicalTrials, 2014). Recently, whole exome sequencing, lesions involving tyrosine kinases and key signalling pathways were identified in near haploid ALL (Holmfeldt et al., 2013). These pathways can certainly be attractive targets for the use of tyrosine kinase inhibitors.

1.2.2 Leukaemia as an evolutionary process

In 1976, Peter Nowell published a landmark perspective on the development of cancer. He suggested that the development of cancer as a process of somatic evolution – much like Darwinian principle of natural selection – with cancer cells acting as organisms and the body as an ecosystem (Nowell, 1976). Beginning in embryonic life, cells are under continuous internal and external factors which may introduce mutations such as DNA damage or chromosomal breaks within the rapidly dividing cells. Postnatally, mutations continue to accumulate in low frequency within the dividing and ageing cells. Fortunately, the majority of these mutations are within the non-coding parts of the genome and therefore are inconsequential (passenger mutations). When these mutations are incurred upon parts of the genome vital for cell survival the cell may die. Rarely, the mutations will involve areas of genomes associated with regulation of cell growth or apoptosis and will result in a phenotype with enhanced proliferative ability or resistance to programmed cell death.

This mutant clone expands along with the normally proliferating cells. However, in a Darwinian manner, selective pressure results in preferential expansion of the biologically

fittest daughter cells of this clone. Subsequent mutations arising in the progeny of such cells allow expansion of subclones with accumulated mutations resulting in further dysregulated cellular processes. Many regulators of cell cycle which are responsible for programmed cell death are inactivated. Such clones have an increased capability to survive further DNA damage and are naturally more suited to survive (Figure 1-2).

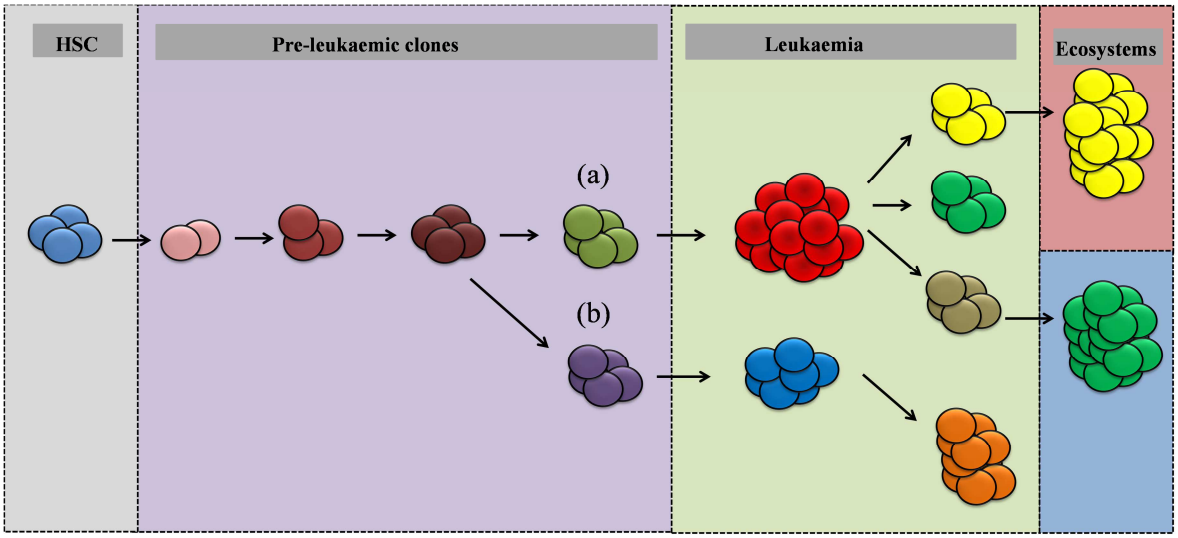

Figure 1-2 Clonal evolution and heterogeneity in ALL
Mutation involving normal haematopoeietic stem/progenitor cells results in limited expansion of the mutant cell. Additional mutations form subclones. Selective pressures allow some mutant subclones to expand while others become extinct or remain dormant. Ecosystems represent the different tissue niches. Relapse may be caused by expansion of (a) a resistant subclone or (b) additional mutations in the ancestral clone. Each differently coloured circle represents a genetically distinct subclone. (adapted from (Greaves and Maley, 2012)

1.2.3 Clonal evolution in ALL

Historically, chromosomal analysis has been the main tool for analysing genetic changes in leukaemic cells. Due to the low resolution power of karyotyping, and reliance upon *in vitro* culture of leukaemic cells, the genetic heterogeneity in ALL was missed. It is certainly true that fewer additional genetic mutations may be required to initiate leukaemia, however, at the time of presentation, leukaemic cells are a heterogeneous population carrying several additional mutations.

The initial convincing evidence for sub-clonal heterogeneity in ALL came from comparison of matched leukaemic samples at the time of diagnosis and relapse. For instance, Raimondi et al. (1993) reported completely unique karyotypes at relapse in approximately 10% children. Like the general consensus at that time, these cases could represent secondary malignancies. However, the authors raised the possibility of a pre-

leukaemic or ancestral clone which might be present in minor proportion at the time of diagnosis. Using multicolour fluorescence *in situ* hybridisation (FISH) analysis, Anderson et al. (2011) identified multiple subclones in cases of TEL-AML1 positive ALL cases in 30 cases with diverse and complex sub-clonal architecture. Selective pressure on the leukaemic cell population could have resulted in elimination of the dominant clone, which could result in expansion of a minor subclone. The convincing evidence of such an ancestral clone was only possible after back-tracking of relapse-specific mutation. Analysis of paired diagnostic and relapse samples by analysis of antigen receptor gene rearrangement identified crucial differences between the dominant clones at diagnosis and relapse (Konrad et al., 2003). Moreover, single nucleotide polymorphisms (SNPs) in samples revealed that the majority of mutations found in the dominant clone at relapse could be traced back to a rare clone present at diagnosis. Importantly, more than half of the relapse-associated clones shared some but not all copy number alterations (CNAs) identified in the diagnostic clone. This suggested that the relapsed clones most likely evolved from an ancestral clone (Mullighan et al., 2008b).

While these genetic abnormalities certainly influence leukaemic behaviour and clinical outcome, a number of other factors are taken into account when making clinical decisions.

1.3 Prognostic factors in ALL

Several factors determine the outcome of patients in ALL. These include demographic factors (e.g age and gender), disease factors (e.g. presenting white cell count (WCC) or cytogenetics) and treatment factors (e.g. drug regimen, treatment duration and intensity). These various factors have been utilized for risk assessment of patients. More recently, therapy response based stratification has emerged as a single most significant prognostic factor in ALL.

1.3.1 Patient characteristics

Age has been a major determinant in the outcome of leukaemic patients. Infants (van der Linden et al., 2009) and adolescents (Ramanujachar et al., 2006) have a much worse outcome than young children. This difference is mainly due to the characteristic MLL-rearrangements seen in infants (van der Linden et al., 2009), and due to the higher frequency of high risk cytogenetics (e.g. BCR-ABL1) and the poor drug tolerability in the older patients. Indeed in young adults the outcome is much superior when treated on paediatric protocols (Ramanujachar et al., 2006, de Bont et al., 2004, Stock et al., 2008).

Boys have historically had a worse outcome than girls. One reason for this poor prognosis is perhaps the increased incidence of T-ALL in boys. Traditionally, testicular relapses have been considered poor risk factors. Even the more recent studies continue to show the slight inferior outcome in boys compared to girls (Escherich et al., 2010).

The diagnostic WCC is considered to be a crucial variable for the outcome of the patient. Whether it represents a high tumour burden or a more aggressive disease is not known. Conventionally, a WCC higher than 50 x 10^9/L is used as a cut-off between better and worse risk. Patients with BCP-ALL and a high WCC at diagnosis are at an increased risk of treatment failure. The relationship of WCC with prognosis in T-ALL is much less clear. This is perhaps because of the low presenting WCC seen with Early T-cell precursor (ETP) ALL – an aggressive subtype (Vaitkeviciene et al., 2011). Signs of extramedullary infiltration such as hepatosplenomegaly, lymphadenopathy and mediastinal involvement are also considered as measures of tumour burden. Overt testicular involvement most commonly seen with T-ALL does not appear to be of prognostic significance when treated with the more intense protocols (Sirvent et al., 2007). The presence of CNS leukaemia at diagnosis is associated with worse outcome. Not only do these patients require additional treatment, but this also significantly increases the risk of CNS-relapses. A more extensive discussion on CNS leukaemia is presented in section 1.3.7.

1.3.2 Immunophenotype

ALL arises from haematopoietic precursors of the B- or T lymphoid origin. The leukaemic cells tend to recapitulate stages of normal B- or T cell development. Expression of lineage specific immunological markers on leukaemic cells is used for the classification of ALL. The initial diagnostic method utilized sheep rosette formation to identify T- lineage blasts and a polyclonal antiserum with affinity to the common acute lymphoblastic leukaemia antigen (CALLA) to identify B-lineage ALL. Emergence of polyclonal antibodies against the lineage-associated markers (cluster of differentiation or CD markers) allowed identification of specific maturation stage of leukaemic cells. As a consequence, ALL was classified into several B- and T- lineage categories by various study groups (Bene et al., 1995). In 2008, the World Health Organization (WHO) classified B- lineage leukaemias as precursor- B lymphoblastic leukaemia (B-cell precursor ALL or BCP-ALL) and Burkitt leukaemia. BCP-ALL identified by expression of B-lineage markers such as cytoplasmic CD79a, CD19, HLA-DR and CD10 whereas Burkitt leukaemia is identified by surface Immunoglobulin (Ig) expression (Swerdlow et al., 2008). T-ALL is characterized by the expression of T- lineage associated markers such as cytoplasmic CD3, CD7 and CD2 or

CD5.

T-ALL is frequently associated with male gender, older age, high WCC and mediastinal mass and is treated as high-risk disease. ETP-ALL is characterized by a very early lineage phenotype (Coustan-Smith et al., 2009) and shows a unique gene expression signature that overlaps with stem-cell and AML (Zhang et al., 2012). Approximately 80-85% cases of paediatric ALL comprise of BCP-ALL and are characterized by good prognosis whereas T-ALL form about 10-15% cases of childhood ALL and carry inferior prognosis. However, the independent prognostic value of T-cell phenotype is disputed. Differences in outcome previously attributed to immunophenotypes can now be classified based upon cytogenetic and molecular genetic abnormalities. Treatment intensification of T-ALL has resulted in an overall improved outcome with a treatment success approaching that of BCP-ALL (Mitchell et al., 2010, Escherich et al., 2010).

1.3.3 Cytogenetic characteristics

As discussed earlier, chromosomal abnormalities play a crucial role in the development of leukaemia, have distinct clinical and phenotypic properties and have a strong impact on the prognosis of disease, especially in BCP-ALL. Chromosomal analysis has been in use for the past several decades and is used for diagnostic classification, risk stratification and monitoring of disease progression. Cytogenetic/FISH analysis can identify chromosomal abnormalities with a high success rate. In the Medical Research Council (MRC) UK ALL trials, chromosomal abnormalities were performed using cytogenetics/FISH analysis in up to 91% patients out of which 89% had identifiable cytogenetic abnormalities (Harrison et al., 2005). The WHO classification has included BCP-ALL with the following cytogenetic abnormalities as distinct disease entities (Swerdlow et al., 2008):

- Numerical chromosomal abnormalities
    - Hyperdiploidy
    - Hypodiploidy
- Structural chromosomal abnormalities
    - t(9;22)(q34;q11.2); BCR-ABL1
    - t(v;11q23); MLL- rearranged
    - t(12;21)(p13;q22); TEL-AML1 (ETV6-RUNX1)
    - t(5;14)(q31;q32);IL3-IGH
    - t(1;19)(q23;p13.3);E2A-PBX1 (TCF3-PBX1)

The most common cytogenetic abnormalities relevant to this thesis are briefly discussed

below. One specific chromosomal translocation t(9;22)(q34;q11.2) (BCR-ABL1) is of particular interest to this thesis and is there discussed in more detail in this section (also in section 1.6.8).

1.3.3.1 High hyperdiploid

High hyperdiploid (chromosome number of 51-68) is the commonest cytogenetic subtype and represent approximately 25-30% of all ALL cases. High Hyperdiploidy is found mostly in BCP-ALL and rarely in T-ALL. The hyperdiploid leukaemic cells have a propensity to undergo apoptosis, and accumulate methotrexate and its active metabolites (Synold et al., 1994); thus explaining the independent favourable outcome in this category. Patients with chromosome numbers 58-66 offer the best prognosis in this category. Near triploid (69-81) or near tetraploid are rare but distinct types of ALL and are associated with ETV6-RUNX1 BCP-ALL, T-ALL and a favourable outcome (Raimondi et al., 2006).

1.3.3.2 TEL-AML1 (ETV6-RUNX1)

The t(12;21)(p12;q21) translocation results in fusion of ETV6 gene on chromosome 12 to the RUNX1 gene on chromosome 21. ETV6 gene is a regulator of haematopoiesis while RUNX1 encodes a transcription factor necessary for haematopoiesis. The fusion gene encodes a protein that binds to Smad3, a transforming growth factor-β (TGF-β) signalling target and alters its ability to inhibit proliferation (Ford et al., 2009). ETV6-RUNX1 translocation is the most common specific genetic rearrangement and is seen in 20-25% of BCP-ALL but rarely seen in T-ALL (Attarbaschi et al., 2004) This rearrangement is associated with good prognosis characteristics and a favourable outcome (Loh et al., 2006). However, the prognostic value is modified by coincidence of other prognostic variables such as age, presenting white cell count (WCC) and response to treatment (Enshaei et al., 2013, Borowitz et al., 2008). Furthermore, some of the patients with TEL-AML1 tend to suffer from late relapses despite initial clearance of disease. The late relapses usually have a better outcome than other categories. Interestingly, some of the relapses represent an independent second hit in a persistent ancestral TEL-AML1 rearranged clone (Ford et al., 2001).

1.3.3.3 Philadelphia chromosome (BCR/ ABL1)

The Philadelphia (Ph) chromosome was the first specific chromosomal abnormality identified in human cancers (Nowell and hungerford, 1960) as well as ALL (Propp and Lizzi, 1970). Philadelphia chromosome is formed as a result of reciprocal translocation

between the long arms of chromosome 9 and 22. Fusion of ABL1 gene with the breakpoint cluster region (BCR) on chromosome 22 generates the BCR-ABL1 fusion gene. The breakpoints on the chromosome 9 are located within the first intron whereas on the chromosome 22 are scattered in three main regions. As a consequence three different sized mRNA and translated products are formed i.e $p190^{BCR-ABL1}$ (190 kDa), $p210^{BCR-ABL1}$ (210kDa) and $p230^{BCR-ABL1}$(230 kDa) (Figure 1-3). $p190^{BCR-ABL1}$is most commonly associated with Paediatric BCR-ABL1 ALL whereas p230 $^{BCR-ABL1}$ is a characteristic feature of chronic myeloid leukaemia (CML). It is not clear whether the intrinsic differences in the three variants of BCR-ABL1 protein account for the clinical phenotypes or whether the differences in clinical disease are merely due to the distinct lineage of the transformed cells – there is evidence for both. Adult BCR-ABL1 positive ALL cases with either p190 or p210 fusion gene present with similar clinical characteristics and prognosis (Kantarjian et al., 1991). On the other hand, $p190^{BCR-ABL1}$ is suggested to be more efficient in promoting secondary mutations necessary for transformation into acute leukemic phenotype (Lugo et al., 1990).

BCR-ABL1 translocation is not sufficient to induce leukaemia and additional genetic aberrations are thought to be necessary for progression to overt ALL. For instance, deletions of IKZF1 with loss of the transcription factor IKAROS are commonly seen in BCR-ABL1 ALL and are thought to play a critical role in leukaemic progression. Other less common mutations such as deletions of CDKN2A and PAX5 are also seen (Mullighan et al., 2008a).

BCR-ABL1 ALL comprises 3-5% of childhood ALL cases and is associated with a poor prognostic outcome and generally treated as high risk patient (Jeha et al., 2014). BCR-ABL1 ALL is associated with older age, higher WCC and CNS disease at diagnosis. Before the introduction of tyrosine kinase inhibitors, BCR-ABL1 ALL presented the worst prognostic type of ALL with a very high likelihood of treatment failure (Ribeiro et al., 1987). However, with the use of tyrosine kinase inhibitors, there has been a dramatic decrease in leukaemia burden and end-of-induction minimal residual disease (MRD) levels similar to non-Ph+ ALLs (Jeha et al., 2014, Conter et al., 2010). With the use of tyrosine kinase inhibitors and accurate measurement of response by MRD monitoring, it has been possible that some of high risk patients can be re-classified as standard risk. BCR-ABL1 ALL with other favourable clinical features such as low WCC count, age <10 years and good response to remission induction can be expected to have better overall prognosis (Bhojwani et al., 2009).

Recent microarray data have identified a subset of paediatric ALL with poor outcome demonstrating genetic signatures that clusters with BCR-ABL1 ALL (e.g. IKZF1 deletion)

(Mullighan et al., 2009b) without the BCR-ABL1 translocation. These patients are classified as BCR-ABL1-like ALL (van der Veer et al., 2013, Den Boer et al., 2009).

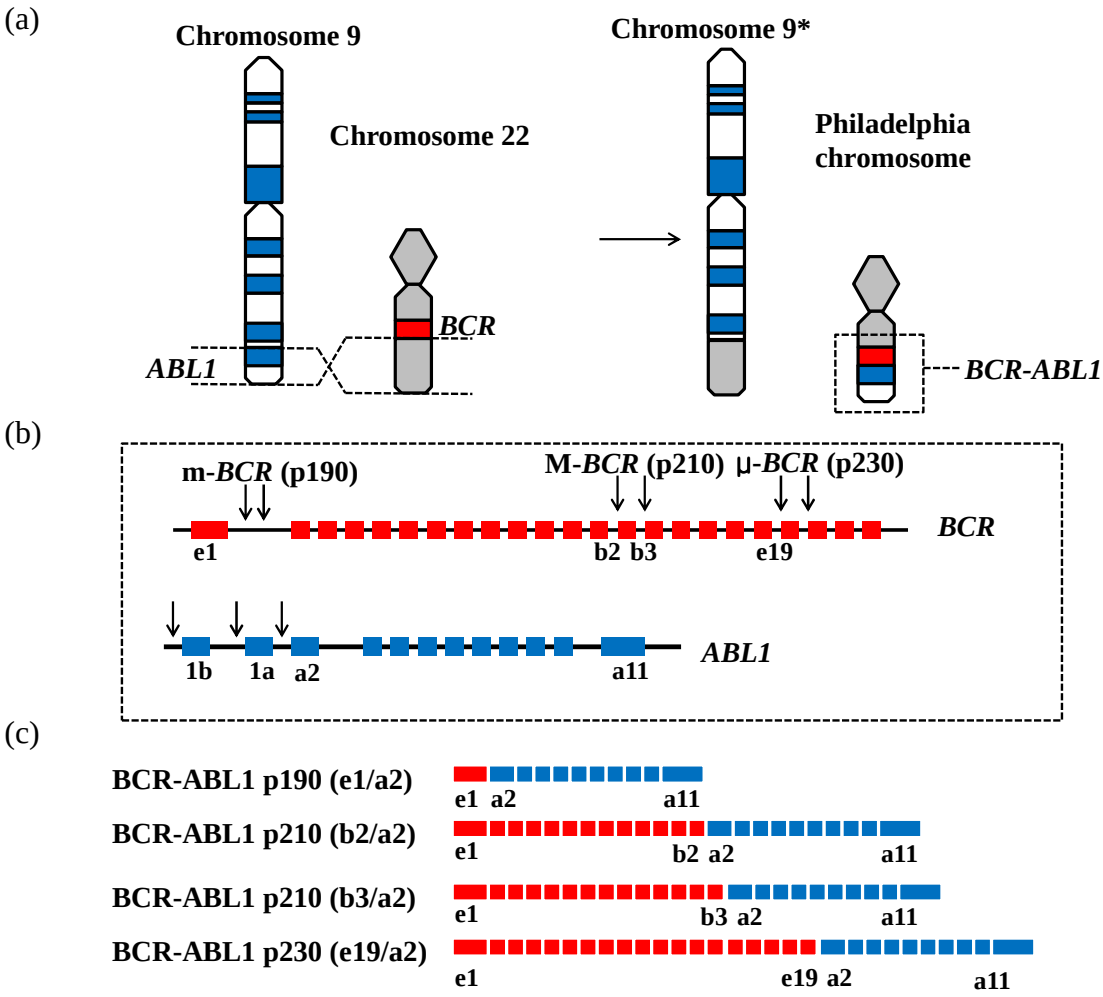

Figure 1-3 Philadelphia chromosome and BCR-ABL1 variants
(a) Chromosomal translocation between 9 and 22 (b) BCR and ABL1 genes with common breakpoints (c) translocated, transcribed and spliced mRNA. *abnormal chromosome 9. Adapted from (Chasseriau et al., 2004)

1.3.3.4 11q23; MLL- rearranged

This translocation represents approximately 2% of childhood ALL. The translocation occurs between MLL- gene on chromosome 11 and any one of a large number of translocation partners. The most common MLL rearrangements are MLL-AF4 found in approximately 50% of MLL-rearranged BCP-ALL. MLL gene is responsible for regulation of haematopoiesis and the translocation leads to abnormal expression of several transcription factors and regulatory genes (eg. FLT3) resulting in a ‘stem-cell like’ state of maturation (Mullighan, 2012). MLL-rearranged ALL patients have a poor prognosis, especially when diagnosed shortly after birth.

1.3.4 Risk assignment

While acknowledging ALL as a heterogeneous group of disorders, efforts have been made to define guidelines for uniform risk criteria, treatment regimen and analysis of the effectiveness of therapy. Treatment for ALL children is based on the theoretical risk of treatment failure and relapse defined by clinical and laboratory features. The aim of risk assignment is to achieve balanced therapeutic regimen where patients with favourable features receive less intensive drug therapy while patients with less favourable features who are likely to have poor outcome receive more intensive therapy.

Several features contribute to the risk assessment of ALL patients. These include:

- Demographic features such as age and sex.
- Presenting clinical and laboratory features such as WCC, presence of extramedullary disease, immunological subtype and cytogenetic characteristics
- Response to therapy.

At the time of diagnosis, the usual clinical decision is to stratify patients according to age, sex, WCC and immunophenotype. The allocated treatment regimens are usually redefined based on subsequent information on cytogenetic subtypes and the response to induction therapy. The National Cancer Institute (NCI) risk group stratifies patients according to the following criteria (Smith et al., 1996):

- NCI standard risk - WCC $<50 \times 10^9$/L and age 1-<10 years
- NCI high risk – WCC $>50 \times 10^9$/L and age <1 / >10 years

Patients with T-ALL are generally stratified as NCI- high risk irrespective of the other variables. Other patient characteristics affecting the prognosis include extramedullary disease such as CNS or testicular involvement at diagnosis. If patients initially stratified in the standard risk category are subsequently found to have high risk cytogenetics (e.g. hypodiploidy, MLL- rearrangement), they are allocated into the high risk category.

1.3.5 Response to treatment

In addition to the recognised clinical and biological factors associated with prognosis, there are several additional features that define individual patient's outcome. The pharmacogenomic and pharmacokinetics factors, the treatment intensity, scheduling and compliance and other yet unrecognised factors may play a complex interactive role in individual patients – thus limiting the sensitivity of predicting the outcome of the individual patient. As a result, response to leukaemic therapy has emerged as an independent prognostic factor which includes all of the above characteristics.

Modern treatment achieves clinical and morphological remission in most patients. However, with complete clinical remission (CCR) (<5% blasts in BM), the disease burden may not be completely eradicated and as many as 10^{10} cells may theoretically persist in the marrow (Pui and Campana, 2000). The morphological examination of the bone marrow is not sensitive for monitoring residual disease, as only 1-5 blasts/100 cells can be identified. Furthermore, morphological examination of the bone marrow is difficult to interpret and presence of increased numbers of blasts may merely represent the regenerating bone marrow – therefore, this method is not specific. In addition, the morphologic examination is subjective to the observer's interpretation; therefore standardization within a laboratory and between laboratories is difficult. Historically, all patients in CCR received the same consolidation treatment irrespective of the extent of submicroscopic disease burden. Some patients in CCR may not have required any treatment at all while others should have received enhanced treatment because of the burden of submicroscopic disease (Figure 1-4). The international Berlin-Frankfurt-Munster (BFM) group has long used 1-week single agent steroid response as a measure for monitoring treatment response (Schrappe et al., 2000). However, more recently, focus has shifted to using more sensitive, specific and reproducible methods for the detection of minimal residual disease (MRD).

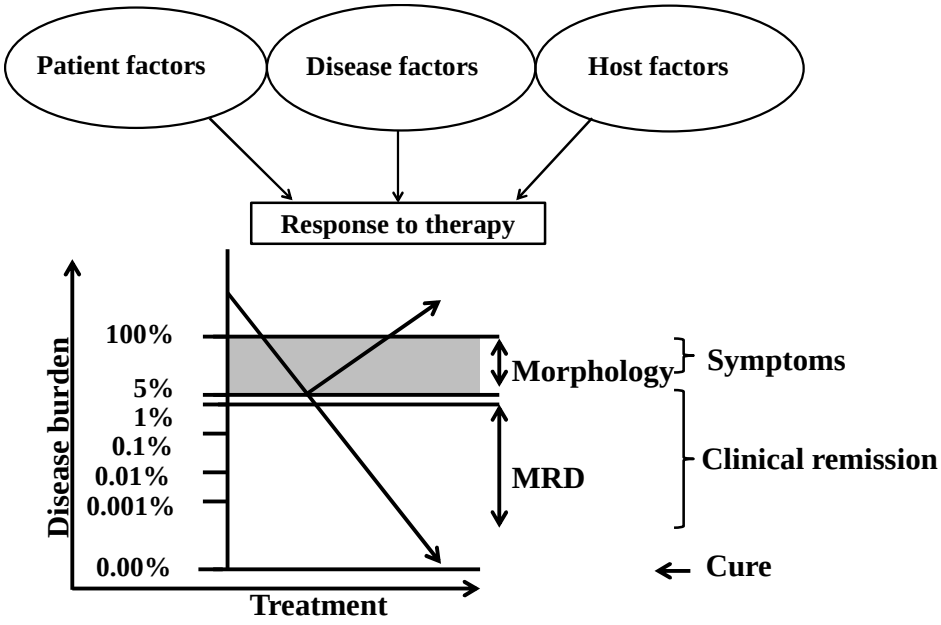

Figure 1-4 Principle of MRD monitoring
Prognosis of individual leukaemia is affected by the host characteristics (e.g. age, pharmacogenomics), leukaemia characteristics (e.g. WCC, cytogenetics) and treatment factors (dose intensity, duration). Submicroscopic residual leukaemic burden can exist wtih morphological remission which is responsible for treatment failure or relapse. (Adapted from Campana (2003)).

1.3.5.1 MRD determination by flow cytometry

Lymphocyte development begins in the bone marrow with pluripotent haematopoietic stem cells (HSC). Upon appropriate stimuli, the HSCs differentiate into lymphoid and subsequently B- and T- lymphoid lineage. A number of surface and intracellular proteins (e.g. cluster of differentiation or CD markers) are expressed during specific stages of development. As discussed in section 1.3.2, leukaemic cells tend to mimic the normal stages of B- and T cell differentiation (Figure 1-5). In addition, leukaemic cells express proteins not seen in any of the normal lymphocytes in the same stage of development and may lack some antigens expressed by their normal counterparts. As a result, individual patient's leukaemic cells can be discriminated from normal developing lymphocytes based on aberrant expression of such markers. This immunophenotypic signature, called Leukaemia associated immunophenotype (LAIP) can be used to monitor residual leukaemic cells over time.

Flow cytometry based MRD detection (flow-MRD) has the ability to detect 1 leukemic cell in a background of 10,000 normal haematopoietic cells (0.01%) (Coustan-Smith et al., 1998, Weir et al., 1999) and can be applied in more than 95% cases of childhood ALL (Weir et al., 1999, Dworzak et al., 2002). However, flow cytometry requires fresh material for analysis and expertise in interpretation of results. In addition, leukaemic relapse may be

accompanied by emergence of a different LAIP thus making accurate monitoring difficult. The Children's oncology group (COG) routinely uses flow cytometry for MRD monitoring (Chen et al., 2012). In one study on 2143 of BCP-ALL patients, MRD at day 29 (end of induction) was able to effectively predict outcome. Importantly, in multivariate anaylsis, MRD at day 29 was the strongest risk factor for event free survival (EFS) while a conventional risk factor ETV6:RUNX1 translocation was not associated with a significant difference in outcome (Borowitz et al., 2008). Efforts at standardization of flow-MRD in the UK in multicentre setting have shown promising results (Irving et al., 2009).

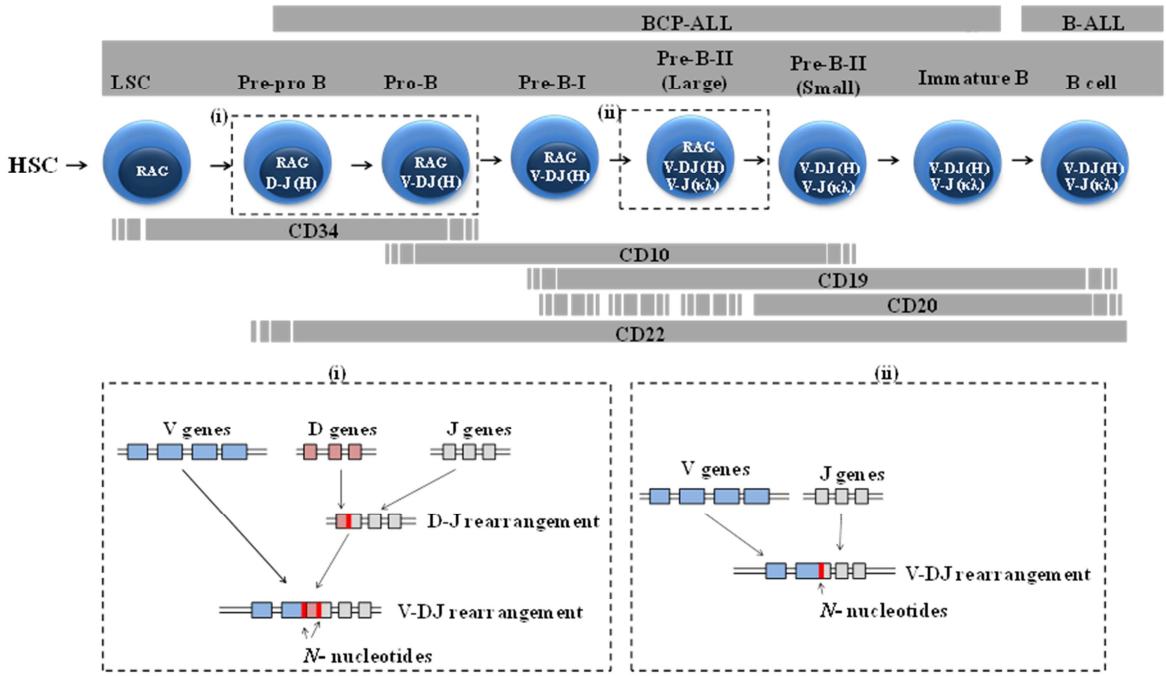

Figure 1-5 Simplified model of (a) B- cell development stages and corresponding BCP-ALL types and (b) V(D)J and VJ rearrangement
Schematic representation of (a) B- cell differentiation stages and expression of relevant CD markers with leukaemic counterparts above. (b)(i) V(D)J rearrangement process with D-J rearrangement followed by a V-DJ rearrangement I (Ig heavy chain (IGH), TCR beta (TCRB), & TCR delta (TCRD) genes (ii) direct V-J rearrangements in case of Ig kappa (IGK), Ig lambda (IGL), TCR alpha (TCRA), and TCR gamma (TCRG) genes. Rearrangement is initiated following expression of recombination activation gene (RAG1 and 2). HSC (Haematopoietic stem cell), LSC (Lymphoid stem cell, CD (Cluster of differentiation) Adapted from (Cobaleda and Sanchez-Garcia, 2009, Bene and Kaeda, 2009).

1.3.5.2 MRD determination by polymerase chain reaction

The main function of normal B- and T cells is to maintain the immune defences by identifying and neutralizing foreign antigens. The ability of lymphocytes to identify potentially unlimited number of antigens is based on the repertoire of antigen receptor molecules expressed by the lymphocytes. This diversity to identify millions of antigens is created by Ig and T-cell receptor (TCR) gene rearrangements. This involves random recombination of variable (V), diversity (D) and junctional (J) region genes (Tonegawa,

1983). In addition, insertion of non-templated (N-) nucleotides provides additional diversity to the Ig and TCR molecules. Consequently, each lymphoid precursor and its progeny differ from the others. This unique identity – a DNA finger-print – forms the basis for monitoring leukaemic cells in the background on normal regenerating bone marrow.

The principle underlying real-time quantitative PCR (qPCR) monitoring of MRD is the specific amplification of leukaemic DNA sequences in the background of predominantly normal DNA from the bone marrow. Using DNA from diagnostic bone marrow specimen as a control to generate standard curve, accurate quantification of minimal levels of residual leukaemia is possible. Since the leukaemic cell population carry identical Ig/TCR gene rearrangement, diagnostic bone marrow DNA is used to identify and sequence the junctional regions of the rearranged genes. These sequences are used to design allele specific oligonucleotide (ASO) primers. A laborious standardization phase involves testing for sensitivity. Comprehensive guidelines for optimum DNA extraction, testing for sensitivity and specificity, and data interpretation have been published (van der Velden et al., 2007, Flohr et al., 2008, van der Velden et al., 2003) . In principal, qPCR is capable of detecting a single copy of leukemic DNA. However, practically, a sensitivity of 1×10^{-5} (1 leukaemic cell/ 100,000 cells) can be achieved in nearly 95% patients with this method. Currently, this method is widely used in many paediatric ALL protocols (van der Velden et al., 2003, Vora et al., 2013, Zhou et al., 2007).

Levels of qPCR MRD after induction therapy are associated with relapse and poor prognosis. In an earlier study, patients with 10^{-3} residual leukaemic cells at any time point (after induction, consolidation or delayed intensification) were at a very high risk of relapse. MRD levels were the most important prognostic factors followed by immunophenotype and WCC (Cave et al., 1998). Since then, molecular monitoring of MRD is applied in several major treatment protocols with strong association of MRD positivity and relapse, treatment failure and other poor outcome variables (Zhou et al., 2007, van Dongen et al., 1998, Flohr et al., 2008, van der Velden et al., 2003, Vora et al., 2013). Based on MRD results, treatment reduction for some low risk ALL types has shown promise. Treatment reduction of MRD negative low risk children and young adults in the MRC UKALL 2003 trial showed that there was no significant difference in EFS in any of the randomized groups (Vora et al., 2013).

In addition to MRD monitoring for rearranged Ig/TCR genes, qPCR can also be used to identify the fusion genes transcript levels in ALL with recurrent cytogenetic abnormalities (e.g. BCR-ABL1). This method carries the advantage of detection of the genetic mutation

associated with the leukaemia and the potential detection of pre-leukemic clone, irrespective of the clonal evolution and clonal heterogeneity. In addition, this method carries the advantage of a fixed set of standardized primers for the fusion gene transcripts (Gabert et al., 2003). Global use of this technique has been limited due to: a small proportion of suitable patients with fusion genes (40%), issues with RNA stability, the levels of fusion gene transcripts produced /cell may vary even for the same fusion gene type and finally, due to the potential variation in the levels of the house-keeping gene to control for sample quantities (van Dongen et al., 1999). Therefore, currently, this method is in use only for BCR-ABL1 ALL (Jeha et al., 2014).

Despite being a strong indicator of treatment response and prognosis, a negative MRD does not always predict outcome and approximately 5-12% patients with a negative MRD at the end of induction still relapse (van Dongen et al., 1998, Cave et al., 1998, Zhou et al., 2007, Flohr et al., 2008). In addition, MRD monitoring only reliably demonstrates the levels of leukaemia in the bone marrow. Theoretically, leukaemic cells in the so-called sanctuary sites (such as the testes and the CNS) can be the cause of relapses in patients who clear bone marrow MRD. In addition, there is not enough evidence to show whether MRD levels can be used as a surrogate marker while testing new therapies. For instance, in the recent UK ALLR3 trial, significantly improved EFS was observed in children treated with Mitoxantrone compared to Idarubicin despite similar levels of post-induction MRD in the two groups (Parker et al., 2010).

1.3.6 Extramedullary disease (excluding CNS)

The clonal concept of leukaemia implies that leukaemic cells originate from the sites of lymphoid development (i.e. bone marrow or thymus), yet at the time of diagnosis, leukaemic infiltration of several extramedullary organs such as the liver, spleen, (Steinherz et al., 1998) testes and the CNS is common (Reiter et al., 1994, Burger et al., 2003).Traditionally, extramedullary involvement at diagnosis has been considered a measure of tumour burden and has been associated with poor outcome (Steinherz et al., 1998). Presence of extramedullary disease at diagnosis can be important therapeutically. Occult leukaemia at the so-called sanctuary sites can seed the bone marrow and result in relapse or treatment failure. Therefore, current treatment protocols include assessment of testicular and nervous system disease.

Overt testicular involvement is seen in 2% children with ALL at diagnosis and is associated with a significantly higher rate of relapse. Isolated testicular relapse is the

second most common site of extramedullary relapse in children. Testicular disease at diagnosis is associated with other high risk prognostic features. As a result, the majority of boys with bulky testicular disease at diagnosis are treated as high risk (Hijiya et al., 2005, Sirvent et al., 2007). The reason for testicular involvement in ALL is not understood completely. A poorly defined blood-testis barrier may protect leukaemic cells from tumour immune surveillance. Alternatively, the external location of the testes may provide survival advantage to leukaemic cells.

Ovaries are the embryological counterparts of testes. A series of autopsies revealed similar incidence of ovarian (58%) and testicular (48.5%) infiltration by leukaemia (Kamiyama and Funata, 1976). However due to their position in the abdominal cavity, clinical signs of leukaemic infiltration appear less often. Current protocols do not actively look for ovarian infiltration at diagnosis and relapse. It is possible that because of same embryological origin, the ovarian environment is also protective to leukaemic cells. Moreover, in girls with leukaemia, cryopreservation and re-implantation of ovarian tissue is a potential method of preservation of fertility. In a recent article, cryopreserved ovarian tissue from 9 girls with ALL showed presence of leukaemia by PCR (5/9 patients) and engraftment of leukaemia in immunodeficient SCID mice transplanted with the ovarian tissue (4/9 patients) (Dolmans et al., 2010).

1.3.7 CNS disease

With improving success rates in control of leukaemia, central nervous system involvement in ALL emerged as a new phenomenon. The longer the patients lived, the greater the chances of them developing CNS disease. Between 1948-1960, the incidence of CNS leukaemia increased from 3% to 40% as the median survival of patients increased from 4 to 12 months (Evans and Craig, 1964). In a series of 126 autopsies on children who died of leukaemia, almost 60% of the autopsies showed evidence of leukaemia in the CNS, predominantly the meninges (Price and Johnson, 1973). In patients surviving for 4 years or longer, up to 75% had CNS disease (Evans et al., 1970). The increasing incidence of CNS disease was attributed to poor penetration of anti-leukaemic agents into the CNS. With the realization that any improvement in survival rates could only be possible with effective clearance of CNS disease, prophylactic CNS therapy quickly reduced the frequency of CNS infiltration and improved survival (Hustu et al., 1973). Over the past few decades, survival from ALL has improved dramatically. Yet, CNS disease continues to pose challenges.

CNS disease is diagnosed and monitored by microscopic analysis of CSF. 1-2 ml of CSF is obtained through lumbar puncture. CSF cells counts are determined using automated cell counters while morphologic examination of CSF cytospin slides is performed to identify and count leukaemic cells. Based on this, CNS disease is classified into CNS disease categories (Table 1-1). At diagnosis, approximately 3% patients have CNS-3, 15-20% present with CNS-2 status (Gilchrist et al., 1994, Mahmoud et al., 1993, Burger et al., 2003) while approximately 10% have traumatic lumbar puncture (TLP) with blood contamination of the CSF at the time of diagnosis (Gajjar et al., 2000). The majority of children with CNS-3 disease are asymptomatic. However, some may present with clinical or radiological signs without leukaemic cells in the CSF.

Category	Definition
CNS-1	Non-traumatic lumbar puncture without leukaemic blasts a
CNS-2	Non-traumatic puncture, $\leq$ 5 WBC/µL CSF with identifiable blasts
CNS-3	Non-traumatic puncture, $\geq$ 5 WBC/µL CSF with identifiable blasts or cranial nerve palsies or cerebral mass
TLP positive	Traumatic lumbar puncture with obvious blasts
TLP negative	Traumatic lumbar puncture without blasts

Table 1-1 Diagnostic criteria for CNS disease

Acknowledging that the current methods of diagnosing CNS disease may not be sensitive enough, a number of researchers have tested novel methods to improve the diagnostic accuracy of CNS disease.

1.3.7.1 Experimental methods for detection of CNS disease

Following the improved survival with prophylactic CNS therapy, it was proposed that sub-clinical level of leukaemia in the CNS were present at diagnosis (Hustu et al., 1973). There was a need to improve the diagnostic accuracy of CNS involvement. Several alternative methods to detect sub-clinical levels of leukaemia in the CSF have been tried. Three main approaches have been reported: increasing sensitivity of detecting blasts in the cerebrospinal fluid samples, and indirect estimation of CNS leukaemia by detecting soluble biomarkers of leukaemia in the CSF, and using radiological diagnostic methods. These are briefly described here.

1.3.7.2 Detection of CNS leukaemia by immunological markers

Leukaemic blasts are difficult to be discriminated from normal leukocytes on cytospin. Use of immunological markers can identify leukaemic cells with accuracy. The initial studies used Terminal deoxynucleotidyl transferase (TdT) (Hooijkaas et al., 1989) and TdT/CD10

(Homans et al., 1990) staining of CSF cytospin preparation. TdT staining from patients with TdT-expressing leukaemias identified approximately 25% patients to be positive for CNS disease. Moreover, TdT staining at diagnosis was predictive of a CNS relapse during the follow up period (Hooijkaas et al., 1989). More recently, multi-colour flow cytometry has added to the accuracy of diagnosing CNS disease (Sayed et al., 2009, Del Principe et al., 2014, Martinez-Laperche et al., 2013, Bromberg et al., 2007, Cancela et al., 2013). For example, in a study on 219 patients with different haematological malignancies, flowcytometry detected CNS leukaemia in 44 (20%) patients compared to 19 (8%) by cytology. Four flow cytometry +ve/cytology-ve patients subsequently relapsed in the CNS (Bromberg et al., 2007). Similarly, in a recent study on 113 paediatric ALL patients, CNS leukaemia was found in 27.8% patients by flow cytometry compared to 2.8% by cytology. Moreover, appearance of leukaemic phenotype during treatment period was predictive of CNS relapse (Martinez-Laperche et al., 2013).

1.3.7.3 Detections of CNS disease by PCR

PCR for clonal Ig/TCR gene rearrangements can be used to determine the clonality of leukaemic cells in the CNS (Scrideli et al., 2004, Scrideli et al., 2003, Pine et al., 2005, Biojone et al., 2012, de Haas et al., 2002, Galoin et al., 1997). DNA is stable and can be recovered from cells with poor viability. Studies utilizing PCR have demonstrated not only a higher incidence of CNS disease, but also poor prognosis in CSF PCR positive patients. For example, using PCR, in a series of 37 paediatric ALL patients, 46% were positive for CNS disease while morphology could only determine 5.4% CNS-3 cases. Moreover, the 4 year EFS in qPCR positive patients was significantly worse than qPCR negative patients (Scrideli et al., 2004). qPCR studies can also be useful in cases suspected of CNS leukaemia. For instance, Scrideli et al. describe a small series of cases with and without CNS disease. In one such patient where CSF cytology was considered positive, heteroduplex analysis of the PCR product identified oligoclonal bands, suggesting reactive lymphocytosis instead of CNS disease (Scrideli et al., 2003). However, presence of clonally evolved leukaemic cells in the CNS may lead to false negative results when tested by qPCR for Ig/TCR rearrangements. It is currently not known whether leukaemic cells in the CNS represent the same dominant clones in the bone marrow.

The worse prognosis associated with sub-clinical levels of CNS disease tends to reduce in more recent trials. In a study using qPCR for clonal Ig/TCR rearrangement 29/62 patients were positive for CNS leukaemia at diagnosis. Patients treated with a low intensity regimen had a significantly poor 5 year EFS and Relapse Free survival (RFS) compared to

CSF negative patient, while there was no difference in the outcome of CSF qPCR positive and negative patients allocated to intensive treatment group. Three CNS relapses were seen in the duration of follow up, all were CSF qPCR positive at diagnosis (Biojone et al., 2012). Similarly, CSF positivity by flow cytometry in adult ALL is associated with worse overall survival (Del Principe et al., 2014). A similar effect of treatment was seen with flowcytometry positive CSF leukaemia where enhanced intrathecal methotrexate was used (Liang et al., 2013).

It is clear that when flow cytometry or PCR is used, CNS disease can be detected at a higher rate than by microscopy. This added information has shown to be useful in predicting relapse, and improving the outcome in some cases with therapy escalation. However, the published literature lacks comparability due to different panels of antibodies used or different PCR techniques employed. Flow cytometric analysis of CNS leukaemia is limited so far by limited number of cells, poor viability of cells after lumbar puncture, different combinations of antibodies used in literature. LAIP may change and result in a false negative result. Low yield of amplifiable DNA for PCR excludes patients who may be true negatives but follow up data from these patients is missing. In addition, analysis by PCR may not detect CNS homing clones if different from the dominant clone. The above described studies are mostly clinical and fail to provide any explanation for discordance between cytology and Flow cytometry /PCR results. More of leukaemic burden is present on the surface of meninges and leukaemic cells may not necessarily be always present in CSF circulation. This prompts for indirect determination of leukaemia in the CNS through soluble biomarkers of CNS leukaemia.

1.3.7.4 Soluble biomarkers of CNS disease

Leukaemia-associated soluble factors may be released by the malignant cells into the extracellular compartment and their levels in the CSF could be an indirect measure of disease burden in the CNS. Early attempts to identify leukaemia specific soluble biomarkers focused on assessing markers of inflammation, cellular activity and the blood-brain barrier integrity such as levels of lactate dehydrogenase (Reeves et al., 1978), and CSF protein levels (Harms, 1974). Few candidate lymphoid cell proteins associated with adhesion, chemotaxis and immune response have shown promise. Not only do the soluble biomarkers associated with CNS disease be useful clinically, but also they can provide clues on disease biology – soluble L-selectin (sL-selectin) is one of such biomarkers. Stucki et al. categorised a group of adult leukaemia patients into plasma sL-seletin^{high} and sL-selectin^{low} groups. The authors observed that patients with confirmed CNS disease had

significantly higher levels of CSF sL-selectin compared to patients without CNS disease or controls (Stucki et al., 1995). The levels of CSF sL-selectin have shown to rise before clinical CNS-relapse, peaking at overt CNS relapse and declining post- treatment (Dagdemir et al., 1998). sL-selectin has been shown to inhibit blast cell adhesion to the endothelium and thus may have been responsible for excessive mobilization of leukaemic cells in the CNS compartment (Spertini et al., 1994).

Soluble Interleukin-2 Receptor alpha (sIL2-Rα) was tested in 19 patients with CNS disease and 134 controls patients. sIL2-Rα level >10U/ml was suggestive of CNS leukaemia with a high sensitivity (89.5%) and specificity (89.6%). However, these values could only be used in conjunction with CSF cytology (Lee et al., 2005). Soluble CD27 (sCD27) was analysed in 70 children with various haematological malignancies. sCD27 levels possessed high sensitivity and specificity, however in many cases there was a considerable overlap in sCD27 levels between CNS cytology positive and cytology negative cases (Kersten et al., 1996). The chemokine CXCL13 has also been investigated in various CNS malignancies expressed on the tumour (Smith et al., 2003), host tissue (Brunn et al., 2007), or secreted in the CSF (Rubenstein et al., 2013). CXCL13 and IL-10 combined had a diagnostic specificity of >99% in primary CNS lymphoma (Rubenstein et al., 2013). Several groups have also tested CCL2 (Eisenkraft et al., 2006), β2 microglobulin (Mavlight et al., 1980), Fibronectin (Rajantie et al., 1989) and Vascular endothelial growth factor 1 & 2 (VEGF1&2) (Tang et al., 2013) in the CSF from leukaemia and lymphoma patients with inconclusive results. In a recent study conducted on B-cell lymphoma patients several candidate biomarkers were tested. In patients with primary CNS lymphoma, higher levels of soluble CD19 (sCD19) were found in the CSF in 88% patients. sCD19 positivity was associated with a poor EFS however, no CNS relapse was seen on follow up (Muniz et al., 2014). Recently, significantly higher CSF osteopontin levels were found in a cohort of paediatric patients with CNS relapse compared to CNS negative controls. However, the findings were limited by a small number of control group and low specificity of the test (İncesoy-Özdemir et al., 2013).

Soluble biomarkers of disease in the CNS are limited by high false negative and false positive results. A possible explanation to this could be the insensitive comparator (CSF cytology) used in these studies. As we have already discussed, CSF cytology lacks sensitivity and many CSF cytology negative cases may harbour disease in the CNS. Such cases are wrongly put in the CNS negative category, thus making adequate comparisons difficult. CSF cytology only identifies 3-5% cases at diagnosis while data from PCR and

flow cytometry suggest that up to 60% cases of paediatric ALL may be positive for CNS disease at diagnosis. A study of CSF biomarkers in flow cytometry/ PCR defined CNS disease has never been performed.

1.4 ALL treatment

Acute lymphoblastic leukaemia was invariably fatal disease until the 1960s. Patients treated with single agents rarely achieved remission and the disease would take over again. It was soon realized that when vincristine, prednisolone and L-asparaginase were combined, the remissions lasted longer. The realization that systemic therapies could not effectively eradicate the subclinical CNS disease was a major breakthrough. The prophylactic cranial and craniospinal irradiation dramatically improved prognosis and within a decade, nearly half of the patients could be expected to achieve long-term survival. Formation of large cooperative study groups meant more uniform approaches for treatment could be employed and smaller differences in survival could be exploited. Understanding of prognostic risk factors and adaptation of risk-adapted therapeutic regimen along with improved management of toxicities resulted in an excellent survival of paediatric ALL patients.

The current treatment of ALL typically involves chemotherapy given for 2-3 years and is intended to achieve cure in patients. Therefore children at a higher risk of treatment failure receive more intense and prolonged chemotherapy. The majority of patients are treated at specialized centres with risk-stratified treatment protocols. The core chemotherapeutic drugs have principally remained unchanged over the last decades. The main classes of drugs used in paediatric ALL include corticosteroids (prednisolone, dexamethasone), anthracyclines (Daunorubicin) and purine analogues (6-Mercaptopurine). The treatment is distributed into different phases spanning over 2 years for girls and 3 years for boys.

1.4.1.1 Remission induction

Remission induction includes intensive chemotherapy for a short period (typically 4 weeks) and is intended to eradicate the bulk of disease along with restoration of normal haematopoiesis. Commonly used drugs include a glucocorticoid (prednisolone or dexamethasone), vincristine and asparaginase. This drug combination allows targeting multiple key pathways in leukaemic cells. High risk patients may receive additional daunorubicin. BCR-ABL1 ALL patients may also receive a tyrosine kinase inhibitor (Imatinib or Dasatinib) (Schultz et al., 2009). Following induction chemotherapy, the

majority of patients achieve clinical and morphological remission (<5% BM blasts, no circulating and CSF blasts, no cerebral mass). MRD studies performed at the end of induction period are used to assess patient response to treatment and re-assign risk.

1.4.1.2 Intensification (consolidation)

The aim of consolidation therapy is to eradicate any residual disease using a combination of chemotherapeutic agents. The combination and intensity is dependent upon clinical risk-status and MRD results. The drug combinations vary in different protocols but include methotrexate, mercaptopurine, asparaginase along with frequent pulses of vincristine and corticosteroids. Intensification is typically administered for 10-12 weeks. (Vora et al., 2013) CNS directed therapy is given to eliminate CNS disease. Many protocols include a delayed intensification phase consisting of a 3 week re-induction and re-consolidation towards the end of intensification phase (Moricke et al., 2008, Schrappe et al., 2011).

1.4.1.3 Maintenance

Maintenance therapy is typically given over a period of 2-3 years of continuous remission - three years for boys while two years for girls (Vora et al., 2013, Gaynon et al., 2010). The maintenance therapy generally includes oral 6-mercaptopurine and weekly or parenteral methotrexate and targets residual slow-cycling leukaemic cells. Therefore, careful monitoring of drug toxicities and compliance to drugs is essential for the whole duration of maintenance therapy. Non-compliance to 6-mercaptopurine is shown to be associated with significant increase in relapse risk (Bhatia et al., 2012) whereas toxicities may arise in patients with deficiency of S-methyltransferase – an enzyme that inactivates mercaptopurine (Relling et al., 1999). CNS prophylaxis continues during maintenance (Mitchell et al., 2010).

1.4.1.4 CNS-directed therapy

At diagnosis, only 3-5% children present with morphological or clinical evidence of CNS disease (CNS-3). However, unless CNS-directed therapy is administered, the majority of children will eventually present with CNS disease. Therefore, CNS- directed treatment is given to all patients irrespective of the evidence of CNS involvement at diagnosis. The initial CNS prophylaxis consisted of cranial or cranio-spinal irradiation (Hustu et al., 1973). However, due to toxicities associated with radiation, the use of radiation in most modern protocols is reserved for patients at high risk for CNS relapse (Richards et al., 2013). CNS- directed therapy comprises of high intensity systemic chemotherapy with

CNS bioavailability, intra-thecal chemotherapy and cranial radiation in some cases. The choice of drugs and intensity is calculated on the NCI-risk, MRD risk and CNS disease status at presentation (Gaynon et al., 2010, Mitchell et al., 2010, Schmiegelow et al., 2010, Salzer et al., 2010).

1.4.1.5 ALL relapse

Approximately 20-25% children with ALL will eventually relapse, mostly in the bone marrow and or CNS (Nguyen et al., 2008, Mitchell et al., 2010). Despite intensive therapy, the prognosis of relapsed ALL has not improved in the past few decades (Nguyen et al., 2008, Roy et al., 2005). Features associated with poor prognosis include NCI- high risk category, early relapse, age >10 years, CNS disease at diagnosis, male gender, T-cell immunophenotype, high risk cytogenetics (Nguyen et al., 2008, Chessells et al., 2003) and MRD at the end of induction (Raetz, 2008). More recently, acquired genetic mutations such as TP53 gene mutations and IKZF1 deletions are found to be associated with a higher frequency of relapse and carry risk of second relapse (Krentz et al., 2013). However, the defining characteristics for risk stratification are the duration of first remission, site of relapse and immunophenotype (Einsiedel et al., 2005, Masurekar et al., 2014, Nguyen et al., 2008).

The duration of first remission is an important determinant of outcome – with late relapses having a much better prognosis than early relapses. For instance, in the UK, 5 year EFS following bone marrow relapse occurring within 18 months from diagnosis was 20% while prognosis after relapses occurring more than 18 months but within 6 months after completion of therapy was 49% (Roy et al., 2005). For patients with CNS relapse, the overall survival in late relapses was 69% compared to 41.9% for very early relapses (Masurekar et al., 2014). This probably could be due to incidence of late relapses in TEL-AML1 ALL cases. On the other hand, T-ALL cases tend to relapse early – both these characteristics are independent poor prognostic features (Einsiedel et al., 2005).

Site of the relapse is an independent prognostic factor. CNS involvement at the time of relapse (isolated or combined with bone marrow relapse) can be seen in 20-40% of patients (Krishnan et al., 2010, Masurekar et al., 2014). CNS relapses are frequently associated with high risk features such as T-cell ALL, WBC > 100,000/ul, BCR-ABL1 and MLL-rearrangement and CNS disease at diagnosis (Pui, 2006) The role of CNS-2 status and traumatic lumbar puncture is debated (te Loo et al., 2006, Mahmoud et al., 1993, Gilchrist et al., 1994, Burger et al., 2003). Despite this risk stratification, CNS relapses are

frequently seen in patients stratified as low risk for CNS disease. The earlier CCG (childhood cancer group) trial data (1983-1989) from 2712 ALL children nearly 1/3rd relapsed with highest number of relapses in the bone marrow, followed by isolated CNS relapse (Gaynon et al., 1998). Moreover, the median time to CNS relapse was shorter (19 months) and 6 year survival of only 48% (Gaynon et al., 1998). In a Dutch Childhood Leukemia study group (DCLSG) study, out of 526 paediatric ALL cases, only 22 cases of isolated CNS relapse were seen; however the majority of CNS relapse patients were from CNS1 category (te Loo et al., 2006). Similarly more CNS relapses were seen in standard risk (SR) patients compared to high risk (HR) in 491 children treated at Dana Farber Cancer Institute (DFCI) (Moghrabi et al., 2007). In the BFM group study, more isolated CNS relapses were seen in medium risk patients compared to high risk group (Moricke et al., 2008).

Isolated CNS relapses tend to respond better to treatment than patients with combined (bone marrow>5% blasts + CNS>5 blasts/µl) relapses (Krishnan et al., 2010) which in turn have a better outcome than isolated bone marrow relapses (>25% blasts). This improved outcome in isolated CNS relapse is attributed to high dose CNS directed systemic and intrathecal chemotherapy followed by cranial radiation (Ritchey et al., 1999). Moreover, it can also be argued that since bone marrow and CNS relapses are competing events, isolated CNS relapses would represent efficient clearance of bone marrow blasts and therefore a less aggressive disease. This hypothesis is supported by identification of a new group of patients with overt CNS relapse with bone marrow disease detectable only by qPCR. Such patients tend to have a worse outcome in comparison with truly isolated CNS relapses (Hagedorn et al., 2007). Therefore, the prognosis of patients with CNS relapse worsens with increasing levels of disease in the bone marrow. Weather the sub-microscopic bone marrow disease is a result of secondary seeding from the CNS blasts or alternately CNS relapse is the result of an early dissemination from sub-microscopic bone marrow disease remains to be clarified. This may have important biologic and therapeutic implications. Leukaemic cells in the bone marrow at relapse can represent expansion from an ancestral clone (Mullighan et al., 2008b) and are frequently found to have additional genomic mutations (Krentz et al., 2013). If the leukaemic cells in the CNS are different from the bone marrow clone at relapse, different therapeutic approaches may be required.

1.4.1.6 Toxicity of ALL therapy

Intensive chemotherapeutic regimen along with the use of CNS prophylaxis has increased chances of survival even in relapsed ALL. This success has not been without the cost of

significant treatment related toxic effects. Therapeutic agents may affect the growth of the developing bodies of the children, may cause acute toxicities or may result in late effects such as secondary neoplasms. The use of multiple chemotherapeutic agents during induction and consolidation can result in neutropenia. Bacterial and fungal infections during this period are an important cause of treatment related mortality. In addition, individual therapeutic agents have specific side effects with may cause complications and limit the use of these drugs. CNS complications of cranial and craniospinal irradiation have reduced in the past few decades due to the reduction in the use of radiation. However, current CNS directed therapies are not without complications either. Children on methotrexate suffer signs of meningeal irritation such as seizures and irritability which have a debilitating effect on the quality of life. CNS infections due to myelosuppression require aggressive treatment and prophylaxis.

The long treatment duration in ALL has resulted in appearance of many delayed adverse events. Long term survivors of ALL continue to present with secondary tumours (Pui et al., 2003). While the majority of these were treated with irradiation, the long-term effects of systemic and intra-thecal chemotherapy are not known yet. The combined effects of chemotherapy and radiation can affect the developing brain – young children especially girls are particularly susceptible to these. While most children treated on contemporary protocols have IQ scores within the normal range (Halsey et al., 2011) some children show significant reduction in the IQ scores (15 points or more) irrespective of the treatment modality (Mulhern et al., 1991).

1.5 Current clinical challenges

Much of the recent improvement in the outcome of childhood ALL has been a result of more intensive therapeutic protocols. Several challenges remain: our understanding of the etiological factors that cause leukaemia are limited. How gene polymorphisms affect the development of leukaemia and response to therapy remains to be investigated. Treatment related toxicities remain a major cause of mortality in ALL patients (Hunger et al., 2012). Risk based treatment assignment has resulted in higher survival; however considerable overlap exists. For instance, standard risk patients and those with a good initial MRD response may ultimately relapse. Earlier trials with low intensity chemotherapeutic protocols resulted in nearly 50% cure rates (Eden et al., 1991). Subsequent trials have progressively escalated dose intensities to cure another 35-40% patients while theoretically over treating patients who would have been cured with much less intense treatment. Recent

trends towards use of less intensive regimen for good risk patients have shown promise (Vora et al., 2013), however, these measures will only be successful after careful assessment of the risk factors. Patients at a high risk of drug toxicity (e.g. thiopurine S-methyltransferase (TPMT) deficiency) can benefit from such dose reduction approaches. Finally, the role of the pre-leukaemic stem cells is not well understood. Whether such cancer stem cells exist in all subtypes of ALL, they must be targeted to achieve complete cure.

With the declining rate of relapse cases over the past few decades, it is becoming difficult to test new treatment modalities. These would require patients in large numbers and long follow up times to prove the superiority of one treatment over the other. In order to test experimental treatments, it has been suggested to use MRD to quantify the differences in the treatment efficacy. However, bone marrow MRD levels do not predict the risk of extramedullary relapse as accurately as bone marrow relapse. Not only are end-induction MRD levels of patients with and without CNS disease (CNS-3 and CNS-1) are similar (Levinsen et al., 2014) but also that CNS relapses are seen in both MRD-low and MRD-high categories with similar frequencies (Bowman et al., 2011).

Effective clearance of CNS disease is another major challenge to be addressed if universal cure of ALL is to be aimed. Currently, all the patients receive some form of CNS-directed chemotherapy. In addition, high risk and relapsed patients receive radiation therapy. Nonetheless, significant numbers of patients in CNS-low risk group suffer from relapse in the CNS. Little is known regarding the biological mechanisms underlying the CNS relapse. Whether blasts in the CNS at the time of relapse are remnants of the initial seeding from the diagnosis or represent secondary involvement following bone marrow relapse is not known. If CNS relapse is a result of secondary infiltration of leukaemic cells, then investigating the mechanisms underlying the dissemination of leukaemic cells from the site of origin to extramedullary organs will aid in developing therapeutic modalities to prevent this spread. If CNS relapse is a result of expansion of CNS-residual blasts, then it would be important to investigate the factors that allow leukaemic cells escape the initial therapy.

1.6 Extramedullary dissemination in ALL – cell entry

It is conceivable that the first leukaemic population reside in a distinct bone marrow site and subsequently disseminate to other medullary and extramedullary sites through blood circulation. This is a crucial step in leukaemic progression, although little is known regarding the biology of leukaemic cells that enable them to enter such sites. Entry of

circulating leukaemic cells into extramedullary organs may result from a number of biological processes. Leukaemic cells may enter the extravascular tissue using an invasive mechanism as seen in many solid tumours. Alternately, leukaemic dissemination may be a result of a more specific trafficking process mimicking normal leukocyte transport. And finally this may be a random event dependent on the total leukaemic burden and/or number of blasts in circulation. It is also possible that these processes may co-exist. These hypotheses are presented in Figure 1-6. This thesis focusses more on the role of normal leukocyte trafficking mechanisms and how these may go wrong in leukaemic dissemination.

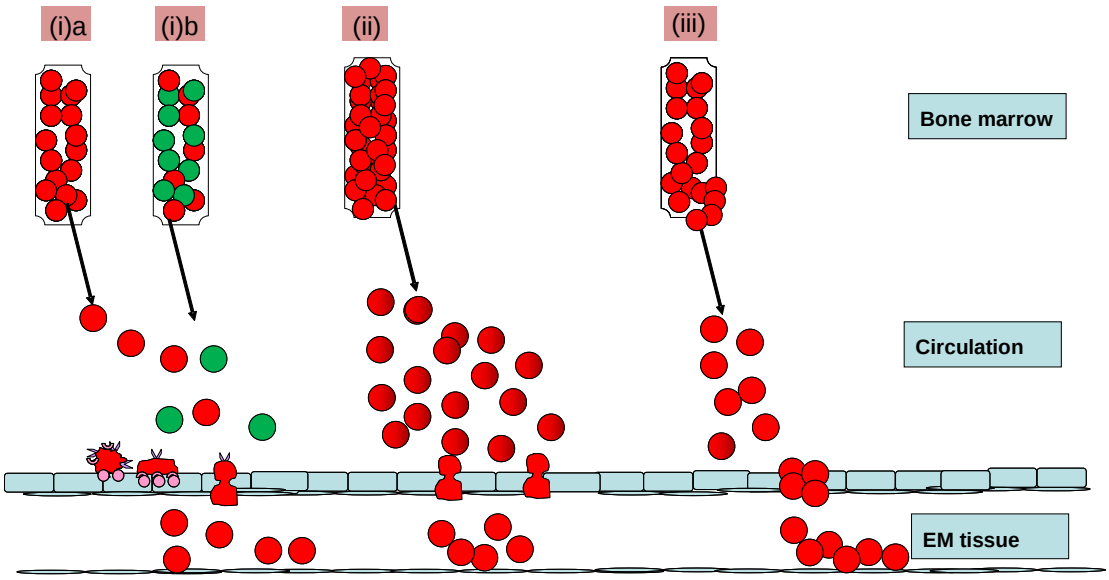

Figure 1-6 Possible mechanisms of leukaemic entry into extramedullary tissues.
Leukaemic entry into extramedullary tissue (i) utilizing normal physiological trafficking mechanism. This property may reside in (ia) all the cells or (ib) within a smaller subclonal population, (ii) random entry due to high tumour burden/over spill, (iii) leukaemic entry as an invasive process.

1.6.1 Physiological leukocyte trafficking

The immune system has the capability to rapidly act against an injury. This capability relies upon trafficking specific subsets of leukocytes to specific tissue sites in a precisely controlled manner. This precision is orchestrated by expression of a combination of leukocyte trafficking molecules (selectins, adhesion molecules and chemokine receptors) expressed in leukocytes. This combination or a molecular ‘post-code’ ensures that the right population of leukocytes home to the tissues exactly where intended, both during homeostasis and inflammation (Ley et al., 2007, Luster et al., 2005). The processes involved in entry of circulating leukocytes into a tissue site have been well described and

consist of various distinct steps. These are briefly described below. The leukocyte trafficking molecules will be discussed in more details in the subsequent sections.

The first step in leukocyte homing to the target tissues is extravasation through the blood vessels. Several stages have been identified and each requires specific sets of trafficking molecules. These steps are described as leukocyte rolling, activation and arrest, adhesion strengthening, intravascular crawling, paracellular and trancellular transmigration, and migration through the basement membrane (Figure 1-7) (Ley et al., 2007).

The first step in leukocyte extravasation is Leukocyte rolling. This involves transient contact of leukocytes with the vascular endothelium resulting in slowing down of leukocytes. Leukocyte rolling is mediated by interaction of selectin molecules (L-selection, E-selectin and P-selectin) on the vascular endothelium with their ligand P- selectin glycoprotein ligand-1 (PSGL1) on the leukocytes. Leukocytes can also interact with each other through these molecules during rolling (McEver and Cummings, 1997, Ley et al., 2007). In addition to the role of selectin molecules, others such as integrins may play an assistive role (Alon et al., 1995). For instance, the integrin (very late antigen-4 (VLA4)) is shown to support lymphocyte rolling on venules of the CNS in conjunction with P-selectin or alone (Kerfoot and Kubes, 2002).

The next steps in this cascade are leukocyte activation and arrest. Slow rolling leukocytes come in contact with chemokines on the vascular endothelial surface. Components of extracellular matrix such as glycosaminoglycans (GAGs) immobilize the chemokines on endothelial surface, thus preventing dilution by blood flow. Chemokine receptor-ligand pairing initiates a cascade of intracellular signalling pathways, and results in ‘activation’ of leukocytes. As a consequence, integrins on leukocyte surface change from low- to high affinity conformation, exposing their ligand binding sites. These high affinity integrins readily bind endothelial adhesion molecules such as ICAM1 (intracellular adhesion molecule 1) and VCAM1 (vascular cell adhesion molecule 1) forming firm adhesions. Consequently, the leukocytes come to a state of ‘arrest’(Shulman et al., 2009). This signalling cascade is called ‘inside-out’ signalling where G-protein coupled receptor (GPCR)-mediated signalling leads to activation of surface integrins, modifying integrins from a low affinity to high affinity conformations (Ley et al., 2007) (Also see section 1.6.1.3). Following leukocyte arrest, adhesion is further strengthened by ‘outside-in’ signalling initiated by integrin activation. The necessary specificity required for leukocyte entry to specific tissues is regulated by the chemokine receptor-ligand pairing. If the leukocytes lack chemokine receptors specific for the endothelial chemokines, activation

and extravasation will not take place and the temporary interactions during rolling will break and the leukocyte would resume circulation.

Just prior to crossing the endothelium, the activated leukocytes seek a preferred transmigration point in a ‘crawling’ movement. This crawling is made possible by cytoskeletal rearrangement. Leukocyte transmigration or diapedesis begins with the extension of membrane protrusions into the endothelial cells. The endothelial cells trigger cytoplasmic signalling leading to formation of channels through which leukocytes can migrate (Greenwood et al., 1995). After passing through the endothelial lining, the emigrating leukocytes encounter the basement membrane and in most venules, the pericytes. Transmigrating leukocytes utilize matrix metalloproteinase enzymes to degrade and pass through the basement membrane (Leppert et al., 1995).

Following transmigration, leukocytes migrate towards the target tissue. It is hypothesised that matrix-fixed chemokines form a physiological gradient which guides the leukocytes towards the target tissues (Ley et al., 2007, Ebert et al., 2005). Thus, the coordinated cascade of events, tightly controlled by chemokines, results in directed migration of leukocytes from the circulation to the target tissues.

The individual types of these trafficking molecules are discussed in subsequent sections.

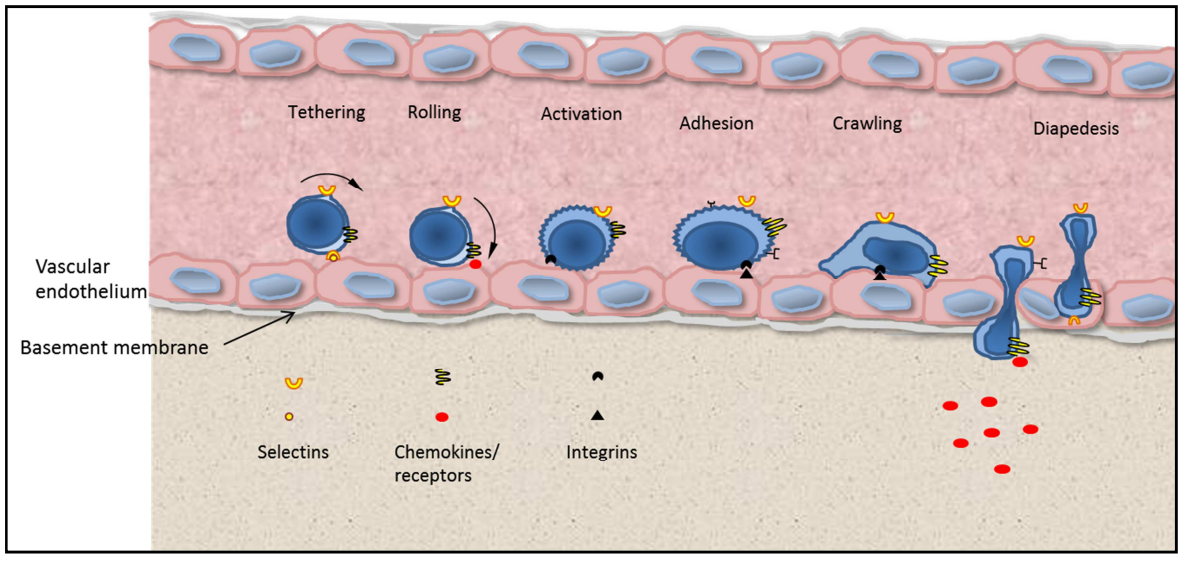

Figure 1-7 Leukocyte migration across the endothelium into the tissue
Circulating leukocytes come in contact with selectins and roll along the vascular endothelium. The leukocyte surface-expressed chemokine receptors interact with immobilized chemokines on endothelial surface. The chemokine receptor-ligand interactions lead to ‘activation’ manifested by conformational change in integrin molecules. The now-high affinity integrins bond with cognate molecules on endothelium, leading to firm adhesion and leukocyte arrest. At this stage the cytoskeletal machinery is active for cellular locomotion. Subsequently, leukocytes crawl with the aim to identify an optimal exit-point and extravasate across the endothelial barrier. Leukocytes then cross the basement membrane and migrate towards a gradient formed by immobilized chemokines. Drawn with information from Ley et al. (2007).

1.6.1.1 Selectins

Selectins are a family of closely related calcium-dependent glycoprotein cell adhesion molecules which bind to carbohydrate moieties on target cells. The selectin family comprises of S- selectin, E- selectin and P-selectin. Selectins are anchored in the membrane by a transmembrane domain and contain a cytoplasmic tail (Patel et al., 2002). P-selectin, the most widely expressed member of the family is present in platelets and endothelial cells in intracellular vesicles. Upon stimulation by appropriate factors, the vesicles quickly fuse with the plasma membrane expressing the P-selectin on the surface. For this reason, P-selectin is the first to respond during leukocyte recruitment for an inflammatory response. E-selectin, is present on the endothelium and its expression can be induced upon inflammatory stimuli. L-selectin is constitutively expressed on the surface of most leukocytes and their precursors in the bone marrow (Patel et al., 2002). Generally, selectins bind to various classes of molecules (e.g mucins, GAGs) but P-selectin glycoprotein ligand (PSGL1) is the most extensively characterized selectin ligand for its role in leukocyte recruitment (Ley, 2003). This is a mucin-like ligand for selectins and is expressed on myeloid, lymphoid and dendritic cells (Laszik et al., 1996).

As mentioned, selectins play an important role in leukocyte recruitment during homeostasis and inflammation. For instance, L-selectin deficient mice display deficient leukocyte-endothelium adhesion and poor recruitment to the lymph nodes (LNs). In addition, these knockouts demonstrate impaired leukocyte recruitment during inflammation (Tedder et al., 1995, Arbones et al., 1994). In addition to their role in physiological processes, selectins and their ligands have also been implicated in pathological states such as cancer metastasis. L-selectin may be cleaved from the cell surface of normal and leukemic cells and levels can be detected in plasma (Spertini et al., 1991). Levels of secreted L-selectin (sL-selectin) reflects leukocyte turnover (Zetterberg and Richter, 1993), and is a candidate biomarker of leukaemic burden and aggressiveness. For example, high sL-selectin levels are associated with poor prognostic subtypes of AML (Extermann et al., 1998) and ALL (Herold et al., 2002, Spertini et al., 1994). This association with poor prognosis can be a reflection of higher tumour burden (Zetterberg and Richter, 1993), or an independent risk factor for it is shown to inhibit ALL cell adhesion *in vitro* (Spertini et al., 1994) thus suggesting it may promote extramedullary dissemination.

1.6.1.2 Chemokines and chemokine receptors

The chemokine family comprises of more than 50 small (6-10 KDa) structurally related proteins. Based on the structural criteria, chemokines are classified into 4 sub-categories, i.e CC, CXC, XC and CX_3C chemokines (Charo and Ransohoff, 2006). CC chemokines are the largest subfamily of chemokines with 28 members (CCL1-CCL28), while CXC sub-family comprises of 17 members. XC and CX_3C sub-families have one member each (Table 1-2). Chemokines play a variety of functions; however their most established role is in the directed migration of leukocytes during homeostasis and inflammation. Chemokines involved in basal leukocyte trafficking are constitutively expressed and are classified as homeostatic chemokines while chemokines which are induced upon inflammatory stimuli are referred to as inflammatory cytokines (Zlotnik and Yoshie, 2000).

Chemokines exert their biological function by binding to chemokine receptors. Chemokines receptors form a family of 7-transmembrane spanning G-protein couple receptors (GPCRs). CC chemokine receptors form the biggest sub-family of chemokine receptors comprising of 10 members (CCR1-CCR10), while CXC family comprises of 6 members (CXCR1-6). XCR1 is the only receptor for XCL1 and CX3CR1 for CX3CL1 (Table 1-2). Chemokine receptor-ligand interaction leads to activation of G-proteins which modulate the second messenger systems and further downstream signalling cascades. The downstream signalling pathways differ depending on the chemokine, the receptors and the cell type. The receptor-ligand pairing rapidly activates receptor internalization/endocytosis machinery whereby the receptor-ligand complex is ‘pinched-off’ from the surface and processed into an endosomal vesicle terminating the downstream signals. The internalized chemokine receptor may be transported for lysosomal degradation or recycled back to the surface (Neel et al., 2005).

In addition to the classical chemokine receptors, a recent addition to the chemokine receptor family is the ‘Atypical chemokine receptor (ACKR) sub-family. These receptors are characterized by alteration in their conserved motif (Figure 1-8), lack of GPCR mediated downstream signalling and a resultant lack of chemokine driven chemotactic response. (Bachelerie et al., 2014b). ACKRs are generally considered to be ‘decoy’ or ‘scavenger’ receptors with the ability to bind and internalize the chemokines without inducing chemokine driven motility (Graham et al., 2012). The chemokine receptors and ligands more relevant to this thesis (CXCL12 and its receptors CXCR4 and CXCR7) are briefly described below.

Receptor	Ligands
CXC receptors	
CXCR1	CXCL5, 6, 8
CXCR2	CXCL1, 2, 3, 5, 6, 7, 8
CXCR3A	CXCL9, 10, 11
CXCR3B	CXCL9, 10, 11, 4
CXCR4	CXCL12
CXCR5	CXCL13
CXCR6	CXCL13
CC receptors	
CCR1	CCL3,4, 5, 7, 13, 14, 15, 16, 23
CCR2	CCL2, 5, 7, 8, 13, 16
CCR3	CCL4, 5, 7, 11, 13, 15, 24, 26, 28
CCR4	CCL17, 22
CCR5	CCL3, 4, 5, 7, 14, 16
CCR6	CCL20
CCR7	CCL19, CCL21
CCR8	CCL1, 18
CCR9	CCL25
CCR10	CCL27, 28
XC receptor	
XCR1	XCL1, XCL2
CX3C receptor	
CX3CR1	CX3CL1
ACK receptors	
ACKR1	CXCL5, 6, 8, 11, 2, 5, 7, 11, 13, 14, 17
ACKR2	CCL8, 2, 3, 4, 5, 7, 8, 11, 13, 14, 17, 22
ACKR3/CXCR7	CXCL11, 12
ACKR4	CCL19, 21, 25
CCRL2/ACKR5	CCL19

Table 1-2 Chemokine receptor nomenclature
Members of the chemokine receptor sub-families including ACKRs and their respective ligands. Drawn with information from Bachelerie et al. (2014a).

1.6.1.2.1 CXCR4-CXCL12 axis

CXCL12 and its receptor CXCR4 are perhaps the most widely characterized chemokine receptor-ligand pair. CXCL12 is a constitutively expressed homeostatic chemokine and is expressed in various tissues of the body during foetal and post-natal life such as the bone marrow, liver, spleen, lymph nodes, lungs and brain. CXCL12 binds to endothelial- and interstitial GAGs to form functional gradients. CXCR4, a typical 7-transmembrane GPCR binds to its only chemokine ligand CXCL12. Ligand binding initiates a downstream signalling cascade which results in a multitude of effects. CXCR4/CXCL12 deficiency in mice results in perinatal death along with severely deranged haematopoiesis and organogenesis (Nagasawa et al., 1996, Zou et al., 1998). In humans, WHIM (Warts, Hypogammaglobulinemia, Infections, and Myelokathexis) syndrome, a genetic disorder caused by a mutated CXCR4, results in enhanced response to CXCL12 and retention of mature leukocytes in the bone marrow and other immune organs. As a result, patients with WHIM syndrome are immunodeficient and susceptible to infections (McDermott et al., 2014). CXCR4 is also a co-receptor for HIV-1 protein gp120 (Feng et al., 1996). Not only

is CXCL12 important in homing and retention of HSPCs but it is also suggested to play a role in proliferation and survival of these cells. For example, CXCR4-CXCL12 axis was shown to directly enhance the survival of myeloid progenitors *in vitro* (Broxmeyer et al., 2003). These critical functions of CXCR4-CXCL12 have led to the development of CXCR4 inhibitor AMD3100 (Plerixafor). AMD3100 irreversibly blocks CXCR4 and inhibits HIV entry, promotes stem cell mobilization for bone marrow transplant and is being tested in WHIM syndrome (Bachelerie et al., 2014a, McDermott et al., 2014). Clinical deficiency of CXCR4 has not been reported in humans.

1.6.1.2.2 CXCR7

Until recently, CXCR4 was the only known receptor for CXCL12. In 2005, Balabanian et al. demonstrated that the orphan receptor RDC-1 had an affinity for CXCL12 (Balabanian et al., 2005). A year later RDC1 was recognised as a member of CXC chemokine receptor family, and named CXCR7. CXCR7 binds to CXCL11 and CXCL12, but unlike typical chemokine receptors, CXCR7 activation does not cause classic chemokine receptor responses such as calcium flux or chemotaxis, but offered some growth and survival advantage and increased adhesion properties (Burns et al., 2006). Since then, CXCR7 has been extensively studied for its expression patterns and role in homeostasis, inflammation and malignancy. CXCR7 has an altered composition in the cysteine motif and therefore classified as an atypical chemokine receptor. In the recent nomenclature CXCR7 has been renamed as ACKR3 (Bachelerie et al., 2014a). However, in this thesis, the alias CXCR7 will be used. CXCR7 is shown to be present on embryonic, juvenile and adult tissue including the haematopoietic cells, endothelial cells and cancerous tissue (Maksym et al., 2009, Sanchez-Martin et al., 2013, Berahovich et al., 2010, Humpert et al., 2012, Wang et al., 2012, Infantino et al., 2006). The discovery of CXCR7 has important implications: (i) CXCR7 binds CXCL12 with a 10 fold higher affinity than CXCR4 (Sanchez-Martin et al., 2013), (ii) the widely used CXCR4 inhibitor AMD3100 is a partial agonist for the CXCR7 receptor (Kalatskaya et al., 2009), (iii) published literature on CXCR4-CXCL12 interaction before 2005 does not take into account CXCR7.

The exact mechanism of CXCR7 function is still under debate. The generally accepted role of CXCR7 is of a CXCL12-scavenging receptor. CXCL12 binding leads to receptor internalization mediated by β-arrestin. The internalized CXCL12 is degraded and the CXCR7 recycled back to the surface. Evidence from Zebra fish embryos demonstrate that CXCL12 scavenging by CXCR7 helps form a CXCL12 gradient for the migration of lateral primordial line (Boldajipour et al., 2008). Inhibition of CXCR7 using a small

molecule inhibitor results in an increase in abluminal CXCL12 (Sanchez-Martin et al., 2013, Cruz-Orengo et al., 2011). In addition, other roles of CXCR7 have been reported by some. CXCR7 has been shown to dimerize with CXCR4 (Hartmann et al., 2008), and alter CXCR4-CXCL12 mediated responses (Levoye et al., 2009). CXCR7 is also reported to function as a G-protein independent signalling receptor activating alternate signalling pathways such as MAP kinases (Rajagopal et al., 2010) and Akt (Zhang et al., 2014). Another report suggests CXCR7 signals through its ligand CXCL11 (Tarnowski et al., 2010).

A number of phenomena make the field of chemokine biology complex and difficult to study. For instance, the majority of chemokines bind to several receptors, while many chemokine receptors can bind to multiple ligands (promiscuity) (Table 1-2). A single receptor type can identify various ligands and activate distinct signalling pathways (Murphy et al., 2000, Zweemer et al., 2014). Moreover, chemokine receptors may form homo- or heterodimers, altering receptor response to ligand binding (Levoye et al., 2009). And thirdly, atypical chemokine receptors may scavenge chemokine ligands affecting the levels of available chemokine (Naumann et al., 2010). These phenomena allow the chemokine system to finely regulate leukocyte migratory responses and provide redundancy in the immune system.

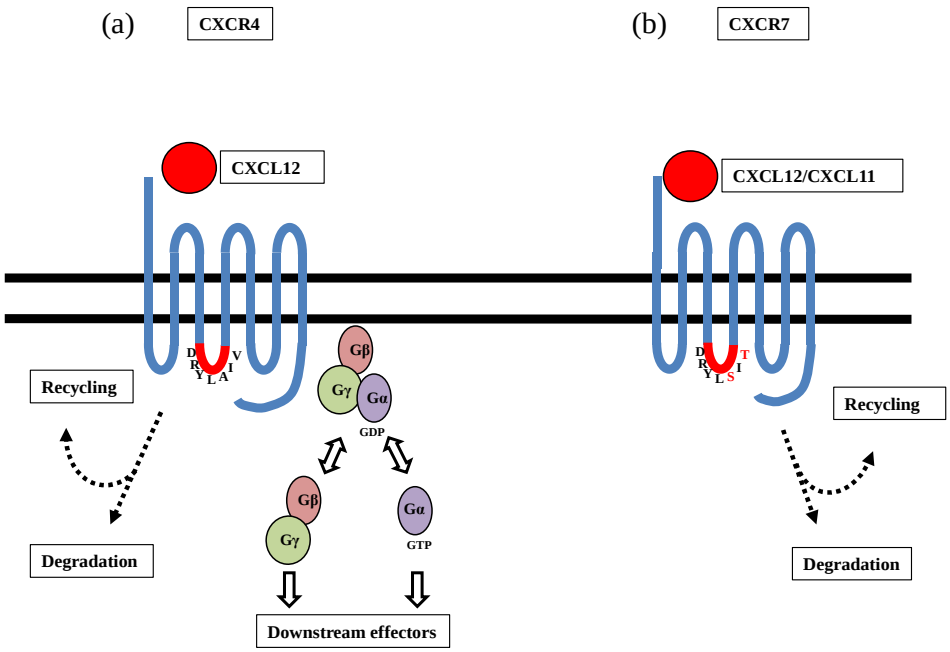

Figure 1-8: Illustration of a typical and an atypical chemokine receptor
(a) CXCR4 has a 7-transmembrane spanning receptor structure which, upon ligand binding,activates the trimeric G-proteins in the vicinity. The GDP associated with the G-protein is replaced by GTP. The sub-units of G-proteins split and initiate signalling. The receptor-ligand complex is internalized and either degraded or the receptor is recycled back to surface. (b) CXCR7 on the other hand has an altered amino acid sequence in the conserved motif (indicated in red). Ligand binding to the receptor does not initiate G-protein response. Ligand binding to CXCR7 initiates internalization. Drawn with information from Bachelerie et al. (2014b), Bachelerie et al. (2014a), Graham et al. (2012), and Comerford and McColl (2011).

1.6.1.3 Integrins

Integrins are members of a family of transmembrane cell-cell and cell-matrix adhesion proteins. Each integrin molecule comprises of heterodimers of different α- and β subunits and this combination forms the basis for their nomenclature (Hynes, 2002). Each subunit of integrin heterodimer contains an extracellular domain, a single spanning transmembrane domain and a cytoplasmic tail. The extracellular domain binds to extracellular matrix proteins (collagens, fibronectin and laminin etc.) or cell surface adhesion proteins (e.g. Intracellular adhesion molecule-1 (ICAM-1)) whereas the intracellular tail binds to intracellular anchor proteins (Hynes, 2002).

In circulating leukocytes, integrin molecules are in a basally inactive state. Chemokine receptor mediated activation signals from within the cell induce activation leading to conformational change in integrin molecules exposing their ligand binding sites. This type of activation signalling is called ‘inside-out signalling’. These high affinity integrin molecules bind to their ligands resulting in signal transduction in the classical ‘outside-in’ fashion. The outside-in signalling is involved in cytoskeletal changes resulting in a multitude of effects ranging from cellular movement to cell division and apoptosis (Srichai and Zent, 2010).

1.6.2 Leukocyte trafficking molecules in site-specific trafficking

Tissue specific homing is determined by specific expression of trafficking molecules during different stages of development in haematopoietic cells. During early foetal life, liver is the primary site for haematopoiesis, and the haematopoietic stem and progenitor cells (HSPCs) are primarily present in liver tissue. However, in later stages, the bone marrow takes the central role – a phenomenon called the 'haematopoietic switch'. It is now well understood that the HSPCs utilize CXCR4 for homing to the bone marrow. CXCR4 or CXCL12 knockout mice present with severe defects in haematopoiesis in the bone marrow (Nagasawa et al., 1996, Zou et al., 1998).This receptor-ligand pair continually mediates haematopoiesis after birth by retaining HSPCs in the bone marrow. In the bone marrow microenvironment, factors such as adhesion molecules strengthen the retention of these cells in the bone marrow supportive niche. For instance, blocking of adhesion molecule VLA-4 leads to prolonged mobilization of haematopoietic progenitors (Craddock et al., 1997).

During differentiation and maturation, haematopoietic subset of cells migrate from the bone marrow and home to appropriate tissue sites such as the thymus and lymph nodes. To make this happen, cells bring about changes in their 'molecular postcode' by altering the expression of leukocyte trafficking molecules, especially chemokine receptors. One classic example of this 'chemokine receptor switch' is observed in migration of T- cell progenitors to the thymus. This is orchestrated in a chemokine dependent manner with up-regulation of CCR7 and CCR9. Engraftment studies using $CCR7^{+}CCR9^{+}$ and $CCR7^{-}/CCR9^{-}$ chimeric bone marrow samples in CCR7/CCR9 double-knockout (KO) mice demonstrate the $CCR7^{-}/CCR9^{-}$ progenitors completely fail to engraft into thymus despite adequate engraftment in bone marrow and mobilization into the blood. This illustrates the importance of chemokine receptors as entry signals into thymus (Zlotoff et al., 2010). The role of PSGL1 is evidenced from homing studies performed in mice. PSGL1-knockout cells have a competitive disadvantage in homing to the thymus compared to wild-type cells. Differential chemokine gradients may further refine the positioning of maturing subsets in specific regions in thymus (Kwan and Killeen, 2004). In a similar manner, mature lymphocytes utilize the leukocyte trafficking molecules to home to peripheral organs and perform their routine functions. For instance, homing of T- lymphocyte subpopulations to the skin is mediated by E-selectin dependent rolling and CCR4, CCR10 dependent positioning in the skin (Reiss et al., 2001).

In summary, leukocyte trafficking molecules drive the process of tissue specific homing

during homeostasis and inflammatory conditions. The organising principles that determine the expression pattern of these molecules is not clearly understood. However, there is clear evidence to suggest that these molecules are the prime factors for entry and retention of leukocytes in tissues.

1.6.3 Leukocyte trafficking into the CNS

The CNS comprises of the brain and the spinal cord (SC), present within the cranial cavity and vertebral column, respectively. The CNS is protected by layers of fibro-collagenous tissue collectively called the meninges. Dura mater is the thicker outer most layer that lines the inside of the skull bones and consists of fibro-collagenous connective tissue and large blood vessels. The arachnoid and pia mater are thinner finer layers and are collectively called the leptomeninges. The pia mater is the innermost layer and lines the brain. The irregular space between the dura and pia is the cerebrospinal space. This CSF filled space is criss-crossed by a dense stroma and contains cerebral and spinal arteries (Ransohoff and Engelhardt, 2012).

Under normal homeostasis, the CNS is protected from a variety of cell populations and molecules that can potentially harm the brain. This property, for which the CNS is considered as immune-specialized site, is characterized by physiological and physical barriers such as: absence of lymphatics, lack of classical antigen-presenting cells (APCs), low expression of antigenic molecules (MHC-I and MHC-II) and the physical barriers between the circulation and the brain parenchyma. Under physiological circumstances, circulating cells do not enter the brain parenchyma, while only a small population of leukocytes is seen in the CSF. Nonetheless, leukocytes are capable of crossing the barriers and entering the CNS in cases of acute injury (e.g meningitis) or chronic insult (multiple sclerosis (MS)) (Ransohoff and Engelhardt, 2012, Romo-Gonzalez et al., 2012). Leukocyte are shown to enter the CNS across a number of routes described below and summarized in Figure 1-9.

1.6.3.1 Blood-brain barrier

The BBB is primarily formed by the brain microvascular endothelial cells (BMVECs) surrounded by basement membrane, pericytes and astrocytic foot processes. The BMVECs maintain the barrier function by the following features: Lack of fenestrations, relatively poor pinocytic ability, and presence of tight junctions. The barrier function is further reinforced by the surrounding basement membrane (Takeshita and Ransohoff, 2012). Moreover, the capillaries are guarded by the astrocytic foot processes, preventing the free

entry of leukocytes and macromolecules into the CNS. Astrocytes almost completely ensheath the brain vessels, separated only by the basement membrane (Hawkins and Davis, 2005). The pericytes cover a minor proportion of the capillaries and post capillary venules. These features almost completely seal the brain from large molecules, and immune cells. In this pathway, the cells are required for transition across the capillary endothelium, the basement membranes on the inner and outer siders of BMVECs to enter the parenchymal perivascular space. To reach the brain parenchyma, leukocytes are further required to cross the Glia Limitans (basement membrane and astrocytic foot processes) (Wilson et al., 2010). During infection, the inflamed endothelium upregulates selectins and adhesion molecules which, in turn, facilitates leukocyte rolling and adhesion (Wilson et al., 2010). In overt brain infections, leukocytes utilize matrix metalloproteinases (MMPs) to disrupt the glia limitans and enter the brain parenchyma (Rosenberg, 2002).

1.6.3.2 Blood-CSF barrier

As the name indicates, the BCSFB is the barrier between peripheral circulation and the CSF compartment. The BCFSB is located in the cerebral ventricles, and is composed of networks of capillaries embedded within a stroma underlying a monolayer of choroid plexus epithelial (CPE) cells. The capillaries of the BCSFB are fenestrated and contain gap junctions. Barrier function is maintained by tight junctions of the choroid plexus epithelium (CPE) cells (Man et al., 2007). The CPE cells generate CSF from the capillaries through diffusion and active transport. The CSF circulates in the CSF space and is re-absorbed through arachnoid villi in the cerebral venous sinuses. Cells migrating through this pathway are required to cross the fenestrated endothelium into the choroid plexus stroma and then cross the CPE to enter the CSF (Ransohoff and Engelhardt, 2012).

1.6.3.3 Virchow-Robin perivascular space

The vessels penetrating the CNS parenchyma are ensheathed by the leptomeninges for some distance giving rise to the Virchow-Robin perivascular space (Figure 1-9). Leukocytes may enter the cerebrospinal space while passing through the post capillary venules at the pial surface into Virchow-Robin perivascular surface (Man et al., 2007). It has been shown that the antigen presenting cells in this region are derived from circulation suggesting Virchow-Robin spaces are involved in cellular exchange between the circulation and the CNS (Hickey and Kimura, 1988).

Leukocyte populations in the CSF compartment are predominantly T lymphocyte subsets involved in routine immune surveillance. The median CSF leukocyte count in neonates and

young infants is 2-3/µl, however upto 20/µl can be normal (Kestenbaum et al., 2010) while in adults, the normal CSF leukocyte count is 1-3/µl. The majority (90%) of these cells are lymphocytes, mostly CD4+ memory T cells, 5% B-cells and monocytes each while infrequent dendritic cells (DCs) and polymorphonuclear cells are also seen (Kivisakk et al., 2003, Svenningsson et al., 1995, Seehusen et al., 2003). CCR7-CCL19 pair has been implicated in the entry of CCR7 expressing CD4+ central memory T (T_{CM}) cells, (Kivisakk et al., 2003) while CCL19 is constitutively present in the CSF (Krumbholz et al., 2007), Thus implying that constitutively present CCL19 at the BCSFB facilitates CCR7 expressing cells' entry to the CSF compartment.

Leukocyte entry into the CNS has been studied extensively in experimental autoimmune encephalomyelitis (EAE) - a murine model of multiple sclerosis (MS). In this model, inflammation is initiated by myelin-specific T- lymphocytes routinely entering the CNS across the BCSFB where they are activated upon stimulation with myelin antigens. As a consequence, inflammatory signals from these 'pioneer' lymphocytes result in active recruitment of inflammatory cells into the brain parenchyma. The initial T-lymphocyte entry across the BCSFB rolling on the vascular surface is mediated by selectins (Sathiyanadan et al., 2014, Carrithers et al., 2000) following which the CCR6-CCL20 dependent interactions is important for leukocyte activation. In one such study, the T lymphocytes entered through the choroid plexus which expressed CCR6 ligand CCL20. Additionally, CCR6 KO mice were refractory to development of EAE (Reboldi et al., 2009). The activated lymphocytes utilize integrins such as α4β1 (Yednock et al., 1992) and VLA-4 (Carrithers et al., 2000) for adhesion and transmigration. CXCR3-CXCL10 interactions have also been reported in EAE with some conflicting results. For instance, using antibodies against CXCL10 were found to have a protective role of EAE (Fife et al., 2001). In contrast, another study showed that CXCR3 knockout mice were equally susceptible to EAE in comparison with CXCR3 wild-type mice (Liu et al., 2006). It can be conceived that the role for CXCR3 may be redundant if at all.

In summary, leukocyte subtypes transit across different compartments of the CNS during homeostasis and inflammation in an immune-privileged manner. There is some evidence to suggest that chemokine receptors may be important in controlling leukocyte migration to the CNS. The complexity of the CNS circulation and the redundancy leukocyte trafficking molecules present challenges in dissecting out the mechanisms of CNS entry of leukocytes.

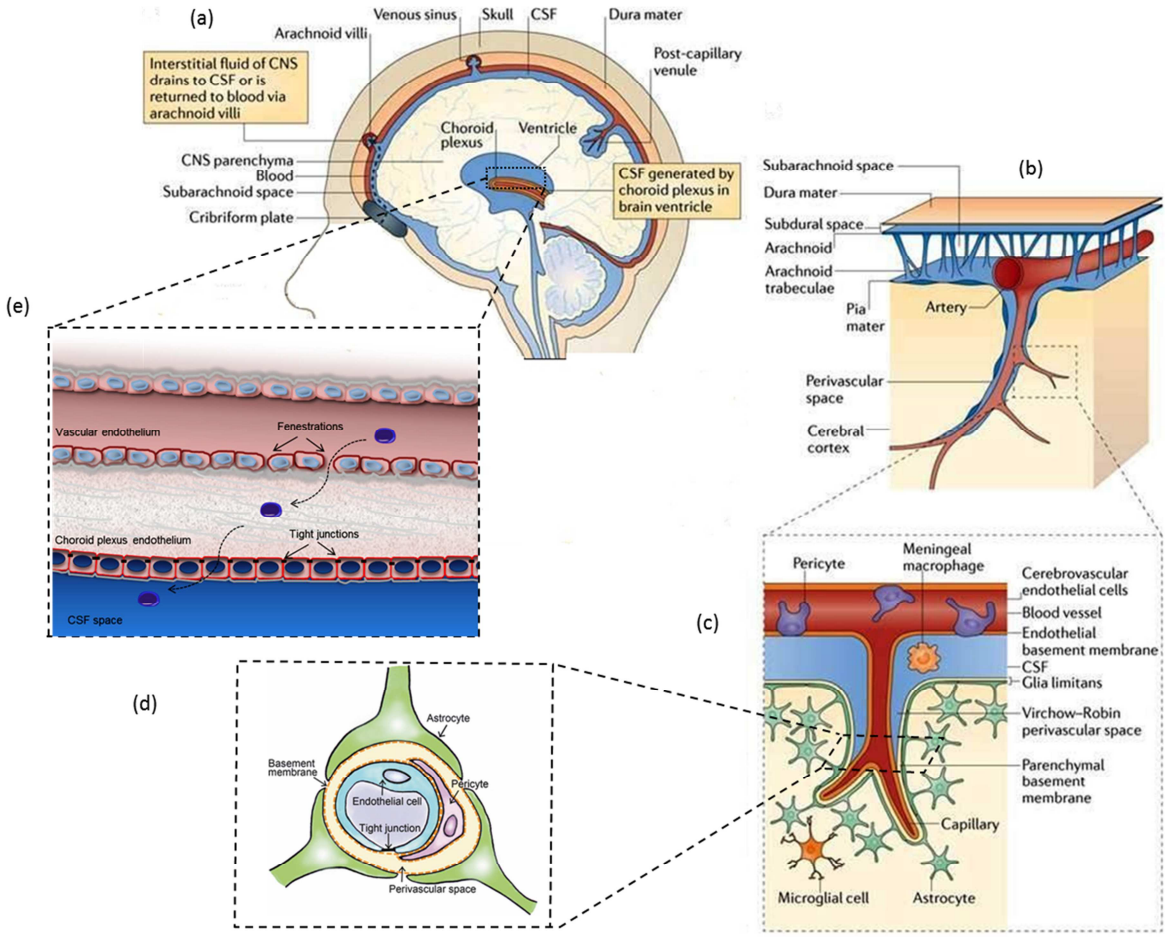

Figure 1-9: Routes of leukocyte entry into the CNS
(a) A human head in the midline sagittal section showing relevant anatomical structures in schematic form. (b) arachnoid granulations in relation to the subarachnoid space and brain parenchyma. (c) Subpial space and Virchow-Robin space. (d) BBB and glia limitans. (e) Choroid plexus structure. Adapted from Ransohoff and Engelhardt (2012), Takeshita and Ransohoff (2012).

1.6.4 Malignant cell trafficking

One defining property of cancers is to form distant metastasis. In fact, at the time of diagnosis, most aggressive cancers are already found to have metastasised to distant tissues. To metastasise to other tissues, cancer cells have to detach from their primary site, enter the circulation, and lodge into another organ suitable for their survival – A process principally similar to tissue specific recruitment of leukocytes. It would not be surprising if the mechanisms governing leukocyte migration and homing would also be involved in malignant cell trafficking. Furthermore, cancer cells appear to have acquired the ability to overexpress chemokine receptors and utilize this for metastasis – They ‘hijack’ the trafficking mechanisms for their advantage (Zlotnik et al., 2011). The following sections discuss the role of chemokine receptor ligand pairing in cancer metastasis relevant to this thesis.

1.6.4.1 CXCL12-CXCR4/CXCR7 axis and site-specific cancer metastasis

CXCL12-CXCR4 interactions are the most widely characterized and perhaps the most important receptor-ligand interactions in cancer metastasis. Overexpression of CXCR4 has been reported in more than 23 cancers (Kakinuma and Hwang, 2006) while its ligand CXCL12 is constitutively present in several tissues including the bone marrow, lymphoid organs and the CNS (Kucia et al., 2004). The initial evidence for CXL12-CXCR4 involvement in cancer metastasis came from studies by Muller and coworkers (2001). The authors screened 7 human breast cancer cell lines for expression of 17 chemokine receptors. Using flow cytometry, CXCR4 was found to be consistently overexpressed in all the cell lines and human breast cancer samples. Furthermore, PCR analysis of the most common sites for breast cancer metastasis (lymph nodes, liver, lung, bone marrow) revealed high mRNA expression of CXCL12. The breast cancer cell lines exhibited avid migration to protein extracts from these tissues in a CXCR4/CXCL12 dependent manner *in vitro.* In addition to this, using a CXCR4 neutralizing antibody showed significant reduction in lung metastasis in xenograft models using breast cancer cell lines in *scid* mice (Muller et al., 2001).

Tumour cells are shown to manipulate the expression of CXCR4 to their advantage. For example, hypoxic stress induces over-expression of CXCR4 via hypoxia-induced factor (HIF) (Schioppa et al., 2003), or human epithelial growth receptor-2 (HER2) in breast cancer (Li et al., 2004). This overexpression of CXCR4 may act in a multitude of ways to promote cancer survival and metastasis. CXCR4-CXCL12 axis may indirectly promote survival by providing cellular attachment to the supportive stromal niches as documented by reduced over-all tumour burden with the use of AMD3100 in xenograft models (Murakami et al., 2002, Muller et al., 2001). Alternately, it may directly promote cell survival (Marchesi et al., 2004). VEGF, a key factor in tumour angiogenesis, is induced by CXCR4 expression in breast cancer cell lines *in vitro,* and reducing vessel formation in xenograft mice treated with CXCR4 antagonist (Liang et al., 2007). CXCR4 is shown to stimulate MMP production which is associated with invasion and metastasis (Singh et al., 2004).

There is growing evidence for the role of CXCR7 in cancer. Not only is CXCR7 expressed in many primary cancer cells and cell lines, it is implicated in multiple cancer types and shown to enhance proliferation and angiogenesis (Wang et al., 2008, Miao et al., 2007), tumour invasion (Burns et al., 2006) and transendothelial migration (Zabel et al., 2011). Despite a lack of typical GPCR signalling response, CXCL12 stimulation results in

activation of alternate signalling pathways such as Akt and β-arrestin (Zhang et al., 2014). Generally, CXCR7 activation has not been shown to be directly chemotactic. However, CXCR7 may indirectly affect tumour metastasis. When co-expressed with CXCR4, CXCR7 enhanced chemotaxis *in vitro* but reduced CXCL12 mediated invasion *in vitro* and *in vivo*. Recently, CXCR7 was shown to be involved in CXCL12 mediated transendothelial migration of Burkitt's lymphoma cell lines. The cell lines exhibited migration in response to CXCL12 which was blocked after using CXCR7 inhibitor CCX771 or CXCL11. The role of CXCR7 in site-specific metastasis is not clear. However, this may be cell-type and context specific.

1.6.5 Chemokine receptors and extramedullary dissemination in ALL

Several lines of investigations suggest that chemokine receptors may be important in dissemination to extramedullary organs. Firstly, chemokine receptor-ligand interaction drives the site specific trafficking of HSPCs, leukaemic cells' presumed normal counterparts. Secondly, there is increasing evidence of chemokine receptor driven site specific metastasis in solid tumours. Thirdly, chemokine receptors are frequently upregulated in acute lymphoblastic leukaemia. And finally, chemokine receptors have shown to interact with aberrant oncogenic pathways in leukaemia (eg. BCR/ABL1). In the following sections, I have presented a review of the current understanding of CXC4 and CXCR7 mediated chemotaxis and their possible roles in ALL dissemination. In addition, the role of BCR-ABL1 signalling in alteration of chemotactic responses is discussed.

1.6.6 CXCR4 in ALL

At the time of ALL diagnosis, most patients present with signs of extramedullary dissemination such as lymph node enlargement or organomegaly. The mechanisms associated with this extramedullary dissemination are poorly understood. It is hypothesised that ALL cells utilize CXCR4-CXCL12 axis to disseminate to extramedullary organs. ALL cells not only also overexpress CXCR4 but also exhibit chemotaxis to CXCL12. Several clinical studies have demonstrated that ALL blasts express CXCR4 (Corcione et al., 2006, Wong and Fulcher, 2004, Wu et al., 2006, Crazzolara et al., 2001, Schneider et al., 2002, van den Berk et al., 2014), and show efficient chemotaxis towards its ligand CXCL12 (Bendall et al., 2005, Corcione et al., 2006). Moreover, higher expression levels of CXCR4 are associated with extramedullary disease and poor prognosis (Schneider et al., 2002, Crazzolara et al., 2001).

Crazzolara et al. (2001) demonstrated that paediatric ALL samples with high levels of CXCR4 expression were associated with extramedullary disease and inferior outcome. Leukaemic cells retrieved from extramedullary organs (thymus, testes and CNS) of ALL patients also exhibited strong expression of CXCR4. Moreover, the leukaemic blasts showed avid transendothelial migration towards CXCL12 *in vitro.* Another study observed that high CXCR4 expression was associated with organ infiltration at diagnosis and a shorter disease free survival. However, an association of CXCR4 with extramedullary relapse could not be confirmed (Schneider et al., 2002). These studies used a relatively small number of patients and insensitive methods to determine extramedullary infiltration. Nevertheless, based on these observations, it is conceivable that circulating blasts may interact with endothelium-presented CXCL12 and extravasate to tissues with high CXCL12 (such as liver, spleen, lymph nodes). Recently, using a murine model of paediatric ALL, it was shown that leukaemic cells engrafted in liver were enriched for CXCR4 expression. The liver retrieved leukaemic cells migrated to CXCL12 *in vitro* and this migration was inhibited with use of AMD3100. Treatment of transplanted mice with AMD3100 resulted in prolonged survival of mice demonstrating the important of CXCR4 in engraftment and survival *in vivo* (Kato et al., 2011). Blocking CXCR4 on ALL cells with antagonists blocks interaction of ALL cells with the bone marrow stromal cells, disturbing the stromal protection of ALL cells from the chemotherapeutic agents making them susceptible to the chemotherapy (Juarez et al., 2003). In addition, CXCR4 expressing ALL can modulate CXCL12 levels in the bone marrow microenvironment and utilize this for extramedullary spread (van den Berk et al., 2014). Taken together, the above data suggest that leukaemic cells expressing functional CXCR4 may migrate and home to sites where CXCL12 is constitutively present.

Cancer cells often acquire aberrant cellular mechanisms for their survival and dissemination. It is plausible that aberrant leukocyte trafficking mechanisms may be seen in leukaemia. These may result from abnormal signalling pathways. For example, in a series using primary ALL samples, Bendall el at. (2005) documented that CXCL12 mediated chemotactic response was mediated through p38-MAPK signalling pathway. Some CXCR4-expressing ALL samples did not exhibit CXCL12 mediated migration. Samples showing CXCL12 mediated chemotaxis exhibited activation of p38-MAPK with CXCL12 stimulation while in samples with poor CXCL12 mediated chemotaxis, this signalling pathway was constitutively activated. Later findings from the same group suggested that the bone marrow homing of leukaemic cells required p38-MAPK signalling pathway (Juarez et al., 2009). It is possible that leukaemic cells acquire aberrant receptor

function at the time of malignant transformation of cells. Compared to normal CD34+ progenitors, CXCL12 stimulation may activate a different set of integrins compared in ALL cells (Spiegel et al., 2004). Leukaemic cells with complex genetic abnormalities have shown aberrant or dysfunctional chemotactic responses. For instance, a subset of human pre-B ALL cell line Sup B15 expressing high levels of 5T4 oncofetal antigen demonstrates high CXCL12 mediated chemotaxis and invasion *in vitro* and ovarian engraftment *in vivo*, despite lower CXCR4 expression than the parent Sup B15 cell line (Castro et al., 2012).

1.6.7 CXCR7 in ALL

As mentioned in the above section, it is clear that CXCR4 signalling and trafficking can be dysregulated in some cases of ALL, it is essential to explore any role CXCR7 may play. So far, few groups have investigated the expression and function of CXCR7 in ALL. A recent study investigated the expression patterns and functions of CXCR7 in leukaemic primary samples and cell lines. CXCR7 gene expression analysis demonstrated CXCR7 expression in myeloid and lymphoid leukaemia cell lines and primary ALL samples. Flow cytometry and western blot analysis for CXCR7 was performed for cell lines only. Differential expression of CXCR7 was observed with T-ALL cell lines (MOLT4 and Jurkat). CXCR7 gene silencing resulted in reduced CXCL12 mediated chemotaxis *in vitro* while no effect on cellular proliferation and apoptosis was documented (Melo et al., 2014). Preliminary reports presented in international meetings show contradicting results with regards to expression patterns and role of CXCR7 in chemotaxis, transendothelial migration and adhesion (Jalili et al., 2008, Sridharan, 2012, Konoplev et al., 2008).

1.6.8 BCR/ABL1 and leukaemic trafficking in ALL

Several studies have demonstrated an association between the extramedullary infiltration in blast crisis with overexpression of $p210^{BCR-ABL1}$, increased activity of $p210^{BCR-ABL1}$ tyrosine kinase and loss of chemotactic response to the chemokine ligand CXCL12. Two different mechanisms have been proposed. First, $p210^{BCR-ABL1}$ tyrosine kinase may affect CXCL12 mediated downstream signalling and adhesion (Ptasznik et al., 2002, Chen et al., 2008), and the second is the downregulaton of CXCR4 surface expression by BCR/ABL1 (Geay et al., 2005). These are briefly discussed here.

Loss of chemotactic response to CXCL12 was initially observed in $p210^{BCR/ABL1}$ transfected myeloid cell lines. Despite surface expression of CXCR4, CXCL12 failed to initiate calcium flux and chemotaxis in transmigration assays. A paradoxical increase in spontaneous motility was seen in these transfected cell lines. This was paralleled by

reduced chemotaxis of $p210^{BCR/ABL1}$ transfected Ba/F3 cell lines *in vivo* (Salgia et al., 1999). There are conflicting explanations to the mechanism underlying this phenomenon. One of these is the cross-talk of the BCR/ABL1 tyrosine kinase and CXCR4 at a common downstream pathway 'Lyn kinase' which is a possible downstream effector for leukaemic cell motility. CXCL12 mediated activation of this tyrosine kinase pathway was seen in peripheral CD34+ precursors and BCR/ABL1 negative cell line HL-60. While BCR/ABL1 transfected HL-60 cells and leukaemic blasts from CML patients, Lyn kinase was constitutively activated and unaffected by CXCL12 stimulation. BCR/ABL1 transfected cell line HL60 showed a 4 fold higher spontaneous motility and lack of CXCL12 directed chemotaxis *in vitro*. BCR/ABL1 inhibition by the tyrosine kinase inhibitor Imatinib (STI-571) restored CXCL12 mediated Lyn kinase activation. However, the authors did not report whether $p210^{BCR-ABL1}$ inhibition restored CXCL12 mediated chemotaxis (Ptasznik et al., 2002). The same group later demonstrated that $p210^{BCR-ABL1}$ transfected human megakaryoblastic cell line Mo7e, exhibited higher affinity to adhesion molecules ICAM-1 – typically associated with chemokine receptor activation. It was postulated that $p210^{BCR-ABL1}$ tyrosine kinase 'hijacks' the CXCL12 mediated integrin activation and resulting adhesiveness which may be responsible for retention of cells in the extramedullary organs (Chen et al., 2008). This hypothesis however does not explain the high spontaneous motility, or increase in circulating blasts in CML. Other groups investigating CXCR4 function in CML have reported somewhat conflicting observations. For instance, in an article megakaryoblastic cell line Mo7e was transfected with BCR/ABL1. Subsequently, two populations of BCR/ABL1-high and BCR/ABL1-low expressing cells were sorted by fluorescence activated cell sorting (FACS). $Mo7e^{BCR/ABL1-low}$ cells demonstrated a signalling defect whereas $Mo7e^{BCR/ABL-high}$ was shown to down-regulate CXCR4 mRNA and surface expression. Treatment of primary CML blasts with Imatinib led to an up-regulation of mRNA and surface expression of CXCR4 (Geay et al., 2005). Overall, these studies consistently show that BCR/ABL1 oncoprotein affects CXCR4 – although the exact underlying mechanism is debated. This raises the question whether similar cross-talk is seen in $p190^{BCR-ABL1}$. P190 oncoprotein differs in molecular behaviour from p210 in a number of ways. P190 tyrosine kinase not only has a significantly higher constitutive activity (Lugo et al., 1990) but also has a different set of downstream effects (Li et al., 1999).

1.6.9 Chemokine receptors and CNS entry

Chemokines are expressed by many cell types in the CNS such as astrocytes, microglial cells, choroid plexus and the neurons (Bajetto et al., 2001). These chemokines may allow entry of specific leukaemic cells. Preliminary evidence regarding a single chemokine receptor-ligand interaction for leukaemic cell entry into the CNS was described in T-ALL. Buonamici et al. (2009) have reported that in a murine model of T-ALL, CCR7-CCL19 interactions are both necessary for CNS infiltration. In this study, the authors used transgenic models of NOTCH-1 activating mutation which develop T-ALL with overt involvement of the CNS. Gene expression profiling of murine haematopoietic progenitors infected with NOTCH-1 carrying retrovirus resulted in up-regulation of CCR7 and efficient chemotaxis towards CCR7 ligands CCL19 and CCL21. Furthermore, T-ALL cell lines and patient samples carrying NOTCH-1 mutations overexpressed CCR7 while treatment with NOTCH-1 inhibitor resulted in reduction in CCR7 expression. This demonstrates the association of NOTCH-1 activating mutations with CCR7 expression. Furthermore, using human T-ALL cell lines (CEM/CCR7^{+}, DND41/CCR7^{-} and CCR7 transduced DND/mCCR7^{+}) transplanted in immunodeficient mice, the authors demonstrate that mice injected with CCR7 expressing cell lines developed aggressive disease with CNS involvement while CCR7 negative line failed to show CNS engraftment – although, the overall leukaemic burden in these mice was also lower. NOTCH-1 transduced in CCR7 knockout mice developed T-ALL but without CNS infiltration, providing further evidence for the role of CCR7 in CNS disease. However, here again CCR7 expressing cells lead to a more aggressive overall disease. Furthermore, CCL19 negative mouse strain was engrafted with NOTCH-1 expressing haematopoietic progenitors. These mice developed aggressive leukaemia but the leukaemic cells failed to infiltrate to the CNS (Buonamici et al., 2009). These findings provide a proof of principle that a single chemokine receptor-ligand pairing can provide access to the leukaemic cells in the CNS compartment. However, little is known about the subsequent mechanisms involved in T-ALL cells after CCR7-CCL19 mediated interactions and no such interactions have been reported in CNS engraftment of BCP-ALL.

Thus, there is some evidence that leukaemic cells may utilize chemokine receptor-ligand interaction for motility and site-specific homing. Nonetheless, little is known regarding leukaemic cell entry into the CNS compartment. Aberrant receptor ligand interactions are frequently seen in leukaemia and to understand site-specific trafficking of leukaemia, a further understanding of molecules interacting with the trafficking pathways is necessary.

1.6.10 CNS entry - alternative mechanisms

Chemokine receptor-ligand interactions may not be the only means by which leukaemic cells gain entry into the CNS compartment. Given the heterogeneity of ALL, it is conceivable that multiple leukaemia subtype-specific factors may be involved in CNS entry of cells. Other possible mechanisms have been proposed. One of these is the leukaemic cellular entry across the BBB or BCSFB through an invasive process. Holland and colleagues have suggested a collective role of invasive proteins, adhesion molecules and cyctoskeletal proteins in ALL cell infiltration to the CNS (Holland et al., 2011). The authors observed that different BCP-ALL cell lines (SD1, Sup B15 and REH) differed in their ability to infiltrate the CNS when transplanted in immunodeficient SCID/beige mice. SD1 cells showed heavy CNS infiltration while Sup B15 caused systemic ALL only without any evidence of CNS infiltration. Histological examination of the murine brains showed presence of leukaemia in the CSF compartment and brain parenchyma. SD1 cells demonstrated *in vitro* invasion which was significantly reduced with inhibition of the enzyme asparaginase endopeptidase (AEP). However, when REH cells were transduced with AEP, the cells showed only a modest increase in invasion suggesting a partial role of AEP in invasion. Ras-related C3 botulinum toxin substrate 2 (Rac-2), a protein related to cytoskeletal organization was overexpressed in SD1 cells. Inhibiting RAC-2 resulted in delayed overall engraftment and CNS infiltration. SD1 cells also had high expression levels of adhesion molecules ICAM-1 and LFA1 (Holland et al., 2011). Together, these findings suggest that many factors play a role in CNS infiltration of leukaemic cell in BCP-ALL cell lines and individual factors may only contribute partially to this phenomenon. Circulating blasts expressing adhesion molecules such as ICAM-1 may adhere to the choroid plexus epithelial cells or brain microvascular endothelial cells. AEP enzyme activity may facilitate invasion across the BBB or BCSFB. RAC-2 may initiate the extravasation of these cells into the CSF space and/or brain parenchyma. However, this postulate fails to address whether AEP mediated invasive process is CNS specific or representative of an overall invasive phenotype.

As discussed under section 1.3.7, CNS relapse may be a result of leukaemic cells gaining entry into the CNS or alternatively, this may be due to expansion of resident blasts once treatment in complete. If the latter is true, then gaining a better understanding of the CNS micro-environmental factors that may protect leukaemic cells from months to years of intensive chemotherapy.

1.7 Extramedullary dissemination in ALL – microenvironmental niche

Leukaemic cells cannot live in isolation in any tissue in the body. The microenvironment of the host tissue must interact with the leukaemic cells and provide a fertile soil that provides shelter to the leukaemic cells and shields them from chemotherapy. This seed-and-soil theory has been extensively studied in leukaemic cell interaction with the bone marrow nice (Sipkins et al., 2005, Burger and Burkle, 2007, Boyerinas et al., 2013). Not only the bone marrow microenvironment provides leukaemic stem cells a place to reside, it also provides essential factors for their growth and proliferation. Moreover, the bone marrow microenvironment interactions with the leukaemic cells provide protections from the chemotherapy (Boyerinas et al., 2013, Iwamoto et al., 2007) and essential signals for mobilization in blood resulting in dissemination (Fukuda et al., 2005). The CNS microenvironment differs from the bone marrow microenvironment in cellular, physical and chemical composition. Yet, the CNS has proven to be a sanctuary site for leukaemic cells. It is necessary to understand the components of the CNS microenvironment and how these interact with leukaemic cells.

1.7.1 CNS stromal support

The CNS differs from conventional leukaemia-host microenvironments in a number of ways. The physical barriers of the CNS compartment may restrict free entry of leukaemic cells into the CNS. In addition, the CNS stromal support network differs from the bone marrow microenvironment. Moreover, CSF is a unique feature which differs from the bone marrow interstitial fluid in physical and chemical properties. Despite these differences, evidence from MS patients shows that B cells can live in the CSF compartment and expand clonally to contribute to the pathogenesis of MS (Owens et al., 2003). However, the mechanisms underlying this protective effect remain poorly understood. This is partly due to the lack of suitable *in vitro* and *in vivo* models to study the effect of CNS niche on ALL (Tenenbaum et al., 2013).

Recently, Akers et al. (2011) provided *in vitro* evidence of interaction of stromal cells of the CNS with leukaemic cells. The authors used BCP-ALL cell lines and CNS stromal cells, namely, normal human astrocytes (NHA), primary human choroid plexus epithelial cells (HCPEpiCs) and human meningeal cells (HMCs) to dissect out critical interactions between the leukaemia cells and the CNS niche. The authors observed that leukaemic cells

migrated towards conditioned media from these three stromal components. Upon using CXCR4 inhibitor AMD3100, there was a significant reduction in migration towards HCPEpic and HMC conditioned media but not with NHA conditioned media. This suggests that while CXCL12 plays an important role in leukaemic cell migration, alternate soluble chemotactic factors may be involved. In co-culture studies, leukaemic cell lines were cultured individually with the stromal components. Leukaemic cells were found to adhere to the cellular layers suggesting physical interactions between the leuakaemic cells and cellular components. Furthermore, ALL cell lines, and primary leukaemic cells from two patients were co-cultured with the stromal components with addition of chemotherapeutic agents. The co-culture provided variable resistance to CNS-directed chemotherapy (Cytosine arabinoside, Dexamethasone and methotrexate) induced death. Additionally, modest protection from chemotherapy-induced death was seen when the cell lines cultured on fixed stromal cell layer, or in conditioned media alone (Akers et al., 2011). These preliminary findings highlight the impact of the CNS microenvironment on disease. However several questions remain unanswered. This study used a limited number of cell lines and primary samples. The factors that allow initial interaction and subsequent adhesion to the stromal components are not known. Further work is required to ascertain whether these observations are reproduced *in vivo* and in patients. Answer to these questions will be of critical importance in understanding disease kinetics and designing novel therapies.

1.7.2 Chemotherapy penetration in the CNS

Another challenge faced in preventing and treating CNS disease in ALL is the drug delivery to the CNS. BBB restricts the entry of chemotherapeutic agents into the brain, the drugs are distributed in the cellular compartments, bind to proteins or reabsorbed into the systemic circulation making it difficult to achieve a high concentration of drugs in CNS. Furthermore, drug delivery to the meninges might equally affect the susceptibility of cells to therapy. Use of prednisolone is associated with a higher risk of CNS relapse in comparison with Dexamethasone. Rapid clearance of prednisolone from the CSF may limit the duration of leukaemic cell exposure to cytotoxic concentrations of the drug (Balis et al., 1987). Therefore, Dexamethasone is preferred despite the several toxicities associated with its use. Regardless of the type of drug used, attention should be paid to the distributions and clearance of the agent. Direct delivery of the chemotherapy through the intrathecal route or intracerebroventricular route through indwelling catheter achieves high concentration of drugs in the cerebrospinal space. Not only is the volume of the drug

injected important, but also factors such as body position plays a role in distribution of the drug within the cerebrospinal space. Injection of a higher volume (6 ml or more) of the drug achieves better distribution of the drug (Pui, 2006) while removal of equal volume of CSF before administration of the drug may prevent leakage from the injection site (Pui and Howard, 2008). Lying in a prone position after the injection is shown to achieve better distribution within the CSF compartment in an animal model (Blaney et al., 1995).

1.7.3 Immune surveillance

The ability of the host immune system to identify and destroy tumours has been a focus of considerable scientific debate. It is proposed that the host immune system has the ability to identify and destroy cancer cells on the basis of expression of aberrant tumour-specific antigens on cancer cells. Identification of cancer cells by cytotoxic T- and NK cells may allow the body to eliminate the cancer. Conversely, cancer cells can evolve to escape identification by immune surveillance mechanisms and cause overt tumour. This idea of immune surveillance is exploited in graft-leukaemia effect after transplant, donor lymphocyte infusion (DLI), and immune-modulation therapy. Graft versus leukaemia effect is now considered to be a key factor in improved prognosis after allogenic bone marrow transplant. The immunological mismatch between the donor and recipient cells leads to activation of NK- and T cells of the donor to identify and target tumour cells in the bone marrow and extramedullary tissue.

Isolated CNS relapse is seen in some patients following Haematopoeitic stem cell transplant (HSCT) (Oshima et al., 2008). The mechanism underlying the selective involvement of extramedullary site remains unclear. Furthermore, the effect of immune surveillance in the CNS compartment is not extensively studied in ALL. Few clinical studies have described the risk factors for CNS relapse after HSCT. For instance, Patients with CNS-3 disease at diagnosis or relapse are at a higher risk of isolated CNS relapse after HSCT (Thompson et al., 1986, Oshima et al., 2008, Ganem et al., 1989). Consequently, these patients receive CNS prophylaxis (Thompson et al., 1986). Although the beneficial effect of CNS directed therapy after HSCT in such patients is debated (Oshima et al., 2008). The incidence of CNS relapse after allogenic transplant is lower than autologous transplant suggesting a role for the immune surveillance provided by the donor immune system in the CNS (Ganem et al., 1989). Moreover, the risk of CNS relapse in patients with chronic graft-versus-host disease (cGVHD) and HLA mismatch in cord blood transfusion tends to be lower supporting this hypothesis (Oshima et al., 2008).

1.7.4 Host factors – IL-15 and IL-15 receptor

An alternative translational approach to explore the mechanisms governing CNS disease in ALL is to analyse the genetic make-up of leukaemias associated with high risk for CNS disease. Host factors may play an important role in leukaemia development and prognosis. However, such studies merely show association between host genomic make-up and the observed disease and it is necessary to investigate the biological association between such observations. One such gene identified by genome-wide studies, IL-15, is relevant to this thesis and discussed here.

In 1994, two groups simultaneously reported a novel cytokine that shared many physiological characteristics with IL-2 (Grabstein et al., 1994, Burton et al., 1994) and named this as IL-15 (Grabstein et al., 1994). Subsequently, cloning of the IL-15 gene identified two distinct isoforms, formed due to alternative splicing: the long signal peptide (IL-15LSP) and a short signal peptide (IL-15SSP). IL-15SSP has a shorter signal peptide (21 compared to 48 amino acids), but has an additional 119 BP sequence in mRNA, however, both the isoforms produce the same mature protein (114 amino acids). The signalling peptides (LSP and SSP) have a profound role in intracellular trafficking of the protein (Tagaya et al., 1997). IL15-SSP is directed to the cytoplasm and the nucleus whereas IL-15LSP is sorted to Golgi complex for presentation on the cell surface and/or secretion (Gaggero et al., 1999). The IL-15 transcript is abundantly expressed in a variety of tissues and cell types, however, due to strict regulation, protein expression is more restricted on the cells (Onu et al., 1997).

IL-15 signals via a hetero-trimeric receptor complex with a specific high affinity α- subunit (IL-15Rα) (Giri et al., 1995), a shared IL15/IL-2 β-subunit (IL-15Rβ) and a common γ-subunit shared by several other cytokines (IL-15Rγc) (Giri et al., 1994). IL-15Rα confers the specificity to IL-15, (Giri et al., 1995) although IL-15 can also bind directly to IL-2 R$\beta\gamma_c$ complex with lower affinity (Giri et al., 1994). Many cell types express IL-15Rα independently of the IL-15Rβ/γ_c subunits and therefore can potentially be activated by IL-15 stimulation. Notably, IL-15Rα also exists in a soluble form (sIL-15Rα) (Budagian et al., 2004), and together with IL-15 forms biologically active IL-15/sIL-15Rα complex. This complex is suggested to be the main active form of IL-15. This may also explain the difficulties in detection of secreted IL-15 in body fluids. The promiscuity in IL-15 biology allows IL-15/IL-15Rα complex to be *cis*- or *trans*- presented to IL-15R$\beta\gamma_c$ and signal in autocrine, paracrine, juxtacrine and even endocrine fashion (Bulfone-Paus et al., 2006)(Figure 1-10). IL-15 stimulation of the IL-15 receptor complex initiates multiple

downstream signalling pathways including JAK/STAT, PI3K/Akt and MAPK pathways resulting in strong proliferative and anti-apoptotic effects.

Perhaps the most important role for IL-15 is in the development and proliferation of T- (Grabstein et al., 1994) and NK cells (Carson et al., 1997). Therefore, it is not surprising that IL-15 is suggested to potentiate a T- and NK cell mediated anti-tumour effect (Roychowdhury et al., 2004). Ironically, for the same pro-survival and anti-apoptotic effect, IL-15 has increasingly been implicated in the development and progression of many tumours including haematological malignancies. Uncontrolled expression in transgenic mice results in expansion of peripheral blood lymphocytes and ultimately develop T-cell leukaemia. This suggests continuous stimulation by IL-15 may overcome the regulatory checkpoints turning the balance in favour of leukaemogenesis (Fehniger et al., 2001). Malignant cells respond to IL-15 by reduced apoptosis and increased proliferation. For example, exogenous IL-15 results in resistance to apoptosis in primary human NK leukaemia cells and cell lines (Yamasaki et al., 2004), and proliferative advantage in B cell chronic lymphocytic leukaemia (CLL) (Trentin et al., 1996) and adult T cell leukaemia/lymphoma cells (Kukita et al., 2002). Additionally, IL-15 has been shown to mediate leukocyte motility. For example, it has been shown to induce T- cell polarization and distribution of integrin molecules (Nieto et al., 1996). Moreover, exogenous IL-15 is shown to be chemotactic for NK cells and pre-incubation of NK cells resulted in enhanced adhesion with endothelial cells *in vitro* (Allavena et al., 1997).

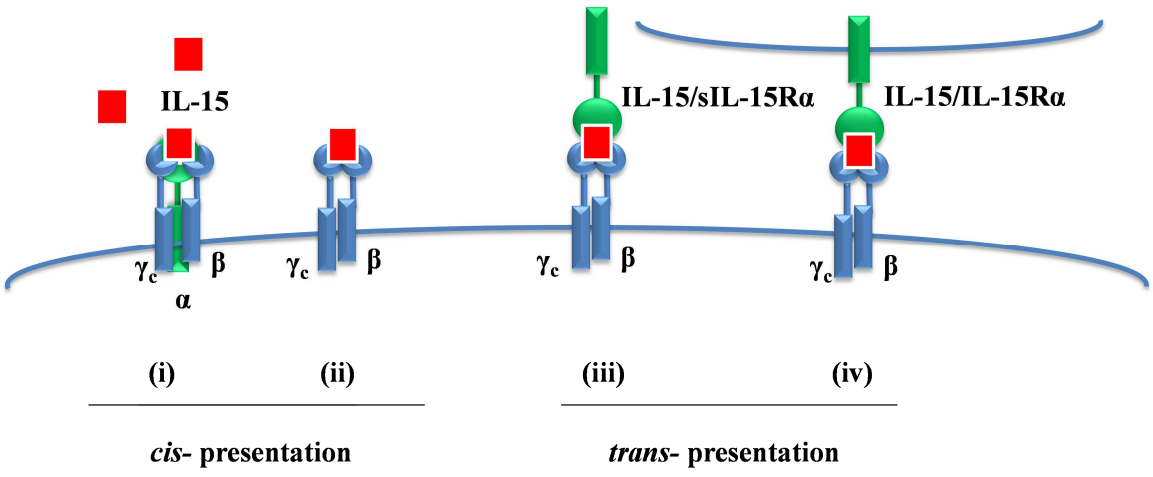

Figure 1-10 Possible modes of IL-15/IL-15 receptor signalling
(i) cis- presentation to the heterotrimeric receptor (ii) trans- presentation of the IL-15/sIL-15Rα complex (iii) trans- presentation of the IL-15/IL-15Rα complex. Drawn with information from Budagian et al. (2006)

Recently, Genome-wide analysis demonstrate single nucleotide polymorphisms SNPs in IL-15 gene associated with a higher risk of leukaemia in adult ALL (Lin et al., 2010) and resistance to therapy in paediatric ALL. It is also suggested that the SNPs in IL-15 gene may be associated with a high expression of IL-15 by leukaemic cells in paediatric ALL (Yang et al., 2009). Clinically, IL-15 expression by leukaemic cells is associated with aggressive disease and extramedullary dissemination. In a series of 87 adult ALL patients, IL-15 expression was found in the majority of patients with a high IL-15 expression associated with T-ALL, mediastinal and nodal infiltration and a poor prognosis. No association was seen with CNS, hepatic or splenic involvement (Wu et al., 2010). In paediatric ALL, using cDNA microarray technology, Cario and co-workers (2007) demonstrated high IL-15 expression was associated with CNS involvement. IL-15 was shown to be significantly overexpressed in patients with CNS-3 disease at diagnosis compared to CNS-1 controls. Despite a high false discovery rate (FDR) of 61% in this technique, this observation was validated by qPCR in an independent group of patients. In CNS-1 patients at diagnosis, a higher IL-15 expression level was significantly associated with a subsequent CNS relapse.

Despite the increasing number of reports describing a link between IL-15 and ALL, questions remain. It is not known whether IL-15 SNPs have a direct role in leukaemia development and dissemination or an indirect role via modulation of anti-tumour immune responses. Further investigation into IL-15 biology may provide crucial insights into the observed associations with ALL in general and CNS disease in particular.

1.8 Study aims

Despite the clinical impact of CNS disease on the outcome of patients, little is known about the true incidence of CNS disease and the mechanisms underlying leukaemic cell migration and survival in the CNS. A number of gaps in the current knowledge regarding the CNS disease exist. The true incidence of CNS disease at diagnosis is a matter of debate. In addition, the mechanisms underlying the entry of leukaemic cells in the CNS compartment and that allow leukaemic cells to survive in the CNS remain to be investigated. It is hypothesised that leukaemic cells utilize a combination of leukocyte trafficking molecules to enter the CNS. If a particular combination or a molecular address code is identified, this information can be used to design and test novel therapies to block the CNS entry of leukaemic cells and prevent CNS relapse. Alternately, leukaemic cells may already be present in the CNS compartment at diagnosis. In this case, mechanisms

which allow leukaemic cells to proliferate in the CNS may be more important.

In order to contribute to the current body of knowledge, the purpose of this thesis is to:

- Develop an *in vivo* murine xenograft model for CNS disease in ALL in order to address specific research questions concerning the leukaemic infiltration of the CNS.

- Develop and test novel biomarkers of CNS disease to identify patients with submicroscopic levels of CNS disease.

The key aims investigated in each chapter are:

Chapter 3 Aim: To Develop and characterise a xenograft model of CNS disease using primary BCP-ALL cells in NSG mice and use this model to describe the frequency and pattern of extramedullary dissemination including an in depth analysis of the CNS infiltration.

Chapter 4 Aim: To utilize *in vivo* techniques to investigate the role of leukocyte trafficking molecules in the leukaemic cell entry into the CNS compartment. Due to the observed CXCR4 dysfunction in a BCP-ALL cell line SD1, an additional aim of this chapter is to characterise the CXCR4-CXCL12 interactions in SD1 cell line.

Chapter 5 Aim: To investigate the reported association between IL-15 and CNS disease using *in vitro* analysis of IL-15 and IL-15 receptors and their impact on cellular proliferation and gene expression in conditions mimicking the CSF.

Chapter 6 Aim: To develop and utilize sensitive assays (qPCR and Luminex) as biomarkers of CNS disease in CSF samples from childhood ALL patients.

The results of these investigations are presented in the following chapters.

2 Materials and methods

2.1 General equipment and reagents

2.1.1 Plastics

All consumable plastic lab-ware were purchased from Starlabs (Milton Keynes, UK) except the following:

Consumable	**Supplier**
Tissue culture plates and flasks	Corning Inc. (Poole, UK)
Microcentrifuge tubes	Eppendorf (Hamburg, Germany)
Falcon conical tubes 15 ml and 50 ml	BD Biosciences (Le pont de Claix, France)
BD Plastipak syringes	BD Biosciences (Le pont de Claix, France)
Polystyrene 5 ml round bottom Flow cytometry tubes	BD Biosciences (Le pont de Claix, France)
96 well round bottom tissue culture plates	Nunc International/Thermoscientific

Table 2-1 Plastic lab-ware used in this thesis

2.1.2 General reagents

The composition of chemical solutions, buffers and reagents that were used in experiments is given in table Table 2-2. Unless otherwise stated, all chemical reagents were purchased from Sigma-Aldrich.

Reagent/solution	Composition
Phosphate buffered saline (PBS)	137 mM NaCl, 2.7 mM KCl, 10 mM Na_2HPO_4, 1.8 mM KH_2PO_4
Tris-buffered saline (TBS)	50 mM Tris-Cl, pH 7.5, 150 mM NaCl
Flow cytometry (FCM) buffer	0.5% Foetal calf serum (FCS), 2.5mM EDTA in PBS
chemotaxis buffer	0.5% Bovine Serum Albumin (BSA) in Rosewell Park Memorial Institute (RPMI) media
Tris-acitate-EDTA (TAE) buffer	40 mM TAE, 1 mM EDTA (pH 8.2 - 8.4)
PBS-Tween buffer	0.5% Tween20 in PBS
TBS-Tween buffer	0.5% Tween20 in TBS
PBS-EDTA buffer (PEB)	2.5mM EDTA in PBS
Citrate buffer	10 mM Citric acid, 0.05% Tween20, pH 6
1% acid alcohol	1% concentrated hydrochloric acid (HCl) in 70% ethanol
Complete media	10% FCS, penicillin (100units/ml), streptomycin (100units/ml), L-Glutamine (2mM) in RPMI.
10% Dulbecco's modified Eagle medium (DMEM)	10% FCS, penicillin (100units/ml), streptomycin (100units/ml), L-Glutamine (2mM) in DMEM (Gibco)
4% Paraformaldehyde (PFA) solution	4% (v/w) PFA in PBS. pH 6.9 with 1N NaOH. Stored at -20C.
Red Blood cell (RBC) lysis buffer	10% (v/v) 10x RBC lysis soln (Miltenye Biotech, Bergisch Gladbach, Germany) in dH2O
Cryopreservation media	90% FCS, 10% Dimethyl Sulphoxide (DMSO)

Table 2-2 Composition of solutions

2.2 Cell culture methods

All procedures involved in cell culture were conducted using sterile conditions in a laminar flow hood with HEPA filtration. All materials such as pipettes, vortices, glassware and pasticware and reagents were sterile. The surfaces and equipment were wiped with 70% ethanol. Unless otherwise stated, all centrifugation steps were performed at 300 g for 5 minutes. All cultures were incubated in a standard tissue culture incubator at 37 ºC with 5% CO_2 and 95% humidity.

2.2.1 Cell lines

SD1 and REH were kind gifts of Professor Vaskar Saha (University of Newcastle). SEM cell line was gifted by Dr Olaf Heidenreich (University of Newcastle). Sup B15 cell line was purchased from DSMZ (German collection of Microorganisms and Cell Cultures). Clinical details of the patients these cell lines and the immunophenotypic features of the cell lines is presented in Table 2-3.

Cell line	Patient age	Sex	Presentation /relapse	Cytogenetics	Immuno-phenotype*	References
SD1	NA	F	Presentation	t(9;22) m-bcr**	CD34+, CD10-, CD19+, Cy79a+	Dhut et al. (1991)
Sup B15	9 years	M	Second relapse	t(9;22) m-bcr	CD10+, sIg -	Naumovski et al. (1988)
REH	15 years	F	Relapse	t(12;21)	CD34+, $CD10^-$, CD19+, Cy79a+	Alkatib et al. (1985)
SEM	5 years	F	Relapse	t(4;11)	CD34-, CD19+	Greil et al. (1994)

Table 2-3 Clinical and immunophenotypic characteristics of the cell lines
** minor breakpoint cluster region

2.2.2 Thawing of cells from frozen stocks

Frozen cell lines stored in liquid nitrogen (-196 ºC) were identified and thawed in water bath at 37 ºC. The cells were washed in 5 ml complete culture media followed by centrifugation. Supernatants were removed and the cells were re-suspended in 5 ml complete media (pre-warmed to 37°C) and transferred to 25 cm^2 flasks for subsequent culture.

2.2.3 Cell counting

Cell counts were performed using Haemocytometer (modified Neubauer chamber). Cells were thoroughly mixed in the suspension and 100 µl of cell suspension was added to 300 µl of Trypan blue. After thorough mixing, 10 µl of this suspension was loaded into the counting chamber. Cells negative for trypan blue were counted in the 4x4 grid. The number of cells counted was multiplied by 1 x 10^4 which represented the counts per ml of the original cell suspension. Viability was measured by dividing number of live cells by total number of cells and multiplied by 100 to get the percentage viability.

2.2.4 Maintenance of cell lines in culture

Cells were grown in complete media (Table 2-2) and passaged as recommended by DSMZ. SD1 cells were cultured in complete media. Cell lines were maintained in 25 ml cell suspension in 75 cm^2 vented tissue culture flasks. Cells were monitored daily using inverted microscope to monitor confluence and general culture conditions. SD1 cells were maintained at a concentration of 0.25-1.2 x 10^6 /ml and were split every third day at a dilution of 1:5 with fresh complete media. Sup B15 cells were maintained in complete media at a concentration of 1-2 x 10^6 /ml and were split at a dilution of 1:5 every third day. REH cells were maintained in complete media at a concentration of 0.5 - 2 x 10^6 /ml and split once every 3 days at a dilution of 1:5 in complete media. SEM cells were maintained in complete media at a concentration of 0.2-2 x10^6 /ml and split 1:4 once every 4 days. Cell lines were grown approximately at a concentration of 1-1.2 x 10^6 /ml just before using in experiments.

2.2.5 Passage of cell lines

SD1, Sup B15 and REH cell lines were thoroughly resuspended using 10 ml pipette and an aliquot of 5 ml was transferred to a 25 ml centrifuge tube. The cells were centrifuged and the supernatant discarded. The cells were resuspended in 25 ml fresh pre-warmed media and transferred to a new 75cm^2 sterile tissue culture flask. For SEM split 1:4, 6 ml of cell suspension was expanded in 24 ml fresh media. Adherent cell lines were grown at a maximum confluence of 80% upon which the cell layers were gently detached using Trypsin or a cell scraper. 10 ml of complete media was added and the cells were thoroughly re-suspended by pipetting. Two ml of the cell suspension was transferred to a new 75cm^2 flask and 13 ml complete media was added on top.

2.2.6 Cryopreservation of cells

Cells were frozen down from the growing cultures at early passage numbers. Cells were supplemented with fresh media one night before freezing down. The cells were counted using haemocytometer with trypan blue dead cell exclusion method. Different cell lines vary in the optimum cell density for freezing as recommended by DSMZ. Cells were resuspended in cryopreservation media (90% FCS, 10%DMSO or for some cell lines 20% FCS, 10% DMSO in 70% RPMI) at the optimum density. For primary cells retrieved from patients or primagraft cells (human leukaemic cells expanded and

retrieved from mice organs), 1 x 10^7 cells were frozen in 1ml of 90% FCS, 10% DMSO solution.

2.3 Patient Methods

2.3.1 Ethics approval

All human research conducted was in accordance the ethical standards of the Helsinki declaration and was approval by West of Scotland research ethics committee (WoSREC reference: 09/SO703/77).

2.3.2 Collection of human CSF

Patients were diagnosed at the Royal Hospital for Sick Children (RHSC or Yorkhill), Glasgow. CSF samples were obtained under anaesthesia using standard lumbar puncture technique. About 1 ml of CSF was withdrawn from children in a sterile tube and sent to the diagnostic lab. About half of the sample was removed for CSF cytology. The remaining sample was transferred to be processed as described below.

2.3.3 Processing of CSF

Samples were transferred to a 1.5 ml eppendorf tube and centrifuged at 1000 g for 10 minutes at 4 ºC. The supernatants were carefully transferred into new 1.5 ml eppendorf tubes in 210 µl aliquots. Tubes were labelled and stored at -80 ºC. DNA extractions were performed from the cell pellet described later in section 2.6.2.

2.3.4 Blood collection

Blood samples were collected in the Schiehallion ward, Yorkhill using heal prick (young children), or cuboital vein or Hickman line (adolescents) by trained phlebotomists using standard techniques. Blood samples were sent to the laboratory where automated full blood counts (FBC) were performed. Leftover blood samples were processed as described under section 2.6.3.

2.4 Animal methods

2.4.1 Mice

NOD.Cg-*PrkdcscidIl2rgtm1Wjl*/SzJ (NSG) mice (Charles River) were maintained at the Central Research Facility, University of Glasgow, in strictly sterile conditions with filtered air and autoclaved food, water and bedding. Mice were used between 6 and 14 weeks of age for all studies. All procedures were carried out in accordance with the United Kingdom Home Office regulations under the authority of the appropriate project licence (number: 60/4092) and personal licence (number: 60/13504).

2.4.2 Intra-femoral injections of primary cells

Primary cells from frozen stocks were thawed and counted. For each injection, between 1 x 10^5- 1 x 10^6 cells were resuspended in 30 µl PBS in 0.5 ml syringe with 29 gauge needle. For intrafemoral injections, the mice were anaesthetised with Isoflurane. Knees were shaved and cleaned with 70% ethanol solution. One of the knees was flexed and the direction of the femur was assessed by palpation with index finger. A 25 gauge needle was inserted at the distal end of the femur just about the knee cap, first puncturing the skin, and then boring through the distal end of the bone. The needle was advanced in the bone marrow cavity in a boring motion. The boring needle was removed and the needle attached to syringe with cells was inserted. Cells were carefully injected and the knee extended. Sterile gauze swab was pressed to prevent any bleeding from skin. Intra-peritoneal carprofen (0.125 mg) was used per mouse as a post-operative analgesia. The mice were monitored until completely recovered and observed for signs of pain or fracture.

2.4.3 Intravenous injections of cell lines

Primary cells from frozen stocks were thawed and between 1 x 105 – 1 x 106 cells/ mouse were used. For cell lines grown in culture, between 1 x 106 – 1 x 107 cells were used. Cells were resuspended in 100 µl PBS and loaded in 0.5 ml syringe with 29 gauge needle. Mice tails were cleaned with ethanol and injections were given through tail veins.

2.4.4 Monitoring of engraftment

Engraftment was assessed by monitoring mice for signs of ill health, weekly weight measurements and quantifying circulating human CD10/CD19 positive cells via tail vein blood sampling (section 2.4.5). Mice were culled following any sign of engraftment (>10% human CD10/CD19 positive cells in tail vein blood sample, signs of ill health, or weight loss of >10% for 3 days or >20% on one occasion). If there were no detectable signs of engraftment, mice were culled 28 weeks post injection

2.4.5 Tail vein blood sampling of xenograft mice

Mice were moved from their cages to a laminar flow cabinet and restrained using a restrainer. Their tails were wiped with 70% ethanol and a small incision given using a blade. Approximately 3-4 drops of blood were collected in a 1.5 ml eppendorf tube containing 30 µl 0.5 mM EDTA to prevent blood coagulation. After collection, mice were transferred back to their cages and blood samples were kept on ice. Red blood cell lysis was performed using RBC lysis solution. Cells were then washed in FCM buffer and stained with human CD10/CD19 antibodies (section 0).

2.4.6 Culling and dissection

All mice were humanely culled with CO_2 asphyxiation. Blood samples were taken from cardiac puncture and anticoagulated using EDTA. Liver, kidneys and gonads were removed, weighed and fixed in 4% paraformaldehyde (PFA) solution. Skulls were isolated after removing skin, facial muscles and bones and fixed in 10% Neutral buffer saline (NBF) (Cell store) unless otherwise specified; in which case brains were removed from the skulls and cells harvested from the brains by vortexing. Spleens were removed, weighed and passed through 40 micron cell strainer to isolate cells. Using a 23-21 gauge needle and a syringe, bone marrow samples were harvested from the femur and tibia by flushing the bones with PBS or, in some cases, by grinding the bones with a mortar and pestle. Spinal cords were removed from the vertebral column by flushing with PBS using a wide gauge needle. The spinal cords were vortexed in PBS in a 50 ml tube at medium speed for 5 minutes. Cells were passed through 40 micron cell strainer.

RBC lysis was performed on cells from blood, spleen, BM and the cells were washed and assessed for quantification and viability. Histology, chemotaxis assays and flow cytometry for chemokine receptor expression assays were performed as described in

the subsequent sections.

2.4.7 *In vitro* imaging of xenografts injected with REH$^{GFP\text{-}Luciferase}$ cells

1 x 10^7 REH$^{GFP\text{-}Luc}$ cells were counted and injected, intravenously, into the tail vein of 4-8 week-old NSG mice. Mice were culled after 4 weeks, and femurs and skulls were removed. Bone marrow was harvested from tibiae using mortar and pestle. Cells from the CNS were isolated by carefully removing the brains from the skull cavity and vortexing the brain in PBS in 50 ml tube at moderate speed for 5 minutes. Cells from bone marrow and the CNS were passed through 40 micron cell strainer and quantified using a haemocytometer and their viability assessed using Trypan blue. Cells from bone marrow/CNS (5 x 10^5) were intravenously injected into 4-8 week-old NSG mice. Bioluminescent-imaging used an IVIS100 system (PerkinElmer, Seer Green, UK). Mice were imaged under 2% isoflurane anesthesia following subcutaneous injection of luciferin (100mg/kg, PerkinElmer). Image-acquisition of whole animals (dorsal and ventral views) used 1-60 seconds exposure at a low binning level. Data analysis used Living Image software v3.1 (PerkinElmer).

2.5 Cell based assays

2.5.1 Flow cytometry

Flow cytometry is a powerful tool to identify a surface or intracellular markers of interest by measuring fluorescence signals from cells. The process involves the preparation of a single cell suspension, labelled with fluorescently-conjugated antibodies. Cells are injected into a complex tubing system that generates a stream of single cells. Each cell passes through an interrogation point where lasers with distinct wavelength shed beams of light. Light scatter and fluorescence emission from fluorochromes are detected by light detectors and provides information about the cell's particular properties. Light scatter and fluorescence are digitally converted to generate Forward Scatter (FSC), Side Scatter (SSC) and fluorescence intensity. A combination of FSC and SSC provides information about the size and granularity of cells while markers of interest are assessed using fluorescence. In this thesis, flow cytometry was used in a number of experiments, each described under appropriate headings.

2.5.2 General equipment, materials and solutions

Cells, labelled with the appropriate fluorescently-conjugated antibodies, were analysed using a MacsQuant™ analyser (Miltenyi). Acquisition parameters for multiparameter flow cytometry were established using unstained cells and cells stained with single fluorochromes. Data were analysed using data analysis software FlowJo (FowJo LLC).

Monoclonal antibodies used were either directly, or indirectly, conjugated with fluorochromes: Fluorescein isothiocynate (FITC), R-phycoerythrin (PE), allophycocyanin (APC), PE conjugated to Cyanine 7 (PE-Cy7). Cell viability dyes used were Draq7, conjugated to APC-Cy7 (Biostatus, shepherd, UK), or Viaprobe (7-AAD)(BD Biosciences). All the antibody concentrations were used according to manufacturers' instructions and were between 1-5 µg/ml. All the dilutions were between 1:10-20. A detailed list of fluorescently labelled antibodies, viability dyes, fluorescently labelled dyes or other materials is given in Table 2-4. Due to the limited variety of available conjugated fluorochromes, and to avoid the overlap of fluorescence emission signals (spectral overlap), it was decided to use PE- and/or APC-conjugated antibodies for CXCR3, CXCR4, CCR6, CCR7, CX3CR1 and PSGL1. Consequently, analysis for each of these molecules was performed individually or a combination of two antibodies (1 PE and 1 APC).

Antibody	Cat.no	concentration	Manufacturer
Anti-Human CCR6-PE	12-6969-42	0.6 µg/ml	eBioscience,
Anti-Human CCR7-APC	17-1979-42	1.25 µg/ml	eBioscience
Anti-Human CD10-FITC	11-0106-42	1.25 µg/ml	eBioscience
Anti-Human CXCR4-APC	17-9999-42	2.5 µg/ml	eBioscience
Anti-Human CD19-PE-Cy7	25-0199-42	2.5 µg/ml	eBioscience
Anti-Human CD45-FITC	11-9459-42	10 µg/ml	eBioscience
Anti-Human CX3CR1-PE	12-6099-41	1.25 µg/ml	eBioscience
Anti-Human CXCR3-PE	121839	2.5 µg/ml	eBioscience
Anti-Human CD184 (CXCR4) Purified	14-9999	2.5-10 µg/ml	eBioscience
Human CXCR7/RDC-1 MAb, Mouse IgG1	MAB42273	2.5-10 µg/ml	R&D systems
Mouse anti human CXCR7/RDC-1-PE	FAB42271P	2.5-10 µg/ml	R&D systems
anti-Human Annexin V-APC	88-8007-72		eBioscience
Secondary antibodies			
Goat Anti-Mouse IgG1, Human ads-TRITC	1070-03	0.3 µg/ml	Southern biotech
Goat Anti-Mouse IgG2b, Human ads-FITC	1090-02	0.3 µg/ml	Southern biotech
Viability dyes			
BD Via-probe	555815	0.5 µg/ml	BD Biosciences
Draq7	DR71000	0.3 µM	Biostatus
Propidium Iodide	00-6990	10 µg/ml	eBioscience
Isotype control antibodies			
CXCR7 inhibitor isotype control ccx704	Non commercial		Chemocentryx
Mouse IgG1 K Isotype Control-PE	12-4714-42	0.6-2.5 µg/ml	eBioscience
Mouse IgG2a K Isotype Control-APC	17-4724-42	0.6-2.5 µg/ml	eBioscience
Chemokines			
Recombinant Human CXCL12-AF647	CAF-11	1-300 ng/ml	Almac group
Recombinant Human CXCL11	300-4	1000 ng/ml	Peprotech
Inhibitors			
CXCR7 small molecule inhibitor CCX771	Non commercial	01-10 µg/ml	Chemocentryx
CXCR7 inhibitor isotype control ccx704	Non commercial	0.1-10 µg/ml	Chemocentryx
Other reagents used			
CellTrace violet cell proliferation kit	C34557		Invitrogen
Apoptosis activator 2 (AA2)	2098	50 µM	Tocris Bioscience

Table 2-4 Antibodies, fluorescent conjugated and native chemokines and reagents for flow cytometry

2.5.3 Analysis of surface receptor expression

Surface expression of various leukocyte trafficking molecules was determined using multi-parameter flow cytometry. Cells (1 x 10^6) were washed twice in FCM buffer and resusupended in 100 µl FCM buffer. FC block was added and incubated on ice for 10 minutes to prevent non-specific binding of antibodies to the Fc receptors. Specific/isotype antibody was added as per manufacturer's recommended concentration. Cells were incubated on ice for 30 minutes, with periodic gentle flicking of the tubes. Cells were washed twice in FCM buffer and resuspended in 100 µl FCM buffer. Suitable viability dye (7-AAD or Draq7) was added just before acquisition. Cells were acquired on MacsQuant with medium acquisition settings, keeping the event rate between 1000-10,000 events/seconds. 50,000-5,00,000 events were counted depending on rarity of the subpopulation of interest. Adjusted mean fluorescence intensities (MFIs) were calculated according to the formula: cMFI = MFI^{test} -$MFI^{isotype}$

2.5.4 Chemotaxis assay

Transwell® transmigration assays were used to determine the chemotactic activity of a particular chemoattractant or inhibitors of chemotaxis for cells. The assay utilizes a microporous permeable membrane positioned between two compartments. Cell suspensions are placed in the top compartment and a chemokine solution was added to the bottom compartment. This forms a chemokine gradient and allows the cells to migrate towards the chemokine. Cells that migrate across the membrane are collected from the bottom compartment and counted using haemocytometer or by flow cytometry.

Working concentrations of the chemokine +/- chemokine receptor inhibitor were prepared in chemotaxis buffer according to the experimental conditions. 600 µl of the prepared chemokine solution was added to wells of a 24 well tissue culture plate and 5µM Transwell® inserts were placed on top. Cells were then counted, washed and resuspended in complete media to a concentration of 5 x 106 cell/ml. The plate was covered and incubated for 3 hours at 37 ºC, 5% CO2. Inserts were then carefully removed and the contents of the bottom well were transferred to a new eppendorf tube leaving no residual cell suspension behind. Cells were centrifuged, supernatants removed and the pellets resuspended in 100 µl sterile ice cold PBS or FCM buffer. Cells were counted using either a haemocytometer with or by flow cytometry.

Migration indices were calculated by the formulae: Cells in the chemokine well/Cells in the control well. Percent migration was calculate by the formula: No of cells in the well/ $5x10^5$ x 100

2.5.5 Chemokine receptor internalization and recycling assay

Receptor internalization and recycling assay was performed to determine the extent of CXCR4 expression levels, reduction in surface expression following exposure to CXCL12 and restoration of surface expression following removal of CXCL12 from media.

Cells were counted and resuspended at a concentration of 1 x 10^6 /ml in a 24 well plate in complete media. CXCL12 was added at a final concentration of 100 ng/ml to the appropriate wells. The plate was then incubated at 37 ºC for 30 minutes. Following the incubation, the cell suspension was transferred to a new eppendorf tube, centrifuged, resuspended in complete media and then transferred to a new 24- well plate. The plate was incubated at 37 ºC, 5% CO_2 for up to 120 minutes. At each time point, the plate was removed from the incubator, and the cell suspension transferred to a new eppendorf tube and incubated on ice to stop metabolism. The time points used were 0, 30, 60, 90, 120 minutes. After the last time point, cells were washed twice and resuspended in ice cold FCM buffer. Cells were stained with $CXCR4^{-APC}$ antibody as described in section 0 and acquired on MACSQuant.

Formula for calculating adjusted/corrected MFI is:

% Adjusted MFI = $(MFI^{CXCR4} - MFI^{isotype}) / (MFI^{n\ min\text{-}CXCR4}\ MFI^{n\ min\text{-}isotype})x100$. Where n= specific time point

2.5.6 Chemokine competition assay

To determine the relative surface expression of CXCR7, a competition assay was performed whereby cells were incubated with alexa-fluor labelled chemokine, CXCL12 ($CXCL12^{AF647}$). As CXCL12 will label both CXCR7- and CXCR4 positive cells, cells were labelled in the presence or absence of a non-fluorescent competing chemokine, CXCL11. CXCL11 binds to CXCR7 (and CXCR3), but does not bind to CXCR4. Consequently, any CXCL12 labelling that is attenuated in the presence of CXCL11, must be due to the specific interaction between CXCR7 and CXCL12.

Cells were counted and resuspended at 1 x 10^7 /ml in a staining buffer (5uM HEPES,

10% FCS in RPMI). 100µl Cell suspension was transferred to a sterile 96 well plate (NUNC) and incubated on ice to stop metabolism. $CXCL12^{AF647}$ was added to a final concentration of 100ng/ml. A tenfold excess of native CXCL11 was added to the appropriate wells at a final concentration of 1µg/ml. An equal volume of PBS was added to the negative control wells. The plate was incubated for 1 hour at 37 ºC, 5% CO2. Cells were then washed twice in FCM buffer to remove excess chemokine. Dead cell discriminator, 7-AAD, was added just before analysis. Using FlowJo, MFIs were calculated and the MFI of control cells was compared to that of CXCL11-treated cells.

2.5.7 Analysis of cellular proliferation using cytoplasmic dye Celltrace Violet

CellTrace Violet (CTV) is a cytoplasmic dye which is cleaved by intracellular esterases to yield a highly fluorescent compound which binds to intracellular amines. With every cell division, fluorescence is halved, giving discrete peaks of fluorescence when analysed using a flow cytometer. Apoptosis was measured by AnnexinV-APC kit (eBioscience, San Diego) and dead cells were measured using 7-AAD staining. Cell numbers were measured using event count on MACSQuant.

Cells (2×10^6/ml), resuspended in pre warmed staining buffer (2% FCS in PBS), were labelled with CTV (5 µM) and incubated at 37 ºC, 5% CO2 for 20 minutes. 30 ml of complete media was added, following which the cell suspension was incubated at 37 ºC, 5% CO2 for 5 minutes to quench the unbound dye. Next, cells were washed and resuspended in staining buffer (30 ml) and incubated for two hours to allow the cells to recover from the toxic effects of CTV. After the incubation, cells were counted and treated with IL-15 (25 ng/ml) or media for the defined time points (72 - 96 hours). Following treatment, the cell suspensions were collected and washed in Annexin V staining buffer twice, and then resuspended in 100 µl of Annexin V staining buffer. Annexin V-APC was added and the cells were incubated for 20 minutes on ice. The cells were then washed twice in Annexin V staining buffer and analysed on the MACSQuant after adding cell viability dye 7-AAD. Cells treated with Apoptosis Activator 2 (AA2, Tocris Bioscience, UK) were used as a positive control for Apoptosis.

2.6 Molecular biology methods: DNA

2.6.1 DNA extraction using Trizol

Cells were counted, pelleted by centrifugations and lysed in 1 ml Trizol (Life Technologies) by thorough pipetting. For cerebrospinal fluid (CSF) samples, cells were pelleted and lysed without counting. Lysates were incubated for 3 minutes at room temperature to complete lysis. 200 µl of chloroform was added and thoroughly mixed by vigorously shaking by hand for 15 seconds. Lysates were incubated at room temperature for 3 minutes and then the tubes centrifuged at 8000 g for 10 minutes at 4 ^{O}C. This formed an upper clear 'aqueous phase' containing RNA, an 'interphase' and a lower 'organic phase' containing DNA. The aqueous phase was carefully removed and stored. In the organic phase from CSF samples, a co-precipitant (Glycogen (sigma, UK) or Pellet paint co-precipitant (EMD Millipore)) was added to the solution containing the DNA and the sample mixed by vortexing. Samples were incubated for 3 minutes at room temperature and centrifuged at 2000 g for 5 minutes at 4 ºC to pellet the DNA. Supernatants were carefully removed leaving the DNA pellet behind. The DNA pellets were washed with 1 ml of sodium citrate/ethanol solution (0.1 M Sodium Citrate in 10% ethanol pH 8.5). Samples were incubated for 30 minutes at room temperature, occasionally inverting the tube to mix. Samples were then centrifuged at 2000 g for 5 minutes at 4 ºC. This wash step was repeated once. 1.5 ml 70% ethanol was added and incubated for 20 minutes at room temperature, periodically inverting the tubes. Sample tubes were then centrifuged for five minutes at 4 ºC. Supernatants were completely removed and discarded. The pellets were air dried by leaving the tubes open for 15 minutes to evaporate the residual ethanol without over drying the pellets. DNA pellets were dissolved in 35 µl nuclease free water by incubating at room temperature for 1 hour. DNA quantification was performed as described in section 2.6.5.

2.6.2 DNA extraction from CSF using QIAmp DNA micro kit

Where specified, DNA extraction was performed using QIAmp DNA micro kit (Qiagen). This kit utilizes spin column technology and is optimized for DNA extraction from small samples. Cells were lysed and passed through silica-gel membranes which bind to DNA and allow contaminants to pass through. Contaminants are further removed in two wash steps followed by high-speed

centrifugation. DNA was then eluted using RNAse free water or an elution buffer provided with the kit. Carrier RNA (cRNA) was used to the cell lysates to increase DNA yield. Cells were pelleted and supernatants removed. Lysis buffer, along with proteinase K and cRNA was added and lysates homogenised by pulse vortexing for 15 seconds. The lysates were then incubated at 56 ^{O}C for 10 minutes to increase the protein digestion activity. Absolute ethanol was added to precipitate the DNA and the whole lysates were transferred to the column and centrifuged. Wash steps were performed according to the manufacturer's instructions. Residual ethanol was removed by centrifugation at 17000 g for 2 minutes. The bound DNA was eluted with 35 µl of nuclease free water in a new eppendorf tube and stored at -80 ºC until use.

2.6.3 DNA extraction from blood, cultured cells and bone marrow samples using Qiagen blood DNA mini kit

The Blood DNA mini kit (Qiagen) utilizes the column based principle of DNA extraction. An appropriate volume of cell suspension (50 µl of whole blood, $10^5 – 10^6$ cultured cells or purified mononuclear cells from bone marrow samples) was taken and lysed usinglysis buffer provided with the kit. Protein digestion was performed by adding proteinase K solution and incubating lysates at 56 ^{O}C for 10 minutes. After adding 100% ethanol, the lysates were transferred to the membrane columns and centrifuged. Wash steps were performed according to the manufacturer's instructions and the DNA eluted in 50 µl of nuclease free water. DNA was quantified as described in section 2.6.5 and stored at -20°C until use.

2.6.4 DNA concentration and cleanup

A DNA cleanup procedure was performed if better quality, or higher concentration, was needed. This step was performed using Qiagen DNeasy mini kit according to manufacturer's instructions. For DNA extracted from very low number of cells, Qiagen QiAmp DNA micro kit was used according the manufacturer's instructions.

2.6.5 DNA quantification by spectrophotometric method

DNA was assessed for quantity and quality using Nanodrop1000 spectrophotometer (Thermofisher). The samples were brought to room temperature and mixed well. The pedestals of the spectrophotometer were wiped clean with lint free tissue soaked in nuclease free water and then with a new dry tissue. Nuclease free water was used as blank and the OD_{260} was measured. Purity of DNA was assessed by measuring the

absorption ratio at 260:280 nm, with normal levels between 1.7-1.9 (optimum 1.9). Readings below 1.7, or above 1.9, indicated phenol or protein contamination.

DNA quantification of patient CSF samples was performed using qPCR for Albumin gene (section 2.9.2)

2.7 Molecular biology: RNA

While performing assays with RNA, measures were taken to prevent RNA degradation. Prior to starting RNA work, all surfaces were decontaminated from RNases using RNAzap RNase decontaminating solution (Ambion). All equipments, reagents, plastics and pipette tips were RNase free. Samples were processed quickly and all steps of the procedures were performed while keeping the samples on ice.

2.7.1 RNA extraction from cells

RNA was extracted using spin-column based RNA isolation technology. Depending on the amount of available cells for RNA extraction, an RNAeasy Mini kit (Qiagen) (>$5x10^5$ cells), or RNAeasy Micro kit (Qiagen) (<$5x10^5$ cells) was used. Cells were lysed using RLT buffer and homogenized using QIAshredder spin column (Qiagen). RNA extraction was performed according to manufacturer's instructions. In order to remove DNA contaminants, lysates were treated with RNase free DNase I (Qiagen) according to manufacturer's instructions. RNA was eluted with RNase free water and quantified using Nanodrop1000.

2.7.2 cDNA synthesis

RNA was converted to complementary DNA (cDNA) using Precision nanoScript Reverse Transcription kit (Primerdesign, Southampton, UK). Depending on the concentration of available RNA, 200-1000 μg RNA was used in each reaction. cDNA synthesis was performed according to manufacturer's instructions. cDNA synthesis involves two main steps: annealing and reverse transcription. RNA samples were mixed with random nanomer primermix and heated to 65 ºC for 5 minutes and to allow annealing of primers to the isolated RNA. Subsequently, reverse transcription was performed by adding reverse transcriptase, dNTP mix, DNAse, buffer and water according to the manufacturer's instructions. For RT-ve controls, RNase free water was added instead of reverse transcriptase enzyme. Samples were incubated at 25 ºC for 5 minutes, 55 ºC for 20 minutes, and 75 ºC for 15 minutes. cDNA samples were

stored frozen at -20°C until use.

2.8 Molecular biology: SYBR Green qPCR

qPCR allows determination of relative and absolute numbers of transcripts of a gene present in a sample. This technique utilizes SYBR Green fluorescent dye which binds to double stranded DNA and emits fluorescence in bound form. With each PCR reaction cycle, the amount of DNA is amplified with a proportional increase in signal from SYBR Green, thus allowing real-time measurement of DNA amplification. Absolute transcript quantification, by SYBR Green qPCR, requires primers specific to the transcript of interest, and standard primers, which are used to generate standard curves for analysis of transcript copy numbers. Absolute numbers of a transcript encoding an appropriate housekeeping gene must also be assessed to normalise for different quantities of template cDNA. The following sections describe design and verification of both qPCR and standard primers, followed by the SYBR Green qPCR method that has been utilized in this thesis.

2.8.1 Primer design

A set of 'inner' and 'outer' primers were designed using online software 'Primer3' (available online at http://bioinfo.ut.ee/primer3-0.4.0/). The outer primers were designed to create PCR products, used to create a standard curve, while the inner primers were used to efficiently amplify a suitable region of the transcript of interest. Three sets of primers were generated for each gene transcrips and one best set of primers was selected based on amplification efficiency determined in qPCR reaction. It was preferred to design intron spanning primes. The following criteria were taken into consideration while designing the primers (Table 2-5):

Factor	Optimal value
Sequence length	18-23 base-pairs (BP)
GC content	40-65% (50% optimal)
Melting temperature (Tm)	59-61 ^{o}C (60 ^{o}C optimal)
Max. self complimentarity	2
Max. 3' self complimentarity	1
Amplicon size	<150bp (250-1000 for outer primers)
GC bases at the end	Not more than two G or C based in last 5' or 3' end of each primer.
GC repeats	<4 or G and/or C in a row

Table 2-5 Criteria for optimal primer design

Outer primers were designed to amplify the region where inner primers would bind. The conditions for these primers were similar to the inner primers, apart from their length which was at least 80 BP larger. Also, as these primers were not to be used in the final qPCR reaction, other conditions for primer design could be slightly relaxed if the software did not suggest suitable primers.

BLAST analysis was performed to confirm the specificity of the primers, and to exclude amplification of splice variants or genomic DNA. Specificity was further confirmed by performing a PCR reaction (section 2.8.2.1) and separating the amplified PCR products according to size, using agarose gel electrophoresis (2% agarose in Tris-EDTA). Amplified DNA was visualized using ethidium bromide. Presence of a sharp clear band of the appropriate size confirmed a specific product, whilst multiple bands suggested non-specific amplification, the presence of primer dimers, or genomic DNA amplification. Unsuitable primers were not used any further. List of primers is presented in Table 2-6.

RT-PCR			
Target	**Sequence**	**Annealing temperature**	**Product size**
IL-15	5′ AAACCCCTTGCCATAGCCAGCTCT T 3′ CTTCTGTTTTAGGAAGCCCTGCAC T	55	201bp LSP-IL-15 320bp SSP-IL-15
IL-15 Rα	5′ GCCAGCGCCACCCTCCACAGTAA 3′ GCCAGCGGGGGAGTTTGCCTTGAC	55 ºC	402 bp
IL-15 Rβ	5′ CACAGATGCAACATAAGCTGG 3′ ACT TCA GGA CCT TCT TCA GCC	52 ºC	403 bp
IL-15 Rγ	5′ AGC CCCAGC CTACCAACCTCACT 3′ TTAAAGCGGCTCCGAACACGAA	55 ºC	447 bp
Serpine 1 Standard	5′ CTCTCTCTGCCCTCACCAAC 3′ TGCCACTCTCGTTCACCTC	60 ºC	261 bp
MMP9 Standard	5’ CCTGGAGACCTGAGAACCAA 3’ CACCAAACTGGATGACGATG	60 ºC	366 bp
PTEN standard	5’ ATGTGGCGGGACTCTTTATG 3’ TCAGGAGAAGCCGAGGAA	60 ºC	241 bp
DENR standard	5’ CAGTAACAGGGGAGGATGAAA 3’ CAGGCAACAGTGCGAGAC	60 ºC	600 bp
TIMP4 standard	5’ CAGACCCTGCTGACACTGAA 3’ GGGAAGGAGAACTGGCTTG	60 ºC	553 bp
CDH11 stanadard	5’ CAGATGACCCCACTTATGGAA 3’ GCTTTATCACCCCCTCCTGT	60 ºC	1051 bp
CXCR4 standard	5’ TCATCAAGCAAGGGTGTGAG 3’ CCTACCACGAGACATACAGCAA	60 ºC	1691 bp
CXCR7 standard	5’ GTCTGGGTGGTCAGTCTCGT 3’ TGCTGTGCTTCTCCTGGTC	60 ºC	654 bp
TBP standard	5’ GGGCACCACTCCACTGTATC 3’ CATCTTCTCACAACACCACCA	60 ºC	723 bp
GAPDH	5′ CAAGGCTGAGAACGGGAA 3′ GGTGGTGAAGACGCCAGT	55 ºC	115 bp
SYBRGreen qPCR			
IL-15	5′ AAACCCCTTGCCATAGCCAGCTCT T 3′ CTTCTGTTTTAGGAAGCCCTGCACT	55	201bp LSP-IL-15 320bp SSP-IL-15
Serpine 1 qPCR	5′ GGTTCTGCCCAAGTTCTCC 3′ CGGTCATTCCCAGGTTCTC	60 ºC	71 bp
MMP9 qPCR	5’ GGCACCACCACAACATCA 3’ GCAAAGGCGTCGTCAATC	60 ºC	79 bp
PTEN qPCR	5’ AGGCGAGGGAGATGAGAGA 3’ CGAAGAGGAGGCGAGAAAC	60 ºC	140 bp
DENR qPCR	5’ TCGTCCTTGGCATTTTCACT 3’ TCTCCCGTTTATTTGACTTTGG	60 ºC	73 bp
TIMP4 qPCR	5’ GCCAACAGCCAGAAGCAG 3’ GCCACAGTTCAGATGGTAGTGA	60 ºC	150 bp
CDH11 qPCR	5’ CCTATTTTTCGGTGGAAGCA 3’ TTGGTTGTCCCTGAGAGTCC	60 ºC	142 bp
CXCR4 qPCR	5’ TGTTGTCTGAACCCCATCCT 3’ ATGAATGTCCACCTCGCTTT	60 ºC	132 bp
CXCR7 qPCR	5’ CCTACCACGAGACATACAGCAA 3’ GTCTCATTGTTGGACGCAGA	60 ºC	122 pb
TBP qPCR	5’ AGGATAAGAGAGCCACGAACC 3’ GCTGGAAAACCCAACTTCTG	60 ºC	137 pb
TaqMan qPCR			
Gene	**Assay ID**		
IL-15	Hs99999039_m1		
PSGL1	Hs00380945_m1		
CXCR3	Hs00171041_m1		
Albumin	5’ TGAAACATACGTTCCCAAAGAGTTT 3’ CTCTCCTTCTCAGAAAGTGTGCATAT		

Table 2-6 Primer details for PCR, SYBR Green qPCR and TaqMan qPCR.

2.8.2 Generation of standards

The ‘outer’ primers were used to generate PCR products containing the amplicon of interest. cDNA from multiple cell lines was tested for expression of the gene of interest. Following a standard PCR reaction, the PCR products were electrophoresed using 2% agarose gel and visualized using ethidium bromide. The appropriate band was excised from the gel using a sharp blade. PCR products were then purified from the excised gel fragment using QIAquick Gel-Extraction kit (Qiagen), according to manufacturer’s instructions. The standard product was tested for specificity by performing a standard PCR reaction using the appropriate inner primers and using the purified standard product as template. Successful amplification was confirmed by gel electrophoresis. These steps are described below.

2.8.2.1 PCR to generate standards

Two microlitre template cDNA and 1 µl diluted primers (1 µM final concentrations) were added to a commercially available pre-mixed ReddyMix (Revolab) containing buffer, MgCl2, dNTPs and Taq DNA polymerase. PCR reactions were performed on a Veriti thermal cycler (Applied Biosystems). The PCR cycling conditions are presented in Table 2-7.

Step	Temperature (ºC)	Time
1.	95	3 minutes
2.	95	15 seconds
3.	60	20 seconds
4.	72	40 seconds
Repeat steps 2-4 for 40 cycles		
5.	72	7 minutes
6.	4	Indefinitely

Table 2-7 PCR cycling conditions for generating standards

2.8.2.2 Agarose gel electrophoresis of PCR standards

PCR products were separated and visualized using agarose gel electrophoresis. 2% Agarose gel was prepared in TAE buffer by boiling till the powder completely dissolved. Ethidium Bromide was added, and the solution carefully poured into a gel cassette with combs inserted. Gel was left to set and then transferred to an electrophoresis tank filled with TAE buffer. PCR products were carefully loaded to wells along with 100 BP DNA ladder (Biolegend). Electrophoresis was conducted at 100V for 30 minutes. The gel was transfer the UV gel imager AlphaImager (Alpha

Innotech) and visualize under ultraviolet (UV) light.

2.8.2.3 Gel extraction of PCR standards

Following gel electrophoresis, gel fragments containing the bands were carefully excised using a sterile scalpel and transferred to a new 1.5 ml Eppendorf tube. DNA from the gels was extracted using QIAquick gel extraction kit (Qiagen) according to manufacturer's instructions.

2.8.2.4 Standard verification with PCR

The PCR product recovered from gel extraction was used as a template for testing the inner primers. PCR was performed as described under 2.8.2.1. PCR products were run on a gel as described under 2.8.2.2 and visualized for specificity of PCR product. A sharp band of expected size with no other bands or primer dimers implied acceptable amplification by primers.

2.8.3 TOPO cloning of vectors

PCR standards were cloned into TOPO vectors using TOPO TA cloning kit with One Shot vector cells (Invitrogen, Paisley, UK). First, the standard PCR products were ligated with the TOPO TA vector (1 µl PCR product, 0.25 µl salt solution, 0.25 µl TOPO vector) by gentle tapping, and incubating at room temperature for 30 minutes. This was followed by transformation of One Shot competent cells. Chemically competent E. coli cells were thawed on ice, mixed with ligation product (12 µl cells + 2µl ligation product) by gentle tapping, and incubated on ice for 5 minutes. The mixture was then heat shocked by incubating at 42 ^{O}C for 30 seconds and immediately transferred onto ice. 250 µl of Super optimal broth (SOC) media was added and the tubes were incubated on a shaking incubator for 1 hour at 37 ^{O}C. LB agar + amplicillin plates were taken and coated with X-gal. 100 µl of transformation product was spread on the agar and incubated overnight at 37 ^{O}C. For each standard cloned, 4 white colonies were then picked using a sterile pipette tip, transferred to 5 ml broth and incubated overnight in a shaking incubator at 37 ^{O}C. Next morning, cloned vectors were purified using QIAprep Spin Miniprep Kit (Qiagen, Venlo, the Netherlands). This purified product was analysed for specificity by determining the sequence of product.

2.8.4 SYBR Green qPCR

Following cDNA synthesis, analysis of gene expression was performed by SYBR Green qPCR. The assays were performed on Applied Biosystem 7500 HT- or 7900 HT real time systems. All assays were performed in triplicates and expression levels were normalised to that of the housekeeping gene, TATA box – binding protein (TBP). TBP expression was analysed on the same assay plate in triplicates. PerfeCta SYBR green supermix (Quanta Biosciences, Gaithersburg, USA) was used for the SYBR green qPCR which contains all the enzymes, nucleotide bases, ROX dye and buffers in a single tube. Standards were serially diluted and a minimum of 5 dilutions were used to form a standard curve. Three no template control (NTC) wells were also analysed to test for contamination.

A Mastermix was created as follows per reaction well:

Reagent	Volume
2x SYBR green mix	10 µl
Primer mix	0.3 µl (at a final concentration of 0.8 µM)
nuclease free water	7.7 µl

Table 2-8 Calculation for SYBR Green qPCR mastermix

10% extra was prepared to account for pipetting errors. 18 µl Mastermix was added per well in a 96 well plate. 2 µl of sample, standard or nuclease free H_2O was added to each well and the plate covered with a clear PCR plate sealing film. In case of 386 well plate, half volumes of the mastermix and samples were used. The plate was then centrifuged at 200g for 1 minute to make sure all the contents were placed at the bottom.

The PCR reactions were performed on 7900HT or 7500 Fast Realtime PCR systems. The thermal cycling conditions for both the machines are presented in Table 2-9.

Step	Temperature (ºC)	Time
1.	94	3 minutes
2.	94	5 seconds
3.	60	15 seconds
Repeat step 2-3 40 times		
4.	Melt/dissociation stage	

Table 2-9 Temperature conditions for SYBRGreen qPCR assay

2.8.5 Analysis of SYBR Green qPCR assay

Following completion of the SYBR qPCR assay, it is crucial to analyse the quality of the assay. A number of quality control checks are required to ensure the data from the assay are valid. Cycle Threshold (Ct) value is the point at which the fluorescence from the sample wells crosses the machine threshold for detection. During a qPCR reaction, the SYBR green signal intensity rises exponentially. Therefore, the fewer cycles it takes for fluorescence intensity of a given well to cross the threshold, the more target cDNA was present in the corresponding sample.

Correlation coefficient (R^2) values represent the quality of the standard curve and relates to how accurately the dilution series was prepared. A R^2 value of >0.97 was considered acceptable. The standard curve slope represents the amplification efficiency of the primers and the optimal value of -3.3 means doubling of the DNA with each 3.3 thermal cycles. Generally, values <-3.3 imply inefficient primers and >3.3 imply presence of PCR inhibitors in the standards. Values between -3.1 and -3.9 were considered satisfactory. A variation in amplification in the triplicates of >1.5 Ct cycles was considered unsatisfactory. There should have been no amplification in the NTC wells. However, if an amplification was seen, the Ct values should be >3 Ct cycles further away from the sample of interest. Melting curve analysis was performed to determine the specificity of amplification.

2.8.6 Normalization of qPCR data

In order to allow comparison of gene expression levels between experimental groups, it is important to normalize for the variations introduced due to sample processing. A number of methods were utilized to control for such potential biases. Wherever possible, equal numbers of cells were utilized for extracting RNA. In addition, equal concentrations of RNA were used for synthesising cDNA, the same cDNA synthesis kit was used in the experimental groups, and subsequently. Following this, equal volumes of cDNA were used in qPCR reactions. Housekeeping genes or reference genes are required for cell metabolism and are expressed in cells with minimal variation in response to the experimental treatment. This implies that the levels of housekeeping genes will be unaffected by the experimental condition and any observed difference in expression levels of a housekeeping gene will be due to the difference in quantity of cDNA. In an initial experiment, a number of housekeeping genes were tested with SD1, Sup B15, REH and SEM. In these cell lines, GAPDH and

TATA binding protein (TBP) were found to be robust and therefore used for the experiments performed in this thesis.

2.9 Molecular biology: TaqMan qPCR

2.9.1 TaqMan qPCR for relative gene expression

TaqMan qPCR system uses a fluorescent probe, specific to the gene of interest, in addition to the primers. This adds to the level of specificity of amplification. However, these primers and probes are difficult to design and usually purchased as a lyophilized mastermix solution. In addition absolute quantification is only possible after purchasing the known standards. Generally, TaqMan gene expression assays are performed to analyse the relative differences between two groups of cells. TaqMan qPCR mastermix solutions containing the primers, probe, enzymes and other reagents in a pre-mixed tube were purchased from Life Technologies (Paisley, UK). The Mastermix solution was prepared according to the manufacturer's instructions. 18 µl Mastermix solution was aliquoted to each well of a 96 well qPCR plate (Starlab) and 2 µl cDNA of each sample was added to wells in triplicate. NTC samples were included to ensure the quality of the assay. qPCR reaction was performed on Applied Biosystems 7900-HT for 40 CT cycles as described (Section 2.8.4). Relative quantitation was analysed on RQ manager software (Applied biosystems)

2.9.2 TaqMan qPCR for Albumin gene

Quantity of DNA extracted from human CSF samples was measured by qPCR using an Albumin gene-specific Taqman assay and a standard curve containing known quantities of DNA. Primer design and verification were performed at Glasgow MRD laboratory according to the guidelines from European study group (ESG) (van der Velden et al., 2007, van der Velden et al., 2003).

2.9.2.1 Preparation of standard dilution

DNA was isolated and pooled from mononuclear cells (MNC DNA), purified from the blood of 20 healthy individuals. Standards containing known quantities of DNA were then prepared as follows. Briefly, stock solution of normal MNC DNA (100 ng/ µl) and DNA diluent Salmon sperm DNA (100ng/ µl) was incubated at 37 ºC for 30 minutes with intermittent vortexing to ensure adequate mixing. First dilution (10:1) (10 ng/ µl) was generated by adding 100 µl of MNC DNA to 900 µl of Salmon sperm

DNA. The sample was incubated at 37 ºC for 30 minutes with intermittent vortexing. Similarly, 5 serial dilutions were prepared and the serial samples stored at -20°C until use.

2.9.2.2 Preparation of qPCR Mastermix for DNA quantification

qPCR Mastermix was prepared as shown in Table 2-10. 20 µl of mastermix was added to each well of a 96 well qPCR plate along with 5 µl of sample or standard DNA template. In some cases, due to limited DNA availability, 15 µl of reaction volume was used. Nuclease free water was added to the appropriate wells as a negative control.

Reagent	Concentration	Volume Added (µl)	Final Concentration
Real-time master mix	2x	12.5µl	1x
Alb Forward primer	10µM	2.25µl	0.9µM
Alb Reverse primer	10µM	2.25µl	0.9µM
Alb Probe	5µM	0.5µl	0.1µM
BSA	2 % (w/v)	0.5µl	0.04% (w/v)
RNAse free water	-	2	-
Template	50 – 200ng/µl	5µl/PCR reaction	-

Table 2-10 Calculation of TaqMan qPCR mastermix for Albumin gene

2.9.2.3 TaqMan qPCR assay for Albumin gene

PCR conditions were as described in Table 2-11.

Step	Temperature (ºC)	Time
1	50	2 minutes
2	95	15 minutes
3	95	15 seconds
4	60	1 minutes
Repeat 2-4 for 40 cycles		
5	4	Indefinitely

Table 2-11 Temperature conditions for TaqMan qPCR assay for Albumin gene

2.9.2.4 Analysis of TaqMan qPCR assay

All quality control checks were performed as described in section 2.8.5.

2.10 Cytology methods

2.10.1 Cytospin preparation

Cells were counted, washed and resuspended at a concentration of 0.5 x 10^6 cells/ml in

PE buffer. Glass slides (VWR Internation, Radnor, USA) were labelled and inserted into a metal slide holder, followed by a cytospin filter and a cuvette. 200µl of cell suspension was added to the cuvette and placed in the cytospin centrifuge. It was centrifuged at 800 rpm for 5 minutes. The slide was carefully removed from the metal slide holder and left to air dry. Slides were fixed in 100% methanol for 20 minutes and air dried overnight before staining.

2.10.2 Blood smear preparation

Blood smears were prepared by placing a 4mm diameter spot of blood about 5 mm from the end of a glass slide. Another slide (spreader) was placed at 45 degree and backed into the blood spot spreading the blood by capillary action. The spreader slide was pushed smoothly towards the other end of the sample slide yielding a smear. The slide was air dried, fixed in 100% methanol and air dried overnight before staining.

2.10.3 Giemsa staining

Blood smear/ cytospin slides were immersed in diluted Giemsa stain (1:20 in ddH_2O) for 20 minutes, rinsed in tap water and then air dried for examination.

2.10.4 Immunofluorescence staining

Cytospin slides were prepared and fixed as described in section 2.10.1. Immunofluorescence (IF) staining was performed to analyse the expression of CXCR4 and CXCR7. A circle was drawn around the cells using a hydrophobic wax pen. Cells were washed in TBS-Tween (5 minutes x 2) and then blocked with 20% horse serum in TBS-Tween for 30 minutes at room temperature. Blocking serum was tapped off and 2.5-10 µg primary antibodies, or relevant isotype control antibodies, diluted in antibody diluent (2.5% normal human serum, 2.5 % horse serum in TBS-Tween) were added to the fixed cells. The slides were carefully transferred to a covered humidified box and incubated at 4 ^{O}C overnight. The slides were then washed in TBS-Tween (5 minutes x 2) and secondary antibody added at 1/300 dilution in antibody diluent for 30 minutes at room temperature protected from light. Cells were washed in TBST (5 minutes x 2). Slides were mounted in 4',6-diamidino-2-phenylindole (DAPI), covered with cover slips and sealed with nail varnish. Slides were visualized under fluorescent microscope.

2.11 Histology methods

2.11.1 Tissue fixation, embedding and cutting

Murine tissue (liver, spleen, kidneys, ovaries and testes) was weighed and fixed in 4% PFA solution for 24 hours. Organs were then put into tissue processing cassettes and processed in automated tissue processor Thermo Shandon Citadel 1000. The sections were gradually dehydrated by treating with 70% ethanol (1hour), 90% ethanol (1 hour), 95% ethanol (1hour), 100% ethanol (5.5 hours) and then treated with Xylene (3.5 hours) and liquid paraffin (9 hours). Tissue sections were then embedded in tissue cassettes on Shandon Histocentre 3. Five micrometer thick slices of tissue were cut on a microtome and transferred on a labelled glass slide. The glass slide was placed on a hot plate to evaporate excess water transferred from water bath.

2.11.2 Haemotoxylin and Eosin staining

Fixed tissue sections, processed as described above, were rehydrated by serially treating with xylene, 96% ethanol, 70% ethanol and water. The tissue was then immersed in Haemotoxylin, rinsed with water and treated with 1% acid alcohol and then Scott's tap water substitute (STWS). Slides were then immersed in eosin and rinsed again. Sections were then dehydrated by serially treating with 70% ethanol, absolute ethanol and xylene. Finally, these were mounted with DPX and covered with coverslips.

2.11.3 Immunohistochemistry

Formalin fixed paraffin embedded tissues were stained using an anti-human CD45 antibody (DAKO). The sections were first dewaxed, after treatment with xylene (10 minutes x 2), and gradually rehydrated by treating the sections with 100% ethanol (5 minutes x2), 90% ethanol (5minutes x2) and 70% ethanol (5 minutes). The cells were then washed with PBS-Tween (5 minutes) and treated with H_2O_2 for 30 minutes to block endogenous peroxidase. Cells were again washed twice in PBS-Tween (5 minutes). Antigen retrieval was carried out using Citrate buffer. The Citrate buffer was boiled in a plastic container in a microwave oven. The slides were submerged completely and boiled in the microwave for 6 minutes. The container was left to cool at room temperature for 30 minutes before removing the slides. The slides were then washed in running water (5 minutes) and PBS-Tween (5 minutes). A wax ring was

drawn around the tissue using a wax pen, after carefully drying the glass with a tissue. The sections were blocked using serum block (20% normal horse serum in PBS-Tween) for 30 minutes. The sections were washed briefly in PBS-Tween, and primary anti-human anti-CD45 (2.5-10 µg/ml) (Dako) was added to the sections. The slides were kept in a humidified contained at 4°C overnight. The slides were then brought to room temperature and washed twice in PBS-Tween (5 minutes). A biotinylated secondary antibody was added and incubated for 30 minutes at room temperature. This was followed by 2 x PBS-Tween washes (5minutes). Sections were then incubated in ABC solution (Vector) as per manufacturer's instructions. Sections were again washed twice in PBST (5 minutes). DAB was prepared as per manufacturer's instructions and applied sections for 1 minute. The DAB reaction was stopped by immersing the slides in tap water. The sections were counterstained with Haemotoxylin and then gradually dehydrated by incubating in 70% ethanol (2 minutes x 2), 90% ethanol (2 minutes x 2), 100% ethanol (2 minutes x 2), and then xylene (2 minutes x 3). The sections were mounted with DPX and covered with coverslip.

2.12 Molecular biology: Protein

2.12.1 Western blotting

Western blot assays were performed for detection of cellular signalling molecules. A list of the antibodies and reagents used is presented in Table 2-12.

Antibody	**Cat.no**	**Manufacturer**	**Dilution**
p38 MAPK Antibody	9212S	Cell signalling/NEB	1:1000
Phospho-p38 MAPK (Thr180/Tyr182) (3D7) Rabbit mAb	9215S	Cell signalling/NEB	1:1000
p44/42 MAPK (Erk1/2) (137F5) Rabbit mAb #4695	4056S	Cell signalling/NEB	1:1000
Phospho-p44/42 MAPK (Erk1/2) (Thr202/Tyr204) (197G2) Rabbit mAb	4377	Cell signalling/NEB	1:1000
Phospho-CrkL (Tyr 207)	3181	Cell signalling/NEB	1:1000
Phospho-Akt (Thr308) (244F9) Rabbit mAb	4056	Cell signalling/NEB	1:1000
Akt (pan) (11E7) Rabbit mAb	4685	Cell signalling/NEB	1:1000
Anti-rabbit IgG, HRP-linked Antibody	7074	Cell signalling/NEB	1:10,000
Reagents and equipment	**Cat.no**	**Manufacturer**	
RIPA buffer (150 nM NaCl, 1 % IGEPAL, 0.5% sodium deoxycholate, 0.1% SDS, 50nM Tris, pH 8.0)	R0278	Sigma-Aldrich	
NuPAGE® MES SDS Running Buffer (20X)	NP0002	Novex/Life technologies	
NuPAGE® MOPS SDS Running Buffer (20X)	NP0001	Novex/Life technologies	
NuPAGE® LDS Sample Buffer (4X)	NP0007	Novex/Life technologies	
NuPAGE® Novex® 4-12% Bis-Tris Gels, 1.0 mm, 12 well	NP0322BOX	Novex/Life technologies	
iBlot® Gel Transfer Device	IB1001UK	Invitrogen/life technologies	
Albumin from bovine serum	A9418-50G	Sigma-Aldrich	
Kodak Carestream Medical X-ray film	814 3059	Kodak	
Novex Sharp protein standard	R028-50ml	Sigma-Aldrich	

Table 2-12 Antibodies and reagents for western blotting

2.12.1.1 Isolation of protein from cells

Proteins were extracted from suspension or adherent cells. Cells were counted and between 1 x 10^6 – 1 x 10^7 cells were used to create lysates. Suspended cells were washed twice in PBS and pelleted by centrifugation. Adherent cell cultures were washed in the flask twice and then trypsinised, scraped and washed again.

Subsequently, cells were pelleted and lysed in 100-200 µl of lysis buffer (RIPA buffer, 1% Protease and Phosphatase inhibitor cocktail) by through vortexing. Lysate was incubated on ice for 10 minutes to complete lysis and vortexed again. Lysates were cleared of debris by centrifugation at 8000 g x 10 min 4°C. Supernatant containing protein were carefully transferred to a new eppendorf tube, mixed well be pipetting and stored at -80°C till further use.

2.12.1.2 Protein quantification

Bicinconic acid (BCA) assay is widely used to quantify proteins for western blotting to ensure equal loading of proteins for electrophoresis. Proteins were quantified using BCA assay. Each sample was analysed in duplicate and PBS and lysis buffer were used as negative controls. BSA assay standards were created by preparing a bovine serum albumin (BSA) solution at 2 mg/ml in PBS. Serial dilutions (1:3) were created from 2 mg/ml down to 25 µg/ml to generate 8 standard dilution points. 200 µl of BCA assay working reagent (prepared as per manufacturer's instructions) was added per well to a 96 well plate. 25 µl of each sample were added to the wells in duplicate. Well contents were mixed well in a plate shaker and incubated at 37°C, 5% CO_2 and protected from light for 30 minutes. The plate was cooled to room temperature and the absorbance at 570 nm was measured on a plate reader. Raw measurements were adjusted by subtracting the blank measurements. A standard curve was created using standard measurements and sample values were generated extrapolating values from standard curves. Data was analysed using Prism (Version 4.0, GraphPad Software, Inc. CA, USA).

2.12.1.3 SDS gel electrophoresis

Proteins were separated using SDS gel electrophoresis. Protein samples were thawed and incubated with 4x LDS sample loading buffer at 70°C for 10 minutes. Commercially available Novex 4-12% SDS gel was loaded in an electrophoresis tank. The tank was filled with MES running buffer as per manufacturer's instructions. 20µl of sample was carefully loaded to each well using extra-long gel loading tips. Protein size marker was added in one well. Electrophoresis was run at 120 volts for 90 minutes until the protein bands had run approximately 80% length of the gel. After the electrophoresis, the gel was removed from its cassette and transferred to the Polyvinylidine fluoride (PVDF) membrane using iBlot (Novex) dry protein transfer system according to manufacturer's instructions.

2.12.1.4 Estimation of protein loading

To ensure equal loading using loading control antibody, the blot was stripped off from antibody using Western stripping buffer. Blot was washed in TBS-Tween buffer (5 minutes) and then incubated with Western stripping buffer (15 minutes), washed again in TBS-Tween (5 minutes) and stained with loading control antibody. Two types of loading control antibodies were used. For example, for a western blot to determine the phosphorylation of p44/42 MAPK in CXCL12 stimulated cells, the signal of interest Phospho-p44/42 MAPK was determined by Phosph-p44/42 MAPK and the loading was determined by total p44/42 MAPK and Histone-H3.

2.12.1.5 Antibody binding and visualization

The blot was blocked in block buffer (5% BSA in TBS-Tween) for 1 hour at room temperature on a plate shaker. Primary antibody (diluted 1:1000 in block buffer) was added and the blot was incubated at 4°C overnight, with gentle continuous agitation, in a sealed container to prevent evaporation. The blot was then washed in TBS-Tween (5 minutes x 6) and HRP linked secondary antibody was added (diluted 1:4000-10,000 in block buffer). The blot was incubated with gentle continuous agitation for one hour. The blot was then washed in TBST (5 minutes x 6). Binding of the antibody was detected by an HRP mediated chemiluminescent reaction using Supersignal West Pico substrate solution (Thermofisher). Depending on the protein and antibody, a more sensitive chemiluminescent substrate, Supersignal West Femto substrate (Thermofisher) solution was used. After incubating the blot in substrate solution for 5 minutes, the blot was placed between two clear plastic sheets and fixed on an X-ray cassette with sellotape. Excess substrate solution was removed using tissue paper. The blot was exposed to X-ray film. Blots were optimized to exposure time of 1 minute where possible, however, in some cases, different exposure times between 10 seconds-10 minutes were used.

2.12.2 ELISA

Enzyme-linked immunosorbent assay (ELISA) is a widely utilized technique for detecting and quantifying proteins. Test antigen is immobilized to the ELISA plate surface and then complexed to an enzyme-conjugated antibody. Subsequently, a suitable substrate is added which is cleaved by the conjugated enzyme to produce a measureable product.

Briefly, 96 well microplates (Ebioscience) were coated with capture antibody diluted in coating buffer and incubated at 4 ºC overnight to allow complete binding of the antibody to the wells. Subsequently, the plate was washed with wash buffer provided and then blocked with 200 µl assay diluent for 1 hour. IL-15 stock solution (1000 ng/ml) was serially diluted 1:2 to generate 7 serial dilutions. Following the incubation, all samples and standards (100µl) were transferred to respective wells. The standards and samples were run in duplicate. The samples were applied to the wells in two-fold, 4-fold and 10-fold dilutions, each in duplicates. The plate was sealed and incubated at room temperature on a plate shaker for 1 hour at~500 rpm. Subsequently, the plate was washed 5 times before adding 100µl of biotinylated polyclonal antibody to each well (binding time?). 100µl of streptavidin-HRP conjugate was then added to each well and the plate was sealed and incubated for 30 minutes at room temperature. The plate was washed for 7 times in TBS-Tween buffer. Substrate solution was added at volume of 100ul/ well and the plate was incubated at room temperature for 15 minutes on a plate shaker. 50µl of stop solution then added to each well. The optical density was measured by an ELISA micro plate spectrophotometer (Multiskan EX, Thermo Electron Corporation) at 430 nm and data collected was compiled using Assent Version 2.6 Software.

2.12.3 Luminex multiplex protein detection assay

Luminex is a multiplex immunoassay designed for simultaneous detection of multiple proteins in one plate. In addition, Luminex assays have a lower sample volume requirement and a lower protein detection limit in comparison to ELISA. The assay principle is similar to that of an ELISA. Capture antibodies directed against the desired protein are conjugated to fluorescence magnetic beads with distinct fluorescence wavelengths for each antibody. Coupled beads bind to the biomarker of interest. Subsequently, a biotinylated detection antibody is added to the samples followed by addition of a reporter streptavidin-PE antibody. The antigen-antibody-reporter complex is analysed with a fluorescence reader.. In this thesis, Luminex assays were performed to determine a number of chemokine ligands in CSF from ALL patients. The assay reagents were purchased from Bio-Rad laboratories (Hercules, CA, US)

Briefly, standards and reagents were prepared according to manufacturer's instructions. Seven standards dilutions were prepared 1:4 with sample diluent supplemented with BSA at a final concentration of 0.5%. The samples were diluted 1:2 with sample diluent. Magnetic beads were reconstituted according to

manufacturer's instructions and 50 µl reconstituted beads were transferred to each well. Subsequently, the plate was washed twice with the buffer provided. Standards, samples and blanks (50 µl each) were added to the respective wells. All standards and samples were analysed in duplicate. The plate was sealed and incubated on a shaking incubator, in the dark, for 1 hour at room temperature. Following the incubation, the plate was washed 3 times with the buffer provided and then detection antibody mix (25 µl) was added to the wells. The plate was incubated for 30 minutes as described above. Following the incubation, the plate was washed 3 times and then 50 µl diluted Steptavidin-PE (dilution factor) was added to each well. The plate was incubated for 10 minutes as before and then washed 3 times. Finally, beads were resuspended in 125 µl assay buffer and analysed on Bio-Plex 100 multiplex plate reader (Bio-Rad). Fluorescence values were adjusted by subtracting values in the negative control wells. Fluorescence values in standard wells were used to generate standard curves, and concentrations of target proteins were calculated by comparing each value to the standard curves. Data were analysed using Bio-Plex Manager software v6.1 (Biorad).

2.13 Statistical analysis

All data were analysed using Prism software (Version 4.0, GraphPad Software, Inc. CA, USA) unless otherwise specified. Normality of data distribution was determined by Kolmonogrov test and by visual inspection of values in case of small number of data points. The statistical tests used for each experiment are described in the figure legends.

3 Investigating frequency and patterns of central nervous system infiltration in xenograft models of acute lymphoblastic leukaemia

3.1 Introduction and aims

Central nervous system (CNS) involvement by leukaemia continues to pose diagnostic and therapeutic challenges. CNS disease is commonly asymptomatic and is usually diagnosed using microscopic examination of the cerebrospinal fluid (CSF). Patients with overt CNS involvement at diagnosis (CNS-3) are considered to be at a high risk for developing CNS relapse. However, without CNS directed treatment, 50-70% children with CNS-1 develop CNS relapse as well (Evans et al., 1970). Even with CNS directed prophylaxis, the number of CNS relapses seen are greater in CNS-1 patients compared to CNS-2 or CNS-3 patients (te Loo et al., 2006). T-ALL patients are considered to be at a higher risk for CNS relapse. However since BCP-ALL is the commonest type of acute lymphoblastic leukaemia (ALL), CNS relapses are more frequently seen in this category (Masurekar et al., 2014). Therefore, there is a clear need for improvement in the risk stratification for CNS relapse. Understanding biological mechanisms underlying CNS infiltration might help in better risk stratification and may lead to development of novel therapies.

Animal models of human disease are widely used in ALL research. However, CNS disease has not been extensively studied. Therefore, there is a need for developing a robust and reproducible animal model of CNS disease that allows us to investigate critical aspects of CNS infiltration in ALL. This chapter begins with a discussion for the rationale of selecting the most suitable mouse strain for xenograft experiments, followed by a brief analysis of the characteristics of the xenograft. The research questions are presented at the end of this section.

Human ALL develops in the bone marrow (or thymus) and disseminates into extramedullary organs including the immune specialised CNS. Since leukaemia originates from the haematopoietic cells, the human immune system does not recognise them as foreign. As a consequence these cells proliferate easily within the nurturing microenvironments. Therefore, to dissect mechanisms of cellular dissemination into the CNS compartment, a model has to be able to:

- Allow leukaemic cells to proliferate without external selective pressures.

- Recapitulate characteristics of human leukaemic cells.

- Have competent physical barriers between the circulation and the CNS.

3.1.1 Selecting an appropriate model

A variety of animal species has been used to model ALL including mice, rats and zebra fish. Mouse models are perhaps the most frequently used *in vivo* model systems since they are easy to maintain and their biology is well understood. Selecting an appropriate mouse model that allows leukaemic cells to function physiologically is a key factor for investigating disease biology.

3.1.1.1 Syngenic mouse models

Syngenic models are usually produced to investigate the role of a particular gene or molecular pathway in disease pathogenesis. Transgenic models (induction of a genetic event at embryonal stage) are produced by introducing a genetic mutation at the embryonal stage. Mosaic models (*ex vivo* manipulation of HSPCs and re-implantation) offer better alternatives to transgenic mouse models in that the genetic abnormality is only present in the cells of interest and not seen ubiquitously as in transgenic mice. Syngenic mice models are frequently utilized in ALL research. For instance, transgenic mice generated *with Bcr-abl1* have been utilized for analysing tyrosine kinase pathways in leukaemia pathogenesis (Voncken et al., 1995). Similarly, the role of NOTCH1 activating mutations in ALL pathogenesis is comprehensively studied. The majority of T-ALL harbour NOTCH1 activating mutations and consequently many groups have developed different *notch1* transgenic mice with various T- cell abnormalities including T- cell leukaemia (Kindler et al., 2008, Kong et al., 2013). The advantage of these models is that the interaction between the leukaemic cells, the immune system and the microenvironment is within a single species. Despite the benefits offered by these models they are limited by multiple abnormalities such as carcinogenesis and variable time to leukaemia development. In addition, the murine leukaemias may not accurately represent the diversity of human ALL.

3.1.1.2 Xenograft mouse models

Xenograft models in ALL rely upon the principle of proliferation of human leukaemic cells in murine hosts, replicating human leukaemia, in a controlled environment. Perhaps the most crucial element affecting the experiment is the immune system of the hosts. When foreign leukaemic cells are transplanted into mice, the cells are rapidly cleared by the host's immune system. Therefore, the success of xenograft models is based on selecting

mice with impaired immune function that is unable to reject the foreign leukaemia cells. Immunodeficient host mice are engineered to provide a non-hostile environment enabling the transplanted leukaemic cells to continue functioning under physiological conditions.

Over the past several decades, numerous genetically engineered mouse strains have been generated with increasing levels of immunodeficiency. Early attempts at establishing xeno-transplants used immunodeficient mice carrying the $prkdc^{Scid}$ mutation (Cesano et al., 1991). Mice homozygous for this 'severe combined immunodeficiency' (scid) mutation at the 'Protein kinase, DNA activated, catalytic polypeptide' (prkdc) locus were deficient in PRKDC enzyme responsible for V(D)J recombination and therefore lacked functional B- and T- cells. $Prkdc^{Scid}$ (SCID) mice nevertheless retain their innate immune system such as NK cells and may spontaneously generate B- and T cells with ageing (called 'leakiness'). Crossing over of the mice with *scid* mutation with non-obese diabetic (NOD) mice led to the development of a highly immunodeficient mouse strain with deficient B- and T-cells (Greiner et al., 1995). Several strains of NOD/SCID mice have been generated since and have been widely utilized in leukaemia research. These mice show additional defects in NK- and macrophage function. NOD/SCID mice lack the age-related 'Immunoglobulin (Ig) leakiness'. However, graft rejection still poses concerns and irradiation is frequently required to overcome this. High rate of engraftment failure have been reported in some studies (Diamanti et al., 2012). Targeted mutations at 'recombination activation gene1' (Rag1) and Rag2 loci lead to a phenotype with defective V(D)J recombination and a resultant lack of mature B- and T- cells. Back-crossing of $Rag^{-/-}$ mice (Mombaerts et al., 1992, Shinkai et al., 1992) with NOD mice (NOD/LtSz-$Rag1^{null}$) generate extremely immunodeficient phenotype and lack the 'leakiness' seen in NOD/SCID mice but are still relatively poor recipients of human grafts (Shultz et al., 2000).

NOD/scid/IL2Rγ null (NSG) mice offer the advantage of additional defects in innate immunity due to the lack of Interleukin-2 Receptor-γ chain which is a component of several cytokine receptors and is essential for NK cell development. Several different strains of NSG mice exist which are comparable in their immune deficient status. NSG mice engraft primary samples with a much higher success and faster speed of engraftment. Samples which are rejected in NOD/SCID mouse strains are frequently engrafted in NSG mice (Agliano et al., 2008). NSG mice are currently the most widely used model in ALL biology with high rates of engraftment of a wide variety of leukaemic cell lines and primary samples (Diamanti et al., 2012, Ito et al., 2002, Agliano et al., 2008). Therefore, the extremely immunodeficient NSG mice with consistently superior engraftment rates

made these as an appropriated model for studies presented in this thesis.

3.1.2 Selecting leukaemic samples for xenograft experiments

Leukaemic cell lines are widely used in ALL research and have the benefit of producing well characterised pure leukaemic populations to study disease mechanisms. Furthermore, leukaemic cell lines are universally available and can be grown in large numbers and rapidly manipulated. Cell lines are suited to investigating effects of individual genes on leukaemia biology using gene transfection, silencing or inhibition of signalling. Use of cell lines is sometime necessary for ethical issues associated with human samples.

Published research on CNS disease in ALL is limited to the use of cell lines for xenograft experiments (Gunther et al., 1995, Holland et al., 2011, Cavallo et al., 1992). However, despite the many advantages offered by cell lines, they are not without limitations. For instance, aggressive subtypes of ALL may be considered interesting/challenging to investigate and may be chosen for establishing ALL cell lines. For example, 8 out of 10 ALL cell lines in American Type Culture Collection (ATCC) are derived from T lymphoblasts (ATCC, 2014). In addition, aggressive clones within a cell line may be more capable of surviving in long-term culture and may overgrow and replace the less aggressive clones in a Darwinian fashion. Furthermore, long term culture may induce technical artefacts. In an study performed by Drexler and colleagues (2003) up to 15% stocks of cells lines from original stocks were found to be cross-contaminated or mislabelled. Similar frequencies of mycoplasma infection have been found in stocks of cells lines (Drexler and Uphoff, 2002). This is a cause for concern since contaminated cell lines may be responsible for inconsistent and sometime contradictory results within published research. Therefore, care must be taken in clinical interpretation of data generated from xenograft models using cell lines.

In comparison to cell lines, primary leukemic cells better represent the genotypic and phenotypic heterogeneity found in leukaemia. Therefore, for the purpose of confirmation of results from the former, primary cells are often used to validate findings obtained from cell lines. Primary human ALL cells have poor viability after isolating from the body and may take longer to engraft. Nevertheless, for the questions addressed in this chapter it was necessary to use primary ALL samples.

3.1.3 Other factors influencing xenograft models

The method of transplantation can also play a key role in engraftment success. The Intrafemoral (IF) route of administration increases engraftment efficiency compared to intravenous (IV) injection of cells (Mazurier et al., 2003). Cells injected via IV route are distributed to various organs and only a fraction reaches the bone marrow niche. In addition, IF route of administration more closely mimics the natural history of human disease with leukaemia first expanding in the bone marrow and subsequently disseminating to the extramedullary tissues. A potential disadvantage of the IF route of administration is the risk of selecting leukaemic cells more suited to the bone marrow microenvironment. Theoretically, the bone marrow microenvironment may not be suited for the cells destined for the CNS microenvironment and coupled with the foreign nature of the murine microenvironment, such cells may be at a survival disadvantage. However, to date no proven literature exists to shed light on this issue.

Following removal from the patient bone marrow, ALL samples have limited viability and cryopreservation of samples may negatively affect engraftment. When engraftment rates in freshly isolated samples were compared with cryopreserved samples, mice were found to engraft fresh samples at a higher engraftment success rate, shorter time to engraft and with a much smaller transplant dose required (Greystoke et al., 2013). Despite the advantages of using fresh samples, cryopreserved samples may be the only practical option in many instances due to logistic issues.

Another crucial step in investigating CNS infiltration would be monitoring the progress of leukaemia in mice. Ideally, the xenograft experiments should allow leukaemic cells to proliferate and follow a course mimicking the natural history of human disease. If the experiments are stopped too early, the biological effects may be missed. On the other hand, if the leukaemia is allowed to proliferate for too long, the results may not truly represent the natural history of the disease course seen in patients. Therefore, a method of monitoring the progress of leukaemia has to be adopted. Monitoring of engraftment in real-time can be analysed with flow cytometry for markers expressed on human cells such as CD45 on blood sampled from tail vein (Cox et al., 2007). Direct bone marrow sampling can also be used for monitoring engraftment, however this method is technically challenging and potentially traumatic to the bone marrow. Alternatively, progress of leukaemia can be monitored by a non-invasive technique using transduction of luciferase gene in leukaemic cells before the transfer into mice (Fazzina et al., 2012, Bomken et al., 2013). This additional step prior to the transplant might risk cell death/selection of clones

within leukaemic cells.

In summary, the development of animal models that can closely recapitulate characteristics of leukaemia has been an ongoing effort. Research on CNS engraftment capabilities and patterns has produced inconclusive results due to differences in animal models and leukaemia types. To investigate biological factors that may affect CNS infiltration, a robust and reproducible *in vivo* model that more closely represents human disease is required. Therefore, an aim of this chapter was to develop and characterize a xenograft model of extramedullary disease using human primary leukaemic samples from patients with and without overt CNS disease. With this and additional xenograft materials obtained from collaborators, the key questions addressed in this chapter are:

1. Do leukaemic cells from patients with CNS-1 disease produce CNS infiltration in xenograft mice?

2. Is CNS disease in xenograft models secondary to bone marrow engraftment?

3. Do xenograft mice engrafted with small numbers of injected cells demonstrate CNS leukaemia?

4. Do xenograft mice engrafted with immunophenotypically sorted leukaemic subpopulations demonstrate CNS leukaemia?

5. Do cells retrieved from the CNS and bone marrow preferentially home to their original site when used in serial transplantation?

In addition to the above aims, a secondary aim of this chapter included *in vivo* expansion and retrieval of cells from the bone marrow and the CNS to address research questions described in chapter 4 and 5.

3.2 Development of a xenograft model of extramedullary disease

In this section, I have presented the methods and techniques used to establish an informative model of extramedullary infiltration of ALL. The general scheme of xenograft experiments is presented in Figure 3-1.

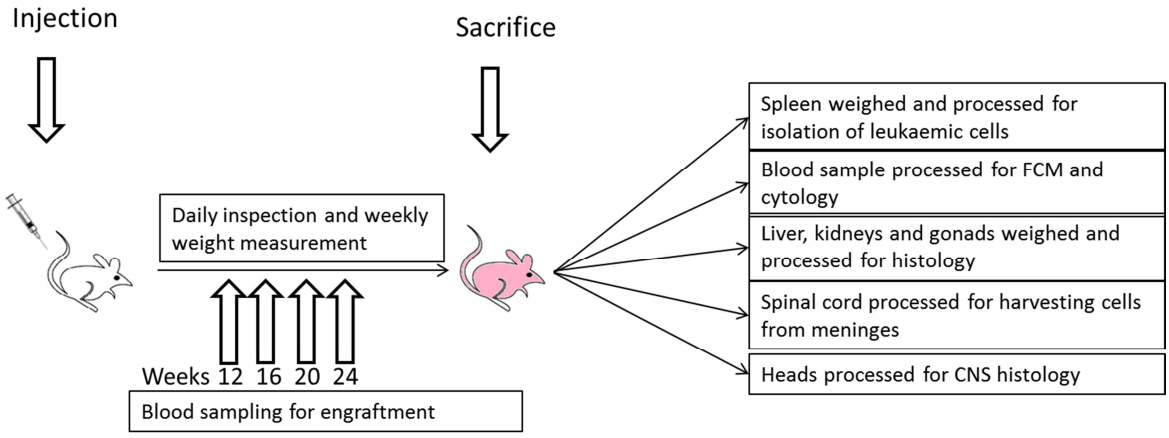

Figure 3-1 Scheme of transplantation experiments
Mice were injected with primary ALL cells using IV or IF routes and were followed for signs leukaemia by inspection, measurement of weights and peripheral blood sampling for circulating blasts. Upon signs of engraftment, mice were culled and organs processed for identification and isolation of leukaemic cells.

3.2.1 Primary leukaemic cells

Following informed consent, diagnostic bone marrow samples from children with BCP-ALL were purified by mononuclear cell enrichment using density gradient centrifugation (Ficoll-Paque; GE Healthcare, Amersham, UK) and cryopreserved in liquid nitrogen until use. Diagnostic bone marrow samples from children with ALL were obtained from the Leukaemia & Lymphoma Research (LLR) Childhood Leukaemia Cell Bank.

3.2.2 Mice

Due to the severe immunodeficiency, NSG mice are at a particular risk for infections. Strict infection control measures and close monitoring is necessary to avoid infection and death during the experiment. Therefore, the mice were kept in sterile isolators with autoclaved bedding, food and water. To ensure reproducibility of results, for each primary sample, at least 3 age and sex matched mice per patient sample. However due to low numbers of viable cells in one case (#6294) only two mice were used. Female mice are better transplant recipient than male mice (Notta et al., 2010). This effect is mediated by

the pro-survival effects of female estrogen hormones on transplant stem cells (Nakada et al., 2014). It was therefore decided to use female mice in the experiments wherever possible. Mice were transplanted at a median age of 10 weeks (range 6-16 weeks) as IF transfer of cells could be difficult in younger mice due to the narrow femoral canal.

3.2.3 Flow cytometry for identification of leukaemic cells

For xenograft experiments, it is essential to accurately identify human leukaemic blasts within the mouse blood and bone marrow. Although, NSG mice lack mature B- and T cells, they possess myeloid cells and haematopoietic precursors. Therefore, it may be difficult to discriminate these from leukaemic cells on microscopy. Expression of specific antigens on the surface of leukaemic cells allows identification for human cells by flow cytometry within mouse background. CD45 (leukocyte common antigen or LCA), CD10 and CD19 are considered lineage markers. High levels of CD45 are present on all human leukocytes and leukaemic cells whereas CD10 and CD19 expression levels together can easily identify leukaemic cells by their location as a cluster on flow cytometry dot-plot. Mouse cells may show some background fluorescence, however a distinct $CD45^{FITC}$ or $CD10^{FITC}/CD19^{PE\text{-}Cy7}$ positive cluster allows identification of human cells. Human specific anti-$CD45^{FITC}$, anti-$CD10^{FITC}$ and anti-$CD19^{PE\text{-}Cy7}$ were utilized. In experiments where it was intended to monitor engraftment, antibodies against CD10 and CD19 were used. In contrast, experiments where expression levels of additional markers were analysed, anti-$CD45^{FITC}$ antibodies were used. As example of gating strategy for CD10-CD19 based identification of leukaemic cells in murine bone marrow is presented in Figure 3-2.

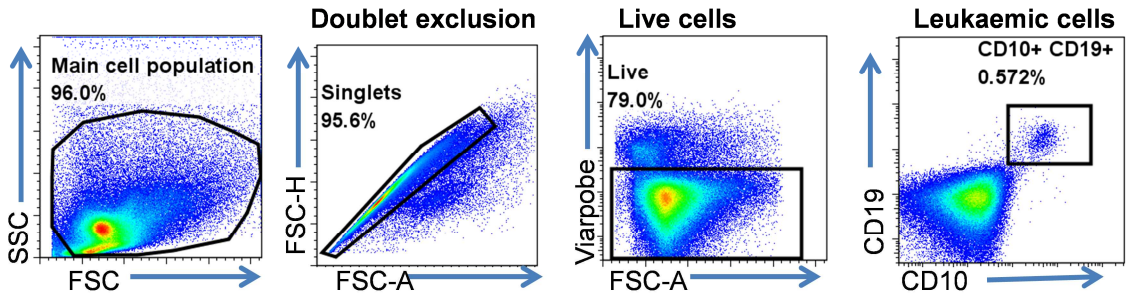

Figure 3-2 Monitoring for engraftment
Representative pseudocolour plots of cells from a xenograft bone marrow showing a cluster of human $CD10^{FITC}$ /$CD19^{PE\text{-}Cy7}$ positive cells. Arrows represent gating strategy. Forward- and side- scatter were used to exclude residual cell fragments and doublets. Dead cells were excluded using the dead cell exclusion dye 'viaprobe'. Data were analysed using Flowjo (version 4.0).

3.2.4 Determining engraftment at early and late time points

In the initial phase of the project, an estimation of the expected time required for successful engraftment could not be made. Therefore, a pilot experiment to determine the time required for engraftment was performed. Leukaemic cells from one patient (#4861) were injected into four age and sex matched mice. One pair of mice was culled at an early time point (12 weeks post injection) and a late time point (24 weeks) each. Mice organs were harvested and assessed for engraftment. Cells were isolated from the bone marrow, spleens and spinal cords, and RNA extracted and reverse transcribed to cDNA. Murine heads were processed for histology. Upon analysis by flow cytometry, no evidence for bone marrow, spleen or CNS engraftment was found in the early-time point mice. Leukaemic growth in mice may follow a lag phase preceding exponential growth. In order to analyse if the cells had failed to survive the new environment or whether submicroscopic levels were indeed present in the bone marrow, a more sensitive method such as PCR could be used (Gunther et al., 1995). Therefore, a TaqMan qPCR assay for human specific GAPDH primers was performed. Analysis by qPCR showed presence of human transcript in bone marrow samples from both mice was found whereas qPCR was negative for samples from the CNS. In the mice culled at late time point, flow cytometry revealed heavy engraftment of the bone marrow however no CNS infiltration was evident. These mice are included in the analysis for CNS engraftment presented in later sections.

Mouse Id	Sex	Age	Route	Cell dose	Duration (weeks)	BM engraftment	CNS engraftment
4861-1	F	11	IF	8×10^5	12	PCR only	No
4861-2	F	10	IV	1×10^6	12	PCR only	No
4861-3	F	10	IF	4×10^5	24	50%	No
4861-4	F	11	IV	2×10^5	24	82%	No

Table 3-1 Analysis of engraftment at early and late time point

3.2.5 Monitoring for engraftment

The results from experiments presented in section 0 implied that engraftment time in primary samples could be longer than observed in cell lines. In addition, leukaemic cells might grow exponentially following a lag phase. It was essential to monitor the progress of engraftment and to end the experiment at a suitable time point where the burden of leukaemia in the mice mimicked human disease course. Leukaemic cells in the bone marrow expand in the bone marrow and subsequently extravasate into circulation. Leukaemic progress was monitored by periodic blood sampling of the transplanted mice and analysis for CD10/CD19 positive cells. Blood samples from tail vein were obtained on

a maximum of four occasions. Blood cells were labelled with anti-human $CD10^{FITC}$/$CD19^{PE\text{-}Cy7}$ antibodies following red cell lysis. In addition, the mice were monitored for the development of leukaemia by daily inspection for clinical signs of leukaemia such as weight loss or hind-limb paralysis. The mice were culled for analysis when leukaemic cells were present at 10% of peripheral blood cells or higher. A representative graph showing percentage of leukaemic cells in blood along with weight measurements is presented in Figure 3-3. For pragmatic reasons, in cases with no circulating blasts till week 28 the mice were culled and organs analysed for engraftment.

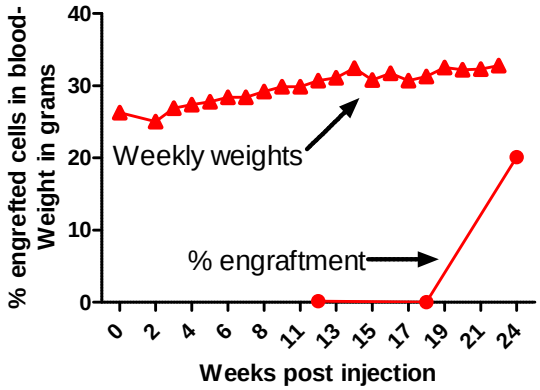

Figure 3-3 Kinetics of engraftment
Representative plots for the weight measurement and circulating blasts. Weights were measured on a weekly basis. Tail vein blood samples were taken at 12, 18 and 24 weeks and analysed for percentage of circulating leukaemic blasts. Percentage = $CD10^{FITC}$/$CD19^{PE\text{-}Cy7}$ cells/total circulating cells x100) Representative plot from one mouse (#5449-2)

In summary, in the initial phase of this project, BCP-ALL samples from CNS-3 and CNS-1 patients were obtained. The initial set of experiments revealed that the progress of leukaemia required careful monitoring and that it could be achieved with peripheral blood sampling and analysis for human specific CD10 and CD19 antibodies.

3.2.6 Analysis of bone marrow engraftment upon cull

During the course of the project, cells from 3 sets of 14 BCP- ALL patients (3 CNS-3 and 11 CNS-1) were used in a total of 43 NSG mice. Leukaemic samples from three cytogenetic subtypes, namely t(12;21), 11q23 (MLL-rearranged) and High Hyperdiploid were chosen. The cytogenetic subtypes represent high-risk (11q23), and low-risk (t(12;21) and high Hyperdiploid) BCP-ALL categories (Table 3-2).

Patent id.	CNS status	Sex	Age at diagnosis (years)	Cytogenetics	WCC ($x10^9$/l)	Outcome
#5094	CNS-3	F	2.1	t(12;21)	84.6	*CCR (6.7 years)
#4630	CNS-1	F	3.0	t(12;21)	103.6	CCR (7.7 years)
#4736	CNS-1	F	3.5	t(12;21)	113.3	CCR (7.3 years)
#5449	CNS-1	F	2.5	t(12;21)	62.2	CCR (6.3 years)
#5705	CNS-1	F	3.4	t(12;21)	221	CCR (5.7 years)
#6112	CNS-1	F	3.6	t(12;21)	120	CCR (4.7 years)
#6240	CNS-3	M	16.6	11q23	800	BM relapse at 8 months, died at 8 months
#4861	CNS-1	F	1.1	11q23	9604	CCR (5.7 years)
#5655	CNS-1	M	1.2	11q23	153	CCR (5.7 years)
#5980	CNS-1	M	2.7	11q23	70.9	not available
#5027	CNS-3	F	1.1	H Hyper	23.3	CCR (6.3 years)
#5969	CNS-1	F	3.0	H Hyper	24.8	CCR (5.2 years)
#6037	CNS-1	F	2.9	H Hyper	14.6	CCR (3.9 years)
#6294	CNS-1	F	1.8	H Hyper	24.5	CCR (4.3 years)

Table 3-2 Clinical and laboratory features of patients
For each sample from CNS-3 patient, 4-5 CNS-1 control samples matched for age, sex, WCC and cytogenetics were used *CCR= continuous complete remission. H. Hyper = High Hyperdiploid.

Transplanted mice were followed up for a median follow up time of 22 weeks (range 14-29 weeks). Upon culling, bone marrows were harvested from the femurs and analysed for leukaemia. If leukaemic cells were >2% of the bone marrow population, the mouse was considered to have successfully engrafted. During the course of experiments, 3 mice died of unexplained causes. In such cases, it was not possible to perform flow cytometry analysis for engraftment. Engraftment was assessed using histology on fixed bone marrow sections. These mice were included in the analysis.

Analysis for engraftment revealed that primary cells from 78% (11/14) patients had successfully engrafted in at least 1 out of 2-4 NSG mice transplanted. Cells from 6/6 t(12;21) patients, 3/4 11q23 and 2/4 high hyperdiploid ALL patients demonstrated successful engraftment in NSG mice. Overall, 2/3 CNS-3 samples and 9/11 CNS-1 samples successfully engrafted in NSG mice (Table 3-3). A comparison of engrafted vs unengrafted samples reveal no differences between the engraftment success and age, sex and clinical outcome (Table 3-3). A tendency of higher engraftment was seen in patients with a high WCC at presentation ($p=0.051$). Samples from 4/8 patients with WCC <100 engrafted in the bone marrow whereas all seven samples with WCC >100 showed successful engraftment. In the cytogenetic subtypes, all t(12;21) samples engrafted successfully while high hyperdiploid samples, another less aggressive subtype, revealed less efficient engraftment (2/4 samples). One 11q23 sample (#5980) also failed to engraft.

This could be due to differences in cell viability of individual samples, or the ability of these samples to proliferate in murine microenvironment.

Variable	Category	Engraftment + n=11	Engraftment - n=3	p-value*
		n	n	
Age	<10 year	10	3	0.588
	>10 years	1	0	
Sex	Male	2	1	0.571
	Female	9	2	
WCC	WCC <100	4	4	0.051
	WCC >100	7	0	
Cytogenetics	High Hyperdiploid	2	2	0.165
	t(12;21)	6	0	
	11q23	3	1	
CNS status	CNS-1	9	2	0.165
	CNS-3	2	1	
Outcome	**CCR	9	4	0.588
	Relapse	1	0	

Table 3-3 Association of successful engraftment with clinical feature
*chi square test, ** continuous clinical remission

Overall, 26/43 (60%) mice demonstrated leukaemia engraftment. A high concordance of leukaemia engraftment was observed in replicate mice. At least 2 replicate mice per primary sample demonstrated successful engraftment except sample #6294 which engrafted in one of the two mice transplanted.

The rate of engraftment was variable between the replicate mice injected with individual patient samples. Some samples exhibited marked similarity of speed of engraftment within replicate mice while others revealed more variable time to engraftment – as seen with variable standard deviations shown in Table 3-4.

Trial No	Route of injection	No of cells /mouse	Duration of experiment (median)	No of engrafted mice	engraftment rate(days mean +/- SD
#5094	IV (x2), IF (x2)	1 x10^6	17.5 weeks	4/4	109.2 +/- 19.8
#4630	IV (x1), IF (x2)	1-4 x10^5	29 weeks	2/3	205.29*
#4736	IV (x1), IF (x2)	6 x10^5	24 weeks	2/3	169.5 +/- 40.9
#5449	IV (x1), IF (x2)	2-4 x10^6	22 weeks	2/3	144.5 +/- 12.7
#5705	IF(x3)	1 x10^6	10 weeks	3/3	71.4 +/- 3.8
#6112	IF(x3)	1 x10^6	28 weeks	2/3	167.9 +/- 38.8
#6240	IF(x3)	8 x10^5	14 weeks	3/3	99.6*
#4861	IV (x2), IF (x2)	2-4 x10^5	12/24 weeks	2/4	156.5*
#5655	IF(x3)	2.3 x10^5	17 weeks	3/3	111.6 +/- 10.4
#5980	IF(x3)	1 x10^6	26 weeks	0/3	-
#6294	IF(x3)	5 x10^5	26 weeks	1/2	182*
#5027	IF(x3)	1 x10^6	28 weeks	0/3	-
#6037	IF(x3)	9 x10^5	27 weeks	0/3	-
#5969	IF(x3)	6 x10^5	28 weeks	2/3	197.8*
Total				**26/43**	

Table 3-4 Details of individual xenograft experiments
Samples are grouped by cytogenetic subtype; Engraftment was determined by FCM analysis of the BM samples at the end of experiment. *The mice were culled simultaneously

3.2.6.1 Engraftment with secondary transplants

As part of the model validation process, a pilot experiment was performed to determine the re-engraftment capabilities of primagraft cells harvested from mice. Primagraft cells from patient #4736 were subjected to secondary transplant using two NSG mice and followed up for engraftment. Leukaemic cells in both the mice successfully engrafted at 20 and 26 weeks post-transplant respectively. In general, serial transplant robustly reproduce engraftment kinetics. However, in a minority of cases may result in a faster rate of engraftment (Lock et al., 2002). This may reflect selection of an aggressive subclone with serial transplants.

In summary, the xenograft experiments show that 78% of BCP-ALL samples from CNS-1 and CNS-3 patients successfully engrafted in the bone marrow. There was some association of the success of engraftment with high WCC (>100 x 109/L) Secondary transplant demonstrated successful engraftment.

3.2.7 Analysis of extramedullary infiltration (excluding the CNS)

At the time of diagnosis, patients with leukaemia often present with hepatosplenomegaly, lymphadenopathy and sometimes with gonadal infiltration. Therefore, at the time of harvest, leukaemic infiltration in the spleen, liver, kidneys and gonads was analysed. All mice were examined for extramedullary involvement irrespective of bone marrow

engraftment to ensure no cases of isolated extramedullary disease were missed. Spleens were analysed for engraftment by weight measurements and flow cytometry for human CD10/CD19 positive cells, whereas the engraftment in liver, kidneys and gonads was assessed using histology. In order to identify patterns of leukaemic infiltration, immunohistochemistry for anti-human CD45 was performed in an initial batch of organs. Subsequently, as an understanding of the patterns of infiltration developed analysis by H&E staining was performed by two observers blinded for identifiers. The patterns of leukaemic infiltration in the organs are briefly described below.

3.2.7.1 Infiltration in the liver

Infiltration of the liver was seen in the majority of the engrafted mice. The leukaemic infiltration involved the perivascular regions and comprised of small clusters to large sheets of small round blue cells, mostly around the blood vessels and portal areas. In most cases, liver architecture was preserved. However, in some cases, extreme leukaemic infiltration resulted in distortion of liver architecture (Figure 3-4). This was paralleled with heavy engraftment in other organs such as the bone marrow and the spleen.

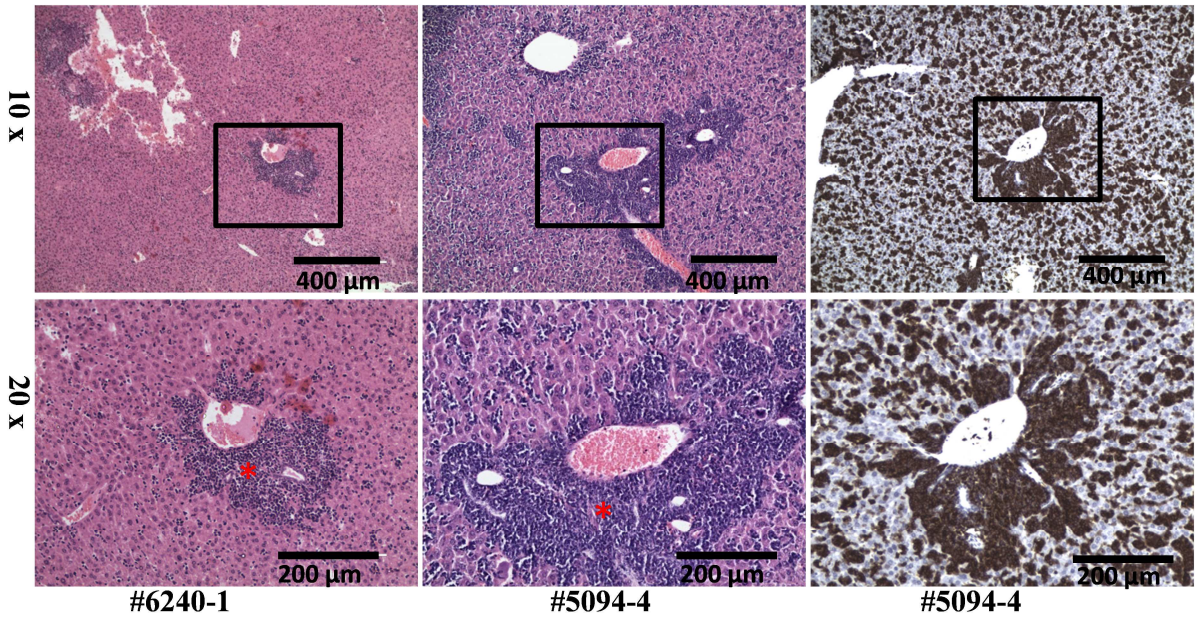

Figure 3-4 Pattern of leukaemic infiltration in the liver
Representative photomicrographs (H&E and CD45) from formaline fixed paraffin embedded liver sections from engrafted mice. Left column shows vascular infiltration by dark purple staining leukaemic cells in mouse #6240-1. Middle column shows extensive infiltration of leukaemic cells around the blood vessels and small clusters scattered in the parenchyma in mouse 5094-4. Right column depicts anti-human anti-CD45 staining from mouse #5094-4 showing leukaemic infiltrates. Top row (10x), bottom row (20x).

3.2.7.2 Infiltration in the spleen

In most of the cases with successful engraftment of the bone marrow, leukaemic infiltration of spleen was observed, manifesting as enlargement in size. In several mice, enlargement of the spleen size was not seen despite heavy bone marrow infiltration. For instance, in one case (#5969), 85% bone marrow engraftment was seen with only 3% engraftment in the spleen. This reflects that the splenic infiltration may be a secondary event after the replacement of the murine bone marrow with leukaemic cells. As can be seen in Figure 3-5, a higher correlation of bone marrow engraftment with splenic infiltration was seen (r^2=0.88). Slightly lower correlation of bone marrow engraftment with splenic weights was observed (r^2=0.75).

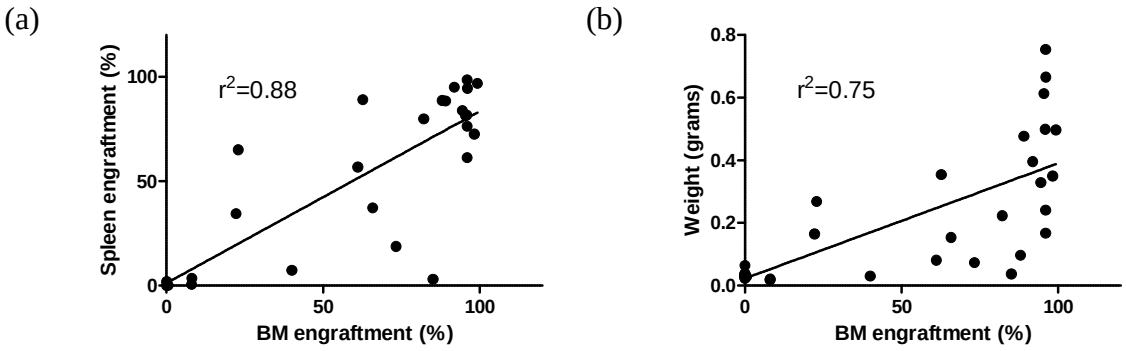

Figure 3-5 Correlation of BM engraftment with splenic infiltration
Percentage of splenic involvement compared to bone marrow engraftment. (a) % splenic engraftment compared to BM engraftment. (b) splenic weights compared to BM engraftment. Analysed using linear regression analysis. r^2=coefficient of correlation

3.2.7.3 Infiltration in the kidneys

Renal involvement was seen in the majority of the engrafted mice. The extent and pattern of infiltration varied with small clusters of leukaemic cells to large patches of leukaemic infiltrates. Leukaemic cells appeared to be clustered between the renal tubules and around blood vessels. In a few cases (e.g. #5655), peri-hilar and renal capsular infiltration was also seen. The renal tubular system was largely preserved with leukaemic infiltrates mainly in the interstitium.

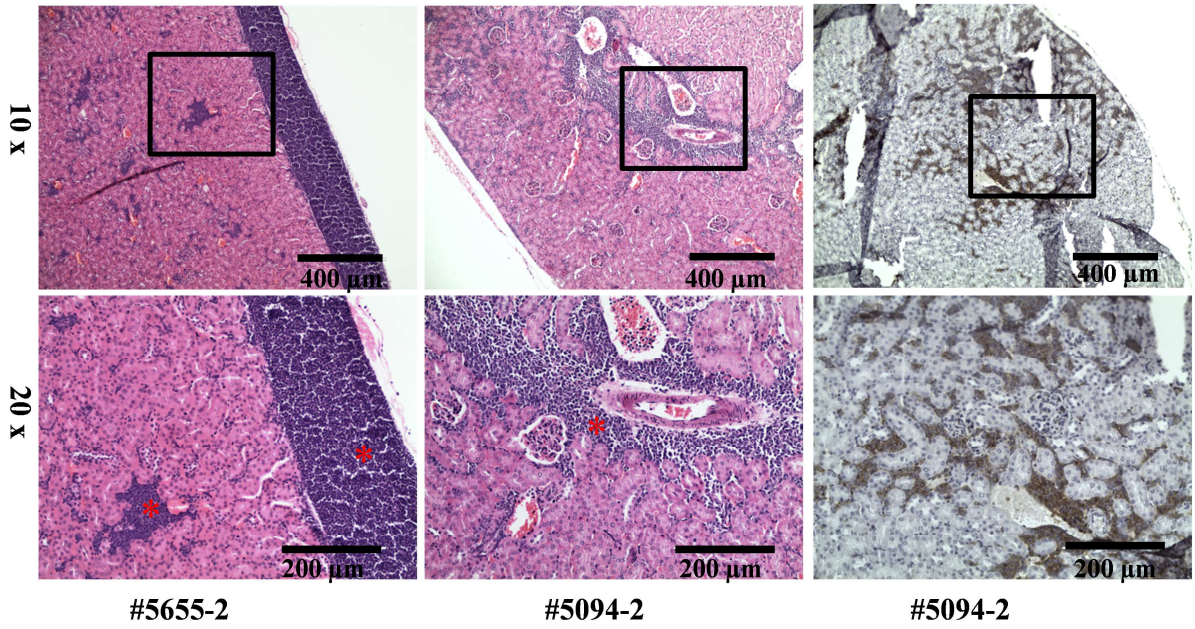

Figure 3-6 Pattern of leukaemic infiltration in the kidneys
Representative photomicrographs (H&E and CD45) from formaline fixed paraffin embedded renal tissue sections from engrafted mice. Left column shows pericapsular infiltration by dark purple staining leukaemic cells in mouse #5655-2. Middle column shows infiltration of leukaemic cells around the blood vessels sparing the renal parenchyma in mouse 5904-2. Right column depicts anti-human anti-CD45 staining from mouse #5094-2 showing leukaemic infiltrates. Top row (10x), bottom row (20x).

3.2.7.4 Infiltration in the gonads

Testes are conventionally considered sanctuary sites for leukaemia, ovaries on the other hand are generally not assessed routinely for leukaemia in girls at diagnosis or relapse. Given that the ovaries are counterparts to testes, assessment of ovarian leukaemia could provide useful insights into the biology of relapse in girls. Ovarian tissue generally contains small round blue cells which could make the analysis of leukaemic infiltration very difficult. Therefore, anti-CD45 staining was performed in all the gonads.

Histological examination of testes from 3 mice transplanted with samples from 2 patients (#5655, #4736) showed minimal infiltration of the testes. Leukaemic cells were seen scattered between seminiferous tubules sparing the parenchymal tissue. In one case, infiltrates were seen in the pericapsular fat around the testes.

Analysis of ovarian tissue revealed variable leukaemic infiltrate. No isolated ovarian infiltration was seen in mice which failed to engraft in the bone marrow. Overall, mice from 6 samples showed ovarian infiltration. A differential pattern of infiltration was observed in murine ovaries. For instance, mice engrafted with cells from patient #6240 exhibited diffuse infiltration with effacement of ovarian parenchyma, but no infiltration in mice engrafted with #6112 was observed. Such examples of specific tropism in the ovaries can be used to further investigate the mechanism ovary specific homing (Figure 3-7).

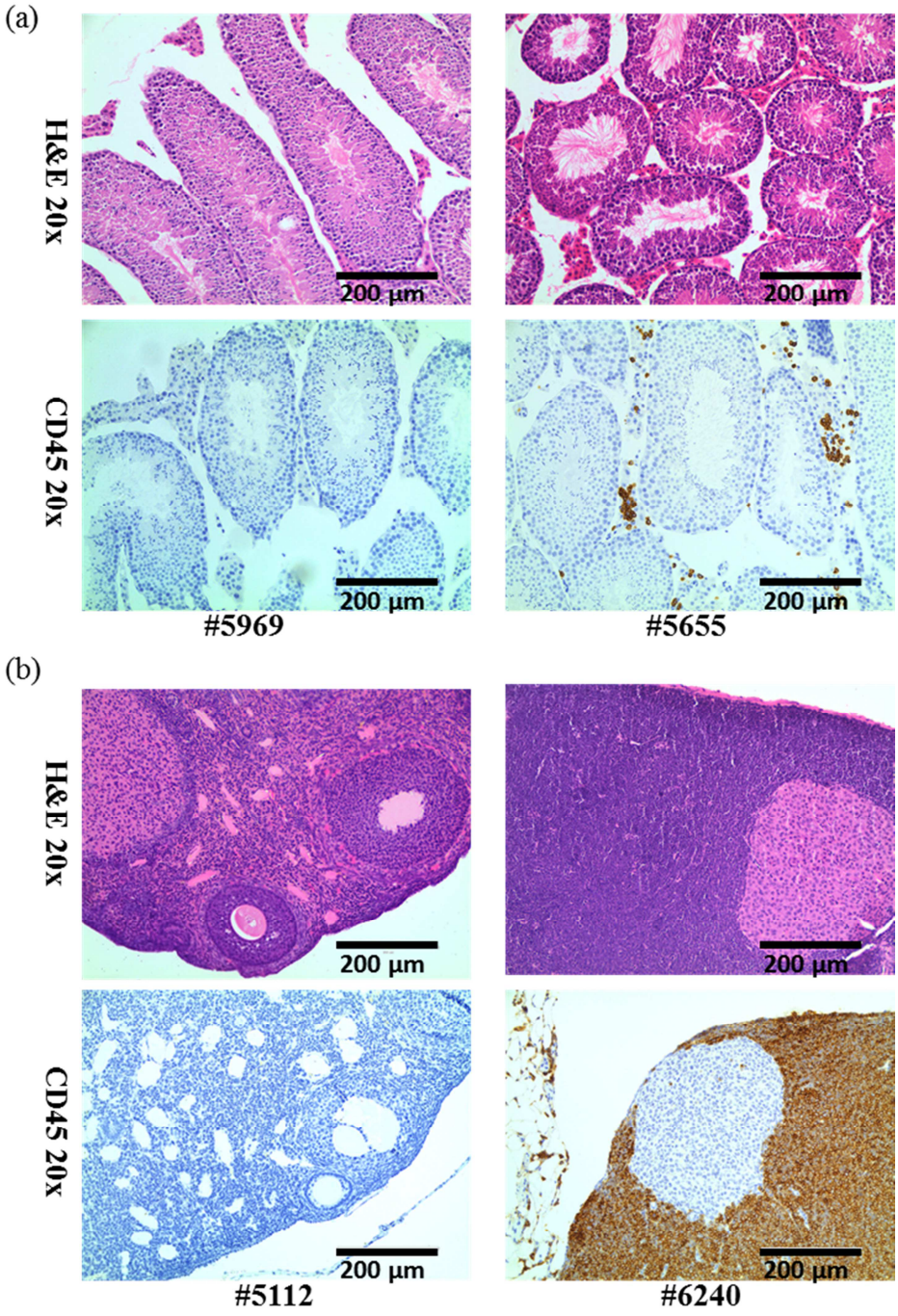

Figure 3-7 Histological sections of gonads showing patterns of leukaemic infiltration
(a) Photomicrographs of testes sections (Top row H&E, bottom row CD45) from mouse with no testicular infiltration (#5969, left) and combined bone marrow and testicular infiltration (#5655, right). (b) Ovarian tissue (Top row H&E, bottom row CD45) from mouse with no infiltration (#5112, left) and combined bone marrow and ovarian infiltration (#6240, right). Images at 20x magnification, scale bar = 200 µm.

3.2.7.5 Extramedullary tumours

Upon dissection of the engrafted mice, the abdominal and thoracic cavities were inspected for gross tumour infiltration. One case (#5655) revealed nodular tumour formation in the abdominal cavity. Upon histological examination, diffuse infiltration of the skeletal muscle and the wall of the uterus was observed (Figure 3-8). This case represents t(11;23) ALL which is a high-risk leukaemia. Uterine wall infiltration was observed in one mouse transplanted with cells from (#6240)

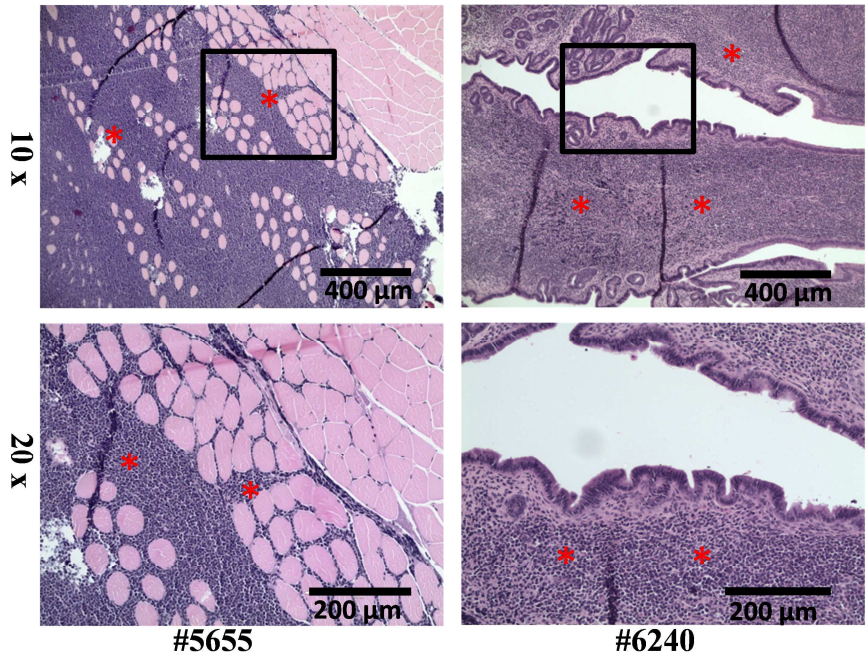

Figure 3-8 Histological sections of nodules showing patterns of leukaemic infiltration in skeletal muscle and uterus
Photomicrographs of H&E staining of a representative section from a nodule in an engrafted mouse showing leukaemic infiltration in skeletal muscle (left) and murine uterus showing infiltration in the smooth muscle wall (right) Top panels x10, bottom panels x20

In summary, at the end of xenograft experiments, murine samples from liver, spleen, testes and ovaries were evaluated for leukaemic infiltration. Leukaemic cells were present in the perivascular regions of liver and kidney specimen. Leukaemic infiltration in the spleen correlated closely with bone marrow engraftment. There was no evidence of isolated extramedullary infiltration in these organs. Solitary nodular deposits of leukaemic cells were found in two cases where leukaemic infiltration of uterine and skeletal muscle was observed.

3.3 Analysis of CNS infiltration

Quantification of CNS leukaemia can be challenging therefore various methods can be used all of which have certain advantages and disadvantages. Histology of whole brain with intact skull allows analysis of the leukaemic infiltrate within the various important landmarks such as brain parenchyma and the CSF compartment, flow cytometric analysis for cells isolated from the brain/spinal meninges identifies small numbers of leukaemic cells and finally quantification of leukaemic cells by immunohistochemistry using anti-CD45 antibodies on histological sections is widely used for assessment of organ infiltration. However, preliminary work in the laboratory using leukaemic cell lines established that quantification with immunohistochemistry was technically difficult. Initially, immunohistochemistry was utilized to identify leukaemic cells in the brain parenchyma however, due to the technical difficulties experienced this was superseded by histology using the H & E staining method. Murine heads with *in situ* brain were fixed and sliced coronally into 6 slices for analysing various regions of the brain. Two independent researchers visualized the brain sections with blinded slide identifiers.

3.3.1 Comparison of IV vs IF route of transplant

Route of injection may influence leukaemic infiltration of the CNS. In order to determine whether CNS infiltration was determined by the initial seeding of cells via IV route, or was more likely a secondary event following bone marrow engraftment, analysis of CNS infiltration in mice injected via IV and IF routes was carried out. CNS engraftment was seen 4/10 mice injected using IF route and 4/8 mice using IV route. No isolated CNS involvement was seen in any IF or IV injected mice (Table 3-5).

mouse ID	Route	BM engraftment	CNS engraftment	
4861-1	IF	PCR only	No	
4861-2	IV	PCR only	No	
4861-3	IF	50% FCM	No	
4861-4	IV	82% FCM	No	-
5094-1	IV	Yes (Histology)	Yes	
5094-2	IV	Yes (Histology)	Yes	
5094-3	IF	Yes (Histology)	Yes	
5094-4	IF	96% FCM	Yes	2 IF, 2 IV
4630-1	IV	0.5% FCM	No	
4630-2	IF	73.3% FCM	No	
4630-3	IF	8.1% FCM	No	
4736-2	IF	61.1% FCM	Yes	
4736-3	IV	22.2% FCM	Yes	1 IF, 1 IV
5449-1	IF	89.1% FCM	Yes	
5449-2	IF	96.1% FCM	Yes	
5449-3	IV	0% FCM	No	1 IF, 1 IV
6294-1	IV	0% FCM	No	
6294-2	IF	8.06% FCM	No	-
Total	**IF(x10) IV(x8)**			**4/10 IF, 4/8 IV**

Table 3-5 Comparison of IV vs IF route of transplant.
Leukaemic samples were injected via IV or IF route. Engraftment in the bone marrow was monitored with flow cytometry (FCM). In case #5094, histological examination was used. In case 4861, submicroscopic levels of leukaemia were determined using qPCR, however these mice were not considered to have engrafted.

In summary, CNS infiltration was seen in NSG mice injected with 2/2 CNS-3 and 6/9 CNS-1 samples. Leukaemic cells were observed within the CSF compartment and in the components of the BCSFB (choroid plexus and meningeal vein). Comparison of IF and IV routes of injection revealed similar rates of CNS infiltration in engrafted mice. Notably, no case of isolated CNS disease was noted with IV injections.

3.3.2 Frequency of infiltration in the CNS

To investigate the frequency and distribution of the CNS engraftment, brain sections were examined from NSG mice. 2/2 samples engrafted with cells from CNS-3 patients demonstrated significant involvement of the CNS in at least one of the transplanted mice. Notably, CNS involvement was also observed in mice engrafted with cells from 6/9 CNS-1 patients. Overall, CNS infiltration was seen in 8/11 primary xenografts (Table 3-4).

Trial number	CNS status	mouse ID	BM engraftment	CNS infiltration	CNS infiltration/ bone marrow engraftment/ mice transplanted
#5094	CNS3	5094-1	Yes	Yes	
		5094-2	Yes	Yes	
		5094-3	Yes	Yes	
		5094-4	Yes	Yes	4/4/4
#4630	CNS1	4630-1	No	No	
		4630-2	Yes	No	
		4630-3	Yes	No	0/2/3
#4736	CNS1	4736-1	No	No	
		4736-2	Yes	Yes	
		4736-3	Yes	Yes	2/2/3
#5449	CNS1	5449-1	Yes	Yes	
		5449-2	Yes	No	
		5449-3	No	No	1/2/3
#5705	CNS1	5705-1	Yes	Yes	
		5705-2	Yes	Yes	
		5705-3	Yes	Yes	3/3/3
#6112	CNS1	6112-1	Yes	No	
		6112-2	No	No	
		6112-3	Yes	Yes	1/2/3
#6240	CNS3	6240-1	Yes	Yes	
		6240-2	Yes	Yes	
		6240-3	Yes	Yes	3/3/3
#4861	CNS1	4861-2	No	No	
		4861-3	Yes	No	
		4861-1	No	No	
		4861-4	Yes	No	0/2/4
#5655	CNS1	5655-1	Yes	No	
		5655-2	Yes	Yes	
		5655-3	Yes	Yes	2/3/3
#5980	CNS1	5980-1	No	No	
		5980-2	No	No	
		5980-3	No	No	0/0/3
#5027	CNS3	5027-1	No	No	
		5027-2	No	No	
		5027-3	No	No	0/0/3
#6294	CNS1	6294-1	No	No	
		6294-2	Yes	No	0/1/2
#6037	CNS1	6037-1	No	No	
		6037-2	No	No	
		6037-3	No	No	0/0/3
#5969	CNS1	5969-1	Yes	No	
		5969-2	Yes	No	
		5969-3	No	No	0/2/3
Total	**3 CNS3, 11 CNS1**				**16/26/43 mice 08/11/14 samples**

Table 3-6 Analysis of CNS infiltration in primary xenografts

3.3.3 Pattern of leukaemic infiltration in the CNS

Histological patterns in majority of cases revealed leukaemic cells as continuous plaques within the leptomeninges with frequent involvement of the central sulcus. Leukaemic cells were frequently observed within the choroid plexus epithelium and the walls of the central meningeal vein (Figure 3.9). Leukaemic infiltrates were also observed in the cerebral ventricles. Notably, parenchymal involvement was rarely seen. However, when observed, parenchymal infiltration was disproportionately low compared to the extent of leptomeningeal plaques. In one sample (#5655), destruction of the cranial bone and direct communication with the CNS was also noted. In this case, leukaemic infiltrates were seen around the optic nerve and the eye ball.

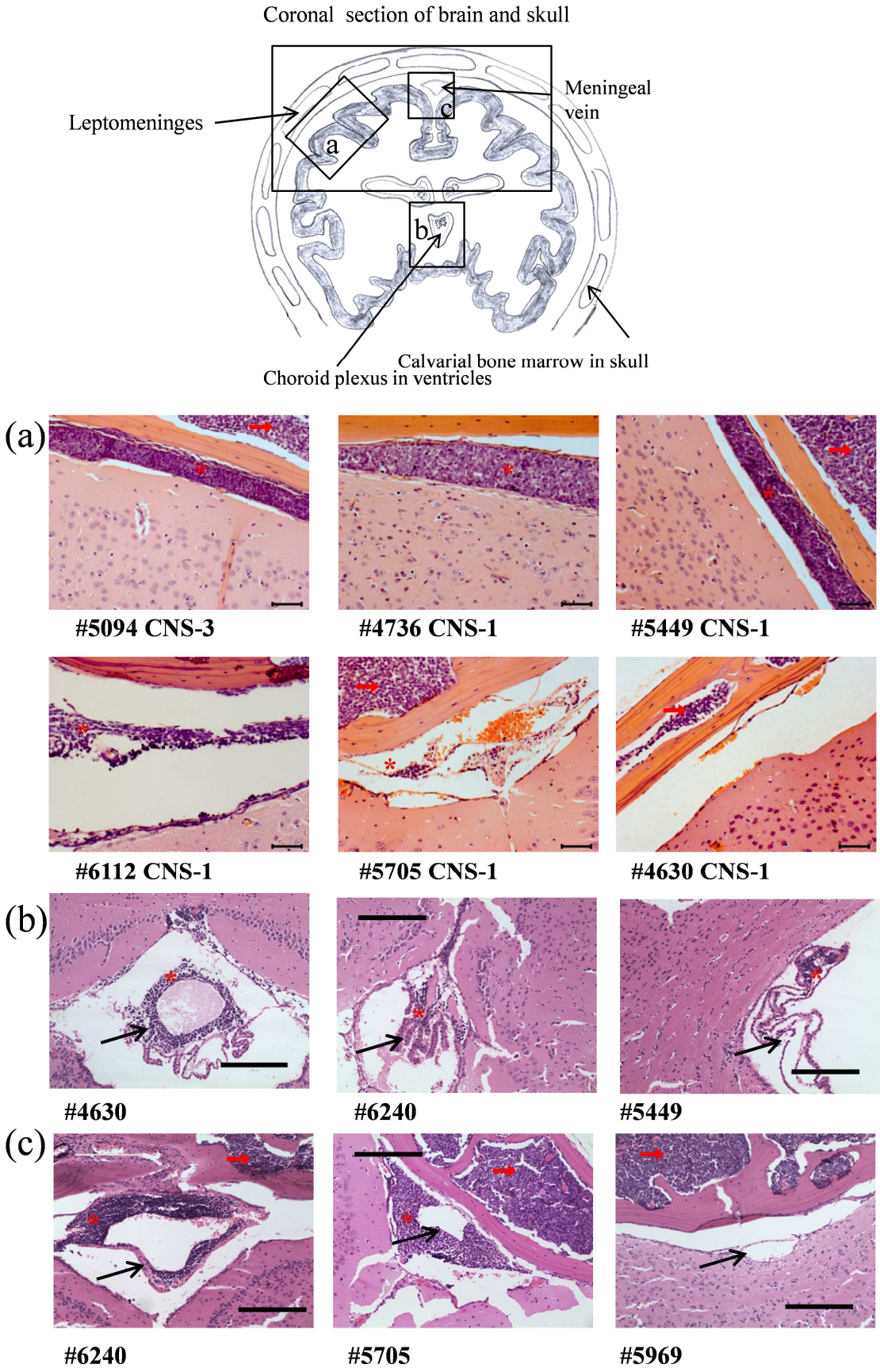

Figure 3.9 Patterns of leukaemic infiltration in the CNS.
(Top) Schematic diagram of a coronal section of brain showing common areas of leukaemic infiltration. Representative H&E sections from CNS of engrafted mice showing leukaemic infiltration (dark purple cells) in (a) leptomeninges from 1 CNS-3 and 5 CNS-1 cases, (x40, scale bar 50µm) (b) choroid plexus (black arrows) and (x20, scale bar 100 µm) (c) central meningeal vein (black arrows) (x20, scale bar 100 µm) showing leukaemic cells in the CNS (red star) and calvarial bone marrow (red arrows).

3.3.4 Validation using independent cohort of primary xenografts

The results presented above demonstrate the leukaemic cells from CNS-1 patients commonly infiltrate the CNS of xenografted mice. However, these only represent a small number of CNS-1 patients and a larger sample size was required for validation. Following a call for surplus brain samples from NSG mice xenografted with primary BCP-ALL samples within the childhood leukaemia research community, murine heads were obtained from 83 mice transplanted with 23 BCP-ALL samples. These samples belonged to various high and low risk cytogenetic subtypes. The majority of samples (16/18) belonged to CNS-1 category whereas 3 samples were from TLP +ve patients. The sample details are presented in Table 3-7. Examination of the murine heads revealed that out of the 4 samples which had failed to engraft in the bone marrow (1 mouse each), none of these showed isolated CNS engraftment. On the other hand, 19 samples had shown engraftment in at least one mouse. Out of these, CNS infiltration was observed in 17 samples. Similar patterns of leukaemic infiltration were observed in these models (Figure 3-9).

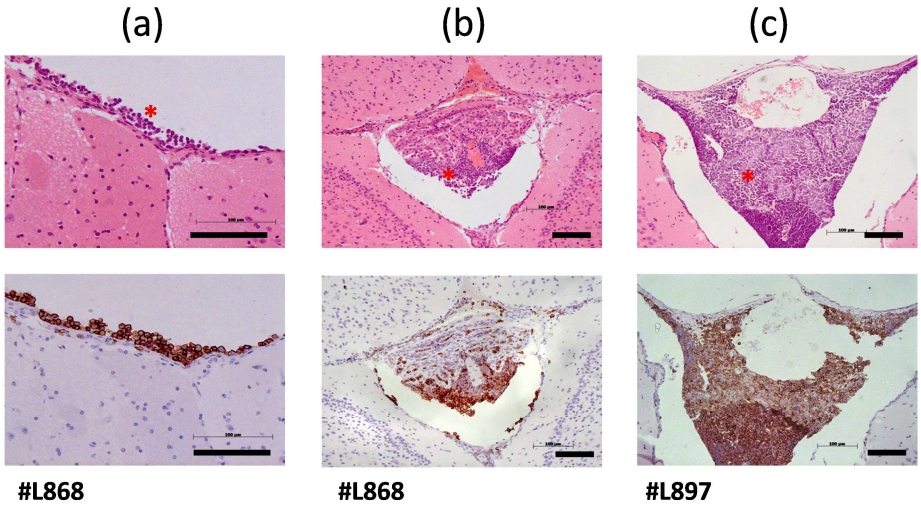

Figure 3-9 Pattern of CNS infiltration in NSG mice in the independent cohort of samples
Representative H & E (top) and corresponding CD45 staining (bottom) for mouse brain sections showing leukaemic infiltrates in the (a) meninges (x40) (b) choroid plexus (x20) & (c) central sulcus of the brain involving meningeal vein (x20). Leukaemic cells in H & E indicated with red stars. Scale bar= 50µm.

Sample ID	Age (yrs)	Sex	WCC*	Cytogenetic characteristic	CNS status	Outcome**	CNS infiltration/bone marrow engraftment/no. of mice examined
#L779	5.5	M	28.1	High hyperdiploiod	CNS-1	CCR (6.9 years)	5/5/5
#21819	1	M	76.8	t(7;9)dic(9;20)	CNS-1	Died (4 months, TRM),	1/1/1
#4540	1.99	M	71	t(9;22)	TLP +ve	CCR (5.1 years)	2/2/2
#M120	16.9	M	66.2	t(9;22)	TLP -ve	Isolated CNS relapse at 7 months, died at 12 months	2/2/2
#WB51	15.8	M	290.2	t(9;22)	CNS-1	BM relapse at 2 months then CCR 6.7 years	7/7/7
#HV101	3.3	F	64.4	t(9;22), del 9p	TLP +ve	CCR 5.7 years	2/2/3
#737c	4.7	M	263.7	BCR-ABL1 like	CNS-1	Relapsed at 28 months, died at 29 months	12/13/15
#758b	6	M	97.5	BCR-ABL1 like	CNS-1	CCR (8.5 years)	3/5/6
#L910	1.8	F	35.8	t(1;19)	CNS-1	CCR (2.5 years)	1/1/1
#BH01	9	M	24.4	t(1;19)	CNS-1	CCR (3.7 years)	0/3/3
#20580	18	F	1.8	t(8;14)	CNS-1	CCR (4.5 years)	4/5/6
#L868	10.6	F	36.1	iAMP21	CNS-1	CCR (3.75 years)	7/7/7
#L904	13.8	F	5	iAMP21	CNS-1	CCR (2.75 years)	0/2/2
#L707	16	F	39.1	t(17;19)	CNS-1	BM relapse at 5 months, died at 7 months	4/4/4
#11538	8	M	400	CRLF2 deletion	CNS-1	BM relapse the combined CNS and BM relapse. Died	4/4/4
#20755	4	M	5.9	del(14q)	CNS-1	Alive	0/0/1
#10671	13	M	2	IgH translocation	CNS-1	Alive	0/0/1
#20951	6.8	F	6.8	IgH translocation	CNS-1	CCR (5.75 years)	3/3/3
#20951	5	F	6.8	IgH transloacation	CNS-1	Alive	0/0/1
#L897	16.8	M	85.9	No result	CNS-1	CNS relapse at 17 months, then CCR (1.75 years)	4/4/4
#L920	4.4	F	22.2	No result	CNS-1	CCR (2.2 years)	1/1/1
#19794	NA	NA	NA	NA	NA	NA	0/0/1
#813Y	NA	NA	NA	NA	NA	NA	2/3/3
23 Primary samples							**64/74/83 mice 17/19/23 samples**

Table 3-7 Clinical characteristics and CNS engraftment

Leukaemic cells from 23 primary samples were transplanted into NSG mice using IF route (except #BH01 cells were injected IV into NOG.Cg-*Prkdc-scid Il2rg-tm1Sug*/JicTac (NOG) mice)* WCC x10^9/l, ** outcome censored at last follow-up. CCR= Continuous complete remission, TRM= treatment related mortality. Contributing researchers with affiliations: Klaus Rehe, Simon Bomken, Paul Sinclair, Katie Dormon, Dino Masic, Helen Blair, Lisa Russel, Olaf Heidenreich, Julie Irving, Josef Vormoor, (Northern Institute for Cancer Research, Newcastle University), Tracey Perry, Victoria Weston, Pamela Kearns (School of Cancer Sciences, University of Birmingham).

When the results from the two datasets were combined, 67.5% (25/37) samples across 13 different cytogenetic subtypes are found to have evidence for CNS involvement. In all samples, no case of isolated CNS infiltration was observed. When samples with no bone marrow engraftment were excluded from analysis, 83.3% (25/30) samples had evidence of CNS infiltration. 79.1% (19/24) samples from CNS-1 patients demonstrated CNS infiltration. The most consistent pattern of infiltration was presence of leukaemic plaques on the meninges, and less frequently in the ventricles, the choroid plexus and meningeal veins. Presence of leukaemia in these components suggests CNS disease to be primarily a CSF compartment disease. Taken together, these findings suggest that in majority of paediatric BCP-ALL cases, the leukaemic cells are capable of infiltrating the CNS, irrespective of the initial CNS status documented by CSF microscopy. Moreover pathological features in murine brains closely resemble clinical disease. Therefore, this appears to be a reproducible xenograft model provides an attractive resource for investigation of molecular mechanisms of CNS disease and pre-clinical studies on primary human samples.

In summary, murine head samples were obtained from research groups working with NSG mouse models of BCP-ALL. Histological examination of the CNS in BCP-ALL samples from CNS-1 patients across 13 different cytogenetic subtypes confirmed frequent CNS involvement, validating the earlier findings.

3.3.5 Analysis of CNS leukaemia in mice engrafted with limiting numbers of leukaemic cells

Limiting dilution experiments are performed in leukaemia research to investigate the frequency of leukaemia-initiating cells in xenograft models. For instance, in AML, not every cell is capable of repopulating a murine bone marrow and this property resides within a small infrequent population of leukaemia-initiating or leukaemic-stem cells. Theoretically, it is possible that CNS-infiltrating capability of leukaemic cells also resides within a minor subclonal population of leukaemic blasts (Figure 1-6). If so, transplanting a very small number of cells in NSG mice will decrease the likelihood of transfer of such a rare CNS infiltrating leukaemic population. As a consequence, mice engrafted with the limited cell numbers might not show CNS infiltration.

In order to investigate whether CNS infiltration was seen in mice engrafted with limiting cell numbers CNS sections were examined from mice engrafted with 10, 100, 1000, and 1500 cells from a cohort of 6 patients (#4540, #M120, #WB51, #HV101, #737c, #758b)

(Table 3-7). These mice were transplanted via IF route. The detailed methods and results on bone marrow engraftment are published (Rehe et al., 2013). Histological analysis of the brain sections revealed CNS involvement in majority of cases. Remarkably, mice engrafted with as low as 10 cells exhibited significant CNS infiltration in 5/6 cases. No relationship between cell numbers used for transplant and frequency of CNS infiltration was observed (Figure 3-10).

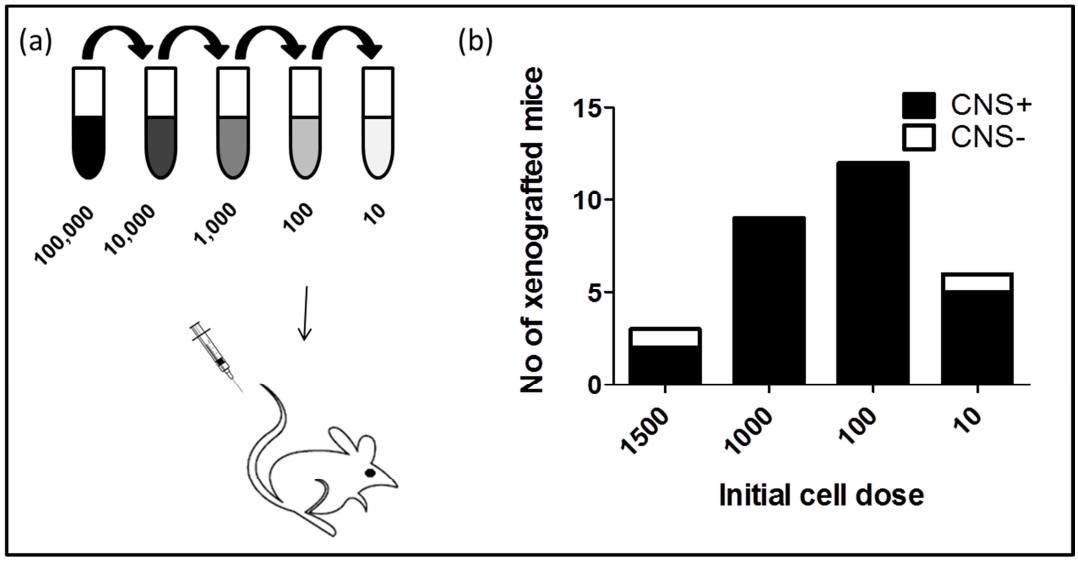

Figure 3-10 Frequency of CNS infiltrating leukaemic cells using limiting dilution experiments
(a) Serial dilution of cells prepared and injected into NSG mice (b) CNS involvement in mice engrafted with 1500, 1000, 100, 10 cells. Black bars represent the number of mice with CNS engraftment (CNS+). White bars represent the number of mice without CNS engraftment (CNS -). Brain samples contributed by Dr Klaus Rehe.

3.3.6 Analysis of CNS leukaemia in mice engrafted with immunophenotypically sorted cells

Leukaemic cells are characterized by aberrant expression of various surface molecules or CD-markers normally associated with maturing haematopoietic cells. Leukaemic cells expressing these markers mimic the various stages of lymphoid cell maturation. Within a leukaemic sample, cells with differential expression of markers associated with ‘immature’ and ‘more mature’ precursors can be identified. During normal haematopoiesis, maturing progeny of HSPCs are characterized by loss of CD34 expression, and acquire the ability to egress from the bone marrow to home to secondary lymphoid organs. It was hypothesised that an absence of CD markers associated with immature HSPCs (which normally reside in the bone marrow) on a leukaemic subpopulation may be associated with a migratory behaviour in this specific subset and mice engrafted with such subset may have increased frequency of CNS disease.

In order to assess CNS infiltrating capabilities of such subpopulations, murine CNS sections engrafted with leukaemic cells ($CD19^{+}$) from patients sorted into $CD34^{high}$ (immature) $CD34^{low}$ (more mature), $CD10^{low}$ (immature), $CD10^{high}$ (more mature) and $CD20^{low}$ (immature), $CD20^{high}$ (more mature) populations (Rehe et al., 2013) were examined.

Histological analysis of brain sections revealed CNS infiltration in mice engrafted with all immunophenotypic subpopulations. 6/7 mice engrafted with $CD34^{high}$ cells showed CNS infiltration while 7/7 mice with $CD34^{low}$ cells showed engraftment. Similarly, 3/4 mice with $CD20^{low}$ cells and 5/5 mice with $CD20^{high}$ cells engrafted in the CNS. All the mice engrafted with $CD10^{high}$ or $CD10^{low}$ subpopulations revealed CNS infiltration.

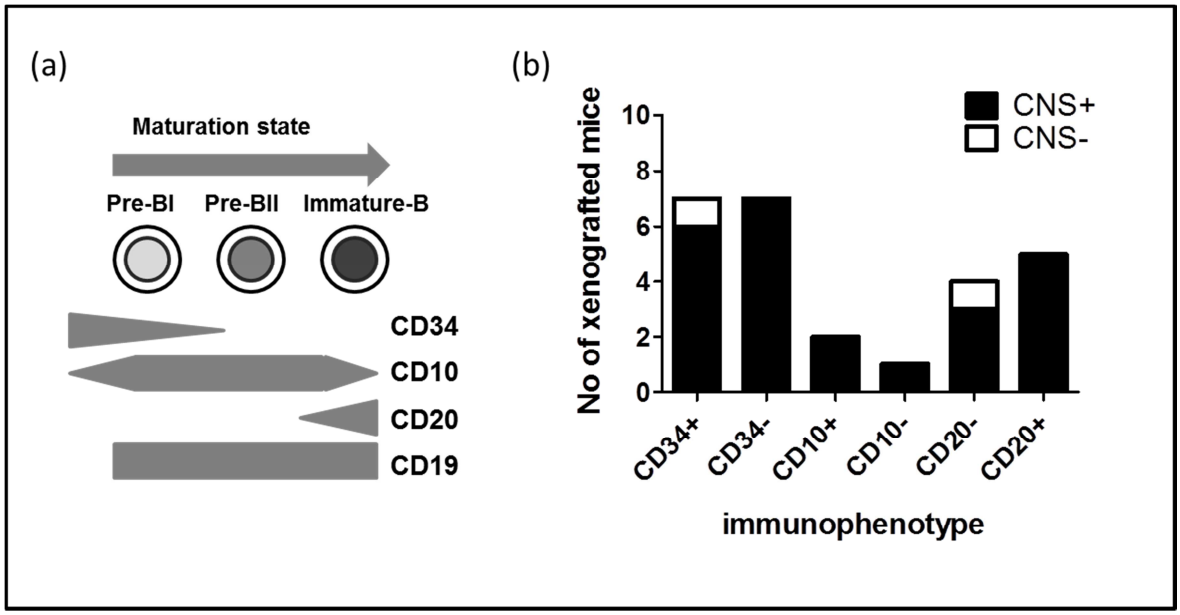

Figure 3-11 Frequency of CNS infiltrating leukaemic cells in various immunophenotypic subpopulations
(a) A schematic representation of CD markers associated with normal cell maturation stages. Leukaemic cells were sorted using FACS into various immunophenotypic subpopulations and subsequently injected into NSG mice via IF route. (b) CNS involvement in mice successfully engrafted with sorted subpopulations. Black bars represent the number of mice with CNS engraftment (CNS+). White bars represent the number of mice without CNS engraftment (CNS -). Brain samples contributed by Dr Klaus Rehe.

In summary, mice engrafted with very small numbers of leukaemic cells, and FACS-sorted immunophenotypic subpopulations demonstrated CNS infiltration. These results suggest that CNS infiltrating capability is a commonly present at least 1/10 leukaemic cells and is not limited to an immunophenotypic subpopulation.

3.3.7 Analysing CNS-specific tropism with serial transplants

It is possible that CNS infiltrating cells belong to an uncharacterised subpopulation not determined by the immunophenotype. Theoretically, cells isolated from the CNS would represent such a CNS-infiltrating phenotype. If these cells are re-transplanted into another generation of mice, higher CNS infiltration would be expected. Studies on breast cancer have identified bone and lung metastasizing subpopulations within a cell line. When cells were isolated from the organ of metastasis and serially transplanted, enriched populations with site-specific tropism were established. Notably, these studies have identified genetic and transcriptional differences between the parent and subpopulations (Minn et al., 2005, Kang et al., 2003).

It was hypothesised that by serially transplanting ALL cells isolated from the CNS of engrafted mice, an enriched population with CNS-specific tropism could be identified. It was also acknowledged that isolating cells from the CNS at an earlier time point would increase the likelihood of isolating a more pure population of cells. Therefore, it was decided to use 'luciferase' expressing REH cell line ($REH^{Luc\text{-}GFP}$) with the '*in vivo* imaging system (IVIS)'. In a mouse engrafted with luciferase expressing cells, injecting 'luciferin' into the mice will result in a chemical reaction detected as bioluminescence on the imaging system. A potential disadvantage of using this technology to assess CNS engraftment is that the luminescence signals from the calvarial bone marrow and the CNS cannot be discriminated.

First, $REH^{Luc\text{-}GFP}$ cells were injected IV into NSG mice and monitored for clinical signs of engraftment. The mice were culled upon engraftment and cells from their bone marrow (REH^{BM}) and the CNS (REH^{CNS}) were isolated. Subsequently, equal numbers of cells were injected into separate NSG mice (secondary transplants). Speed of onset of CNS infiltration was monitored using weekly bioluminescence imaging (Figure 3-12).

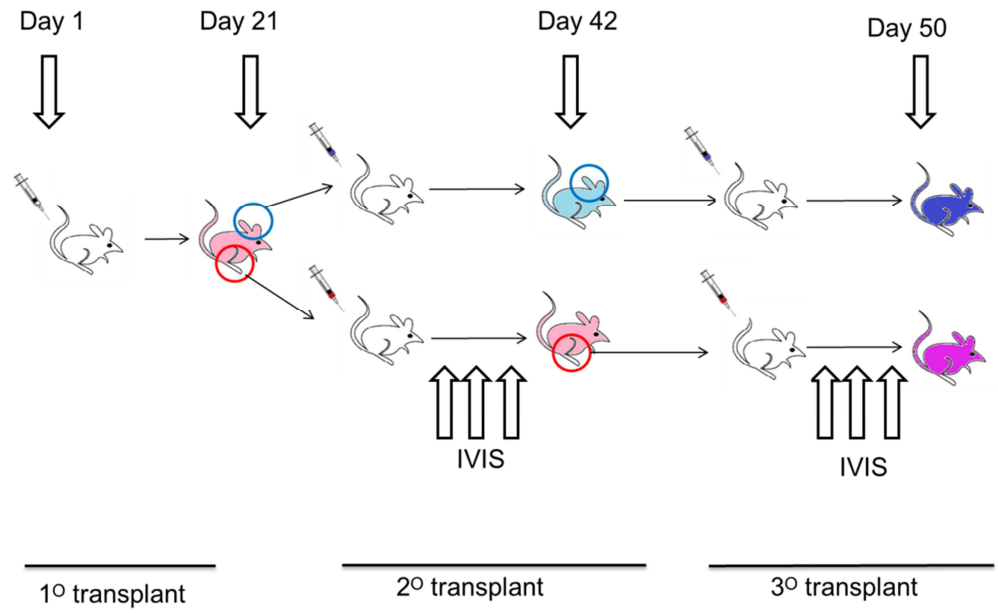

Figure 3-12 Experimental scheme for analysing CNS-specific tropism of REH$^{Luc\text{-}GFP}$ cells

Weekly measurements of bioluminescence revealed slightly higher (p-value =0.05) luminescence signal from the head in REH^{CNS} mice at day 8. This difference was reduced at days 15 and day 21. On day 21, the mice were culled. Examination of the end-point bone marrow and the CNS revealed similar engraftment in mice from both groups (Figure 3-13). The early CNS engraftment in REH^{CNS} mice suggested that specific entry of blasts into the CNS compartment could be an early event. It was therefore decided to investigate early time points for the tertiary transplant. Bone marrow and CNS isolated cells from secondary transplant mouse were injected into tertiary mice (3 in each group). Unfortunately, immediately after the injection, the mice in the CNS group suddenly became morbid and the two of the mice died in this group. It was presumed that during the process of harvesting leukaemic cells from the CNS, neuronal fibrillar material may have contaminated the cell suspension. As a consequence, intravenous injection of this cell suspension may have resulted in a compromise in pulmonary circulation causing death.

The method of leukaemic cell isolation required further optimization. Two methods of purification can be applied. CD19- magnetic bead sorting method allows isolation of CD19 positive leukaemic cells. However, it contains the risk of removal of CD19- negative leukaemic cells population. Alternatively, Ficoll based density purification system allows non-selective isolation of mononuclear cell population. Given the small number of cells retrieved from the CNS, initial attempts at this method resulted in loss of the majority of purified cells. Further experiments on serial transplantation from CNS retrieved cells could not be performed due to constraints of time.

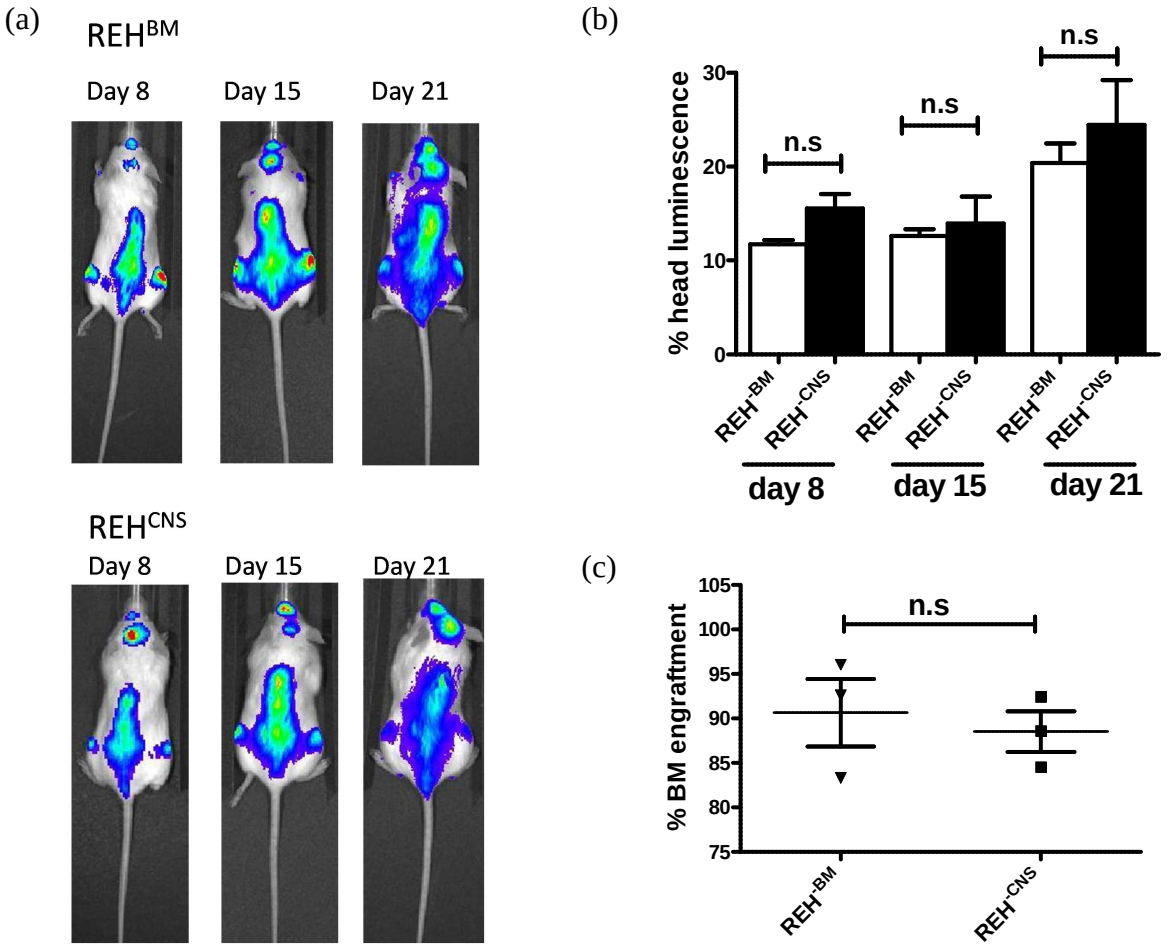

Figure 3-13 Analysis of CNS tropism of CNS- and BM-isolated cells using *in vivo* bioluminescence

(a) Representative serial IVIS images from mice demonstrating increasing leukaemic burden after injection with cells harvested from the BM (REH^{BM}) and the CNS (REH^{CNS}). (b) Measurement of bioluminescence signals from head plotted as percentage of luminescence from the head/whole body at day 8, 15 and 21 using the formula ($luminescence^{head}/luminescence^{total\ body}$ x100) (c) % bone marrow engraftment at the end of experiment measured using flow cytometry. Data represent mean ± SEM and were analysed using two tailed unpaired Student *t* test.

In summary, in this pilot experiment, serial transplant of $REH^{Luc\text{-}GFP}$ cells from the CNS showed a trend toward early site-specific tropism. However, the experiment had to be terminated due to sudden death of mice upon tertiary transplant.

3.4 Discussion

In order to assess the CNS engraftment potential of leukaemic cells, xenotransplantation of paediatric ALL cells from CNS-3 and CNS-1 patients into NSG mice were carried out. Murine heads and organs (liver, kidneys, spleen and gonads) of the transplanted mice were examined for the presence of leukaemic cells. The majority of mice transplanted with cells from CNS-3 and CNS-1 patients successfully engrafted in the bone marrow and the CNS. Analysis of the frequency and pattern of CNS infiltration by primary ALL cells identified a number of key points, the most important being that the majority of leukaemic samples from ALL patients possess the ability to infiltrate murine CNS irrespective of the CNS status of the patient. Further analysis of an independent set of primary xenografts showed a similar frequency and pattern of CNS infiltration in CNS-1 and CNS-3 cases. Histological examination of the brain sections revealed leukaemic cells in the CSF compartment predominantly manifesting as leukaemic plaques in the meninges. Cells were also noted in the choroid plexus epithelium and meningeal veins. Although previous reports have shown successful engraftment of primary leukaemic cells in immunodeficient mice, and have described CNS infiltration using cell lines, this study is the first of its nature to analyse CNS engraftment potential of primary leukaemic samples based on the CNS status of patients. Further studies identified that CNS-leukaemia initiating cells are present in a high proportion in ALL samples, irrespective of the immunophenotype of the leukaemic populations. Results from these models indicate that cells from CNS-1 patients indeed possess the capabilities to infiltrate the CNS. Very few CNS-3 cases were analysed in this study to identify the quantitative differences between CNS engraftment with samples from these two categories.

The majority of primary ALL samples successfully engrafted in severely immunodeficient NSG mice. The use of less immunodeficient strains has been shown to result in significantly poor engraftment rates (Agliano et al., 2008, Uckun et al., 1998). For instance, in a large study conducted by the COG, only 15.3% (104/608) of primary pre-B ALL samples were able to engraft SCID mice (Uckun et al., 1998). On the other hand, 90% engraftment of diagnostic bone marrow samples was seen when a more immunodeficient strain (NOG) was used (Kato et al., 2011). These cause considerable challenges for *in vivo* assessment of the relatively low-risk leukaemic subtypes. Therefore, NSG mice appear to be more suitable for studies in leukaemia research.

Analysis of the engraftment patterns demonstrated a number of key findings. Samples from

CNS-1 patients engrafted with a similar efficiency compared with CNS-3 cases. A high WCC was associated with higher engraftment. These observations are generally consistent with the published literature on xenografts using paediatric ALL cases from diagnosis and relapse. In the CCG study using paediatric high-risk BCP-ALL samples, successful engraftment correlated with a higher age, higher WCC, and clinical risk. Furthermore successful engraftment in mice were found to have a significant risk of relapse (Uckun et al., 1995). CNS status was not shown to be associated with different engraftment success rates (Uckun et al., 1998).

The xenograft model recapitulated several characteristics of human disease. These included retention within the bone marrow, replacement of the normal murine haematopoiesis, and dissemination into extramedullary organs. Most of the engrafted mice exhibited leukaemic infiltration of the liver and the spleen. This is in keeping with the clinical features observed in humans. The majority of ALL children show signs of overt leukaemic involvement of the liver and spleen evident by hepatosplenomegaly. The histological patterns of liver infiltration are in agreement with reports by other authors, both in mice (Kato et al., 2011) and humans (Raghavendra and Naveen, 2006, Vagace and Gervasini, 2011). On the other hand, overt gonadal involvement was seen in few cases. Clinical reports suggest that leukaemia may be present in the ovarian tissue at the time of diagnosis at submicroscopic levels (Greve et al., 2012), and can cause leukaemia in mice (Dolmans et al., 2010). While cryopreservation of ovarian tissue for subsequent post-treatment re-implantation is may be potentially useful for the preservation of gestation, it may bear the risk of leukaemic relapse. This study lends support for the cautious use of this strategy.

The analysis of CNS histology has shown that CNS engraftment is detectable microscopically in 83% of a variety of diagnostic primary pre-B ALL subtypes. Histological analysis provided crucial insights into the patterns of CNS infiltration by leukaemia and suggested key mechanisms by which leukaemic cells may gain access to this immune-specialized compartment. In all the murine samples with CNS disease, leukaemic cells were seen as cohesive plaques on the surface of meninges. This indicates that CNS disease is primarily present in the cerebrospinal compartment rather than the brain parenchyma itself. Involvement of the choroid plexus suggests that leukaemic cells transit across the BCSFB. Involvement of the meningeal vein, located in the CSF compartment, was also frequently noted. Leukaemic cells were observed within the wall of the vein. However, it is difficult to comment whether meningeal vein involvement was a

secondary event with CNS leukaemic cells infiltrating the vein to access the circulation or was the other way round. Presence of leukaemic cells within the walls of meningeal vessels points to the possibility of direct extension of leukaemic cells across the vessel wall. Furthermore, direct extension of leukaemic cells from the calvarial bone marrow cannot be excluded. Clinical studies suggest this as a possible gateway for leukaemic cells into the CNS (Gunther et al., 1995, Thomas, 1965, Cavallo et al., 1992).

In an earlier report on a mouse model of CNS disease, using T-ALL cell lines with immunodeficient nude mice, CNS infiltration of leukaemic cells was seen as a direct extension from the calvarial bone marrow. The authors argue that expansion of leukaemia in the bone marrow causes erosion of the cortical bone and a communication with the CSF space (Cavallo et al., 1992). In another model using BCP-ALL cell line Nalm6 in SCID mice, the authors showed similar findings suggesting direct extension from spinal and calvarial marrow with the CNS. However, in these experiments, clinical signs of CNS infiltration (e.g. hind-limb paralysis) were used (Gunther et al., 1995). In these studies, differences in the immune status of the mice, and the type of leukaemic cells used and clinical assessment of progress of CNS disease may have resulted in an aggressive and late-stage disease pattern. More recently Holland et al. (2011) documented that BCP-ALL cell line SD1 produced invasive disease with infiltration of the CNS parenchyma and optic nerve in SCID/beige mice. In the studies presented in this chapter, in mice engrafted with sample #5655, not only infiltration of the optic nerve and bulb was seen, also infiltration of the skeletal muscle was noted. This might represent a particularly invasive subtype of leukaemia. This highlights the fact that ALL is a heterogenous disease and observations from cell lines may not be applied to the spectrum of characteristics seen in primary samples.

There was some indication that leukaemic blasts isolated from the CNS preferentially home to the CNS when re-transplanted in the mice. This represents a pilot experiment using a BCP-ALL cell line and needs further investigation using primary cells and a larger sample size. If this line of investigation demonstrates any differences between the CNS engraftment potential of bone marrow and CNS engrafting cells, molecular mechanisms guiding these differences should be investigated.

An aim of this chapter was to analyse if CNS engraftment was an intrinsic property of all the leukaemic cell population or a property of a subclonal population within the bulk of disease. The studies performed indicate that CNS infiltration capability was present in mice engrafted with as low as 10 cells. In addition, mice engrafted with sorted cells at

various maturation stages also demonstrate CNS infiltration. The fact that leukaemic infiltration was identified in a wide variety of leukaemic subsets, clinical phenotypes, and low inoculation dose, indicate that CNS engraftment capability is common and not restricted to a rare subclone.

Previous research on CNS disease using xenograft models has been largely limited to ALL cell lines and has produced conflicting results. The differences in CNS infiltration capability and patterns of CNS infiltration may be due to the residual immune status of the mice and the nature of the samples used. The xenograft models presented in this chapter indicate that CNS disease using primary BCP-ALL samples mimics human CNS disease. However, modelling human disease across species require careful interpretation of results. NSG mice lack a competent immune system and therefore do not represent leukaemia in an immunocompetent human. The possibility that leukaemic infiltration of the CNS in mice may be due to lack of leukaemia-immune system and leukaemia-CNS microenvironment interactions cannot be ruled out. In addition, direct monitoring of the progress of leukaemia in the CNS could not be performed. Furthermore, analysis of the CNS infiltration is a non-quantitative method and cannot measure the extent of CNS leukaemia. Nevertheless, the consistent observation of CNS leukaemia in the majority of samples engrafted with a variety of primary BCP-ALL samples provides evidence that BCP-ALL cells from CNS-1 patients possess the capability to infiltrate the CNS.

4 Investigating leukocyte trafficking molecules in association with central nervous system disease in acute lymphoblastic leukaemia

4.1 Introduction and aims

Leukocyte entry into an extravascular compartment requires a coordinated expression of chemokine receptors, selectins and integrins which provide the molecular 'address code' for tissue specific entry of leukocytes. Chemokine receptors provide tissue selectivity in this process. For instance, circulating haematopoietic precursors require CXCR4 to home to the bone marrow (Nagasawa et al., 1996) and CCR7 to enter the thymus (Kwan and Killeen, 2004, Zlotoff et al., 2010). In similar ways, it is suggested that leukaemic cells might disseminate to extramedullary organs by utilisation of such normal physiological trafficking mechanisms. Indeed, evidence of a single chemokine receptor-ligand interaction being important for site-specific dissemination has been shown in murine models of cancer metastasis in melanoma (Murakami et al., 2002) and breast cancer (Muller et al., 2001). Furthermore CXCR4 expression in ALL has been linked to dissemination to liver (Kato et al., 2011) and spleen (Crazzolara et al., 2001). T-ALL cells expressing CCR7 efficiently infiltrate the CNS in comparison with CCR7 negative cell lines, suggesting a role for CCR7 in T-lymphoblast entry into the CNS (Buonamici et al., 2009). However, no such associations have been identified in BCP-ALL.

It is hypothesised that leukaemic cell entry to the central nervous system (CNS) compartment is the result of interactions of a distinct set of leukocyte trafficking molecules on leukaemic cells and the CNS vascular components. Such CNS-leukaemia initiating cells may represent a minor subclone within the bulk disease. Despite the observation that mice engrafted with FACS sorted immunophenotypic subpopulations show CNS leukaemia, a peculiar leukaemic phenotype with the 'CNS address code' may exists. Identifying these mechanisms may be useful as biomarkers for CNS infiltrating capability of leukaemic cells. These can then potentially be used as therapeutic targets. Identification of such a sub-population may provide important clues on the biology of CNS disease.

Figure 4.1 illustrates these hypotheses.

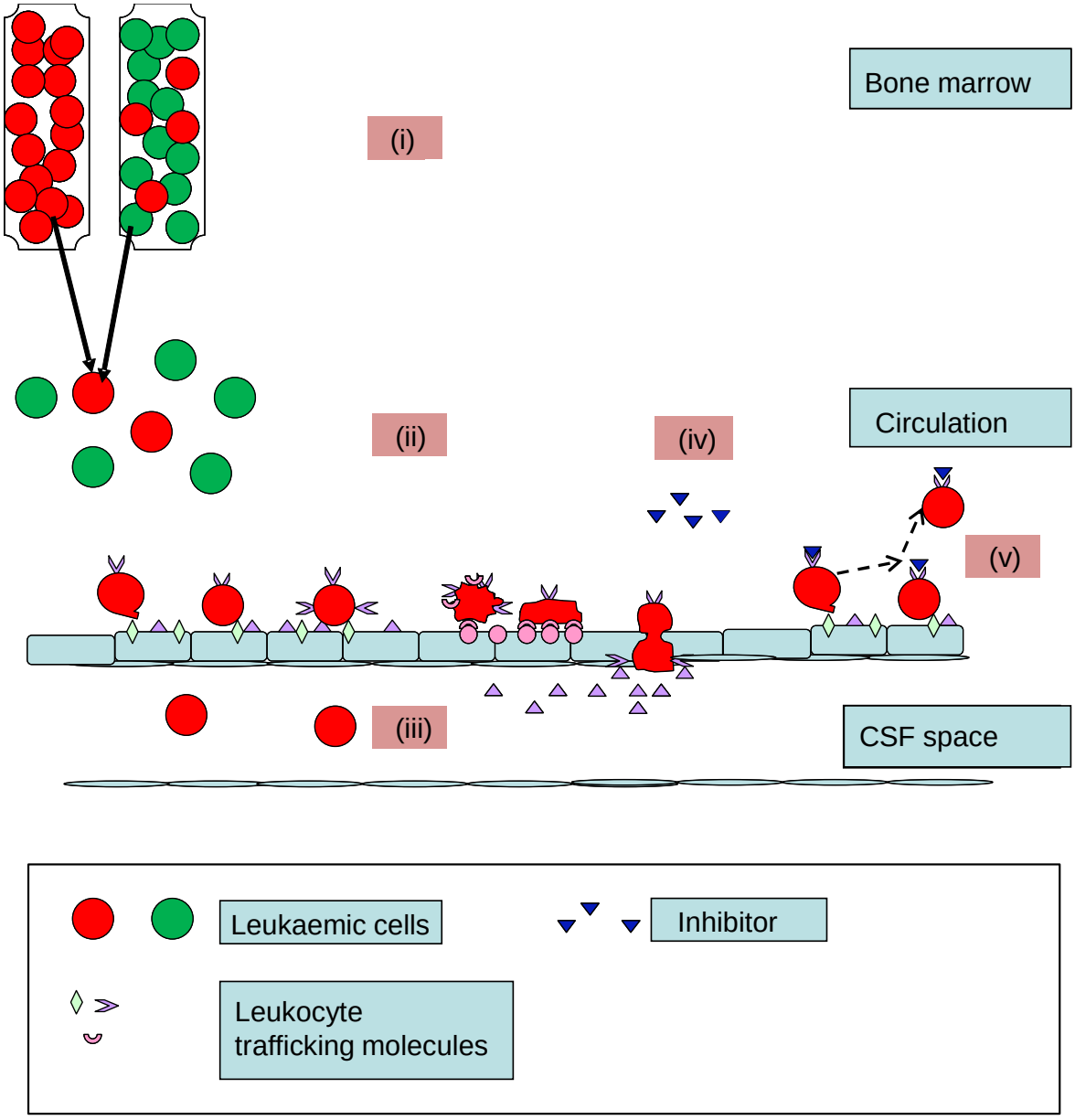

Figure 4-1: The potential utility for identifying mechanism of CNS entry of leukaemic cells.
(i) The ability to enter the CNS compartment may reside in the bulk population (left) or a minor sub-clone (right) of cells. Leukaemic cells with the specific address code for CNS entry (red) in the BM. (ii) Leukaemic cells enter the circulation and come in contact with vessels at the blood-CSF barrier. (iii) Using the leukocyte trafficking molecules, cells transit across the blood-CSF barrier to enter the CSF space. The molecules can be used as biomarkers for CNS disease potential. (iv) Inhibiting the molecule required for CNS entry. (v) The molecules required for CNS entry are inhibited, preventing the cells to enter the CSF space.

To examine the role of leukocyte trafficking molecules in determining CNS disease in BCP-ALL, leukaemic cells were transplanted into NSG mice. Samples with rapid infiltration of the CNS in mice were analysed for expression of candidate leukocyte trafficking molecules. In addition, cells retrieved from primary xenografts (primagrafts) (chapter 3) were utilized for addressing the research questions presented in this chapter.

The primary questions addressed in this chapter are:

- Is there an association between expression of candidate leukocyte trafficking molecules and CNS disease in xenograft models of BCP-ALL?

- Can a CNS-infiltrating phenotype be identified based on expression levels of leukocyte trafficking molecules?

During the course of experiments performed to address the primary aims, an interesting phenomenon was observed. BCP-ALL leukaemic cell line SD1 exhibited minimal CXCL12 mediated migration despite the presence of surface CXCR4. Given that similar phenomenon is seen in maturing lymphoid cells enabling them to enter the circulation, it was decided to investigate the nature of migration defect in SD1 cells.

- Therefore, a secondary aim of this chapter was to investigate the dysfunctional CXCR4-CXCL12 axis in SD1 cells. These results are presented in detail under section 4.4.

4.2 Differential CNS homing and chemokine receptor expression in BCP-ALL cell lines

Paediatric BCP-ALL cell lines SD1, Sup B15 and REH differ in their ability to infiltrate the CNS when engrafted in immunodeficient mice. SD1 cells are known to produce CNS disease whereas Sup B15 and REH do not show evidence of CNS infiltration in SCID/beige mice (Holland et al., 2011). SD1 and Sup B15 carry the BCR-ABL1 translocation – a cytogenetic risk factor for CNS disease. Given the different CNS engraftment potential of these cell lines, they could be a suitable case-control model for investigation of CNS disease and were therefore chosen for our studies. In addition, the cell line SEM with unknown CNS engrafting potential was utilized. Characteristics of leukaemic patients these cell lines were generated from are presented in Table 4-1.

Cell line	Patient age	Sex	Presentation /relapse	Cytogenetics	Immuno-phenotype*	References
SD1	NA	F	Presentation	t(9;22) m-bcr**	CD34+, CD10-, CD19+, Cy79a+	Dhut et al. (1991)
Sup B15	9 years	M	Second relapse	t(9;22) m-bcr	CD10+, sIg -	Naumovski et al. (1988)
REH	15 years	F	Relapse	t(12;21)	CD34+, $CD10^-$, CD19+, Cy79a+	Alkatib et al. (1985)
SEM	5 years	F	Relapse	t(4,11)	CD34-, CD19+	Greil et al. (1994)

Table 4-1: Clinical and cytogenetic features of BCP-ALL cell lines
*Williams et al.(2014) **minor-breakpoint cluster region

NSG mice were injected with the cell lines via tail vein injections and monitored for the signs of CNS infiltration (hind limb paralysis, or other neurological symptoms) or overt leukaemia (weight loss, ill health) – upon which the mice were culled. Examination of the xenografted mice revealed bone marrow engraftment and distinct patterns of extramedullary involvement. Mice injected with Sup B15 cells showed gross ovarian infiltration, REH-engrafted mice demonstrated enlargement of the spleen and the liver while SD1-engrafted mice revealed enlarged kidneys and relatively smaller spleens in comparison with other xenografts. This implies that the organ infiltration is not merely a reflection of non-specific invasive behaviour, but is reflective of a more directed migration to distinct extramedullary organs. Mice injected with SD1 cells rapidly developed signs of CNS infiltration (23.1±1.5 days) and heavy CNS infiltration on histological examination. Remarkably, mice engrafted with other cell lines also exhibited signs of CNS leukaemia, although the time to hind limb paralysis was significantly delayed. SEM engrafted mice developed hind-limb paralysis at a median of 30.5±2.0 days while REH and Sup B15

produced CNS disease at 35.5 ± 2.9 and 46.8 ± 5.1 days respectively (Figure 4-2a). CNS disease in these mice was confirmed by histological examination of the brains. These observations were in contrast to the study reported by Holland et al. (2011). This could perhaps be due to differences in animal models. SCID/beige mice used by the researchers are relatively poor recipients of human cells (Lepus et al., 2009). The residual immune system in the SCID/beige mice might have adversely affected engraftment of REH and Sup B15 cells, evident by reduced overall leukaemic burden in Sup B15 injected mice (Holland et al., 2011).

In order to test if the repertoire of candidate leukocyte trafficking genes expressed by the cell lines could provide clues to the phenotypic 'address code' required for cells to enter the CNS, a screening approach using TaqMan low density array (TLDA) technology was undertaken. Using TLDA plates, gene expression of 30 selected chemokine receptors, selectins and integrins was investigated. As shown in Figure 4-2b, analysis of relative gene expression revealed notable differences in the cell lines. SD1 cells demonstrated more than 50-fold upregulation of CCR3, CCR6, interleukin-15 (IL-15), Integrin-αL (ITGAL) and PSGL1. On the other hand CXCR4, CCR4 and Integrin-β1 (ITGB1) transcripts expression was significantly down-regulated in SD1 in comparison Sup B15.

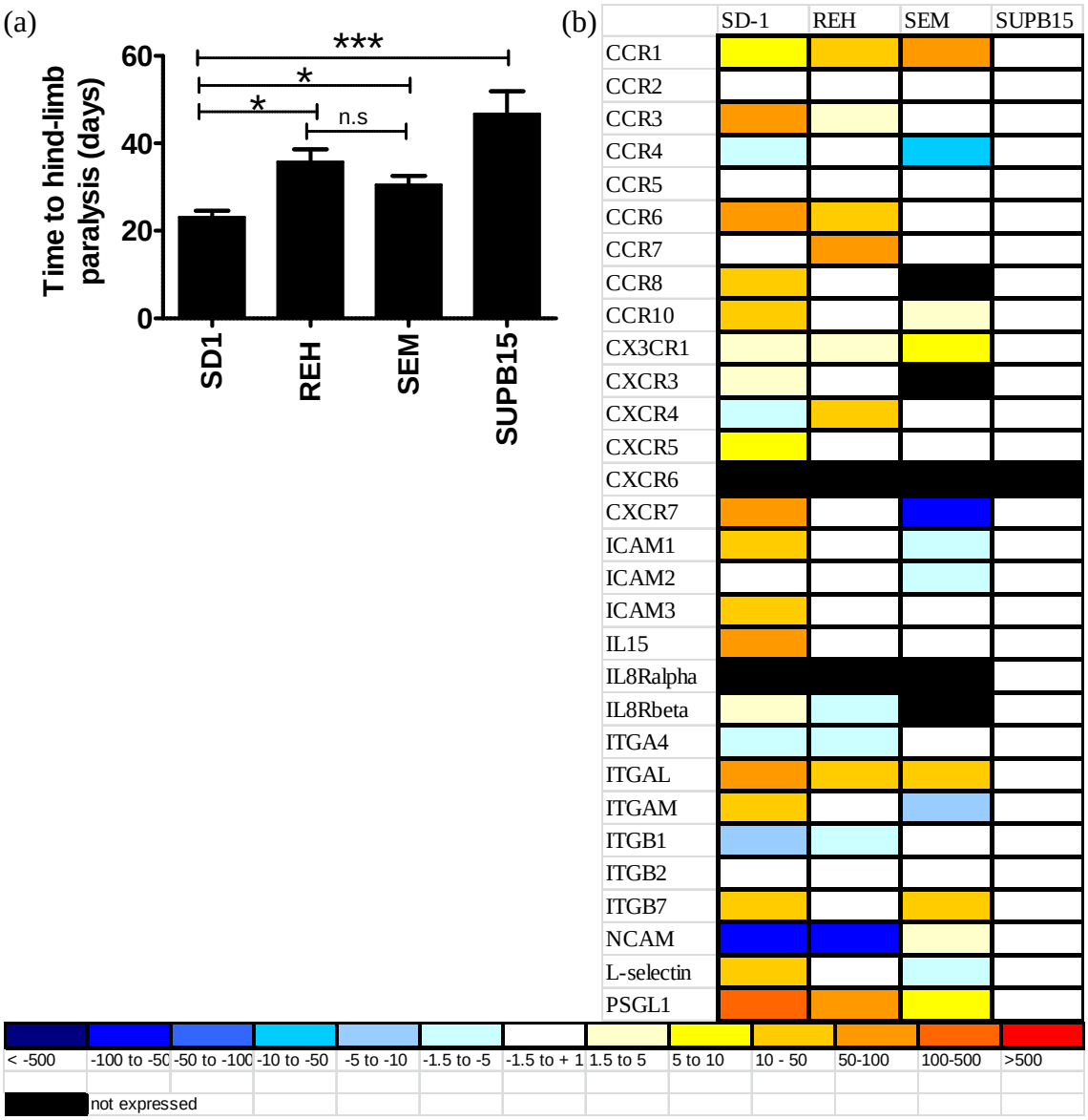

Figure 4-2: Time to hind-limb paralysis and expression of leukocyte trafficking molecules.
(a) SD1, REH, SEM and Sup B15 were injected in NSG mice and monitored for signs of CNS infiltration. The mice were culled when symptomatic. Data represent 4-8 mice/cell line and presented as mean ± SEM. Data were analysed by two-tailed unpaired student *t* tests comparing each of the cell line to the other. ***<0.001, **<0.01, *<0.05. (b) Heat map created from TLDA analysis of mRNA expression of 30 chemokine receptors, selectins and integrins in SD1, REH, SEM and Sup B15. Three independent cultures were analysed per cell line, and all results are expressed relative to the levels in Sup B15 cells, arbitrarily set to 1.0. Contributed by (a) Dr Mark Williams (b) Dr Christina Halsey.

In summary, BCP-ALL cell lines produced CNS infiltration when injected into NSG mice. SD1 demonstrate the most rapid onset of CNS disease amongst the cell lines tested while Sup B15 exhibited slowest CNS engraftment. Gene expression profiling of leukocyte trafficking genes reveal differential expression patterns of the tested genes.

4.2.1 Validation of surface expression using flow cytometry

In order to test if leukocyte trafficking molecules could be detected on the surface of leukaemic cells, flow cytometry using directly conjugated antibodies was performed. Taking a more focussed approach, a panel of candidate genes that could potentially be implicated in cellular transit across the blood-CSF barrier was selected for further investigation. This panel included CXCR3 (Sporici and Issekutz, 2010, Fife et al., 2001, Balashov et al., 1999), CXCR4 (Crazzolara et al., 2001, Burger and Burkle, 2007, Sipkins et al., 2005, McCandless et al., 2006, Juarez et al., 2007, Shen et al., 2001), CCR6 (Serafini et al., 2000, Reboldi et al., 2009), CCR7 (Buonamici et al., 2009), CX3CR1 (Marchesi et al., 2010) and PSGL1 (Carrithers et al., 2002, Bahbouhi et al., 2009, Kivisakk et al., 2003).

In order to determine the expression the selected trafficking molecules, cultured cell lines were labelled with directly conjugated antibodies and analysed on a flow cytometer. As shown in Figure 4-3, flow cytometric analysis revealed differential expression patterns in the cell lines. CXCR3 was highly expressed in all cell lines, while CXCR4 expression varied. SD1 cells exhibited intermediate CXCR4 expression while Sup B15 and REH showed strong expression of CXCR4. A small proportion of $CCR6^{+}$ SD1 cells were observed whereas the other cell lines were negative for surface CCR6. Similarly, low-intermediate CCR7 levels of expression could only be documented in SD1 with all of the other cell lines showing no surface CCR7. Expression of CX3CR1 could not be documented in these cell lines by flow cytometry despite detectible mRNA levels by qPCR. PSGL1 was highly expressed in SD1 but minimally in other cell lines. Overall, CXCR3 and CXCR4 were consistently expressed at high levels on the surface of all the cell lines while CCR6, CCR7 and PSGL1 could only be detected on SD1.

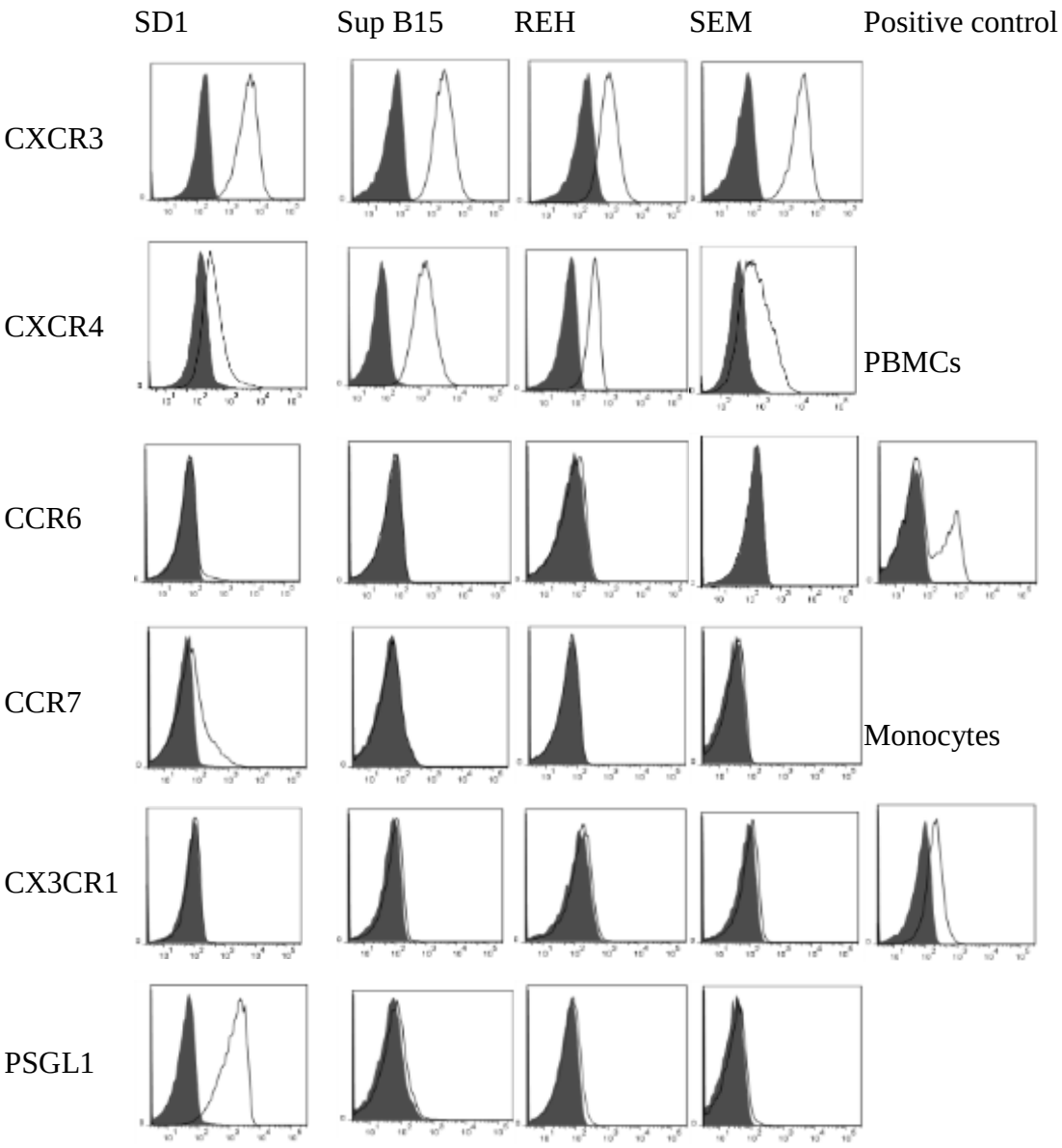

Figure 4-3: Chemokine receptor and PSGL1 expression in BCP-ALL cell lines
Flow cytometric analysis of selected chemokine receptors (CXCR3, CXCR4, CCR6, CCR7 and CX3CR1) and selectin ligand (PSGL1) in BCP-ALL cell lines SD1, Sup B15, REH and SEM. Isotype control – shaded histogram, specific antibody – open histogram. Peripheral blood mononuclear cells (PBMCs) were isolated using Ficoll density gradient separation; Monocytes were isolated using anti-CD14 magnetic bead separation method.

In summary, using flow cytometry, surface CXCR3 and CXCR4 were observed in all the cell lines, whereas high levels of PSGL1 and low levels of CCR6 and CCR7 expression was documented in SD1 only.

4.2.2 Functional analysis using chemotaxis assays

Chemokine receptor-ligand binding results in activation of a number of cellular processes resulting in directional migration or chemotaxis. Transwell® chemotaxis assays are used to quantify the migratory response of cells towards increasing concentrations of a chemokine. Migration index is calculated by normalizing the number of cells migrating to the chemokine with the number of cells migrating towards medium alone. Plotting the migration indices against chemokine concentrations typically reveals a bell shaped curve, with the highest number of cells migrating towards the most physiologically optimum concentration of the chemokine. Fewer cells migrate at lower concentrations as the chemotactic signals are not strong enough, whereas at higher concentrations the cells lose polarity and thus fail to migrate towards the chemokine (Reichman-Fried et al., 2004).

The potential interactions between chemokine receptors expressed by the cell lines and their cognate ligands shown to be expressed on the blood-CSF barrier and/or CNS microenvironment were analysed. CXCR3 binds to CXCL9-11, CCR7 binds to CCL19 and CCL21 whereas CCR6 binds to CCL20. Studies performed in the laboratory showed no significant migration of the cell lines towards CXCR3 ligand CXCL10, CCR7 ligand CCL19 or CCR6 ligand CCL20. CXCL12, a potent chemokine, which binds to the chemokine receptors CXCR4 and CXCR7 was investigated next.

4.2.2.1 Determining CXCL12 mediated chemotaxis

Analysis of CXCL12-mediated chemotaxis demonstrated a differential pattern of chemotaxis in the cell lines. As can be seen in Figure 4-4, Sup B15, REH and SEM cells exhibited avid chemotaxis with a classic bell-shaped distribution with maximum chemotaxis at a concentration of 100 ng/ml. On the contrary, SD1 showed minimal chemotaxis to a range of concentrations (1-1000 ng/ml). The migration indices at a concentration of 100 ng/ml for SD1, Sup B15, REH and SEM were 1.58±1.37, 46.9±5.05, 46.8±27.21, & 46.7±24.97 respectively. These results show that BCP-ALL cell lines Sup B15, REH and SEM expressing surface CXCR4 can migrate in response to CXCL12. However, the significantly poor response by SD1, despite surface expression of CXCR4 was startling, and required further investigation. These experiments are described in section 4.4.

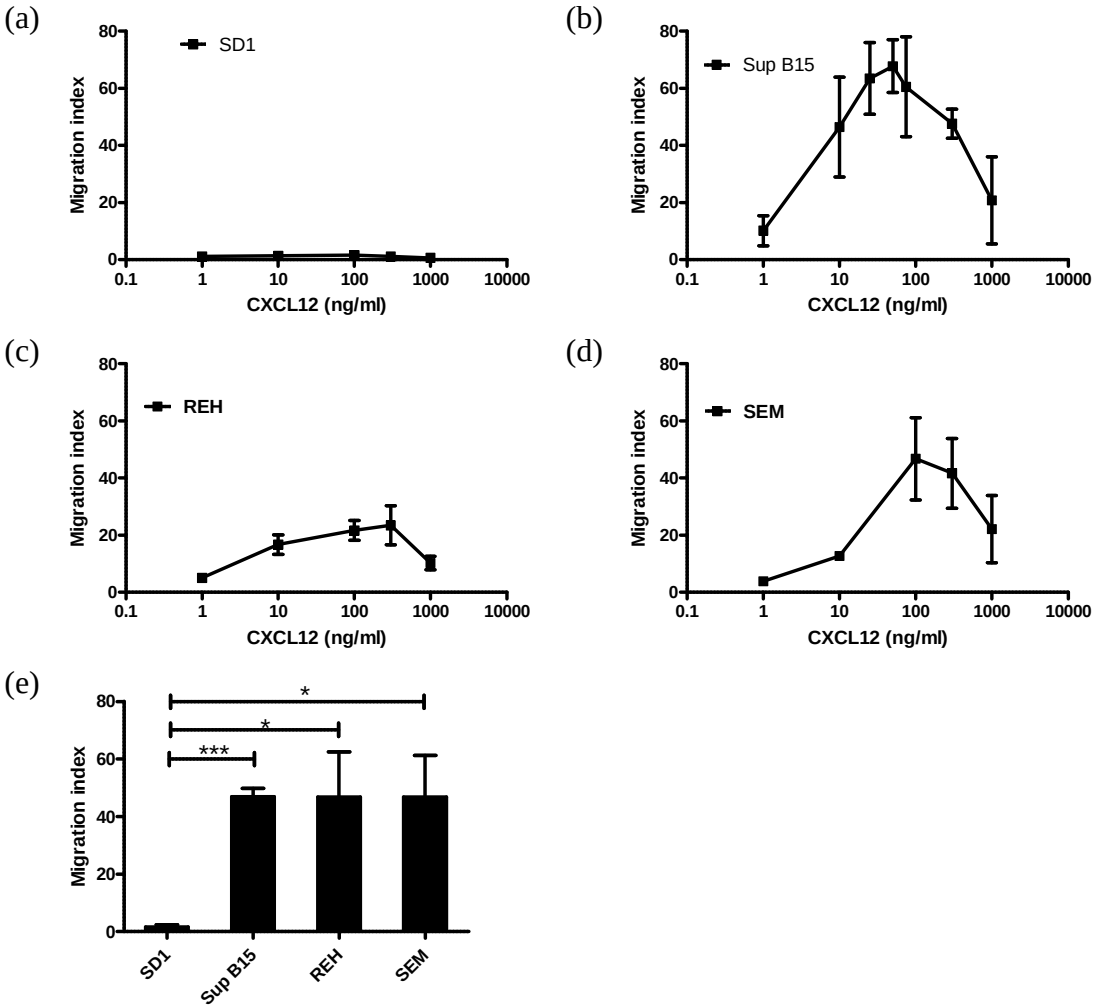

Figure 4-4: CXCL12-mediated chemotaxis in BCP-ALL cell lines
Chemotaxis of (a) SD1, (b) Sup B15, (c) REH and (d) SEM towards increasing concentrations of CXCL12 (1, 10, 100, 300 and 1000 ng/ml) in a Transwell® transmigration assay. Migration indices were calculated using the equation: Number of cells migrating towards CXCL12 (x ng/ml) / Number of cells migrating towards media control. x= specific CXCL12 concentration. Data represent mean ± SEM and are representative of 1 of 3 independent experiments each performed in triplicate. (e) Bar chart showing migration indices of the cell lines at a CXCL12 concentration of 100ng/ml. Data represent mean ± SEM and are pooled from 3 independent experiments each performed in triplicate. Data were analysed using two tailed unpaired student *t* tests and present comparison of SD1 with each of the other cell lines. ***p<0.001, **p<0.01, *p<0.05

In summary, Sup B15, REH and SEM demonstrated avid chemotaxis towards the CXCR4 ligand CXCL12 whereas SD1 showed minimal chemotaxis despite moderate levels of surface CXCR4.

4.2.3 CXCL12 mediated chemotaxis in primagraft cells

Given the interesting association between CXCR4 dysfunction and rapid onset of CNS disease in SD1 cells, it was aimed to test whether leukaemic samples which had produced CNS disease in mice exhibit a similar CXCR4 dysfunction. Accordingly, single cell suspensions were prepared from murine bone marrow/spleens harvested from primary xenograft mice from two CNS-3 and six CNS-1 cases. Subsequently, the samples were analysed for CXCL12 mediated chemotaxis using the Transwell® assays. Migrating cells were quantified by flow cytometry using anti-human CD45 antibodies.

As shown in Figure 4-5, the majority of samples exhibited profound chemotaxis towards as low as 10 ng/ml CXCL12. The majority of the samples exhibited a typical chemotaxis pattern with peak chemotaxis at a concentration of 10-100 ng/ml. There was no correlation between CNS disease status of the patient and CXCL12 mediated chemotaxis. Variable CXCL12 mediated chemotaxis was seen in samples from patients with CNS-3 disease: Sample #5094 demonstrated efficient chemotaxis (41.6%) whereas sample #6112 showed relatively poor chemotaxis (11%) Similarly, samples from CNS-1 patients demonstrated considerable variation. For instance efficient chemotaxis was seen in #6112 and #4630 (39.9% and 37.8% respectively) but cells from #5449, #5655, #4736 showed less avid chemotaxis (6.1%, 8.1% & 8.6% respectively). Similar trend was seen when analysed against the murine CNS-engraftment capability of these samples. Chemotaxis in samples with a 100% rate of CNS engraftment in mice (#5094, #5705, #6240) were 41.6%, 19%, and 11% respectively, whereas the only sample that failed to infiltrate the CNS in xenograft mice showed efficient chemotaxis (i.e. 37.8%). These results lead to the conclusion that CNS-engraftment is not associated with the degree of chemotaxis towards CXCL12 in leukaemic cells harvested from the bone marrow.

(a)

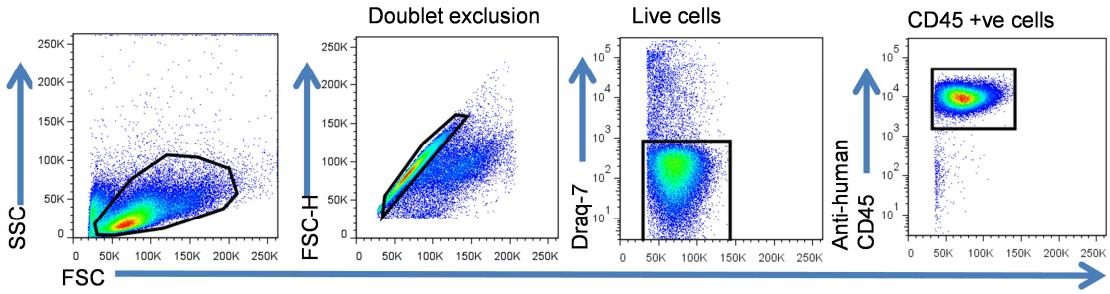

(b)

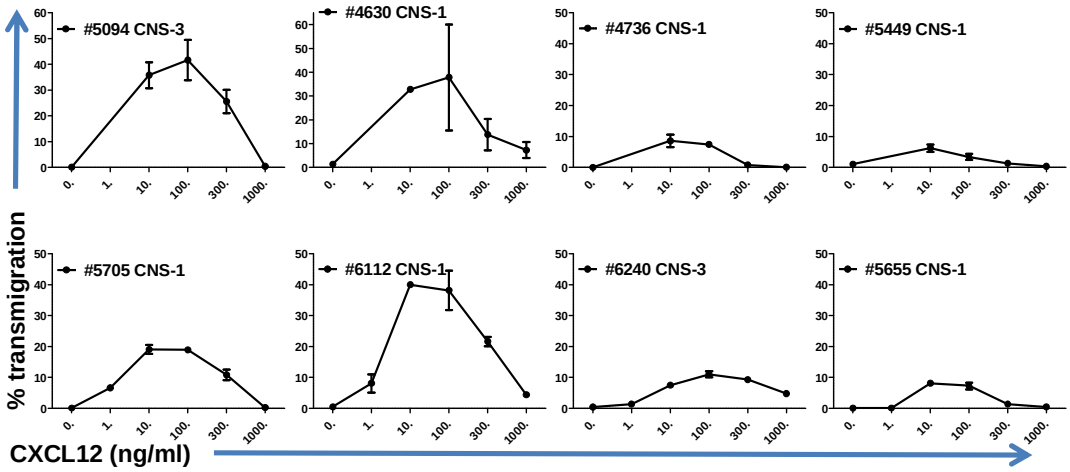

(C)

Patient	CNS status	CNS disease in Engrafted mice	MI	% transmigration
#5094	CNS-3	4/4	526.7	41.6
#5705	CNS-1	3/3	213.3	19
#6112	CNS-1	1/2	84.7	39.9
#4630	CNS-1	0/2	26.7	37.8
#4736	CNS-1	2/2	265.9	8.6
#5449	CNS-1	1/2	6.2	6.2
#6240	CNS-3	3/3	36	11
#5655	CNS-1	2/3	266.6	8.1

Figure 4-5 CXCL12 mediated chemotaxis in primagraft cells

(a) Gating strategy to identify human CD10/CD19 positive cells in xenograft BM/spleen cell suspension. Main cell population was gated on the forward- and side-scatters, followed by doublet exclusion. Subsequently, live cells were identified by Draq-7 viability dye and human leukaemic cells were identified by anti-human CD45 staining. (b) Chemotaxis of primagraft cells towards increasing concentrations of CXCL12 (1, 10, 100, 300 and 1000 ng/ml) in transwell transmigration assay. Percentages of migrating cells (% transmigration) were calculated using the equation: Number of $CD45^+$ cells migrating towards CXCL12 (x ng/ml) / Total number of input $CD45^+$ cells on top of transwell inserts x100 where x= specific CXCL12 concentration. Data are presented as mean ± SEM of triplicate values. (c) Summary of patient characteristics and chemotaxis. CNS status refers to the CNS status of patients at diagnosis. CNS1 (CSF white cell count<5/µl, no blasts), CNS-3 (CSF white cell count>5/µl)

In summary, analysis of CXCL12 mediated chemotaxis in primagraft cells reveal differential chemotaxis patterns of cells. There appears to be no correlation with CNS engraftment capability and CXCL12 mediated chemotaxis in these samples.

4.3 Analysing expression levels of selected leukocyte trafficking molecules in cells from the CNS and the bone marrow

CNS disease could result from a subset of the leukaemic population – a minor sub-clone. Such a subset may escape identification when the whole population from the bone marrow is examined. To test whether cells expressing high/low levels of any particular leukocyte trafficking molecule were being positively selected in the CNS compartment, cells from the bone marrow and CNS were retrieved from mice engrafted with primary samples. Subsequently, these paired cell suspensions were assessed for expression levels of selected leukocyte trafficking molecules. Bone marrow cells from one primary sample with no CNS engraftment were also used for analysis. Cells from the CNS compartment were retrieved as described below.

4.3.1 Retrieval of cells from the CNS compartment

Following mouse cull, the vertebral columns were transacted at upper cervical and lower thoracic regions and removed from the cadaver. Next, using a wide-bored needle fitted to a PBS-filled syringe, the spinal cord sections were expelled out of the spinal canal by flushing with PBS. The spinal canal was rinsed with PBS to increase the cell yield. Cells on the spinal meninges were gently separated by vortexing in PBS at low speed.

Isolating cells from neural tissue typically results in contamination of cells with myelin debris that could interfere with antibody staining. Therefore, attempts were made to remove the debris from cell suspension prior to use in flow cytometry. Ficoll density gradient separation method and CD19-magnetic bead sorting method were tested. While both the methods yielded a purer cell suspension, they resulted in significant decrease in cell counts. CD19-magnetic bead sorting method carried an additional risk of losing CD19-low sub-population of leukaemic cells which could affect the analysis. Therefore, a more conservative approach was followed comprising of following steps: gentle vortex of spinal cords to minimize debris, passage through a cell strainer to remove larger particles, repeated washes of the cell suspension, addition of Fc- receptor blocking agent to minimize non-specific binding of the antibodies, and gating-out of the neuronal debris on forward- and side-scatter on the flow cytometer.

Following retrieval, cells were evaluated for counts and viability using haemocytometer

and trypan blue dead cell exclusion. 1 x 10^6 cells were used/sample where possible, in cases with lower yield, the entire cell suspension were used for staining. Cells from the bone marrow and the CNS compartment were incubated with directly conjugated CD45, CXCR3, CXCR4, CCR6, CCR7, PSGL1 and CX3CR1 antibodies. Appropriate isotype control antibodies were used for each bone marrow- and CNS- cell samples to normalize for non-specific staining. While analysing on the flow cytometer, acquisition conditions for the bone marrow and the CNS samples were kept unchanged.

4.3.2 Expression of selected leukocyte trafficking molecules on primagraft samples retrieved from the bone marrow

Analysis of leukaemic cells from the bone marrow samples revealed a pattern similar to the cell lines. Intermediate-high levels of surface CXCR3 were seen in 7/8 samples, whereas moderate-low levels of CXCR4 were observed in all samples. Low levels of CCR6, CCR7 expression could be detected in 3/8 and 6/8 samples respectively. Differential levels of PSGL1 were observed in 6/8 samples. As seen with the cell lines, CX3CR1 surface expression could not be detected in primagraft samples (Table 4-2)

Sample no.	CXCR3	CXCR4	CCR6	CCR7	PSGL1	CX3CR1
#5094 CNS-3	180	225	5	2.3	119	6.7
#4736 CNS-1	ND	29	ND	52	80	ND
#5449 CNS-1	264	34.6	9	13.9	ND	4.1
#5705 CNS-1	197.7	12	44.7	ND	ND	ND
#6112 CNS-1	53.1	102.8	16.8	26	11.2	ND
#5655 CNS-1	1684	90	42	43	137	10
#6240 CNS-3	941	70	ND	142	15	ND
#4630 CNS-1	684	319	ND	59	3	ND

Table 4-2 FCM analysis of primagraft cells for selected trafficking molecules
Primagraft samples corrected MFI values for the indicated molecules. ND= Not detected. MFI values for specific antibody staining not greater than isotype control antibody.

4.3.3 Comparing bone marrow- and CNS- retrieved leukaemic cells for expression of selected leukocyte trafficking molecules

In order to investigate sub-clonal selection for a particular CNS-engrafting phenotype, 7 paired bone marrow and CNS samples were compared for surface expression of selected leukocyte trafficking molecules. Analysis by flow cytometry revealed no evidence of a positive selection of any of these trafficking molecules in cells isolated from the CNS compartment (Figure 4-6). Although small differences expression levels of CXCR3 and CCR7 were noted in individual pairs, it is clear that the CNS infiltrating subset of cells was

not enriched for expression of particular molecules. It is also clear that CNS isolated cells did not have lower expression levels of CXCR4. Together, these data strongly suggest that a CNS homing signature cannot be identified based on expression levels of the selected chemokine receptors and PSGL1.

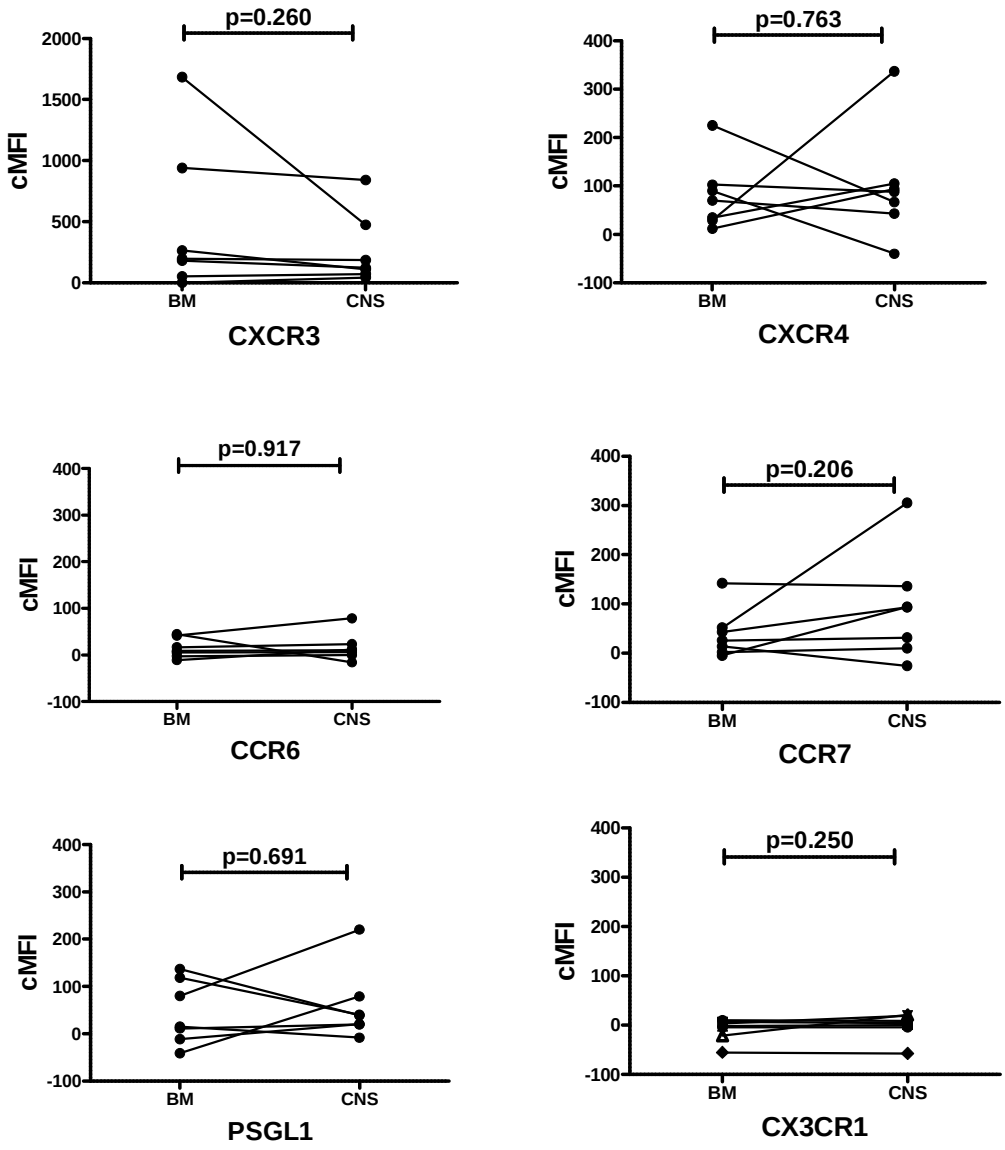

Figure 4-6 Comparison of expression of chemokine receptors and PSGL1 in primagraft cells retrieved from the BM and the CNS compartments.

Cells were retrieved from murine BM and CNS compartments upon engraftment with primary BCP-ALL samples. Live human leukaemic cells (Draq7-/CD45+) were analysed for expression of indicated leukocyte trafficking molecules using directly conjugated antibodies. Data represent corrected mean fluorescence intensity (cMFI) ($MFI^{specific}$ - $MFI^{isotype}$) of the leukaemic cells. Differences between CNS and BM expression were analysed using two-tailed paired student t tests. Values above horizontal bars represent p values.

In summary, these results demonstrate that the cells from the CNS compartment do not appear to be significantly different from cell from the bone marrow compartment in the expression levels of the selected chemokine receptors and PSGL1. Therefore the CNS infiltrating population of cells do not appear to be enriched for phenotype identifiable by selected leukocyte trafficking molecule expression.

Together, these results show that selected chemokine receptors and selectin ligand PSGL1 are expressed in leukaemic cells in the bone marrow and the CNS compartment. Although these trafficking molecules may be required by leukaemic cells for transit across the blood-CSF barrier, they do not appear to play an instructive role in determining the site-specific homing of these BCP-ALL cells in either of these compartments.

In order to investigate whether any of the leukocyte trafficking molecules are necessary for transit across the blood-CSF barrier, it was aimed to perform further experiments by inhibiting the surface expression/function and analysing the effect on CNS engraftment. CXCR3 and CXCR4 were the most consistently and highly expressed surface receptors amongst the analysed trafficking molecules. Given the implicated role of CXCR4-CXCL12 axis in leukaemic dissemination to the liver and spleen, it could also have a similar role in leukaemic dissemination to the CNS compartment. In order to determine whether CXCR4-CXCL12 interaction was required by leukaemic cells for CNS engraftment, *in vivo* studies were carried out in the laboratory. NSG mice were injected with REH$^{luc\text{-GFP}}$ cells and subsequently treated with CXCR4 inhibitor AMD3100 or vehicle control. Engraftment was monitored using bioluminescence imaging system.

At the end of the experiment, bone marrow and extramedullary leukaemic infiltration was evaluated. As expected, the analysis of the murine tissue revealed significant reduction of leukaemic burden in the bone marrow and other extramedullary tissues in AMD3100 treated mice compared to the controls. Strikingly, no reduction in the extent of CNS leukaemic burden was observed. Heavy CNS engraftment was seen in both AMD3100-treated and control treated mice, implying that CXCR4 inhibition does not affect CNS engraftment. Overall, these data strongly indicate that unlike the bone marrow, liver and spleen, CNS engraftment is independent of CXCR4-CXCL12 axis (manuscript submitted). Further investigation would be required to determine whether CXCR3, CCR6, CCR7 and PSGL1 play a similar non-essential role.

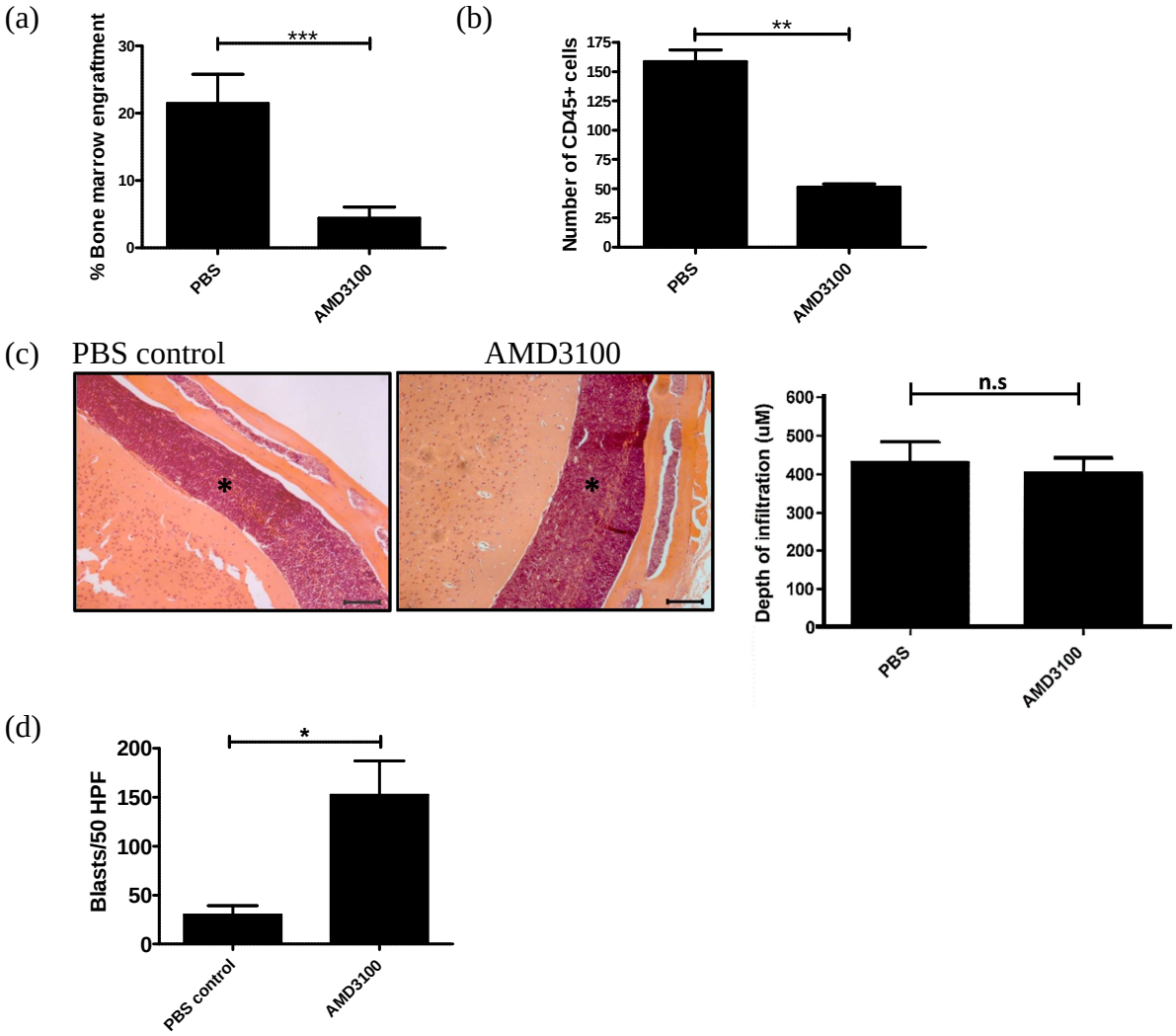

Figure 4-7 Effect of AMD3100 on REH engraftment in NSG mice.
(a) Bone marrow engraftment in AMD3100 vs PBS control treated mice as measured by numbers of $REH^{GFP\text{-}luc}$ cells on flow cytometry. Data show mean ± SEM in n=7 and n=6 mice for PBS and AMD3100 groups respectively. (b) Liver engraftment as measured by numbers of human CD45 positive cells in 8 random fields of view per section. Data show mean ± SEM in n=4 and n=5 mice for PBS and AMD3100 groups respectively. (c) Histological analysis of murine brain sections from xenografts (n=5 mice in each group). Representative H&E stained sections showing dark purple leukaemic cells infiltrating the meninges (black star). Each brain was divided into 5 segments and sections were cut from each segment, the maximal depth of meningeal infiltrates was recorded for each section using Axiovision Rel 4.3 software (Carl Zeiss) and presented as mean ± SEM. (d) Peripheral blood smaears taken at the end of the experiment (n-4 mice each group) were stained with H&E and the number of blasts per 50 high-powered fields was recorded. Data were analysed using two-tailed unpaired Student *t* tests. *p<0.05, **p<0.01, ***p<0.001. (a-c contributed by Dr Mark Williams).

4.4 Investigating the dysfunctional CXCR4-CXCL12 axis in SD1 cells

With the observed dysfunctional CXCR4-CXCL12 axis in SD1 cells, it was aimed to dissect out the underlying molecular mechanisms responsible. Chemokine ligand-induced migration involves a number of critical steps including: ligand binding to the receptor, receptor internalization and recycling, induction of downstream signalling and activation of cytoskeletal machinery for locomotion. Any abnormality in one of these steps could potentially result in abnormal chemotaxis. In addition, other plausible mechanisms in SD1 could be counter-regulation by other cellular mechanisms such as CXCR4-CXCR7 axis and/or BCR-ABL1 tyrosine kinase signalling. Therefore, a reductionist approach was utilized to identify the potential causative factor. For some of the experiments the Sup B15 cell line was used as a comparator as it possesses the same leukaemic translocation but shows avid chemotaxis towards CXCR4. The key questions addressed in this section are enlisted below:

- Do SD1 cells have a normal functioning CXCR4 receptor?
- Is CXCL12-unresponsiveness due to CXCR7 mediated CXCL12 scavenging?
- Does the presence of the $P190^{BCR/ABL1}$ affect CXCR4 expression or function?
- Is the lack of CXCL12 responsiveness due to loss of key chemotaxis-associated signalling pathways?

4.4.1 Functional assays of CXCR4

In order to determine if the surface expressed CXCR4 had normal receptor-ligand interactions, CXCR4 structure and function was analysed in a step-by-step manner. Initially, sequence analysis of CXCR4 exons was performed by Dr Chris Halsey and revealed a normal wild-type CXCR4 gene in SD1 cells.

4.4.1.1 Blocking CXCR4 results in inhibition of chemotaxis

To evaluate the specificity of CXCR4 in CXCL12 mediated chemotaxis, the CXCR4 small molecule inhibitor AMD3100 was utilised. Cells were treated with AMD3100 (10µM) or control and chemotaxis towards CXCL12 assessed. Treatment with AMD3100 significantly reduced CXCL12-mediated transmigration in SD1 and Sup B15 – confirming the specificity of CXCR4-CXCL12-mediated migratory response (Figure 4-8).

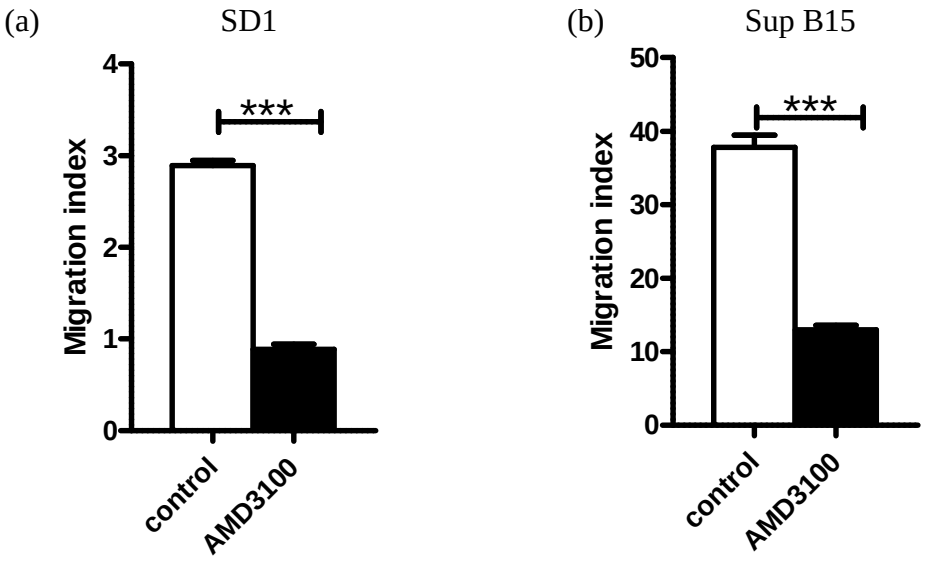

Figure 4-8: Effect of CXCR4 blockade on CXCL12 mediated chemotaxis
CXCL12 mediated chemotaxis in (a) SD1 and (b) Sup B15 subsequent to treatment with CXCR4 small molecule inhibitor AMD3100 (100 µM) or media control for 1 hour at 37ºC. Migration indices were calculated using the equation: Number of cells migrating towards CXCL12 (100 ng/ml) / Number of cells migrating towards media control. Data show mean ± SEM and are representative of 1 of 3 independent experiments each performed in triplicate. Data analysed using unpaired two-tailed Student *t* test. ***p<0.001. Note the different scale in the two graphs.

4.4.1.2 SD1 cells bind alexa-fluor labelled CXCL12

In order to determine whether CXCR4 had a functional CXCL12 binding domain, the binding efficiency of fluorescently labelled CXCL12 ($CXCL12^{AF647}$) was tested. SD1 and Sup B15 cells were incubated with increasing concentration of alexa-fluor (AF647) labelled CXCL12 and fluorescence of cell-bound $CXCL12^{AF647}$ measured by flow cytometry. As can be seen in Figure 4-9, both SD1 and Sup B15 cells bind to $CXCL12^{AF647}$ in a dose dependent manner. Approximately 92% SD1 cells adequately bind to CXCL12 at a concentration of 100 ng/ml. In comparison, Sup B15 had a higher $CXCL12^{AF647}$ binding efficiency and nearly 100% binding was seen at 100 ng/ml.

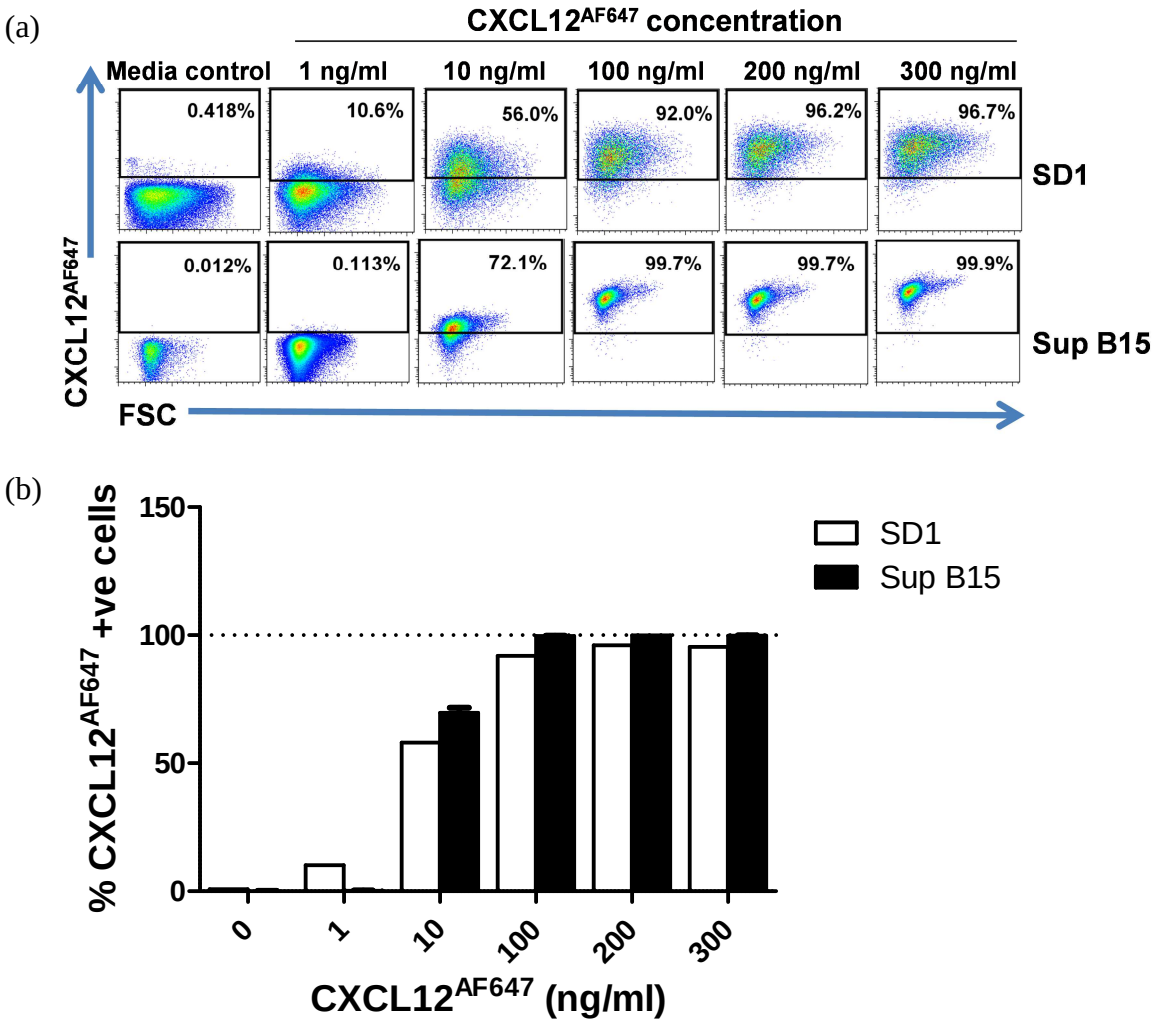

Figure 4-9: Dose-dependent binding of $CXCL12^{AF647}$ in SD1 and Sup B15
(a) Representative pseudocolour density plots of live SD1 and Sup B15 cells showing fluorescence in cells treated and $CXCL12^{AF647}$ (1, 10, 100, 200 and 300 ng/ml) (b) Bar charts representing percentage of $CXCL12^{AF647}$ positive cells calculated by gating on control treated cells. Data presented as mean ± SEM and represent one experiment performed in triplicates.

4.4.1.3 Determining CXCL12 mediated CXCR4 internalization

Upon ligand binding, chemokine receptors are rapidly internalized (Neel et al., 2005). Generally, stimulation of CXCR4 by CXCL12 results in activation of internalisation within a few minutes which plateaus within 30 minutes (Venkatesan et al., 2003). The ability of ligands to internalise chemokine receptors is used as an indicator for ligand-induced receptor activation. In order to test if binding of CXCL12 stimulated equal internalisation of the CXCR4 in SD1 and Sup B15 cells, flow cytometric analysis of receptor internalisation was performed. SD1 and Sup B15 cells were incubated with CXCL12 for 30 minutes at 37 ºC to allow maximal ligand binding and internalisation and subsequently analysed for surface expressed CXCR4. As shown in Figure 4-10, CXCR4 stimulation with 100 ng/ml CXCL12 resulted in efficient internalisation of CXCR4 in Sup B15 (72.5% ± 6.1) but less so in SD1 (21% ± 13).

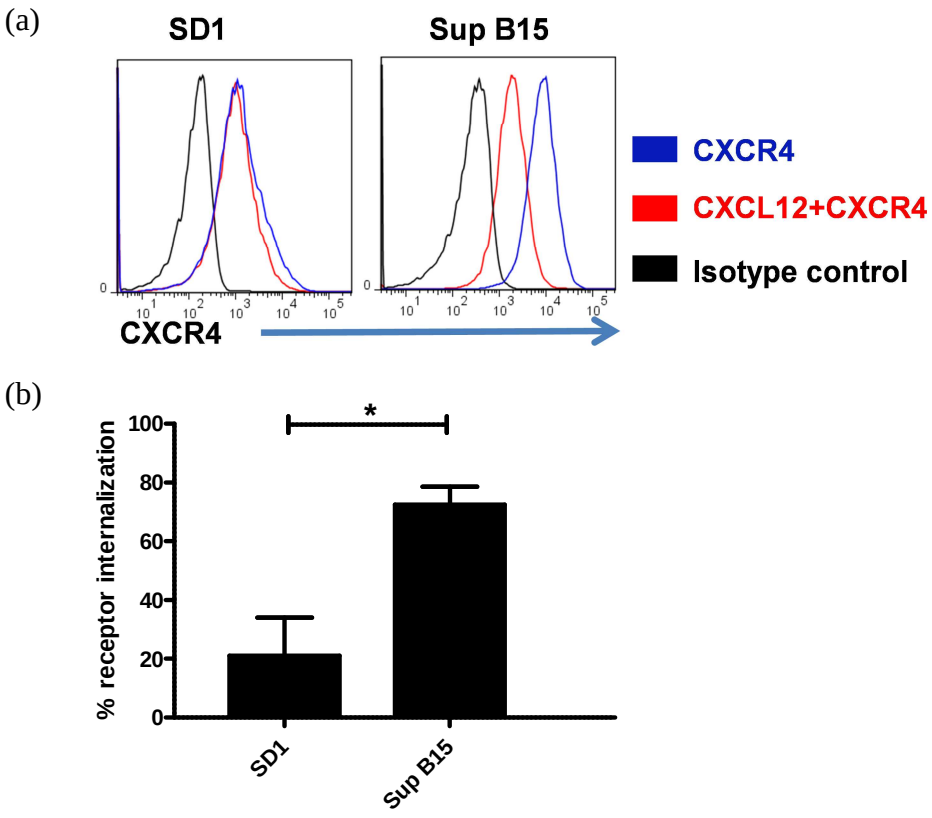

Figure 4-10 CXCR4 internalisation in response to CXCL12 stimulation:
(a) FCM analysis of surface CXCR4 in SD1 and Sup B15 following incubation in CXCL12 (100ng/ml) for 30 minutes at 37 ºC to measure CXCR4 internalisation. Representative histograms showing surface CXCR4 expression levels in CXCL12-treated (red histogram), control-treated (blue histogram) and isotype control staining (black histogram). (b) Bar graph showing CXCL12-mediated CXCR4 internalisation in SD1 and Sup B15. CXCR4 MFI values for control-treated cells were adjusted to a 100% and percent receptor internalisation calculated as reduction in surface CXCR4 expression. Data shown are pooled from 4 independent experiments and presented as mean ± SEM. Data were analysed using two-tailed unpaired Student *t* test. *p<0.05

4.4.1.4 SD1 cells are capable of restoring surface CXCR4 following internalization

Following ligand-induced internalisation, the pool of surface chemokine receptors are rapidly replenished by intracellular machinery by either recycling of the internalised receptor, or by transport of stored receptors to the surface. To determine the kinetics of re-appearance of surface CXCR4 following CXCL12 mediated internalisation, SD1 cells were treated with CXCL12 for 30 minutes at 37 ºC and then incubated in fresh culture media for 30, 60, 90 and 120 minutes at 37^{O}C. As shown in Figure 4-11, both SD1 and Sup B15 exhibited partial restoration of surface CXCR4. Remarkably, CXCR4 on SD1 cells had a more efficient (79.3% ± 13.9) restoration compared to Sup B15 (51.9% ± 9.6). This shows that despite lower surface expression and internalisation, SD1 cells are capable of restoring CXCR4 expression after CXCL12 mediated internalisation.

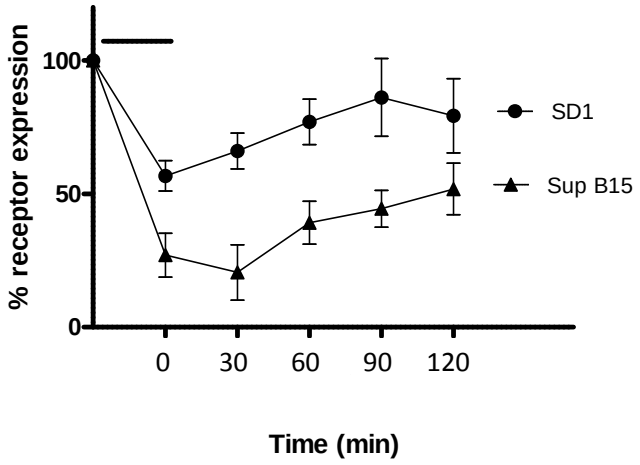

Figure 4-11: Time-dependent restoration of surface CXCR4 following CXCL12-mediated internalization
Graph showing CXCL12-stimulated internalisation and subsequent restoration of surface CXCR4 after removal of CXCL12 from the media. MFI values for untreated cells were taken as 100% and changes in surface CXCR4 expression calculated as % receptor expression. Data shown are pooled from 4 independent experiments and represent mean ± SEM. Horizontal bar represents treatment with CXCL12 (100ng/ml)

In summary, these experiments show that CXCL12 mediated chemotaxis is CXCR4 specific in SD1 and Sup B15. SD1 cells are capable of binding CXCL12; however only a minor proportion of surface CXCR4 is internalised. Following internalisation, SD1 cells are capable of rapidly restoring the pool of surface CXCR4. Together, these data imply that along with lower CXCR4 levels compared to Sup B15, a smaller proportion of the total CXCR4 on SD1 cells maintain the critical chemokine ligand-receptor interactions.

4.4.2 Analysing the effect of CXCR7 on CXCL12 mediated chemotaxis

The initial TLDA analysis revealed higher expression of CXCR7 in SD1. CXCR7 is an alternative receptor for CXCL12 with high affinity binding and can alter the CXCR4-CXCL12 axis in a number of ways (section 1.6.4.1) One alternative explanation for the lack of CXCL12-mediated migration in SD1 is that CXCR7 might be scavenging CXCL12, thus limiting the availability of CXCL12 to bind with and stimulate CXCR4. In order to test this hypothesis, first, CXCR7 mRNA expression was confirmed using qPCR. Next, protein expression was confirmed using immunofluorescence staining and chemokine competition assays. Finally, the effect of blockade of CXCR7 on CXCL12-mediated chemotaxis was evaluated.

4.4.2.1 Determining CXCR7 mRNA levels in SD1 cells

In order to validate the TLDA results, SYBR green qPCR was utilised to compare the CXCR7 mRNA expression in SD1 and Sup B15. Analysis of the qPCR results revealed significantly higher expression of CXCR7 in SD1 compared to Sup B15 ($p<0.001$) (Figure 4-12).

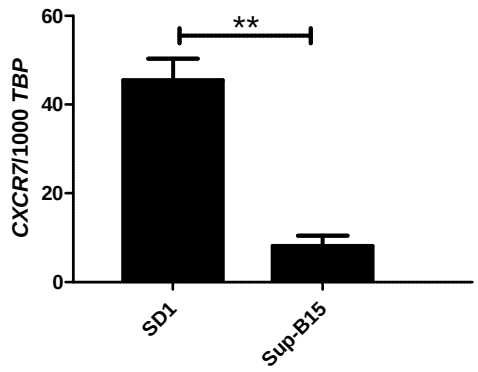

Figure 4-12: Comparison between CXCR7 mRNA in SD1 and Sup B15
SYBR Green qPCR analysis of CXCR7 transcript in SD1 and Sup B15 normalised to TBP as housekeeping gene. Data are pooled from 3 independently grown cultures analysed in triplicate and presented as mean ± SEM. Data were analysed using two-tailed unpaired Student *t* test. **p<0.01

4.4.2.2 Determining CXCR7 protein expression on SD1 cells

In order to confirm the higher expression levels of CXCR7 on SD1, it was decided to examine CXCR7 expression using immunofluorescence staining. This method allows qualitative assessment of both surface and intracellular proteins. Cytospin preparations of SD1 and Sup B15 cells were labelled with mouse anti-human CXCR7 antibody (11G8). A fluorescently-conjugated secondary antibody (goat anti-mouse IgG conjugated to TRITC)

was used to visualize CXCR7. (Figure 4-13) Fluorescent microscopic examination revealed scattered expression in a small proportion of SD1 cells. Sup B15 only showed minimal staining.

(a)

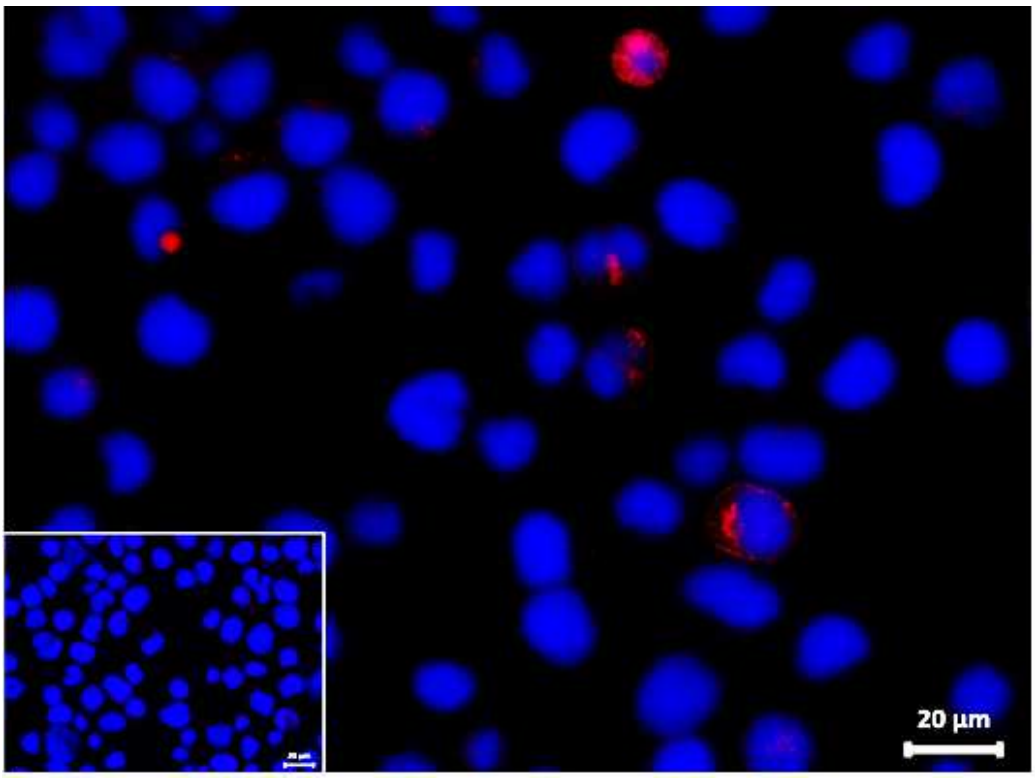

(b)

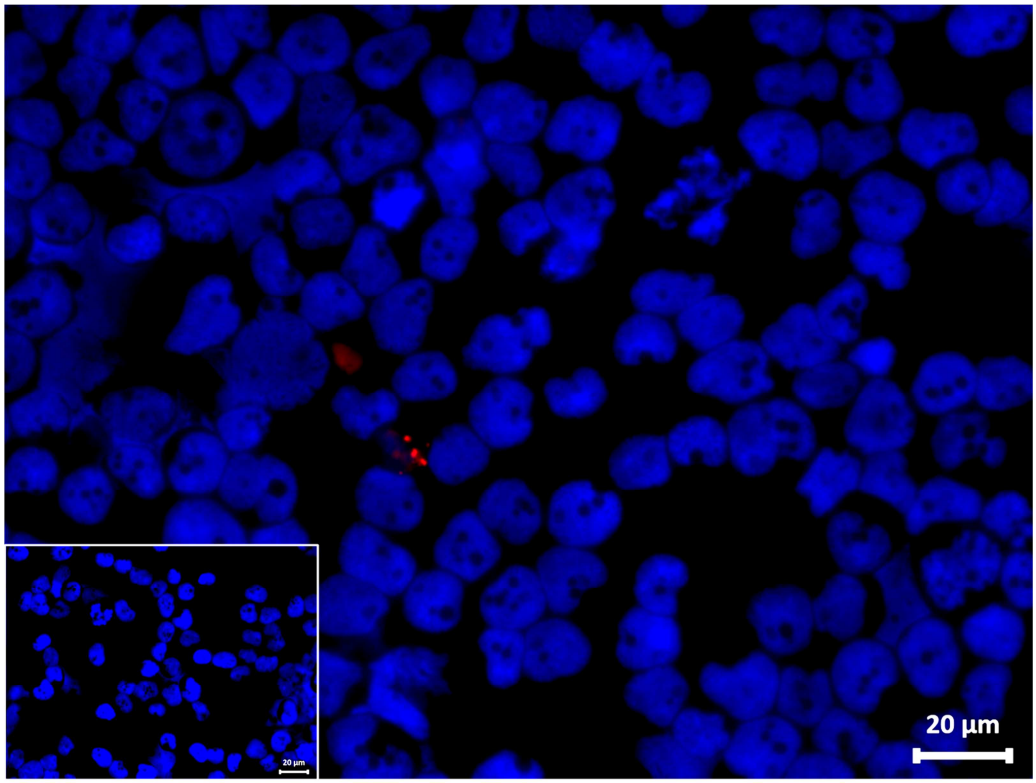

Figure 4-13: CXCR7 protein expression in SD1 & Sup B15
CXCR7 staining in fixed and permeabilised (a) SD1 and (b) Sup B15 cytospin slides. Mouse anti-human CXCR7 antibody and Mouse anti-human IgG1 isotype control antibodies (Inset) were used at 10 µg/ml and visualized using TRITC labelled goat anti-mouse IgG1. Nuclei were visualised using DAPI. Scale bar = 20µm. Images are representative of 2 independently performed staining experiments.

4.4.2.3 Determining CXCR4 & CXCR7 co-expression on SD1 cells

CXCR4/CXCR7 co-staining with CXCR4 confirmed higher levels of surface CXCR4 in Sup B15 whereas intermediate levels were also noted in SD1 (Figure 4-14 a & b). CXCR7 was frequently observed in CXCR4 expressing SD1 cells. Rarely, co-localization of CXCR4 and CXCR7 was observed. (Figure 4-14c)

(a)

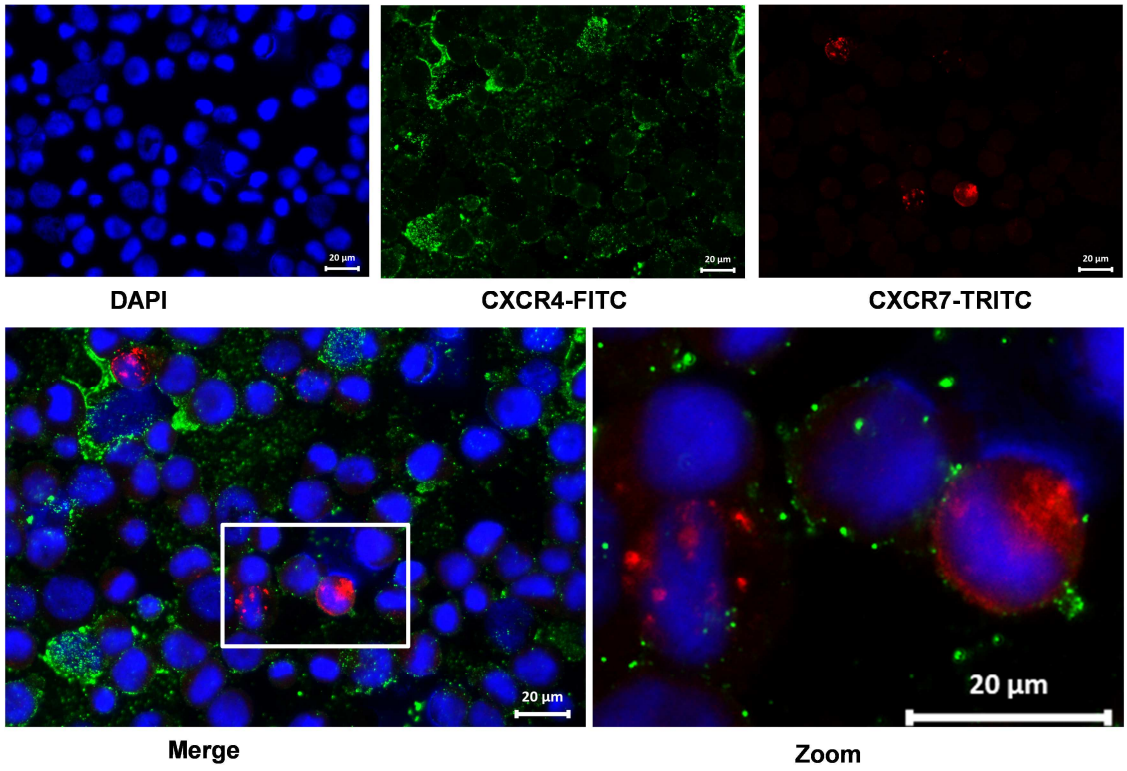

(b)

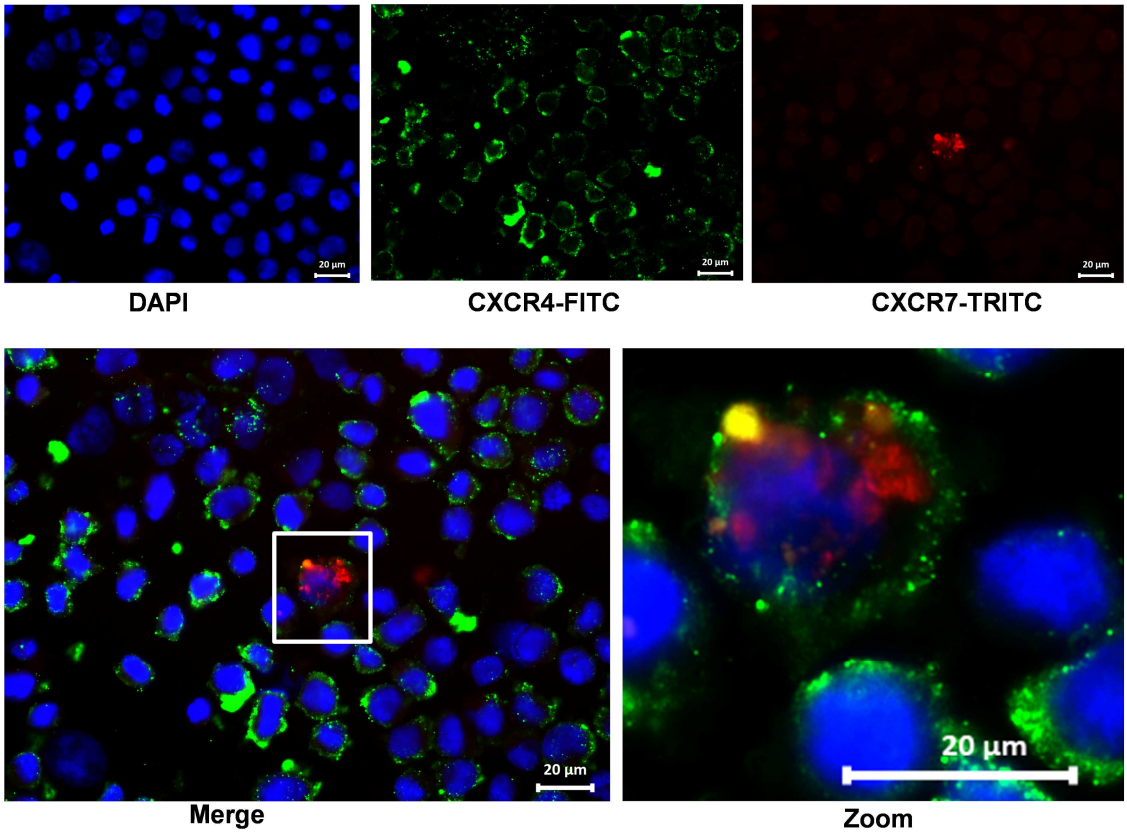

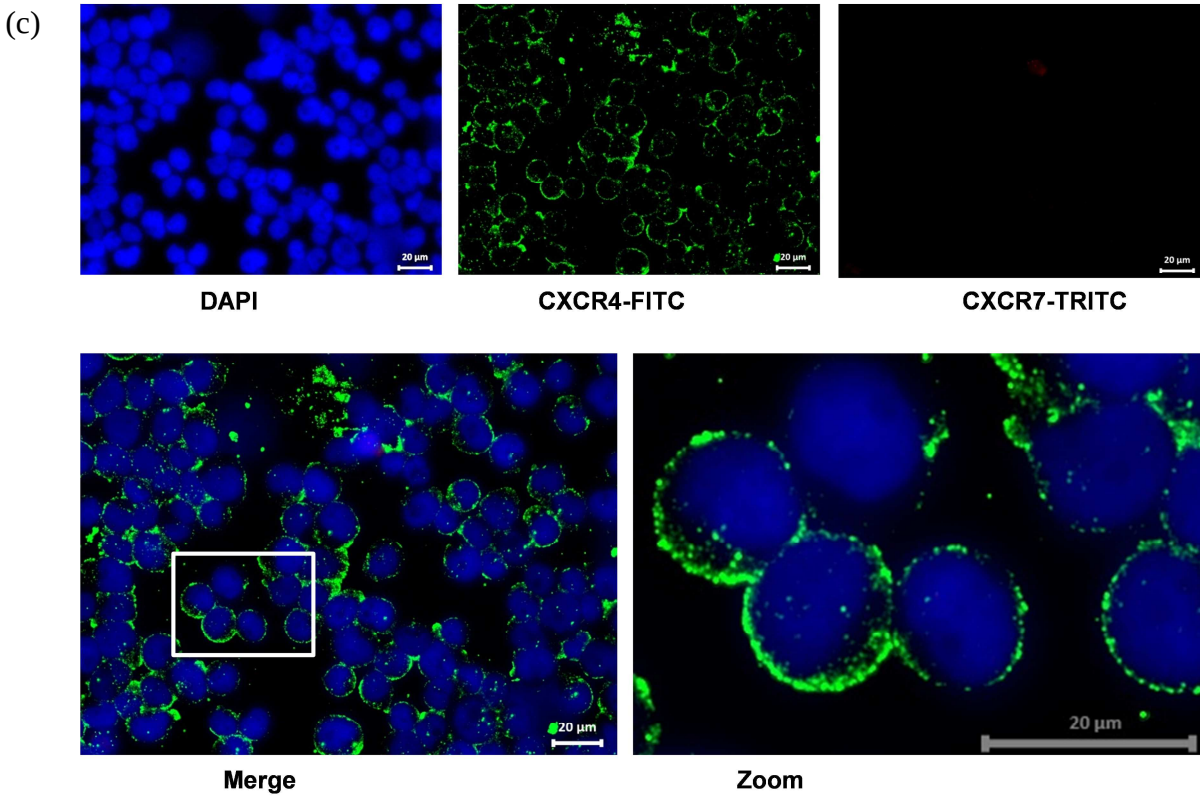

Figure 4-14: CXCR7/CXCR4 co-expression in SD1 and Sup B15
CXCR4/CXCR7 co-staining in fixed and permeabilised cytospin slides in (a & b) SD1 and (c) Sup B15. Mouse anti-human CXCR7 antibody and Mouse anti-human IgG1 isotype control were used at 10 µg/ml and visualised using TRITC labelled goat anti-mouse IgG1. Mouse anti-human CXCR4 antibody and isotype control were used at 2.5 µg/ml and visualised using FITC-labelled mouse anti-human IgG2b. Nuclei were visualized using DAPI. Top panel represent individual channel colours and bottom panels show merged images. Scale bar = 20µm. Images represent staining at 3 different occasions using independently grown cultures.

4.4.2.4 CXCR7 competitively inhibits CXCL12 binding to CXCR4

In order to determine the degree of CXCL12 binding to CXCR7, competitive binding assays were performed. CXCR7 binds to chemokine ligands CXCL12 and CXCL11. When CXCL12 ^{AF647} is added to cells co-expressing CXCR4 and CXCR7, both the receptors bind CXCL12 ^{AF647}. Subsequently, unlabelled CXCL11 is added in high concentration which displaces the CXCR7-bound CXCL12^{AF647}. This displacement is quantified by measuring reduction in fluorescence. SD1 and Sup B15 cells were loaded with CXCL12^{AF647} (100 nM) with or without an excess of unlabelled CXCL11 (1 µM) at 4ºC and subsequently analysed for fluorescence by flow cytometry. As can be seen in Figure 4-15, adding excess unlabelled CXCL11 resulted in significant reduction in cell-bound CXCL12 ^{AF647} in SD1 (33.3% ± 10.2) but not in Sup B15 (3.7% ± 3.1) ($p<0.05$). These results indicate that SD1 cells also bind CXCL12 via CXCR7 whereas Sup B15 cells almost exclusively bind CXCL12 via CXCR4.

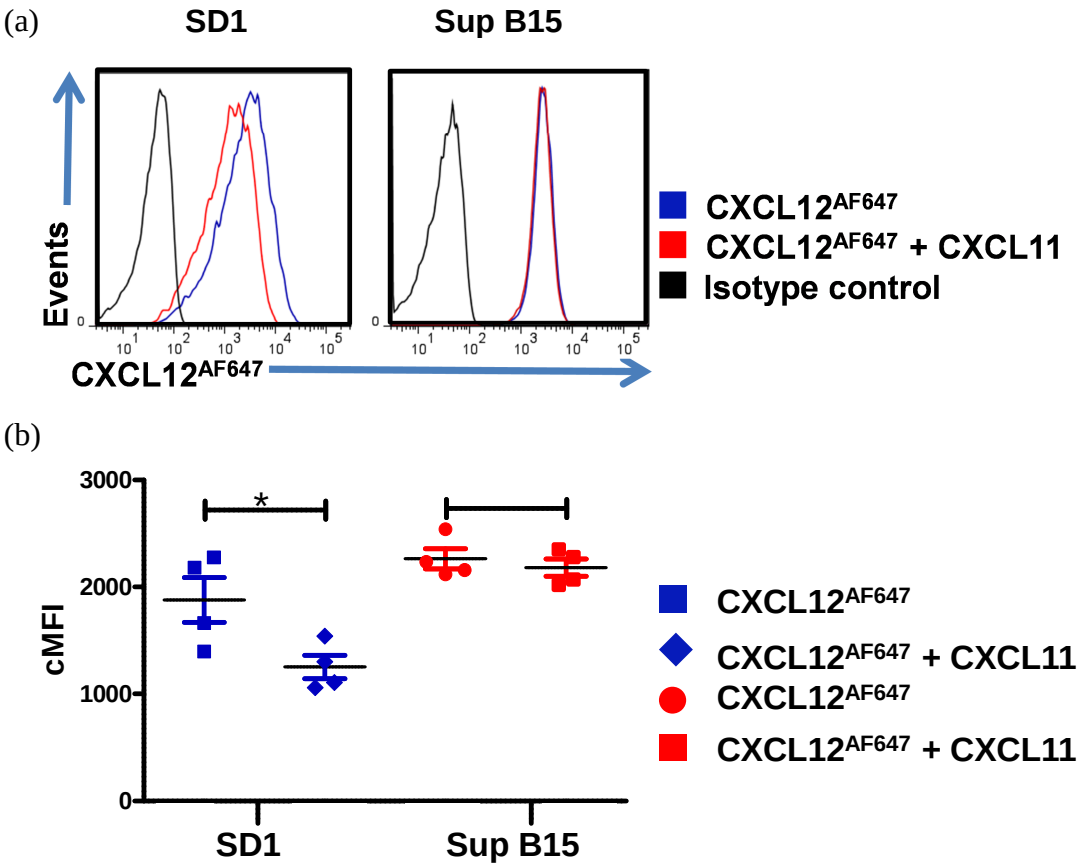

Figure 4-15: CXCL12-CXCL11 competition assay
(a) Representative histograms showing CXCL11-mediated reduction in binding of $CXCL12^{AF647}$ in SD1 and Sup B15. The blue histograms show $CXCL12^{AF647}$ (100 ng/ml) fluorescence, the red histograms show $CXCL12^{AF647}$ fluorescence in presence of excess CXCL11 (1µg/ml), the black histograms (isotype control) show the background fluorescence. (b) Corrected MFI values for $CXCL12^{AF647}$ staining ± CXCL11 (1 µg/ml) in SD1 and Sup B15. Data are pooled from 4 independent experiments and presented as mean ± SEM. Data were analysed using two-tailed unpaired Student *t* test. *p<0.05

4.4.3 Analysing the effect of CXCR7 blockade on CXCL12 mediated chemotaxis

In order to examine whether CXCL12 binding to CXCR7 could affect CXCL12 mediated chemotaxis, CXCR7- small molecule inhibitors (CCX771 & CCX 754) (Chemocentryx) were utilized to block CXCR7 binding domains. SD1 cells were incubated with increasing concentrations of CCX771/CCX754 or isotype control antibody and subsequently tested for CXCL12-mediated chemotaxis. As can be seen in (Figure 4-16), inhibition of CXCR7 did not improve CXCL12-mediated migration in SD1. In fact, a reduction in migration index was seen with increasing concentrations of the blockers.

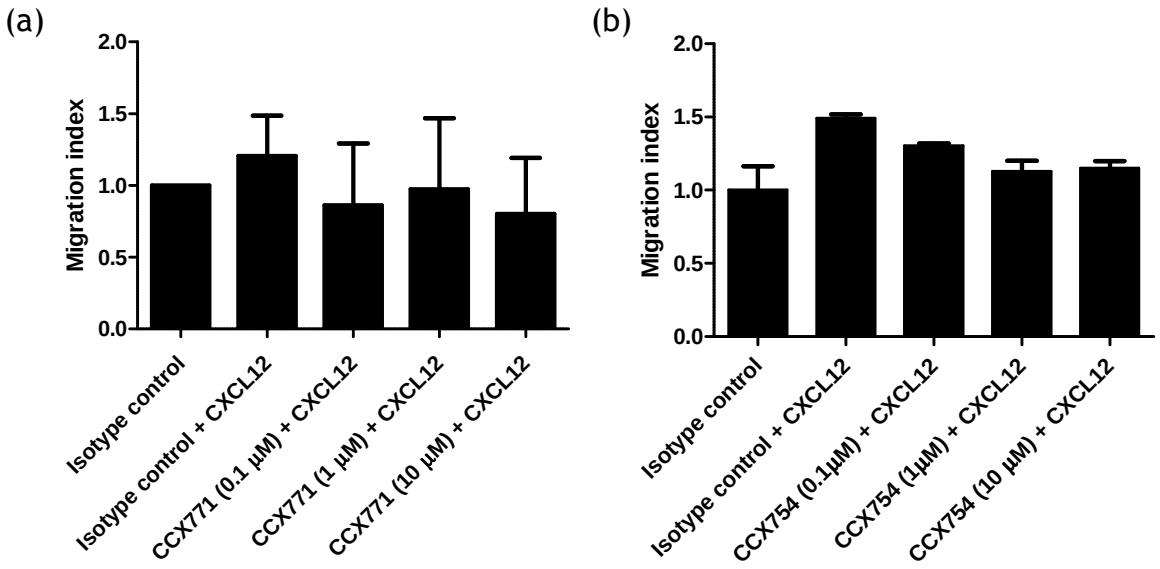

Figure 4-16: Effect of CXCR7 blockade on CXCL12-mediated chemotaxis in SD1.
(a) CXCL12-mediated migration of SD1 cells following treatment with CCX771 (0.1 µM, 1 µM or 10 µM) or isotype control (CCX704 1 µM) for 1 hour at 37ºC. Data are pooled from 3 independent experiments each performed in duplicate wells and represent mean ± SEM. (b) CXCL12-mediated migration of SD1 cells following treatment with CCX754 (0.1 µM, 1 µM or 10 µM) or isotype control (CCX704 1 µM). Data from one experiment performed and represent mean ± SEM of individual wells.

In summary, these results show that CXCR7 mRNA is highly expressed on SD1 cells. CXCL12 binds CXCR7 on SD1 surface, however, no restoration of CXCL12-mediated migration is noted when CXCR7 inhibitors are used; making this unlikely to be the reason for the decreased CXCL12 mediated chemotaxis in SD1 cells.

4.4.4 Does inhibiting BCR/ABL tyrosine kinase restore CXCL12 mediated chemotaxis?

As detailed in section 1.6.8, $P210^{BCR-ABL1}$ tyrosine kinase is associated with down-regulation of CXCR4 mRNA, surface expression and downstream signalling. SD1 and Sup B15 cell lines both express the $P190^{BCR-ABL1}$ protein. It was hypothesised that $P190^{BCR-ABL1}$ fusion protein could interfere with CXCR4 expression and/or CXCL12-mediated chemotaxis in SD1 cells. Given that both the cell lines carry BCR-ABL1 translocation but migration defect is only seen in SD1, it was decided to compare the BCR-ABL1 levels and activity in these cell lines. If BCR-ABL1 levels were found to be similar in SD1 and Sup B15, counter-regulation of BCR-ABL1 with CXCR4-CXCL12 axis would be less likely. To test this hypothesis, first, BCR-ABL1 expression was determined in SD1 and Sup B15 cells. Next, the effect of BCR-ABL1 inhibition on CXCR4 levels and CXCL12-mediated chemotaxis was determined.

4.4.4.1 Determination of relative expression of BCR-ABL1 mRNA and protein in SD1 and Sup B15

To quantify the BCR/ABL1 transcript levels, TaqMan qPCR with primers specific for $p190^{BCR/ABL1}$ fusion gene were utilised. RNA from SD1 and Sup B15 cells was isolated and reverse-transcribed to cDNA and subsequently analysed for BCR/ABL1 levels using qPCR. ABL1 was used as a housekeeping gene (Foroni et al., 2011). Analysis of p190 BCR-ABL1 revealed significantly higher expression in SD1 compared to Sup B15 (Figure 4-17a). To confirm this at the protein level, western blot analysis for phospho-Crkl (p-CrkL) was performed. CrkL is a substrate of the BCR-ABL1 fusion protein and is constitutively phosphorylated in BCR-ABL1-positive leukaemias, and is therefore used as a surrogate marker for BCR-ABL1 tyrosine kinase activity. Western blotting confirmed the higher activity of BCR-ABL1 in SD1 compared to Sup B15 (Figure 4-17 b & c).

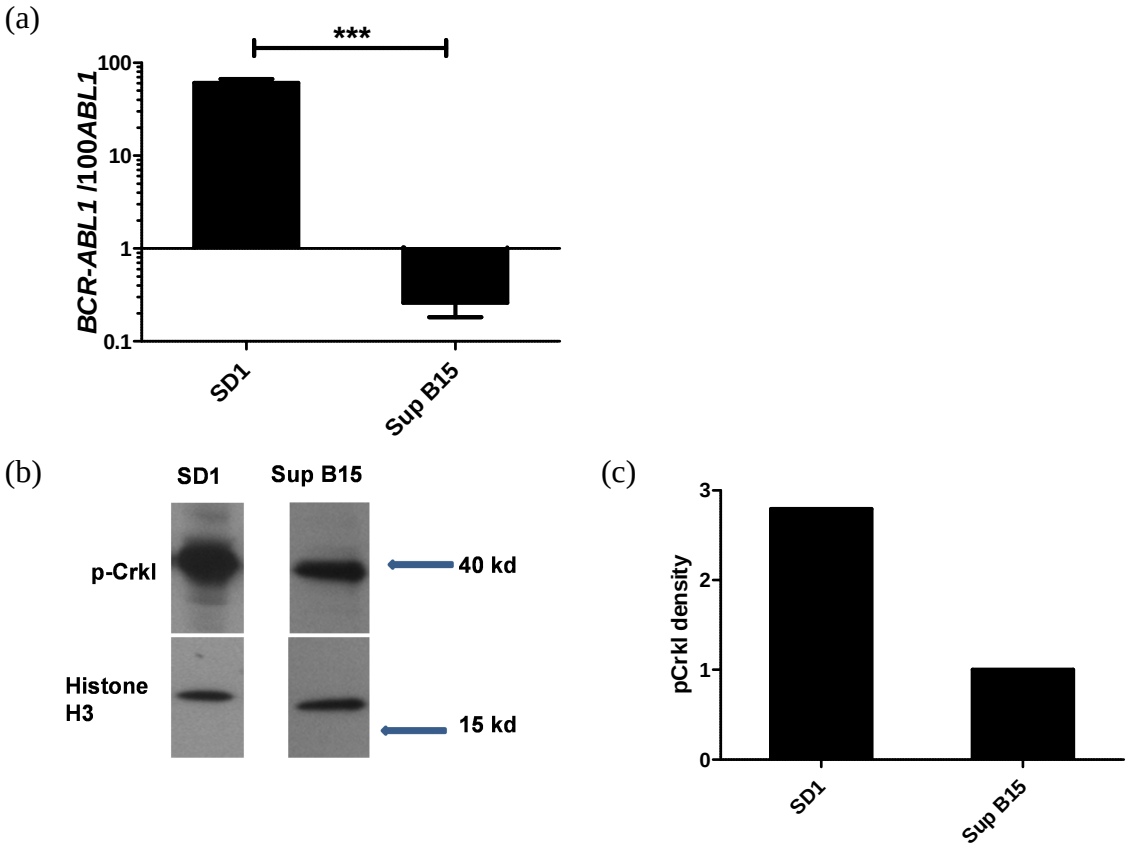

Figure 4-17: BCR-ABL1 expression in SD1 and Sup B15

(a) TaqMan qPCR quantification of BCR-ABL1 transcript in SD1 and Sup B15 normalized to ABL1 as housekeeping gene. Data are pooled from 3 independently grown cultures analysed in triplicate and presented as mean ± SEM. Data are analysed using two-tailed unpaired Student *t* test. ***$p<0.001$ (b) Western blot analysis of Crkl phosphorylation (39 KDa) as a surrogate marker for BCR/ABL1 tyrosine kinase activity in SD1 and Sup B15. Histone H3 used as a housekeeping protein to ensure equal protein loading. (c) Western blot band density analysed using imageJ software (National Institute of Health) and adjusted density calculated by dividing relative density for p-Crkl by the relative density for Histone-H3.

4.4.4.2 Effects of inhibition of BCR-ABL1 tyrosine kinase in SD1

To test whether BCR-ABL1 tryrosine kinase was interfering with CXCR4-CXCL12 axis in SD1, the effect of inhibition of BCR-ABL1 tyrosine kinase on SD1 chemotaxis was investigated. First, a dose-response experiment was performed to measure the adequate concentration of BCR-ABL1 tyrosine kinase inhibitor Imatinib (STI-571). SD1 and Sup B15 cells were treated with increasing concentrations of Imatinib for 3, 6, 12, 24 and 48 hours. To rule out any effect of Imantinib on cell viability, cells were monitored for counts and viability using haemocytometer and trypan blue dead cell exclusion method. Western blot analysis on the cells revealed effective inhibition of p-CrkL at a concentration of 10uM at all the time points. However, due to the cytotoxic effects on viability, it was decided to use shorter treatment time (3 hours) for experiments. (Figure 4-18a & b)

Next, in order to determine the effect of BCR-ABL1 tyrosine kinase inhibitors on CXCR4 mRNA and surface receptor expression, SD1 cells were treated with Imatinib and then analysed for CXCR4 mRNA using SYBR Green qPCR and CXCR4 surface expression using flow cytometry. No effect on CXCR4 mRNA or surface expression was observed in Imatinib treated cells (Figure 4-18c & d). Therefore, $p190^{BCR\text{-}ABL1}$ tyrosine kinase does not seem to regulate CXCR4 transcription or surface expression in SD1.

Finally, in order to determine whether BCR-ABL1 tyrosine kinase perturbs CXCR4 signalling and hence CXCL12 mediated chemotaxis, SD1 cells were treated with Imatinib and CXCL12-mediated chemotaxis was assessed using transwell assays. The results reveal that BCR-ABL1 tyrosine kinase inhibition did not result in an increase in CXCL12 mediated chemotaxis in SD1 cells (Figure 4-18e). Imatinib, besides inhibiting BCR-ABL1 tyrosine kinases, is known to non-selectively target other key cellular pathways (Hantschel et al., 2008). In order to determine whether the reason for failed restoration of chemotaxis could be the non-specific inhibition of chemotaxis pathways, BCR/ABL1 negative cell line REH was treated with Imatinib and analysed for CXCL12-mediated chemotaxis. No effect on CXCL12 mediated chemotaxis was observed with Imatinib treatment (Figure 4-18f).

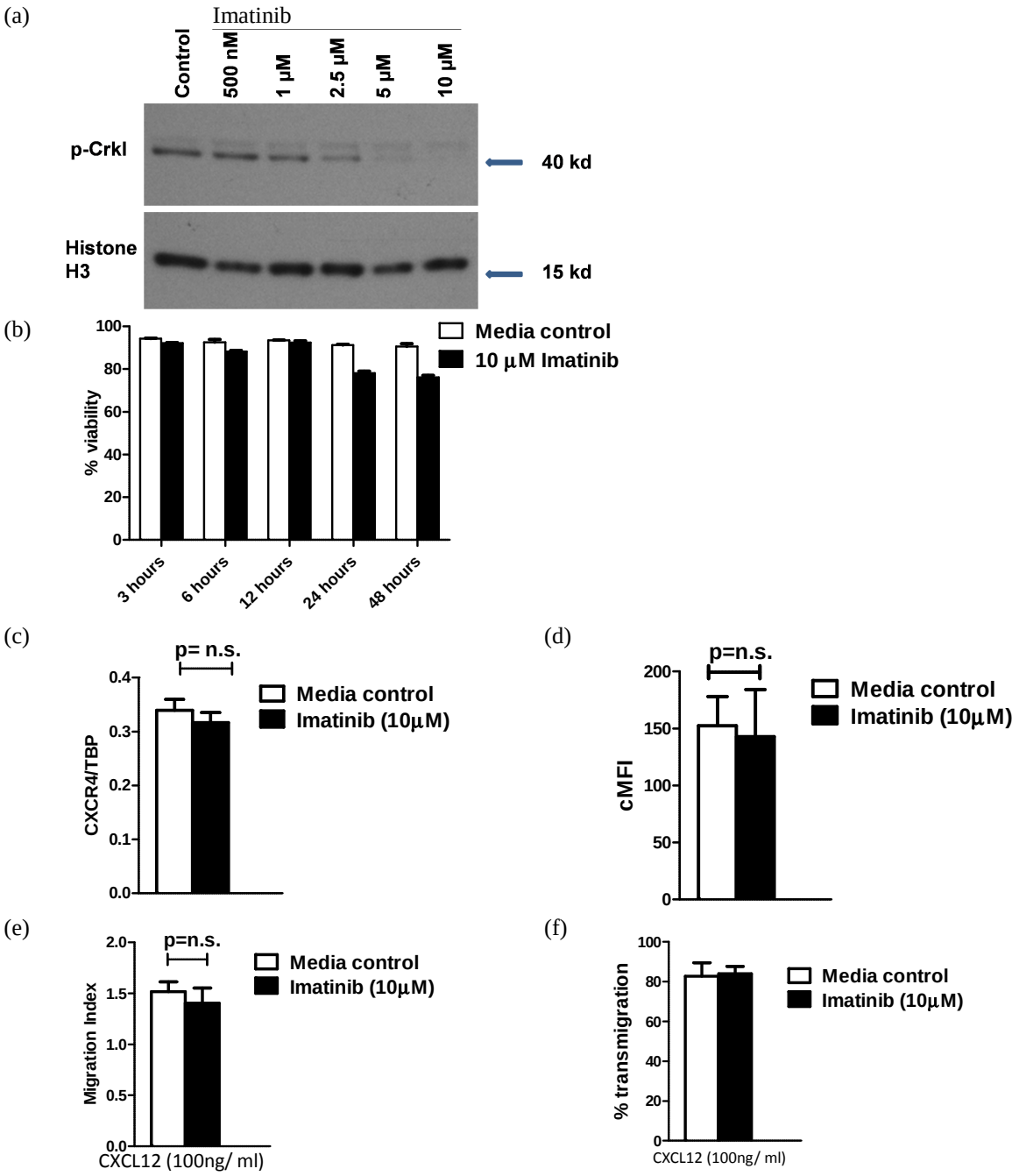

Figure 4-18 Effect of BCR-ABL inhibition on CXCR4 expression and function.
(a) Dose-dependent inhibition of p-Crkl activity in SD1. SD1 cells were treated with increasing concentrations of Imatinib (500 nM, 1 µM, 2.5 µM, 5 µM and 10 µM) for 6 hours followed by western blot analysis for p-Crkl and Histone-H3. (b) SYBR Green qPCR analysis for CXCR4 mRNA were analysed following treatment with Imatinib (10 µM) or media control for 6 hours. Relative quantities were calculated using TBP as housekeeping gene. (c) FCM analysis for CXCR4 surface expression following treatment with Imatinib (1 µM) or control for 6 hours. Corrected MFI (cMFI) represents MFI^{CXCR4} – $MFI^{isotype\ control}$. Data were pooled from 3 independent experiments performed and represents mean ± SEM and were analysed using Student *t* test. (d) CXCL12-mediated chemotaxis in SD1 cells were analysed following treatment with Imatinib (10 µM) or media control for 6 hours. Migration indices were calculated using the equation: Number of cells migrating towards CXCL12 (100 ng/ml) / Number of cells migrating towards media control. Data were pooled from 5 independent experiments performed in triplicates and presented as mean ± SEM. Data were analysed using Student *t* test. (e) CXCL12 mediated chemotaxis in Imatinib treated REH cells.

In summary, these data suggest that CXCR4 mRNA or protein expression is not up-regulated by inhibition of BCR-ABL1 tyrosine kinase. Furthermore, the deficient migration does not appear to be a result of cross-talk of tyrosine kinase signalling and CXCR4 signalling, as inhibition by Imatinib failed to enhance CXCL12-mediated migration in SD1.

4.4.5 Investigating key CXCL12-activated signalling pathways

CXCL12 binding to CXCR4 has been shown to activate a number of downstream signalling pathways. In ALL cells, chemotaxis has been shown to be mediated by p38 MAPK and to a lesser extent by ERK and PI3K/Akt pathways (Bendall et al., 2005). To assess if deficient migration in SD1 was a result of a dysfunctional downstream signalling pathways, SD1 and Sup B15 cells were stimulated with CXCL12 at various time points and analysed for phosphorylation of p38 MAPK, pERK1/2 and pAkt. As shown in Figure 4-19 and summarised in Table 4-3, western blot analysis revealed profound differences in SD1 and Sup B15. Rapid activation of phosphorylated p38 MAPK and pERK1/2 proteins was observed within 5 min of CXCL12 stimulation in SD1, with levels returning to baseline within 15-20 minutes after stimulation. In contrast, no activation of these pathways was noted in Sup B15. p38 MAPK demonstrated modest levels of autophosphorylation in SD1 and Sup B15 whilst minimal constitutive activity of p-ERK1/2 was noted in SD1 but not in Sup B15. No phosphorylation of Akt was observed in the two cell lines. No conclusion could be drawn based on the lack of activation of these pathways in Sup B15. Therefore, REH and SEM cell lines were also investigated for CXCL12-mediated activation of these signalling pathways. Western blot analysis in CXCL12-stimulated REH revealed rapid phosphorylation of p38 MAPK and ERK1/2 as early as 5 minutes with levels returning to baseline in approximately 30 minutes. Analysis of CXCL12 stimulated SEM cells showed constitutive phosphorylation of p38 MAPK with minimal increase in signal over the course of the experiment. Again, Akt phosphorylation was not noted in any of these cell lines. Levels of total p38 MAPK, ERK1/2, Akt and the housekeeping protein (Histone H3) remained largely unchanged over the period of stimulation (Figure 4-19).

These results fail to identify a common intracellular pathway in the 4 BCP-ALL cell lines that might be vital for chemotaxis, and dysfunction of which could explain the lack of chemotaxis in SD1 cells. In contrast to the previously reported association of non-chemotaxing ALL cells with dysfunctional p38 MAPK (Bendall et al., 2005), no such correlation was found in these cell lines (Table 4-3). The simplest explanation is that there are alternative signalling pathways in leukaemia subsets. Further investigation would be required to identify the intracellular signalling pathways involved in SD1 or Sup B15 chemotaxis.

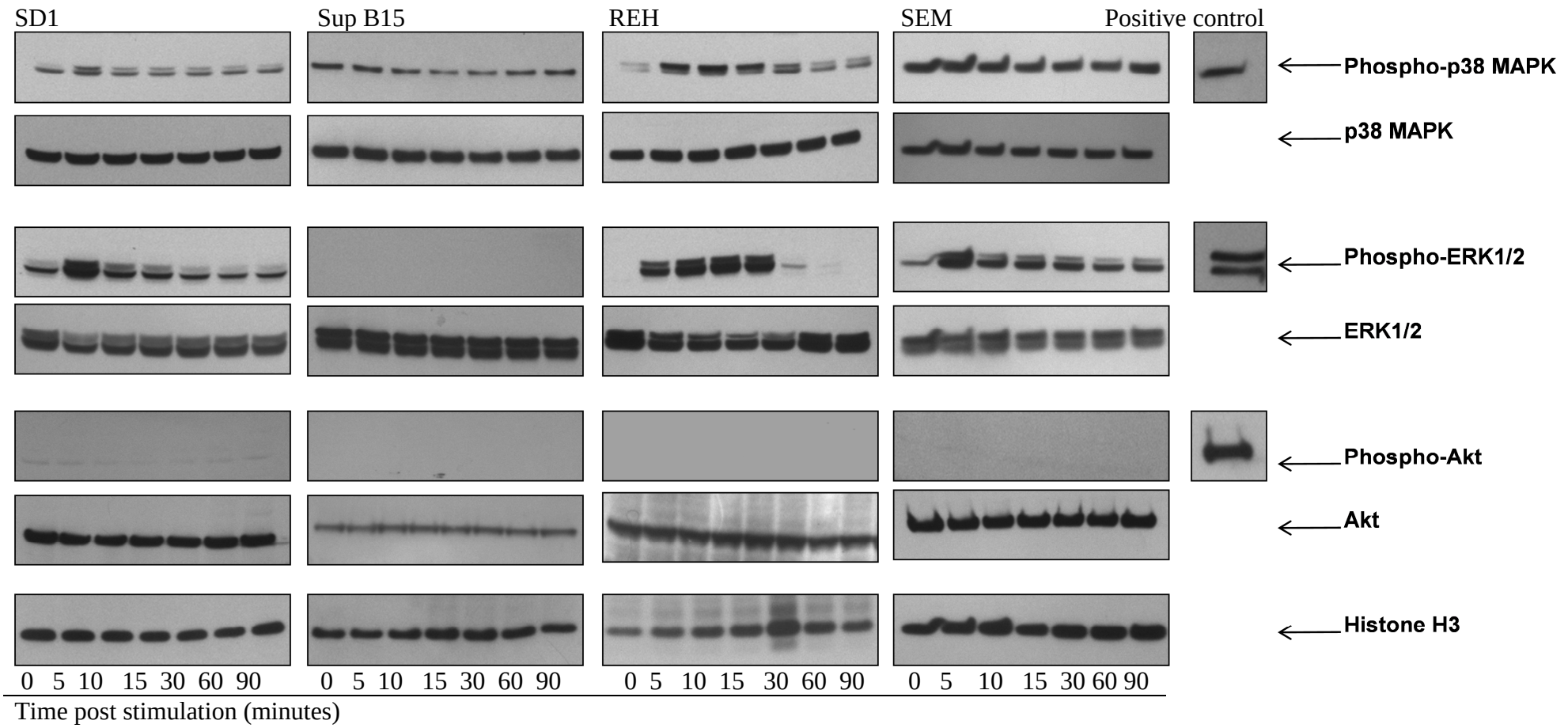

Figure 4-19: Downstream signalling pathways activated by CXCL12 in cell lines
Cells were treated with CXCL12 (100 ng/ml) for 5, 10, 15, 30, 60 or 90 minutes or with media control. Cell lysates were analysed by western blot using antibodies against the indicated signalling pathway molecules. Representative positive controls: IL-15 treated SD1 cells for phospho-p38 MAPK, LPS treated Raw264.7 cells for phospho-ERK1/2, Calyculin-A treated Jurkat cells for phospho-Akt. Representative blots for Histone H3 used to ensure equal loading.

Cell line	Chemotaxis	p38-MAPK	p-ERK1/2	p-Akt
SD1	-	+	++	-
Sup B15	+++	-	-	-
REH	++	++	+++	-
SEM	++	+	++	-

Table 4-3: Correlation of chemotaxis with signalling molecules
Tabular presentation of findings from western blots as shown in Figure 4-16.

In summary, the results show that SD1, Sup B15, REH and SEM, upon stimulation with CXCL12, initiate different signal transduction pathways associated with chemotaxis.

4.5 Discussion

In this chapter, a combination of approaches was utilised to determine whether specific leukocyte trafficking molecules associated with leukaemic cell entry in the CNS compartment in BCP-ALL could be identified. Our initial screening using gene expression analysis identified a range of chemokine receptors, selectins and integrins expressed in cell lines with variable potential to infiltrate the CNS in xenograft mice. Validation by flow cytometry identified down-regulated CXCR4 as a potential candidate for CNS infiltration. Analysis of chemotaxis revealed disproportionately reduced chemotaxis to CXCR4 ligand CXCL12 in SD1 cells. Subsequent analysis of primagraft samples failed to show any correlation between CXCL12 mediated chemotaxis and CNS disease. Leukaemic cells isolated from the CNS of xenograft mice did not differ from cells from the bone marrow compartment in expression of selected leukocyte trafficking molecules. Further in-depth analysis of CXCR4 function in SD1 cells failed to reveal a single mechanism responsible for this dysfunctional chemotaxis.

BCP-ALL cells lines SD1, Sup B15 and REH are reported to differ in their ability to infiltrate the CNS (Holland et al., 2011). However, when injected into NSG mice, all the cell lines were found to cause CNS disease; although the kinetics of CNS infiltration differed significantly. As reported previously, when mice injected with leukaemic cells are monitored for long observation times, almost all mice show signs of engraftment. However, samples with short time-to-leukaemia predict early patient relapse and a distinct gene expression signature (Meyer et al., 2011), suggesting that using engraftment kinetics as a surrogate marker has a rational scientific basis. Therefore, time-to-CNS-leukaemia was used as a marker for CNS engraftment capability in our studies. Out of the 4 cell lines tested, SD1 cells were associated with the most rapid onset of CNS disease followed by SEM, REH and Sup B15 respectively.

Among a wide panel of leukocyte trafficking molecules analysed using TLDA, CXCR3, CXCR4, CCR6, CCR7, PSGL1 and CX3CR1 were chosen for further analysis. Analysis by flow cytometry indicated that SD1 cells had comparatively lower levels of CXCR4, higher expression levels of PSGL1 and a minor proportion of CCR6 and CCR7 expressing cells. In addition, SD1 cells demonstrated minimal CXCL12 mediated chemotaxis. This suggested that dysfunctional CXCR4-CXCL12 axis response correlated with rapid onset of CNS disease. Maturing haematopoietic precursors down-regulate response to CXCL12 to egress from the bone marrow and enter the circulation (Fedyk et al., 1999, Bleul et al.,

1998, Honczarenko et al., 1999). Inhibiting CXCR4 results in egress of cells from the bone marrow and extramedullary organs such as the liver into the circulation (Welschinger et al., 2013, Juarez et al., 2007). Interestingly, a high peripheral blood white cell count in ALL is associated with increased incidence of CNS disease at diagnosis and increased risk of CNS relapse (Pui et al., 2008). However, when an independent cohort of primagraft samples was analysed, no significant association of CNS disease with a particular chemokine receptor could be identified. Further investigation of CXCR4-CXCL12 interaction showed no association of CNS disease with CXCL12 mediated chemotaxis. In addition, use of CXCR4 anihibitor in xenografted mice resulted in similar extent of CNS disease despite a reduction in overall leukaemic burden. Using AMD3100 with Imatinib in a mouse model of chronic myeloid leukaemia (CML) showed similar results with reduction in overall leukaemia but an increase in CNS infiltration (Agarwal et al., 2012). Overall, these observations indicate that CNS engraftment is independent of CXCR4-CXCL12 axis.

Leukaemic cells in a patient are composed of phenotypically diverse subsets which could differ in their ability to enter the CNS compartment. The CNS compartment did not show enrichment of a particular leukaemic sub-population with higher/lower levels of the selected trafficking molecules. It is clear from our results that BCP-ALL cell entry into the CNS compartment cannot be attributed to a particular subset of cells expressing a CNS 'address code'. It is also clear that a single chemokine-receptor ligand pair is unlikely to be essential or sufficient for leukaemic cell entry into the CNS compartment. These findings are in contrast to studies reported by Buonamici et al. (2009) showing CCR7 expression to be critical for CNS entry of T-lymphoblasts. These differences may be explained by a number of reasons. Firstly, a different experimental model was used by Buonamici et al. Secondly, it is possible that CNS infiltration seen in $CCR7^{+/+}$ T-lymphoblasts may be a mere representation of non-specific lymphoblast dissemination. Mice transplanted with CCR7 expressing lymphoblasts showed a higher overall leukaemic burden and a significantly shortened survival of the transplanted mice. Thirdly, B- and T- cells are intrinsically different in cellular behaviour. $CCR7^{+}$ memory T-cells are the most abundant leukocytes in the CSF and it may not be surprising if T-lymphoblasts conserved the CCR7-CCL19 axis to enter the CNS. Interestingly, pilot data presented on cells carrying BCR/ABL or MLL fusions failed to show any reduction in CNS infiltration in mice lacking the CCR7 ligand CCL19 (Buonamici et al., 2009).

One secondary aim of this chapter was to investigate the dysfunctional chemotaxis of SD1 by characterising the functional expression of CXCR4. The majority of SD1 cells exhibit

ligand-binding at 100ng/ml CXCL12 demonstrating slightly lower, but comparable, binding efficiency. The incomplete receptor internalization in SD1 is rather paradoxical. Typically, more rapid CXCL12-mediated CXCR4 internalization is associated with a dysfunctional migratory response (Shen et al., 2001), whereas leukocytes carrying mutated CXCR4 in WHIM syndrome show sluggish internalization and an exaggerated chemotaxis. (Gulino et al., 2004) However, in SD1, one may argue that a fraction of ligand-bound receptor might be non-functional.

Analysis of CXCR7 expression in SD1 showed elevated levels of CXCR7 transcripts. Staining of SD1 cytospins allowed visualization of CXCR7 in SD1 cells. CXCR7 was shown to be present in a subset of SD1 cells – rarely co-localised with CXCR4. It was also shown that CXCR7 out-competed CXCR4 in binding CXCL12. Blocking CXCR7 binding to CXCL12 showed no improvement in the chemotaxis of SD1 cells. This implies that CXCR7 scavenging of CXCL12 would not be enough to critically reduce the amount of CXCL12 present in the chemotaxis chamber. This inference is also supported by the fact that SD1 chemotaxis to CXCL12 remains minimal even at high CXCL12 concentrations (1µg/ml). However, the role of CXCR7-scavenging in tissue micro-environment, where chemokines are not in a free suspension state, small differences in chemokine concentration can potentially be important.

SD1 and Sup B15 cells both harbour the BCR-ABL1 translocation – a chromosomal translocation resulting in a constitutively phosphorylated tyrosine kinase. In CML, the BCR-ABL1 tyrosine kinase has been shown to interfere with CXCR4 expression and signalling (Ptasznik et al., 2002, Salgia et al., 1999, Lichty et al., 1998, Geay et al., 2005). Inhibiting BCR-ABL1 tyrosine kinase activity by Imatinib did not increase CXCR4 mRNA or surface levels, or chemotaxis to CXCL12. It appears that $p190^{BCR/ABL1}$ tyrosine kinase does not counter-regulate CXCR4 signalling in the same way as seen in $p210^{BCR/ABL1}$. This is also supported by the fact the Sup B15 cells carrying the same translocation, albeit at a much lower level, exhibit efficient CXCL12-mediated chemotaxis. This raises the question whether this phenomenon is limited to $p210^{BCR/ABL1}$. If so, this could be due to the different lineage and maturation status of cells carrying the BCR-ABL1 translocation variants (i.e myeloid vs lymphoid). On the other hand, this could also be explained by the intrinsic differences in these variant oncoproteins - $p190^{BCR/ABL}$ exhibits a higher tyrosine kinase activity and leukaemic transformation potential (Quackenbush et al., 2000, Li et al., 1999). However, this hypothesis requires further validation. These results could be replicated by inhibiting $p190^{BCR/ABL1}$ tyrosine kinase with novel tyrosine kinase

inhibitors or by inhibiting transcription of p190 $^{BCR/ABL1}$.

CXCL12 stimulation resulted in modest but rapid increase in phorphorylated p38-MAPK and ERK1/2 on some background phosphorylation of these pathways in SD1. A common pathway could not be identified in CXCL12-responsive cell lines. These results contradict studies carried out by Bendall et al. (2005) where primary ALL samples are shown to require p38-MAPK signalling for chemotaxis. The authors further showed that in primary samples lacking CXCL12-mediated chemotaxis (despite presence of surface CXCR4), p38-MAPK induction was not seen – hinting towards an uncoupled of CXCR4-p38-MAPK pathway. Contrary to this observation, CXCL12 stimulation of SD1 activates p38-MAPK phosphorylation. This raises the question whether the lack of CXCL12-mediated chemotaxis in SD1 may be a result of a dysfunction further down the MAPK pathway or perhaps in the cytoskeletal machinery of the cell. To support the second, studies on Nalm6 (CXCL12-responsive) and Fc4M (CXCL12-unresponsive) cell lines have shown a critical role for activation of RhoGTPases Rac1 and Cdc42 – crucial for actin polymerization (Palmesino et al., 2006). Taken together, the observations made from investigating the signalling pathways activated following CXCL12 stimulation suggest that the intracellular downstream pathways may be cell- and context- specific. It can be suggested that CXCR4 dysfunction at multiple levels (i.e moderate levels of CXCR4, only a minor proportion of signalling receptor evident by inefficient internalisation, and constitutive p38-MAPK and ERK1/2 pathways) collectively result in an inefficient chemotactic response in SD1 cells.

Overall, two main conclusion can be drawn from data presented in this chapter: (i) that BCP-ALL cells do not require a specific combination of leukocyte trafficking molecules to enter the CNS, & (ii) that CNS infiltration appears to be CXCR4 independent. However, the studies performed are not without limitations. The observations presented in this chapter are drawn from a limited samples size and based mainly on xenograft models. Moreover, all the cell lines and majority of primary cells showed CNS engraftment, making adequate comparison between CNS-infiltrating and non-infiltrating samples difficult. Furthermore, time-to-hind-limb paralysis represents CNS-related symptoms which may appear late in the course of CNS disease and/or may reflect cord compression due to expansion of vertebral column bone marrow. The initial screening for leukocyte trafficking molecules identified several chemokine receptors, selectins and integrins, however, a candidate approach was carried out subsequently. The role of integrins was unexplored in this study. Furthermore, chemotaxis assays were utilised to test chemokine receptor-ligand function. These assays lack the essential leukaemic cell-endothelium

interaction necessary for extravasation into extramedullary compartment. More complex models of blood-CSF barrier could be utilised instead of transmigration assays. Finally, pharmaceutical inhibitors (Imatinib, AMD3100, CCX771 & CCX754) were used in these studies. As with any pharmacological agent these potentially carry the risk of incomplete inhibition of the target receptor, or non-specific effects on other pathways. These studies could be supplemented by inhibition of chemokine receptors at the transcriptional level.

These data could be strengthened by using a larger cohort of patients with and without CNS disease. Cells taken directly from the CNS compartment could be tested for the expression patterns of leukocyte trafficking molecules and analysed for factors associated with disease dissemination such as chemotaxis, transendothelial migration and invasion. However, due to the relatively low incidence of CNS disease in patients and the ethical issues in taking large volumes of CSF to isolate sufficient cells from the CNS compartment, this can prove challenging. From a translational aspect, attempts at blocking the CNS entry of leukaemic cells do not appear to be feasible, since the cells are likely to have entered this compartment by the time the patient presents to the hospital. Alternatively, identifying factors that enable long-term survival of leukaemic cells may be a better therapeutic target. The role of bone marrow microenvironment in the survival, proliferation and evasion of therapy is well known. Preliminary data also suggests a similar role of the components of the CNS microenvironment in survival and chemotherapy evasion of ALL (Akers et al., 2011).

5 Investigating interleukin-15 mediated proliferative advantage in B- cell precursor acute lymphoblastic leukaemia cells

5.1 Introduction and aims

As discussed in chapter 4, the established xenograft model which utilized NOD.Cg-*PrkdcscidIl2rgtm1Wjl*/SzJ (NSG) mice and B-cell precursor (BCP) acute lymphoblastic leukaemia (ALL) cell lines demonstrated variable rate of central nervous system (CNS) engraftment by the cell lines. It was further shown that CNS entry of leukaemic cells is not governed by the leukocyte trafficking molecules investigated. Importantly, it was shown that CNS infiltration is not determined by selective entry of leukaemic cells with a high or low expression of a particular combination of chemokine receptors and P-selectin glycoprotein ligand -1 (PSGL1). Consequently, in order to understand the molecular mechanisms underlying CNS disease, other possibilities such as the retention and proliferation of leukaemic cells once they have entered the CNS compartment may be considered.

Interleukin-15 (IL-15), a member of the cytokine family, is one such candidate. Previous studies have identified single nucleotide polymorphisms (SNPs) in IL-15 gene to be associated with leukaemia development (Lin et al., 2010), minimal residual disease (MRD) at the end of induction therapy (Yang et al., 2009) and poor event free survival (EFS) (Lu et al., 2014). Furthermore, gene expression analysis has linked high IL-15 mRNA expression with aggressive disease features in ALL such as T-ALL and mediastinal leukaemia (Wu et al., 2010) and the risk for CNS relapse (Cario et al., 2007). However, these studies merely demonstrate association between the IL-15 gene and disease factors. A number of possible mechanisms could explain this association: Firstly, IL-15 could be directly influencing leukaemic cells in the CNS environment, via its well documented proliferative/anti-apoptotic actions. Secondly, IL-15 could be promoting retention of leukaemic cells in the CNS compartment by affecting cellular localization. Thirdly, IL-15 could indirectly affect leukaemia by modulating effectors of the host immune surveillance effectors, such as NK- and T- cells. And finally, IL-15 production by the host microenvironment may affect leukaemic behaviour irrespective of IL-15 expression by the leukaemic cells.

This chapter aims to investigate the direct biological effects of IL-15 on leukaemic cell

survival and behaviour. BCP-ALL cell lines and primary cells were utilized to investigate the association of high IL-15 expression levels and CNS disease. Additionally, this chapter aims to ascertain the effects of IL-15 on leukaemic cells proliferation and gene expression. The key questions addressed in this chapter are:

1. Do BCP-ALL cell lines and primary cells express IL-15 and IL-15 receptor subunits?

2. Can secreted IL-15 be readily detected in human cerebrospinal fluid (CSF)?

3. Can BCP-ALL cell lines respond directly to IL-15?

4. Via inhibition of IL-15 stimulated signalling pathways, can the effect of IL-15 be blocked?

Data presented in this chapter are part of an ongoing project in the laboratory. Contributions by other members of the laboratory are presented in brief and acknowledged in text. More detailed description of the work is presented in Appendix 1.

5.2 Expression patterns of IL-15 and IL-15 receptors in BCP-ALL

Prior to investigating IL-15 function, it was necessary to determine whether IL-15 and IL-15 receptor subunits were expressed by BCP-ALL. Therefore, 4 BCP-ALL cell lines (SD1, Sup B15, REH and SEM), 13 primary ALL samples and 6 primagraft samples were utilized for analysis. The clinical details of the cell lines and primary samples are presented in Table 4-1 and Table 5-1 respectively. Cells were homogenized in Trizol® and total RNA was isolated following DNAse digestion of the lysates. RNA samples were quantified by spectrophotometric method using Nanodrop. 200 ng total RNA was utilized for cDNA synthesis. However, in some primary samples, due to limited RNA yield, the entire extracted RNA was used for cDNA synthesis and the relative transcript for the housekeeping gene (GAPDH) was used for comparison following qPCR.

Patient ID	Sex	Age (Years)	WCC (x109/l)	Cytogenetics	CNS status	Outcome
#G01	M	2	23	11q23	1	CCR (19 months)
#G02	F	5	29	t(12;21)	1	CCR (19 months)
#G06	M	4	52	t(12;21)	1	CCR (13 months)
#ED7	M	10	3	Normal	1	CCR (13 months)
#G08	F	11	35	dic(7;9)	1	CCR (13 months)
#G09	F	6	23	Hyperdiploid	1	CCR (13 months)
#G11	M	10	14	High Hyperdiploid	TLP+ve	CCR (11 months)
#G16	M	2	90	High Hyperdiploid	1	CCR (10 months)
#G17	F	3	50	t(12;21)	1	CCR (9 months)
#E2	F	3	34.4	Hyperdiploid	1	CCR (21 months)
#E3	F	6	9.6	t(12;21)	1	CCR (21 months)
#E4	M	3	16.8	Hyperdiploid	1	CCR (20 months)
#E5	F	2	4.3	t(12;21)	1	Died during induction* (week 3)
#5449	F	2.5	62.2	t(12;21)	1	CCR (5.3 years)
#4630	F	2.9	103.6	t(12;21)	1	CCR (7.0 years)
#5094	F	2.1	84.6	t(12;21)	3	CCR (6.6 years)
#4736	F	3.5	113.3	t(12;21)	1	CCR (6.1 years)
#5705	F	3.4	221	t(12;21)	1	CCR (4.7 years)
#R3276	M	5.5	98	NA	1	CNS relapse (4.2 years)
#6539	M	1.3	NA	NA	NA	CNS relapse
#4336	F	7	NA	NA	NA	CNS relapse

Table 5-1: Clinical features of patients
CCR = continuous clinical remission, CNS = central nervous system NA = not available, TLP = traumatic lumbar puncture.

5.2.1 ALL cells express differential levels of IL-15 mRNA

First, the expression pattern of the two IL-15 isoforms, IL15-long signal peptide (IL-15-LSP) and IL-15-short signal peptide (IL-15-SSP), and three IL-15 receptor subunits (IL-15 Rα, β and γ) was analysed. To allow identification of the two IL-15 isoforms differing in their sizes due to insertion of 119 bp sequence to IL-15 SSP, standard RT PCR followed by agarose gel electrophoresis was utilized. All samples expressed IL-15-LSP whereas only 6/18 primary/primagraft samples and 3/4 cell lines expressed the cytoplasmic IL-15-SSP. Representative gel images from 3 samples (SD1, #ED-7 and #5449) are shown in Figure 5-1, whereas results from individual samples are presented in Table 5-2.

Next, in order to assess the relative expression of IL-15 gene in the leukaemic samples, SYBR Green qPCR was utilized. Using GAPDH as the housekeeping gene and setting SD1 IL-15 expression to a value of 1, relative expression was calculated. Figure 5-1b and Table 5-2 shows that IL-15 is differentially expressed in primary ALL samples. Due to limited availability of primary ALL samples, validation of IL-15 or the IL-15 receptor subunits expression by flow cytometry could not be possible.

These results not only confirm differential IL-15 expression in BCP-ALL cells as previously shown by Cario et al. (2007), but also extend to show that the cell-surface/secreted IL-15-LSP is the predominant isoform expressed in ALL, while the cytoplasmic IL-15-SSP is expressed in a minority of samples. It can be implied that BCP-ALL cells can potentially express and secrete IL-15.

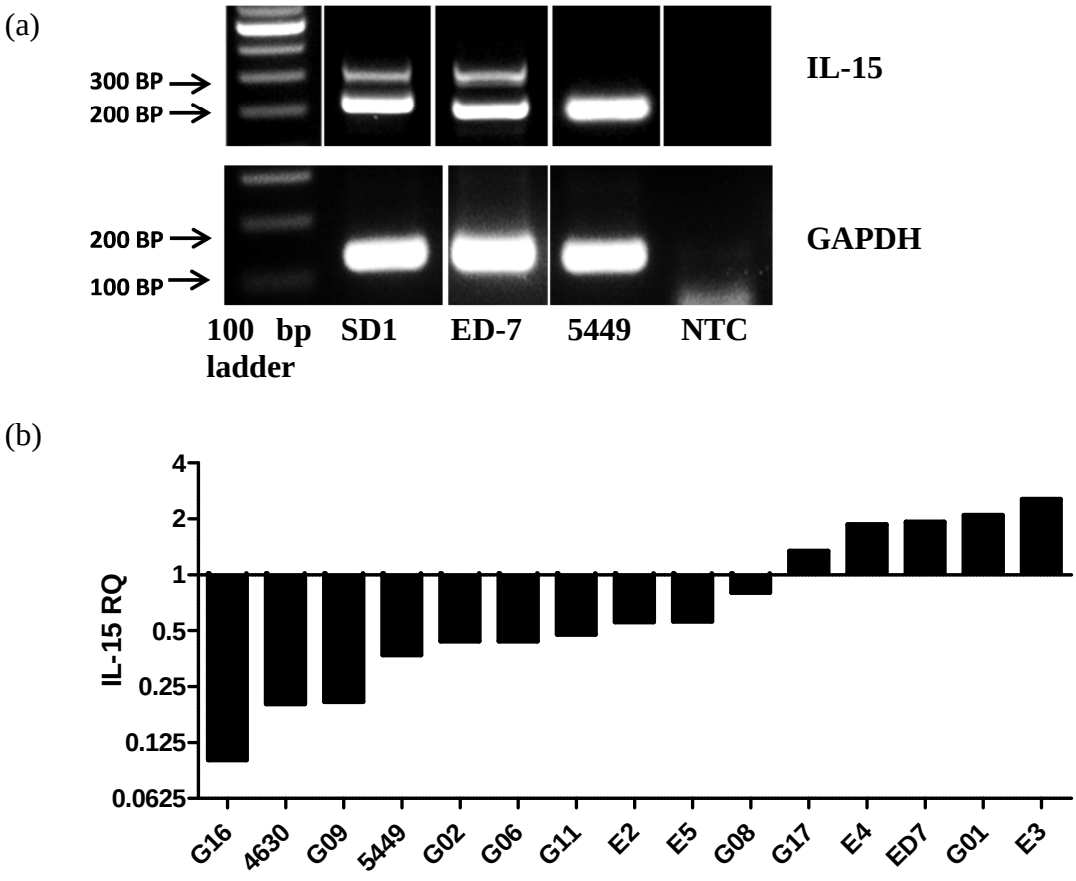

Figure 5-1: IL-15 mRNA expression in BCP-ALL cells
(a) RT PCR analysis of IL-15 isoforms in ALL samples. Nucleotide sizes shown in brackets: IL-15 LSP (201 bp), IL-15 SSP (320 bp). Sizes measured with reference to 100 bp DNA ladder (black arrows). Representative samples from BCP-ALL cell lines, primary samples and primagraft samples are shown. (b) SYBR Green relative quantification of IL-15 mRNA in primary samples using GAPDH as housekeeping gene and IL-15 mRNA expression in SD1 set to the arbitrary unit 1. Calculated using ABI RQ manager software.

5.2.2 ALL cells differentially express IL-15 receptor sub-units

The IL-15 receptor complex, is comprised of a specific high affinity IL-15Rα subunit, and shared β- and γc- receptor subunits. In order to assess if leukaemic cells could potentially respond to IL-15, analysis of IL-15 receptor subunits was performed using RT-PCR. Analysis by gel electrophoresis revealed that the majority of ALL samples express IL-15 receptor subunits. IL-15 Rα and γc subunits were expressed in all the samples whereas IL-15 Rβ was detected in 4/4 cell lines and 14/17 primary/primagraft samples. Representative gel images from 3 samples (SD1, #ED-7 and #5449) are presented in Figure 5-2 and the results from individual samples are presented in Table 5-2. IL-15 receptor expression could not be evaluated in two primagraft samples due to lack of amplification of GAPDH implying inadequate cDNA. These results imply that BCP-ALL samples can potentially respond to IL-15.

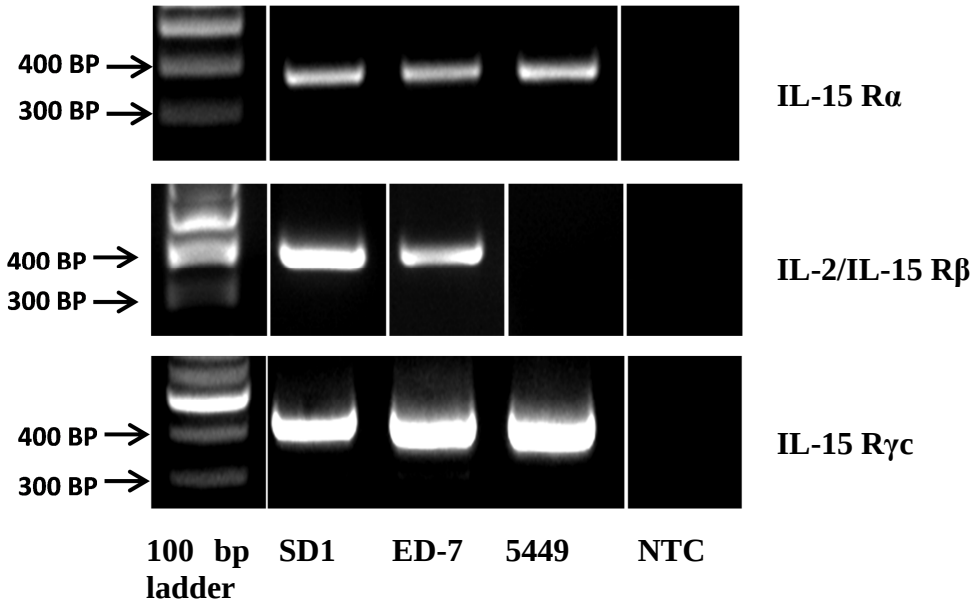

Figure 5-2 IL-15 receptor subunit mRNA expression in BCP-ALL cells
RT PCR analysis of IL-15 Rα, IL-2/IL-15 Rβ and IL15-Rγc in ALL samples. Nucleotide sizes shown in brackets: IL-15 Rα (402 bp), IL-2/IL-15 Rβ (403 bp) and IL15-Rγc (447). Sizes measured with reference to 100 bp DNA ladder (black arrows). Representative samples from BCP-ALL cell lines, primary samples and primagraft samples are shown.

Sample ID.	IL-15 RQ	IL-15 LSP	IL-15 SSP	IL15 Rα	IL15 Rβ	IL15 Rγ
SD1	1	Y	Y	Y	Y	Y
Sup B15	0.082	Y	Y	Y	Y	Y
REH	0.384	Y	Y	Y	Y	Y
SEM	0.337	Y	N	Y	Y	Y
#G01	2.09	Y	Y	Y	Y	Y
#G02	0.44	Y	N	Y	Y	Y
#G06	0.44	Y	Y	Y	Y	Y
#ED7	1.93	Y	Y	Y	Y	Y
#G08	0.80	Y	N	Y	Y	Y
#G09	0.21	Y	Y	Y	Y	Y
#G11	0.48	Y	N	Y	Y	Y
#G16	0.10	Y	N	Y	Y	Y
#G17	1.34	Y	Y	Y	Y	Y
#E2	0.56	Y	N	Y	Y	Y
#E3	2.56	Y	N	Y	Y	Y
#E4	1.86	Y	N	Y	Y	Y
#E5	0.56	Y	N	Y	Y	Y
#5449	0.37	Y	N	Y	N	Y
#4630	0.20	Y	N	Y	N	Y
#5094	n.d	Y	N	Y	N	Y
#4736	n.d	Y	Y	Y	Y	Y
#5705	n.d	Y	N	n.d	n.d	n.d
Total: 22		**22/22**	**9/22**	**21/21**	**18/21**	**21/21**

Table 5-2: Individual results of IL-15 and IL-15 receptor expression data in 4 cell lines, 13 primary samples and 5 primagraft samples.
RQ= relative quantitation. ID = identity. Y= yes, N= No, n.d= not determined due to unavailability of material.

5.2.3 Association of IL-15/IL-15 receptor expression with CNS disease in xenograft models

In the previous chapter, it was documented that BCP-ALL cell lines vary in their time to develop overt CNS disease once engrafted into NSG mice. As shown in table 5.2, SD1 with the shortest time to CNS disease demonstrated elevated expression of IL-15, in contrast to Sup B15 with the slowest onset of CNS disease. RT PCR analysis also confirmed expression of IL-15 receptor subunits in these cell lines. However, to accurately understand IL-15/IL-15 receptor interactions, it was necessary to quantify IL-15 receptor expression. Therefore the relative expression of IL-15 receptor subunits in SD1, Sup B15, REH and SEM was determined. TaqMan qPCR analysis for IL-15 Rα, IL-15 Rβ and IL-15γ_c revealed remarkable differences in the expression of IL-15 receptor subunits. SD1 exhibited highest expression levels of all the three IL-15 receptor subunits whereas Sup B15 demonstrated lowest levels among these 4 cell lines (Figure 5-3). These data show that SD1 cells can not only express both soluble and cytoplasmic isoforms of IL-15, but they also possess the potential to respond to IL-15.

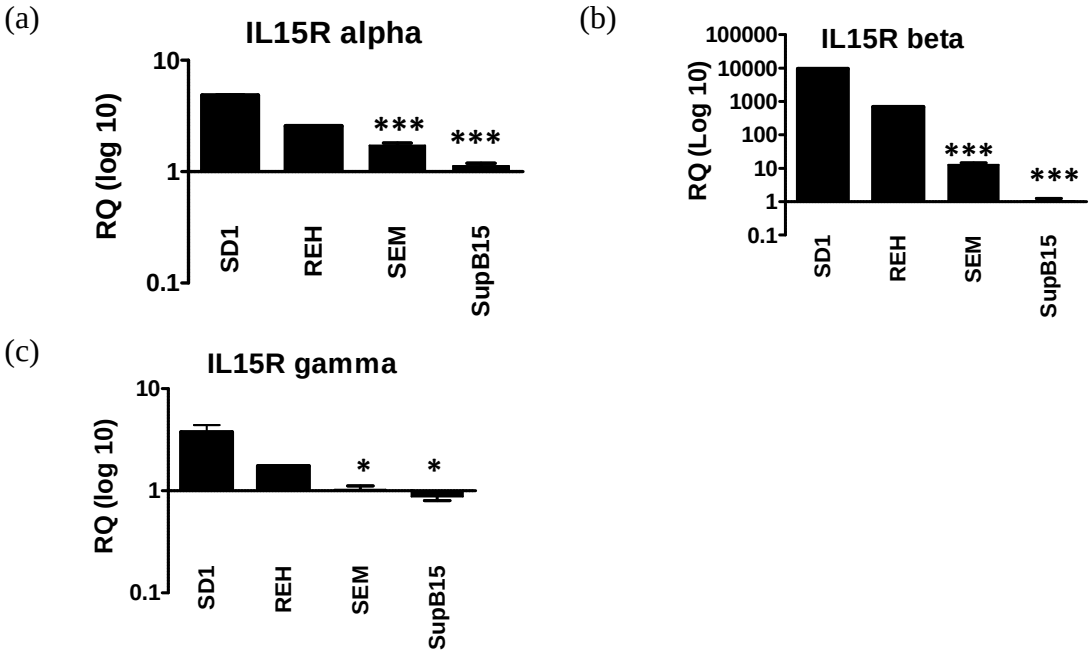

Figure 5-3: Relative expression levels of IL-15 receptor subunits in BCP-ALL cell lines.
cDNA from SD1, REH, SEM and Sup B15 was analysed for expression of (a) IL-15 Rα, (b) IL-2/IL-15 Rβ and (c) IL-15 Rγ_c. Relative expression was calculated using ABI RQ manager software. GAPDH was used as a housekeeping gene and gene expression in Sup B15 was set to arbitrary unit of 1 as a calibrator. Three independently grown cultures were analysed in triplicate. Data are presented as Mean ± SEM and analysed by Two-tailed unpaired Student *t* tests comparing SD1 to each of the other cell lines. ***p<0.001, **p<0.01, *p<0.05. RQ, relative quantification. (Contributed by Dr Chris Halsey)

Overall, these results demonstrate that BCP-ALL samples consistently express IL-15 and IL-15 receptor subunits at the mRNA level, the majority of samples express the cell-surface/secreted IL-15-LSP isoform, and all IL-15 receptor subunits suggesting that ALL cells can express and potentially respond to IL-15. RQ PCR analysis of IL-15/IL-15 receptor subunits in cell lines suggests a correlation with onset of CNS engraftment kinetics in mice.

5.2.4 Detecting IL-15 in CSF samples from BCP-ALL patients

IL-15 secretion is known to be tightly controlled and difficult to detect in culture supernatants in cells shown to express IL-15 (Tinhofer et al., 2000). Nevertheless, detection of secreted IL-15 in fluid compartments might potentially be very informative. Secreted IL-15 could influence the behaviour of not only the leukaemic cells, but also cells of the immune system. Furthermore, detection of IL-15 could be a useful biomarker of disease. Therefore, it was decided to assess whether readily detectable levels of IL-15 were present in CSF samples from patients with CNS-3 disease. A pilot experiment was performed using sandwich ELISA assay (catalogue no. 88-7158-22, eBioscience) to quantify IL-15 levels in 6 CSF samples from 3 patients with CNS-3 disease (#R3276, #6539 and #4336). Three standard dilutions (1:2, 1:4 and 1:10) of each CSF sample were assayed to ensure accurate quantitation. Analysis of CSF IL-15 levels by ELISA failed to show detectable levels of IL-15 in any of the samples (Figure 5-4). Consistent with previous studies (Tinhofer et al., 2000, Bergamaschi et al., 2012, Tagaya et al., 1996), these results are suggestive of a more controlled secretion of IL-15. It can be implied that the routine ELISA screening methods with a relatively high limit of detection (>15 pg/ml) may not be suitable for measurement of IL-15 levels in CSF supernatants.

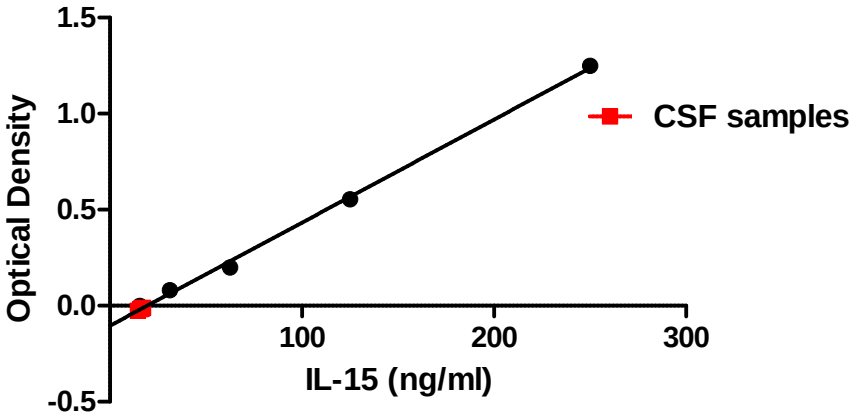

Figure 5-4: ELISA detection of IL-15 levels in CSF supernatants from patients with CNS disease.
CSF supernatants from 3 BCP-ALL patients were analysed for IL-15 levels by ELISA. Absorbance (430 nm) from standard and sample wells was measured on a microplate reader. CSF IL-15 levels (red) were interpolated from standard curve generated from standard concentrations of IL-15 (black dots). Data were analysed using GraphPad prism software and represents means of duplicate values.

5.3 Investigating mechanisms of the association of IL-15 with the CNS disease

Given the well documented role of IL-15 in proliferation of malignant cells in T-ALL (Barata et al., 2004), CLL (Trentin et al., 1996), multiple myeloma (Tinhofer et al., 2000) and T-cell lymphomas (Dobbeling et al., 1998), it was decided to investigate whether IL-15 plays a direct role in growth and survival of BCP-ALL. Furthermore, it is not known how IL-15 affects cell proliferation under hostile conditions such, as the CSF compartment which contains lower levels of proteins (Huhmer et al., 2006) and glucose (Nigrovic et al., 2012) compared to serum. This section describes experiments performed to assess the effects of IL-15 stimulation on the growth of BCP-ALL cells under normal and serum depleted conditions, followed by analysis of genes associated with leukocyte trafficking or metastasis in IL-15 treated cells.

5.3.1 Analysing effect of exogenous IL-15 on growth of BCP-ALL cells

SD1, Sup B15, REH and SEM were chosen for analysis. In order to determine effects of IL-15 on cell growth, cells grown in normal culture media (10% FCS in RPMI) were exposed to exogenous IL-15 and growth assessed by measuring viable cell counts are 24, 48, 72 and 96 hours. First, a dose-response experiment was performed on SD1 and Sup B15 using three different IL-15 concentrations (1, 5 and 25 ng/ml). SD1 exhibited a dose-dependent increase in cell numbers in response to IL-15. Significant increase in cell counts was observed at 72 and 96 hours with 25ng/ml IL-15. Sup B15 on the other hand appeared to be non-responsive to IL-15 induced growth advantage at these concentrations. Similarly, minimal effect was observed in REH and SEM cells at concentrations of 25 ng/ml.

The growth promoting effect of exogenous IL-15 was only seen in 1 out of 4 cell lines tested. However, IL-15 unresponsive cell lines Sup B15, REH and SEM carry IL-15 receptor subunits and therefore can potentially respond to IL15. Furthermore, these results were subsequently validated in primary BCP-ALL samples. Using a primary cell suspension culture model, addition of exogenous IL-15 resulted in a consistent increase in cell counts and significantly enhanced growth rates. (Williams et al., 2014)

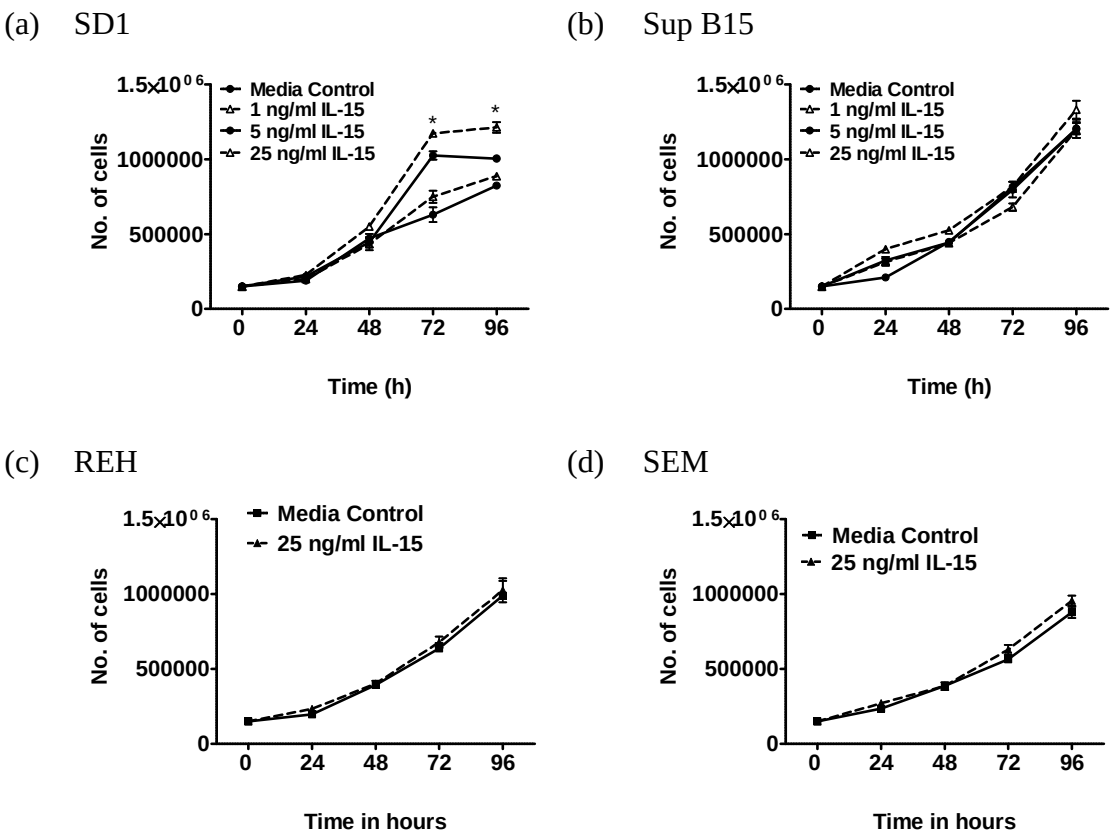

Figure 5-5 Effect of exogenous IL-15 on growth of BCP-ALL cell lines
Growth of (a) SD1 and (b) Sup B15 cells in response to increasing concentrations of exogenous IL-15 (media control, 1, 5, 25 ng/ml) at 24, 48, 72 and 96 hours. Growth of (c) REH and (d) SEM in response to media control or 25 ng/ml IL-15. Data are representative of 3 independent experiments, each performed in triplicate. Data are presented as mean ± SEM and analysed using an unpaired Student *t* test. **p*<0.05. (a &b contributed by Dr Mark Williams).

5.3.2 Determining the role of endogenous IL-15 on growth by IL-15Rα blockade

In order to determine whether endogenous IL-15 also affects growth, cells were treated with IL-15Rα neutralizing antibody (catalogue no. AF247, R&D systems) to inhibit IL-15 mediated receptor stimulation in the absence of exogenous IL-15. Cell counts were monitored at 24, 48, 72 and 96 hours. IL-15Rα blockade resulted in significantly reduced cell numbers in SD1 at 72 and 96 hours ($p<0.05$). As seen previously, the other cell lines did not show any differences in growth in control treated and IL-15 Rα neutralized groups (Figure 5-6). These results show that endogenous IL-15 production plays a significant role in the growth of SD1 cells.

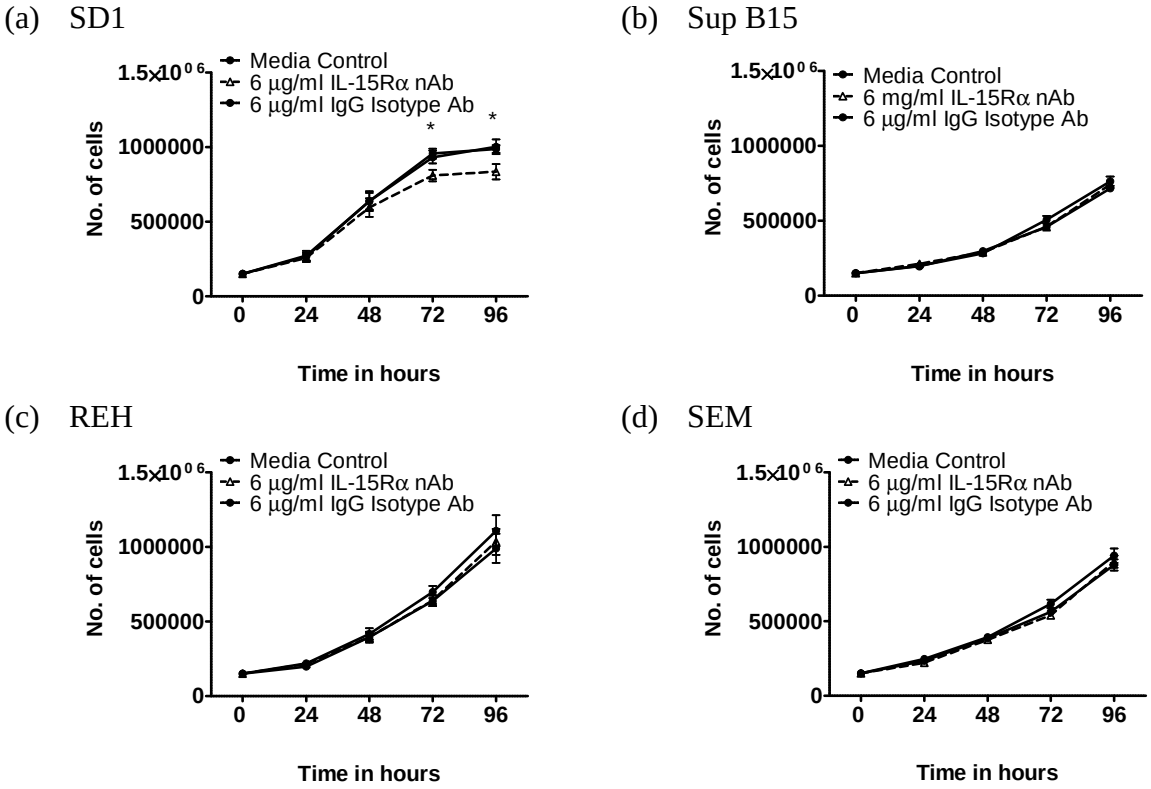

Figure 5-6: Growth of BCP-ALL cell lines following blockade of IL-15 Rα.
Growth of (a) SD1, (b) Sup B15, (c) REH and (d) SEM cells exposed to media control, IL-15 Rα neutralization antibody (6µg/ml) or isotype control antibody (6 µg/ml). Data represents mean ± SEM. Data were analysed using Student *t* test and are representative of 3 independent experiments per cell lines, each performed in triplicates. **p*<0.05 (a & b contribute by Dr Mark Williams)

In summary, these results show that IL-15 promotes dose-dependent growth in SD1 cells expressing the IL-15 receptors. Stimulation of IL-15 receptor by endogenous IL-15 is an important mechanism of cell proliferation evident by significant reduction in cell growth subsequent to blockade of IL-15Rα.

5.3.3 Determining IL-15 mediated growth advantage under serum depletion

In order to analyse the effect of IL-15 stimulation on leukaemic growth under serum depleted conditions, cells were cultured in various low serum conditions (0% FCS, 1% FCS, 5% FCS and 10% FCS) with exogenous IL-15 or with IL-15 neutralizing antibody (HuMax-IL-15, Amgen) for 96 hours. Analysis of the cell counts revealed a significant increase in cell counts under conditions of 0% serum, 1% serum and 5% serum in IL-15 treated cells compared to media control (Figure 5-7a). Maximum % increase in cell counts in response to exogenous IL-15 was seen under serum free conditions although this failed to reach statistical significance (Figure 5-7b). A consistent reduction in cell counts was seen in cell treated with HuMax-IL-15 although this difference was small and failed to reach statistical significance, suggesting that there is a greater role for exogenous IL-15 stimulation compared to endogenous stimulation (Figure 5-7c).

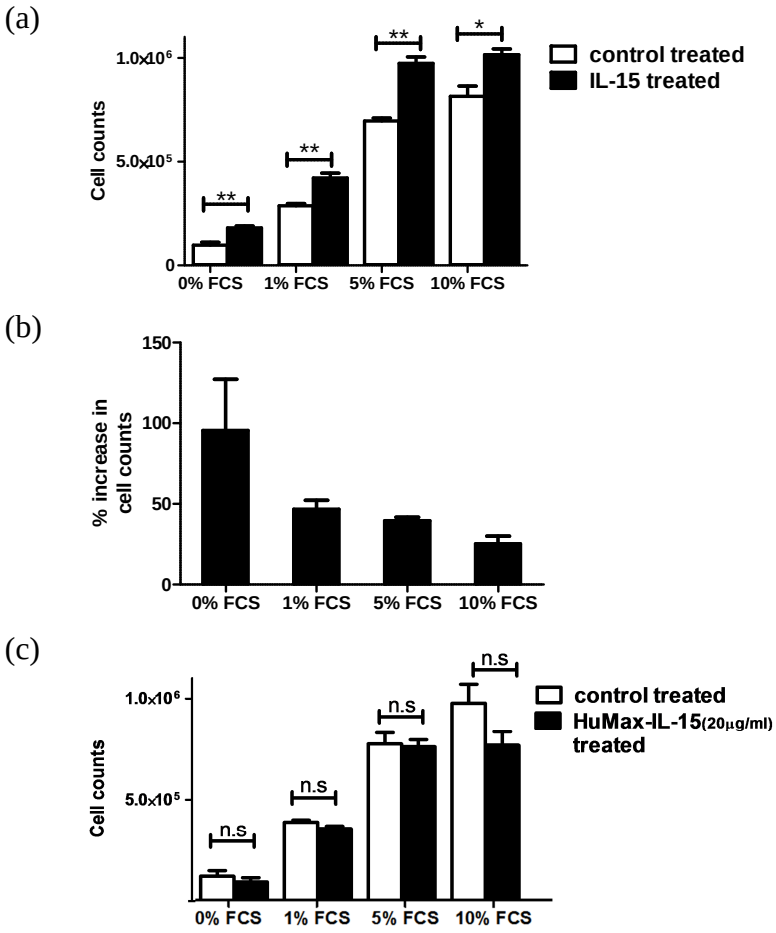

Figure 5-7: Growth of IL-15 treated SD1 cells under low serum conditions:
SD1 cells were cultured in RPMI supplemented with 0%, 1%, 5% and 10% FCS with or without IL-15 (25 ng/ml) for 96 hours. (a) Total numbers of viable cells in each group after 96 hours. (b) Precentage increase in cell counts of IL-15 treated SD1 cells. (c) Cell counts in HuMax-IL-15 treated cells vs isotype control. Data are pooled from 3 independent experiments performed in triplicates and presented as mean ± SEM. Data were analysed using two-tailed unpaired Student's *t* tests. **p<0.01, *p<0.05

5.3.4 IL-15 mediated growth is a result of increased proliferation

The increase in SD1 cell numbers in response to IL-15 stimulation could be a consequence of reduced apoptosis or increased cellular proliferation. A number of methods can be used to measure apoptosis along with other members of the laboratory. One of these is the flow cytometry based detection using Annexin V staining. This method allows identification of cells in early apoptosis by measuring Annexin V fluorescence coupled with dead cell discriminator 7-AAD. SD1 cells were cultured in various serum conditions with/without IL-15 for 96 hours and then labelled with Annexin V and 7-AAD. Analysis using flow cytometry revealed no significant differences in the percentage of cells undergoing early apoptosis (Figure 5-8a). Other measures of apoptosis such as Caspase-3 cleavage, poly(ADP ribose) polymerase (PARP) cleavage or the levels of anti-apoptotic proteins BCL-xL and BCL-2, were tested by the members of the laboratory, with no differences evident in IL-15 treated vs control treated SD1 cells (Appendix 1, Williams et al. 2014). These results clearly demonstrate that the IL-15 mediated growth advantage is unlikely to be due to an effect on apoptosis.

Next, to demonstrate whether the IL-15 mediated growth advantage was due to increased proliferation, cell division analysis was performed using a non-toxic cytoplasmic fluorescent dye CellTrace Violet (CTV). The cells are labelled with the fluorescent dye, and each time the labelled cell divides, the fluorescence intensity is reduced in its progeny. In some cell types, this manifests as a halving of fluorescence intensity with each cell division leading to peaks on histogram plots (Quah and Parish, 2012). In other cases, reduction in intensity is more variable and mean fluorescence intensity (MFI) can be used as a surrogate marker (Sisirak et al., 2011). In the case of SD1 cells considerable variation in cell size leads to smearing of peaks. Therefore, the MFI values were used instead. SD1 cells were labelled with CTV and cultured under various serum conditions with or with IL-15. Upon analysis by flow cytometry, consistently lower MFIs were observed in cells treated with IL-15 compared to controls, confirming higher cell proliferation in IL-15 treated SD1 cells (Figure 5-8b).

(a)

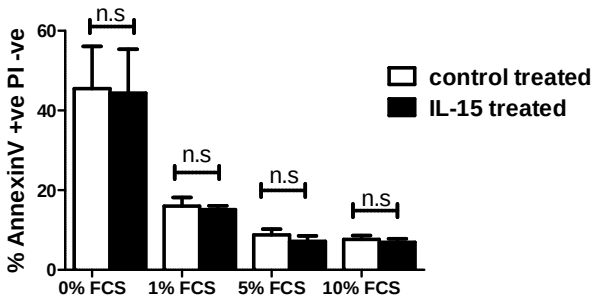

(b)

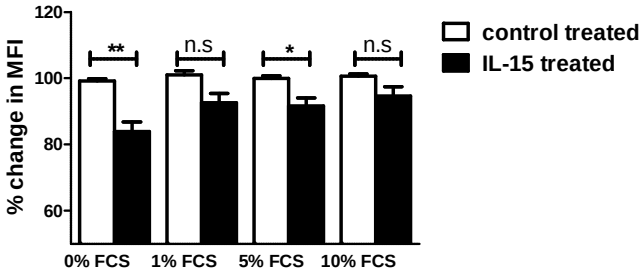

Figure 5-8: Effect of IL-15 treatment on apoptosis and cell proliferation:
(a) SD1 cells were cultured in RPMI supplemented with 0%, 1%, 5% and 10% FCS with or without IL-15. The percentage of live cells positive for Annexin-V in each group at 96 hours is shown. (b) SD1 cells were labelled with CTV and subsequently grown in RPMI supplemented with 0%, 1%, 5% and 10% FCS with or without IL-15. Cells were analysed for CTV fluorescence using flow cytometry. Fluorescence in control treated SD1 cells was calibrated as 100% and percent decrease in MFIs of IL-15 treated SD1 cells calculated. Data are pooled from 3 independent experiments performed in duplicates and presented as mean ± SEM. Data were analysed using two-tailed unpaired Student *t* test. **$p<0.01$, *$p<0.05$

5.3.5 Investigating the effects of IL-15 - induced signalling on the growth of SD1 cells

IL-15 stimulation results in the activation of a number of downstream signalling pathways in normal lymphocytes. These include JAK/STAT, ERK1/2, PI3K/Akt and NFκb/IκBα pathways. IL-15 stimulation of SD1 cells results in the rapid phosphorylation of ERK1/2 and STAT5 accompanied by minimal phosphorylation of Akt and NFκb. With other members of the laboratory, using specific inhibitors of ERK1/2 and STAT5, it was shown that IL-15 elicited growth advantage is dependent on the Ras/Raf/MEK/ERK pathway. Using specific MEK inhibitor to block ERK1/2, it was shown that IL-15 mediated growth advantage was completely abolished with affecting the overall growth of SD1 cells. STAT5 inhibition, on the other hand reduced overall growth but the IL-15 mediated growth advantage remained (Appendix 1, Williams et al. 2014). To analyse whether PI3K/Akt and NFκb/IκBα pathways are also implicated in IL-15 mediated proliferation in SD1, inhibitors of PI3K (LY 294002, Calbiochem) and NFκb (IKK-2 inhibitor IV, Calbiochem) were used along with exogenous IL-15. Treatment with either of the inhibitors resulted in profound inhibition of growth of cells along with elimination of any growth advantage due to exogenous IL-15. Given that both PI3K and NFκb are constitutively phosphorylated in SD1, and that the inhibition of these pathways results in complete arrest of proliferation, it appears that these pathways are vital to cellular proliferation. The slight increase in phosphorylation in response to IL-15 may be directly or indirectly involved in proliferation in response to IL-15. However, it is difficult to draw conclusions based on these results. Further investigation into the role of these pathways will be required.

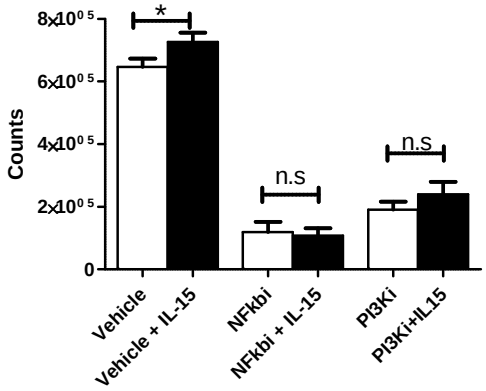

Figure 5-9: Effect of inhibition of downstream signalling pathways on IL-15 mediated growth.
SD1 cells were treated with 5 µM NFκb inhibitor (IKK2 inhibitor IV) or 20 µM PI3K inhibitor (LY 294002) or vehicle control (0.1% DMSO) ± IL-15. The total number of viable cells in each group after 72 hours. Data are pooled from 3 independent experiments performed in triplicates and presented as mean ± SEM. Data were analysed using two-tailed unpaired Student *t* test. *p<0.05, n.s. = Not significant

5.3.6 Regulation of genes associated with leukaemic dissemination following exposure to IL-15

In addition to the growth advantage under serum depletion, other possible mechanisms could account for the association of IL-15 with the CNS disease. For instance, IL-15 could indirectly regulate chemotaxis and homing of leukaemic cells into the CNS. In order to assess whether IL-15 could be involved in regulation of genes associated with leukaemic dissemination, two separate realtime qPCR gene expression arrays on IL-15 treated SD1 cells were performed. First, RT^2 human tumour metastasis profiler array (catalogue no. PAHS-028Z-2, SABiosciences) comprising of 96 genes associated with cancer metastasis was used. Next, custom designed TLDA (Applied Biosystems) plates comprising 30 selected chemokine receptors, selectins and integrin genes were utilized. Overall, out of 126 genes associated with leukocyte trafficking and cancer metastasis, 9 genes were identified to be up-regulated or down-regulated with IL-15 treatment (Appendix 1, Williams et al. 2014) . Although these arrays are marketed as gene validation arrays, this technology is not without limitations (Gaj et al., 2008). Therefore, to confirm these results, qPCR assays for individual genes identified in array analysis were performed.

First, SYBR Green qPCR primers were designed against 7 genes (CDH11, MMP9, PTEN, SERPINE1, DENR, MMP3 and TIMP4) identified by RT^2 profiler arrays. SD1 cells had shown maximum growth advantage to IL-15 treatment at 72 and 96 hours. However, it could be possible that regulation of gene expression occurs at earlier time points. Therefore, both early (4, 6 and 24 hours) and late (72 hours) time points were chosen. Analysis by qPCR showed only SERPINE1 mRNA levels to be significantly up-regulated in IL-15 treated SD1 cells at 72 hour time points (Figure 5-10). None of the genes showed any difference between control- and IL-15 treated SD1 cells at the earlier time points (data not shown). MMP3 validation could not be performed due to lack of a suitable positive control. Therefore, MMP3 was excluded from the analysis.

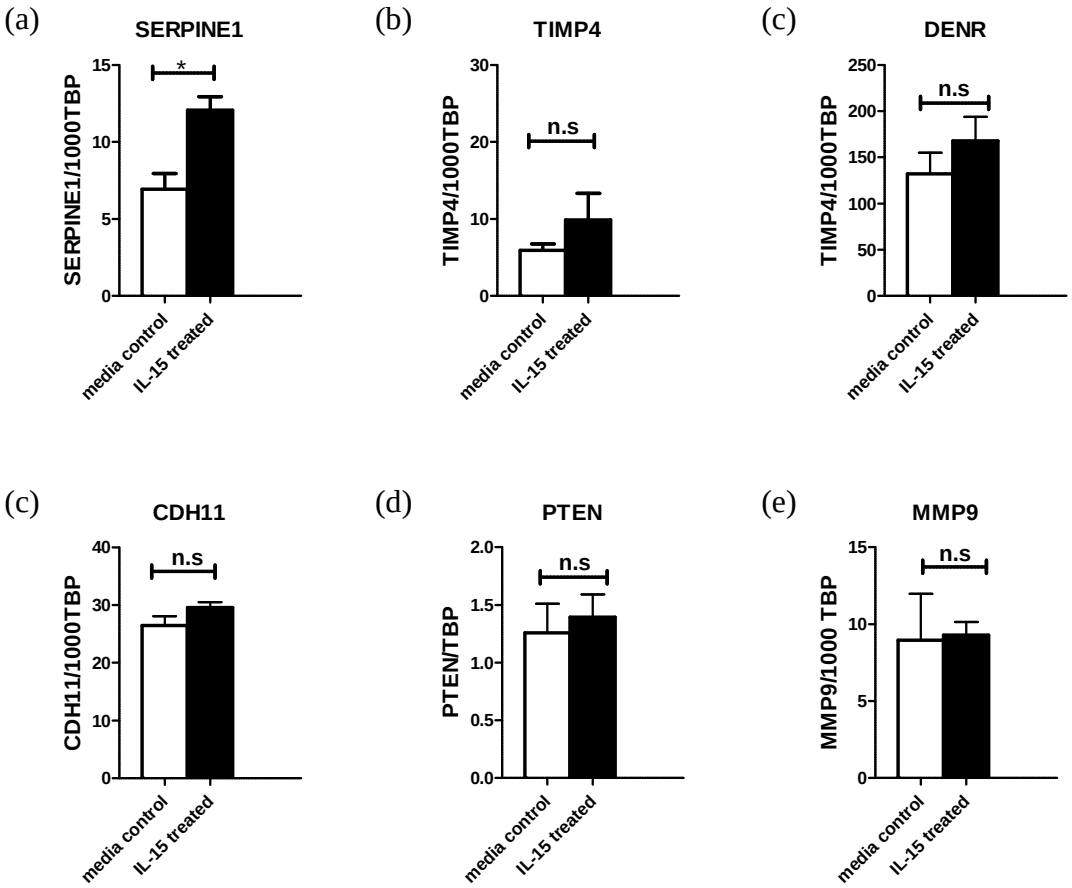

Figure 5-10: qPCR analysis of metastasis-associated genes identified by RT^2 profiler array
SD1 cells were grown in complete culture media ± IL-15 (25 ng/ml) for 72 hours. SYBR Green qPCR analysis of (a) SERPINE1 (b) TIMP4, (c) DENR, (d) CDH11, (e) PTEN and (f) *MMP9* using tata-binding protein (TBP) as housekeeping gene. Data are pooled from 3 independently grown cultures analysed in triplicates. Data were analysed using two-tailed unpaired Student's *t* test and presented as mean ± SEM. *p<0.05. n.s= non-significant.

Next, in order to confirm targets (PSGL-1 and CXCR3) identified by TLDA analysis, TaqMan qPCR analysis was performed on SD1 cells treated with IL-15. Relative quantitation confirmed significant up-regulation of PSGL-1 and CXCR3 (Figure 5.9 a & b). To establish whether these genes were also up-regulated at surface protein level, flow cytometric analysis was performed. Comparison of surface protein expression levels confirmed significant up-regulation of PSGL-1 in IL-15 treated SD1 cells. (Figure 5-11 c & d)

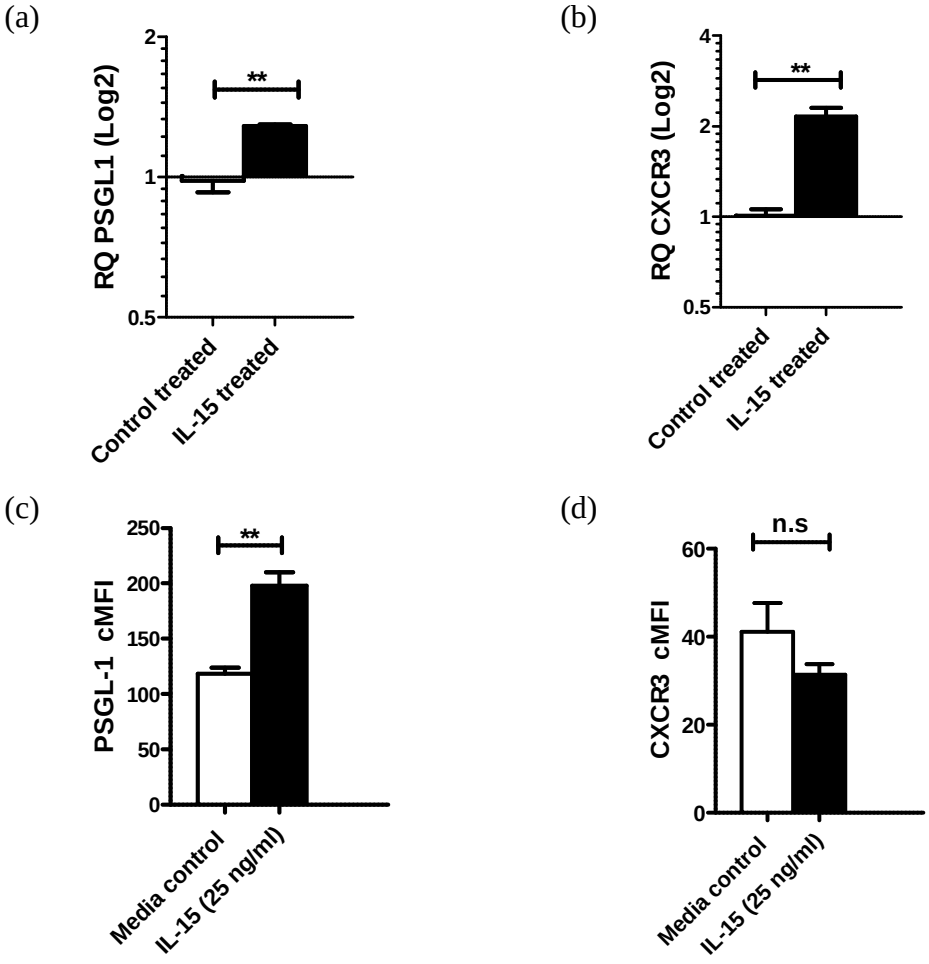

Figure 5-11: qPCR and FCM analysis of IL-15 treated SD1 cells.
SD1 cells were grown in complete culture media ± IL-15 (25 ng/ml) for 72 hours. TaqMan qPCR analysis of (a) *CXCR3* and (b) *PSGL-1* using *GAPDH* as housekeeping gene. Data are pooled from 3 independently grown cultures analysed in triplicates. Surface expression of (c) CXCR3 and (d) PSGL1 were analysed using flow cytometry. Corrected MFIs (cMFI) represents $MFI^{specific\ antibody} - MFI^{isotype\ control}$. Data are pooled from 3 independent experiments and presented as mean ± SEM. Data were analysed using two-tailed unpaired Student's *t* test. *p<0.05, **p<0.01. n.s= not-significant.

In summary, these data support the hypothesis that in addition to providing proliferative advantage, IL-15 stimulation may result in increased interaction of leukaemic cells with CNS barriers by up-regulating molecules involved in leukocyte trafficking (CXCR3/PSGL-1) or invasion (SERPINE1).

5.4 Discussion

In this chapter, mechanisms underlying the association of IL-15 expression with CNS disease in ALL were examined. Using BCP-ALL cell lines, the effect of IL-15 stimulation at multiple time points on the growth of leukaemic cells under normal and serum depleted conditions was analysed. SD1, which exhibited the highest IL-15 and IL-15 receptor expression among the cell lines, showed significantly elevated cell numbers under normal and serum depleted conditions in the presence of exogenous IL-15. Moreover, growth was significantly reduced with IL-15-Rα blockade in the absence of exogenous IL-15, suggesting IL-15 production by leukaemic cells may play an important role in their growth. The IL-15 mediated growth advantage was demonstrated to be a result of an increased cell division and with no apparent effect on markers of apoptosis. Secreted IL-15 could not be detected in CSF samples of patients with CNS disease. Gene targets identified by high throughput arrays were analysed by qPCR. CXCR3, PSGL-1 and SERPINE1 were found to be significantly up-regulated by qPCR. IL-15 stimulation results in modest activation of PI3K and NFκb pathways. Using specific pathway inhibitors to determine their specific role in IL-15 mediated growth showed inconclusive results due to profound inhibition of overall growth. Briefly, this chapter focusses on determining mechanistic explanation of a clinical phenomenon, namely, the association of high IL-15 expression and CNS disease in ALL.

Several studies have identified IL-15 as a candidate gene for leukaemia development (Lin et al., 2010), treatment response (Yang et al., 2009), survival (Lu et al., 2014), and CNS disease (Cario et al., 2007). However, these studies do not provide a mechanistic link between IL-15 and such high-risk factors. In the cohort of patients tested for IL-15 expression, all samples were shown to express IL-15 – highlighting the relevance of IL-15 in the context of ALL. Increased cell growth in response to exogenous IL-15, and growth reduction in response to IL-15 receptor blockade and IL-15 neutralization demonstrate that both exogenous and endogenously produced IL-15 may be simultaneously involved.

The role of IL-15 receptor levels in ALL is not known. Analysis of IL-15 receptor expression in primary ALL samples and cell lines showed heterogeneous expression of IL-15 receptor subunits. In the cohort of patients assessed, the majority of samples expressed IL-15 receptor subunits. Whether expression levels of IL-15 receptor subunits influence outcome, remains to be elucidated. Larger sample size and longer follow-up would be required to draw associations between IL-15 receptor expression and patient outcome.

High IL-15 mRNA expression is predictive of CNS relapse (Cario et al., 2007). In chapter 3, we have shown that CNS leukaemia is predominantly limited to the CSF compartment – a site presumably less conducive to cellular growth compared to the bone marrow microenvironment. IL-15 has a more potent proliferative effect under conditions mimicking the CSF. Consistent with our findings, IL-15 is also involved in NK cell survival under serum free conditions (Carson et al., 1997). IL-15/IL-15 receptor mediated growth advantage may be more important in the CNS compared to the bone marrow.

Several reports have shown suppression of apoptosis as the main mechanism of IL-15 mediated survival in neutrophils (Bouchard et al., 2004), Large granular lymphocytes (Hodge et al., 2009), NK cells (Carson et al., 1997), and malignant plasma cells (Tinhofer et al., 2000). On the contrary, IL-15 stimulation resulted in increased proliferation evident from dye-dilution in IL-15 treated cells whereas measures of apoptosis such as Annexin V expression remained unchanged. Although intriguing, these data are limited to SD1 and require further investigation. ALL is a heterogeneous disease with complex acquired mutations. Study of a larger cohort of primary samples would be needed to confirm this mechanism.

In addition to proliferation, exogenous IL-15 was also shown to up-regulate CXCR3, PSGL1 and SERPINE1 transcripts. These observations provide an alternative explanation to the association of IL-15 with CNS disease. The IL-15 receptor is shown to regulate lymphoid homeostasis and IL-15 knockout mice have shown reduced numbers of circulating T- and B cells and fewer leukocytes in lymph nodes (Lodolce et al., 1998). The up-regulation of leukocyte trafficking molecules provides a link between IL-15 and leukaemic cell trafficking. As shown in chapter 3 and 4, PSGL1 and CXCR3 are unlikely to be essential for entry into the CNS compartment. However, an assistive role for these receptors in CNS infiltration cannot be excluded. Human CD4+ T cells are shown to transit across the BCSFB via P-selectin/PSGL1 interactions (Kivisakk et al., 2003). In addition, CXCR3 expressing T cells are found in CSF in multiple sclerosis (MS) patients (Balashov et al., 1999). Upregulation of SERPINE1 following IL-15 stimulation can explain the aggressive disease characteristics associated with IL-15 expression. SERPINE1 is a serine protease inhibitor, which has been implicated in metastasis and invasion (Bajou et al., 1998). Interestingly, SERPINE1 expression in melanoma cells is linked to site-specific metastasis to the skin. (Klein et al., 2012) Whether SERPINE1 up-regulation in response to IL-15 represents merely an aggressive behaviour of disease or is associated with CNS-specific tropism of leukaemic cells, requires further clarification.

IL-15 treatment stimulates several downstream signalling pathways such as ERK1/2, STAT5, PI3K and NFκB. Inhibition of the MEK/ERK pathway abrogated IL-15 mediated growth advantage without affecting overall cell growth. However, the role of other pathways, such as PI3K and NFκB resulted in an overall reduction in cell proliferation. It remains to be investigated whether IL-15 mediated activation of these pathways indirectly affect leukaemic cells behaviour by IL-15 regulated genes (CXCR3, PSGL1 and SERPINE1).

The GWAS data provides a list of SNPs in the IL-15 gene statistically associated with various ALL disease factors (Yang et al., 2009, Lin et al., 2010). However, these do not provide any direct evidence on how these genetic changes can affect the disease phenotype. For instance, it is not known whether IL-15 SNPs lead to an increase or decrease in IL-15 production. Also, no distinction can be made between IL-15 production by leukaemic blasts themselves or the tumour microenvironment. However, such statistical associations together with functional analysis of the candidate gene help us generate hypotheses about the mechanism of the underlying clinical phenotype. Our studies demonstrate that exogenous IL-15 production provides a greater growth advantage compared to endogenous IL-15 production by leukaemic cells, suggesting that IL-15 production by host microenvironment may be more important than IL-15 production by leukaemic cells. The growth advantage is maximal under serum depleted condition. Additionally IL-15 up-regulates genes associated with leukocyte migration and invasion. We hypothesise that IL-15 may facilitate engraftment and long-term survival in the hostile CNS microenvironment. In the bone marrow – where serum starvation is unlikely to be a selective pressure – IL-15 may play a less important role in leukaemic cell growth. Alternately, high IL-15 in the bone marrow may activate anticancer immune response which may be more efficient in the bone marrow compared to the CNS due to efficient barriers between the circulation and the CNS. Further investigation into the role of host micro-environment/immune system in leukaemia is required. Our studies are based on observations from xenograft NSG mice which lack mature B- and T- cells and are IL-2Rγ_c deficient, and therefore are not suitable for investigating IL15/IL-15 receptor interactions between leukaemia and the host microenvironment/immune system. In order to discriminate between IL-15 production by leukaemic cells vs the microenvironment, and autocrine vs paracrine signalling, other models such as transgenic or knock-down models would be required.

6 Investigating novel biomarkers to improve diagnostic accuracy of central nervous system disease in childhood acute lymphoblastic leukaemia

6.1 Introduction and aims

The involvement of central nervous system (CNS) by acute lymphoblastic leukaemia (ALL) cells is routinely determined by microscopic examination of a small amount of cerebrospinal fluid (CSF) obtained by lumbar puncture. With this method approximately 4% children are considered to have CNS leukaemia at diagnosis (Marwaha et al., 2010). However, the following lines of clinical and experimental investigation suggest that the frequency of CNS involvement at diagnosis may be higher:

1. The majority of children with ALL, if left untreated, rapidly develop signs of overt CNS disease (Evans and Craig, 1964).
2. Historic autopsy data prior to CNS prophylaxis) reveals involvement of the meninges in up to 70% cases (Azzarelli and Roessmann, 1977, Price and Johnson, 1973, Thomas, 1965).
3. CNS relapses are seen in patients with no evidence of CNS disease at diagnosis.
4. In some, studies using more sensitive techniques such as flow cytometry and polymerase chain reaction (PCR), up to 50% patients test positive for the presence of leukaemia in their CSF samples (Scrideli et al., 2004, Martinez-Laperche et al., 2013).

Notably, data from murine models (chapter 3) reveal a distinct histological pattern of CNS involvement by ALL. Leukaemic cells are seen to adhere to the meningeal surfaces rather than in a free-floating state. It can be argued that sampling a small volume of the CSF (from the lumbar spine) carries the risk of underestimating the true incidence of CNS disease. Therefore, it is necessary to test alternative methods to diagnose CNS disease. Various Studies have tested soluble biomarkers for the detection of CNS disease (Section 1.3.7.4) However, many CNS-1 patients may potentially have submicroscopic CNS involvement (these could be considered to be false-negative cases). Consequently, any comparison between CNS-1 and CNS-3 patients will lack sensitivity. Therefore, it is hypothesised that using a more sensitive technique such as quantitative PCR (qPCR) will more accurately define the group of patients with CNS disease and therefore be more likely to identify soluble biomarkers of CNS disease with good predictive value.

The long term aims of using such accurate diagnostic methods would be diagnosis, monitoring and prediction of overt CNS relapse. The envisaged potential of this is presented in Figure 6.1.

This chapter present preliminary data that could lay the foundations for a larger multicentre clinical trial to address the aforementioned aims. The key questions addressed in this chapter are:

1. Can qPCR using patient specific minimal residual disease (MRD) reagents be used to detect and monitor sub-microscopic levels of CNS disease?
2. Can the levels of selected chemokines in the CSF correlate with sub-microscopic levels of CNS disease?

In order to address these questions, CSF samples from children with ALL were collected and an ethically approved CSF Biobank was established to efficiently store and catalogue samples and clinical information. As DNA extraction from the low number of cells normally found in CSF could prove challenging, various DNA extraction and storage methods were compared. In order to test the frequency of sub-microscopic CNS disease, qPCR assays using patient specific TaqMan qPCR primers were utilized. Finally, levels of a panel of chemokines were analysed in CSF supernatants from CSF qPCR+ve vs. CSF qPCR-ve patients to assess whether these could be used as disease biomarkers.

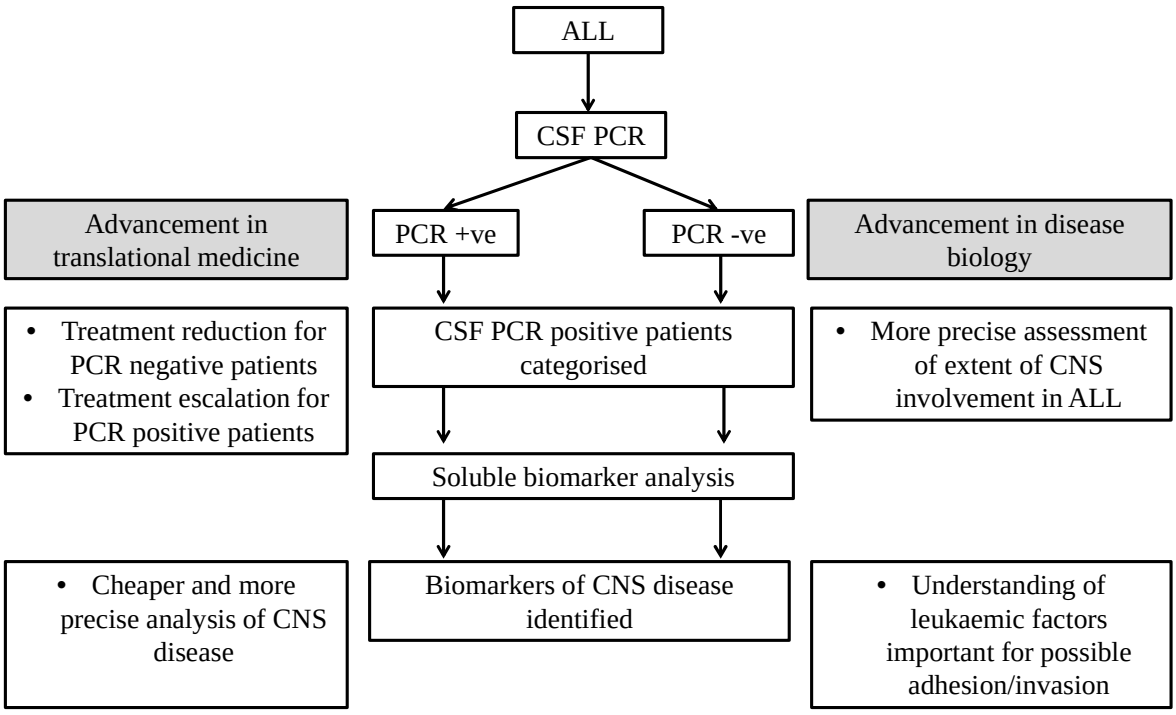

Figure 6-1: Envisaged potential for using more sensitive methods for the diagnosis of CNS disease in ALL.

6.2 Study design

6.2.1 Ethics

The study was conducted in accordance the ethical standards of the Helsinki declaration and was approval by West of Scotland research ethics committee (WoSREC reference: 09/SO703/77).

6.2.2 Study population

From the period between July 2011 and July 2014, all patients diagnosed with ALL at the Royal Hospital for Sick Children (Yorkhill henceforth) were assessed for recruitment on the inclusion criteria.

6.2.3 Inclusion criteria

- All patients under the age of 18 years at the time of diagnosis with a first diagnosis of ALL diagnosed using standard criteria.
- Willing to participate in the study.

6.2.4 Exclusion criteria

- Infants less than 1 year of age at diagnosis.
- Patients diagnosed with mature B-ALL (Burkitt-like) or Lymphoblastic lymphoma.
- Patients who have received prior ALL therapy except clinical urgency for no more than 1 week prior to their first lumbar puncture.

6.2.5 Patient selection and enrolment

Potentially eligible patients were identified at Yorkhill. All persons taking informed consents had received training in Good Clinical Practice (GCP). Parents were approached and the study aims and objectives were explained verbally and by written parent information leaflets. In case of children >6 years of age, and >10 years of age, separate patient information leaflets were also provided. It was explained to the parents that they were under no obligation to enter the study and they could withdraw at any time during the study. Following their interest, written informed consents were obtained from parents of patients. In cases where patients were enrolled in UK MRC trials and had given blanket

consent allowing the researchers to use leftover samples, additional consents were not obtained. Patients enrolled in UK MRC trials who had refused to give permission for the use of leftover samples, were not contacted for enrolment in the study. If patients chose to withdraw from the study, no further sample collection or analysis was performed.

6.2.6 Treatment protocols

Patients were treated under UKALL2003 (Vora et al., 2013), UKALL2011 or EsPhALL (Biondi et al., 2012) protocols. Patients with BCP-ALL received NCI risk assessed induction where NCI- low risk patients received 3 drug induction and NCI- high risk patients received 4 drug induction therapy. Patients with BCR-ABL1 positive ALL received additional Imatinib along with National Cancer Institute (NCI)- high risk induction therapy. All patients with T-ALL received NCI- high risk induction therapy. Subsequently, post induction therapy was stratified based on day 29 MRD results. Details of the UKALL2011 trial can be found online at:
http://www.haematologyclinicaltrials.co.uk/trials/123.

6.2.7 Data collection

Following patient recruitment, patient clinical and demographic details were recorded from patient treatment files on a study proforma and stored in the study site file, located at Yorkhill. Data, managed electronically, were stored in a secure and encrypted computer at the Glasgow Biomedical Research Centre (GBRC).

6.2.8 Initial sample processing

Patients underwent lumbar puncture for sampling of the CSF. This procedure is performed under general/local anaesthesia. The procedure was performed by appropriately qualified and registered staff at Yorkhill. Approximately 1 ml fluid was withdrawn and transferred to the haematology laboratory for cytospin preparation and automated cell counting. Presence of leukaemic cells/normal leukocytes was recorded and CSF cell count was measured on an automated cell counter. After the appropriate diagnostic tests were performed, and verified by trained haematologists, leftover samples were transferred to the GBRC. Patient identifiers were replaced with the unique patient number (UPN) allocated at the time of recruitment. CSF cell pellets, supernatants and matched peripheral blood samples were stored at the CSF Biobank at -80 ºC till further use. A study flow chart is presented in the Figure 6-2

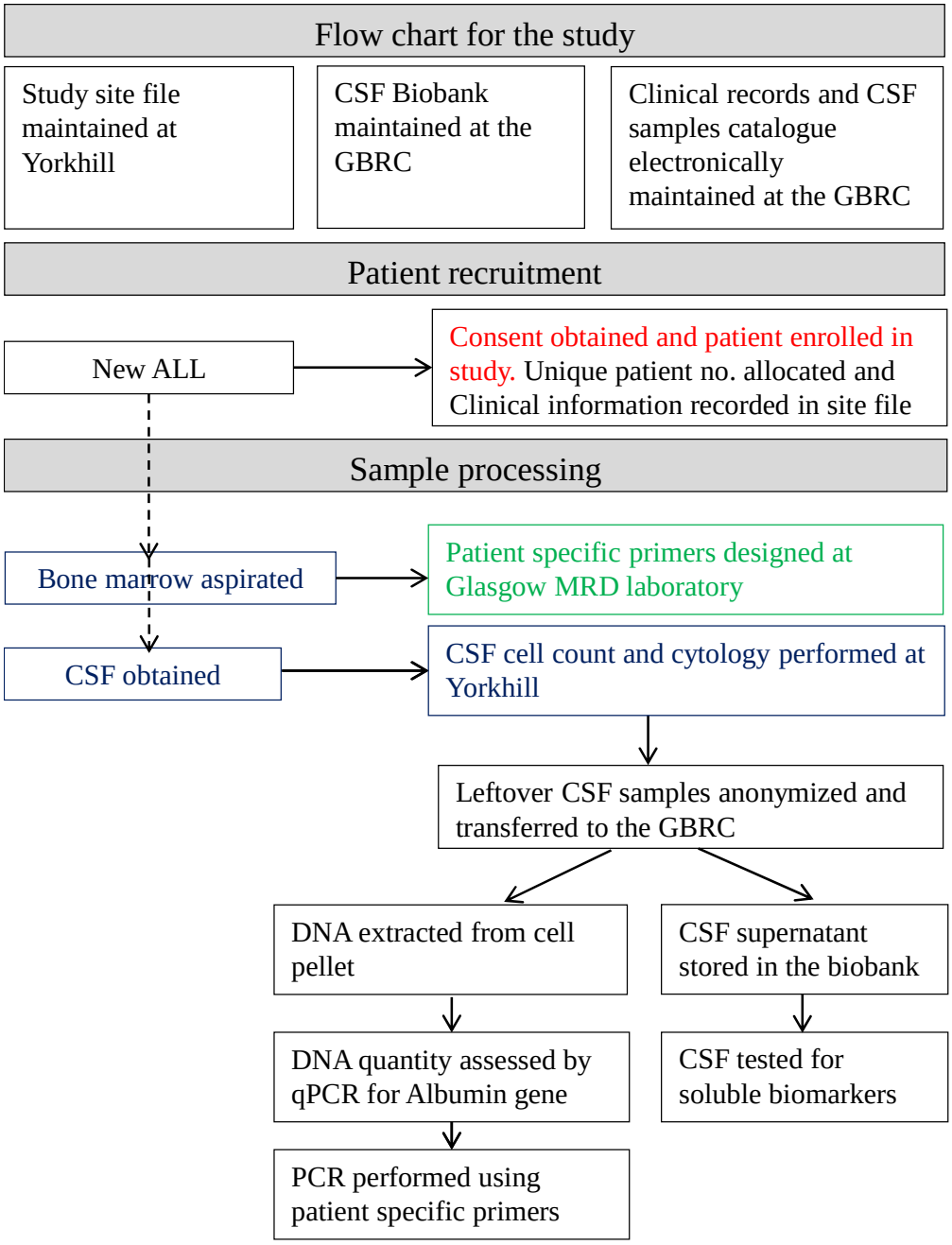

Figure 6-2 Scheme for patient recruitment and sample analysis
Procedures indicated with: red font were performed by the research nurses Alison Spence and Wendy Taylor, green colour were performed by team led by Sandra Chudleigh, and blue by clinical registrars and specialists. Procedures indicated with black font were my responsibility.

6.2.9 Detection of leukaemic DNA

During development, B- and T cell precursors undergo immunoglobulin (Ig) and T-cell receptor (TCR) gene rearrangement resulting in V(D)J sequences unique to the cell and its progeny. The clonal concept implies that leukaemic cells in a patient would carry identical Ig/TCR rearrangements. This principle is utilized for monitoring MRD by qPCR. The Glasgow MRD laboratory is part of the larger UKMRD laboratory network specialized for the analysis of MRD with a sensitivity of up to 1 leukaemic cell in 1 x 10^5 cells. This

process involves identification of MRD targets by a screening method, designing and testing patient specific junctional primers (allele specific oligonucleotides or ASO primers), and testing for sensitivity and specificity of the targets. Standard curves constructed by serial dilution of diagnostic DNA are used to test the sensitivity of the assay and control (mononuclear cell (MNC)) DNA is used to test the specificity of the assay.

6.3 Method optimization

The CSF is a pauci-cellular fluid. The mean CSF cell count in neonates is approximately 9 cells/µl (Kestenbaum et al., 2010), and sharply declines with age to approximately 2 cells/µl in young children (Portnoy and Olson, 1985). Given the small volume of CSF available for analysis (300-500 µl), it was anticipated that the amount of amplifiable DNA extracted from the cell pellet might be extremely low. Therefore it was vital to test if conventional methods could achieve adequate DNA yield required for qPCR analysis. In addition, methods for DNA quantification were optimized.

6.3.1 Optimization of DNA quantification

In order to discriminate between samples truly negative for leukaemic cells and false negatives, it was essential to accurately quantify the extracted DNA. Spectrophotometric methods are widely used for DNA quantification. NanoDrop (Thermofisher) offers DNA measurement using UV- absorbance and requires a small volume for measurement (1 µl). However, this method was found to be unsuitable for our studies. NanoDrop lacked accuracy for two reasons: firstly the absorbance measurements were found to be affected by residual trace amounts of RNA and phenol, secondly, this method was not precise at low DNA quantities (data not shown). Therefore, it was decided to use qPCR based method to accurately assess DNA quantity and quality.

qPCR is routinely used by the UK MRD labs to assess the quantity of DNA and provides accurate quantification of amplifiable DNA. TaqMan primers are designed to amplify a sequence in the albumin gene and a fluorescent probe is utilized to quantify the amplification of DNA. A drawback of this method is the requirement of up to 15 µl sample volume for the assay. CSF samples were analysed against known quantities of control DNA. This control DNA was extracted using peripheral blood mononuclear cells pooled from 20 healthy individuals (mononuclear cell DNA or MNC DNA). First, two different commercial TaqMan master mix solutions, QuantiTect Probe PCR Master Mix (Qiagen), and Gene expression Master Mix (Applied Biosystems), were tested to assess qPCR

efficiency. Both the solutions demonstrated equally efficient amplification when tested with control DNA serial dilutions (Figure 6-3a). Given that the QuantiTect probe PCR master mix is routinely used by the UK MRD labs, it was decided to use the QuantiTect probe PCR master mix henceforth.

Next, DNA from primary CSF samples quantified using qPCR. Figure 6-3b demonstrates qPCR amplification in standard dilution of MNC DNA and DNA from a CSF sample. Unfortunately, the majority of CSF DNA samples were found to be below the quantifiable range. Therefore, it was necessary to use an arbitrary cut-off value to define adequate DNA amplification. DNA was considered as low quantity/poor quality and was excluded from the analysis if: (i) DNA amplification not seen until a Ct value of 38, (ii) there was greater than 1.5 Ct cycles difference between the triplicate wells, (iii) there was non-specific amplification in the NTC or MNC wells less than 3 Ct- from the samples, or (iv) there was no amplification in any of the triplicate wells.

(a)

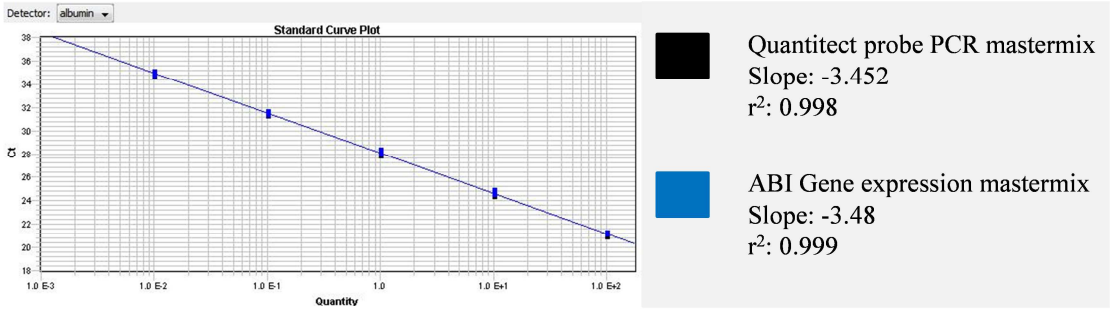

(b)

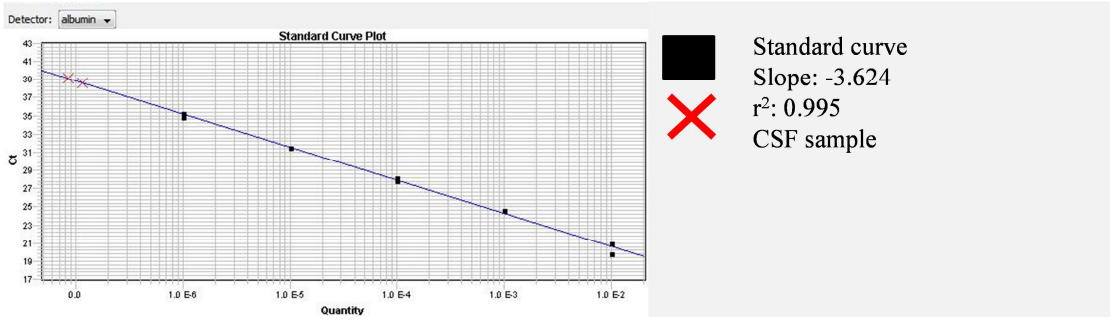

Figure 6-3: Optimization of DNA quantification
Pooled DNA extracted from healthy controls (MNC DNA) was serially diluted. TaqMan primers against control gene (albumin) were used to amplify DNA. (a) Comparison between QantiTect Probe PCR master mix and Applied Biosystems Gene Expression master mix, (b) amplification of CSF DNA sample.

In summary, two qPCR master mix solutions tested achieved comparable amplification efficiency. Due to the small quantities of DNA extracted from the CSF samples, qualitative measures for DNA amplification in qPCR were used.

6.3.2 Optimization of DNA extraction

A number of methods exist for DNA extraction from primary samples. These include phenol/chloroform based methods such as Trizol®, bead based methods or silica-membrane column based commercial kits. Trizol® based DNA extraction is widely used for isolating DNA from primary human samples, and offers the additional benefit of simultaneous extraction of RNA and proteins. However, this method has not been widely tested for DNA extraction from low cell numbers. To increase the DNA yield using Trizol®, DNA co-precipitants such as Glycogen or carrier RNA (cRNA) are frequently used. The co-precipitants reduce non-specific adsorption of DNA and reduce the chances of loss of the DNA pellet during extraction due to improved visibility of the pellet. It was decided to initially test these methods on leukaemic cell lines grown in culture before testing on clinical samples.

An initial set of experiments was performed to compare extraction efficiency of Trizol® with/without co-precipitants. SD1 cells (1×10^3- 10^5) grown in culture were lysed in Trizol® with or without co-precipitants (Glycogen, cRNA, and PelletPaint). DNA was extracted and subsequently assessed for amplification using qPCR primers specific for a sequence in albumin/CXCR7 gene. The results as shown in Figure 6-4a, demonstrate that the amplifiable DNA yield from 1000 leukaemic cells is extremely low even with co-precipitants (Glycogen & cRNA). Although, the co-precipitant PelletPaint® significantly increased the DNA yield from cultured cells and CSF samples (Figure 6-4b & c). To test whether low amplification of DNA was due to PCR inhibitors in the eluted DNA, it was decided to test DNA-cleanup methods. Four DNA cleanup methods were tested including three commercial kits: Zymo Qick-gDNA® Micro prep (Zymo), Zymo DNA clean and concentrator kit (Zymo), and QiAMP DNA micro kit (Qiagen) and a manual clean-up method developed in our laboratory. None of these improved qPCR amplification of the extracted DNA (Data not shown).

Next, column based commercial kits were tested for DNA extraction. Of these (Qiagen DNEasy mini kit, Gentra puregene blood kit, High pure PCR cleanup micro Kit, QiAMP DNA micro kit) only QIAmp DNA Micro kit achieved adequate yield of DNA from small samples. As can be seen in Figure 6-4d, whilst Trizol® based method had a better DNA extraction efficiency at higher cell numbers, more amplifiable DNA was recovered with the QiAMP DNA micro kit at low (1×10^3-10^4) cell numbers.

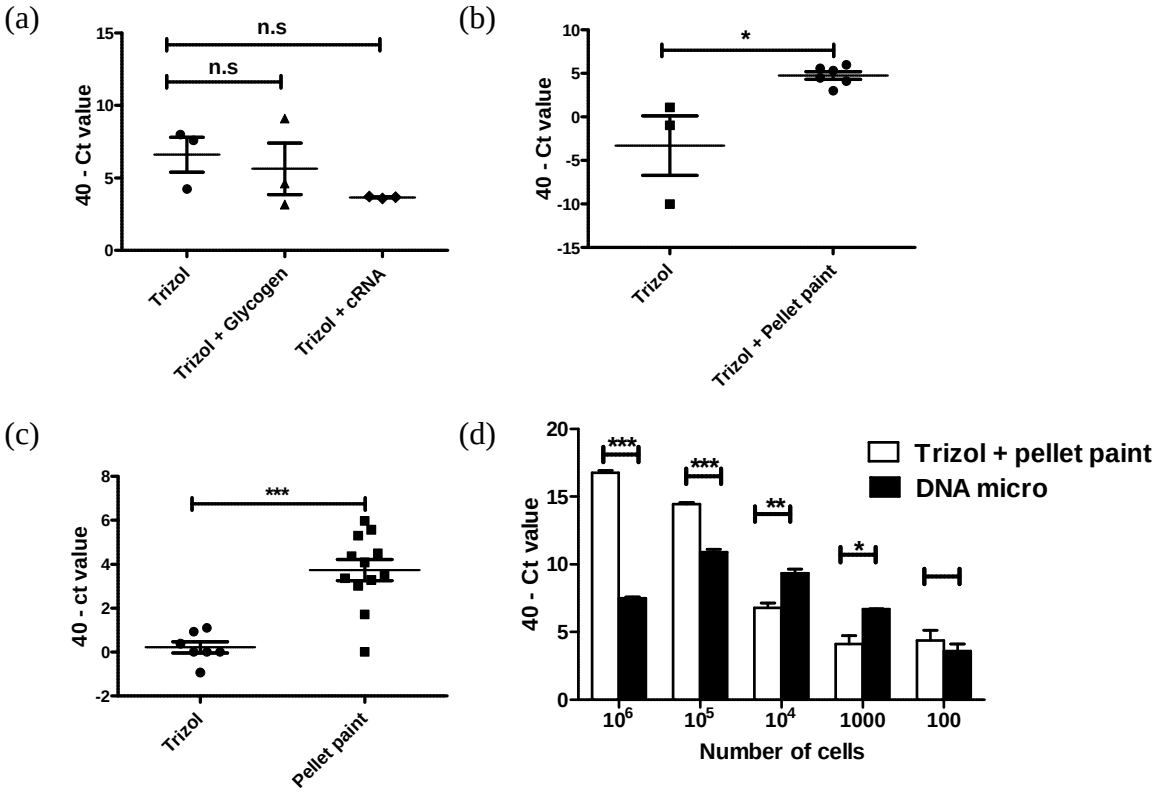

Figure 6-4: Optimization of DNA extraction methods

DNA was extracted from cultured SD1 cells/ patients CSF samples, and relatively quantified using real time qPCR. Primers were specific for Albumin/CXCR7 gene. (a) DNA from 1000 cells using Trizol®, Trizol plus Glycogen as carrier, and Trizol® plus cRNA (n=3), (b) DNA from 1000 cells with Trizol® alone & Trizol® plus PelletPaint® (n=3 & 6 respectively). (c) DNA extracted from randomly selected CSF samples from ALL patients using Trizol® and Trizol® plus PelletPaint® (n=7,13 respectively). (D) DNA from serial dilutions (10^6-1000 SD1) using Trizol or QIAmp DNA micro kit (n=3). PCR Cycle threshold was subtracted from 40 (40-Ct) and plotted with bars representing mean ± SEM. Data were analysed using Mann-Whitney U test. *p<0.05, **p<0.01, ***p<0.005

In summary, a number of methods for DNA extraction were compared. Use of the co-precipitant PelletPaint improved yield from samples lysed in Trizol. QiAmp DNA micro kit significantly improves DNA yield from 1000-10000 cells in comparison with any of the other methods tested.

6.3.3 Effect of storage and shipment on DNA yield

Leukaemic cells have a limited viability in the CSF following removal by lumbar puncture. One aim of this study was to determine if qPCR based analysis could be conducted in a multi-centre setting with a core facility performing the qPCR assays. This would permit standardization and increase patient numbers. For this purpose, it was necessary to assess the effect of storage and shipment conditions on the quality of DNA. In order to test whether amplifiable DNA could be recovered from samples sent from national centres, CSF samples were exposed to postal conditions and then assessed for DNA yield.

The CSF sample was then centrifuged and the acellular supernatant was divided in 18 tubes (1ml/tube), and spiked with 1 x 10^6 SD1 cells. Subsequently, the cell suspension was diluted with equal volumes of RPMI or DNAGuard® Blood (Biometrica), or left untreated. RPMI has been shown to be a preservative for CSF DNA (Pine et al., 2005), whereas DNAGuard® blood is marketed as a DNA preservative. These samples were subjected to storage at ambient temperature for various time points up to 7 days. One set of samples was subjected to postage through the Royal Mail postal services. DNA was extracted after each time point and was assessed for amplifiability using qPCR. Figure 6-5 shows DNA ampifiability after (a) 7 days storage at room temperature, and (b) 7 days with shipping at ambient temperature. The results show that amplifiable DNA could be achieved without any additives or with addition of RPMI after incubation at these time points and shipping conditions. DNAGuard blood showed inferior DNA preservation.

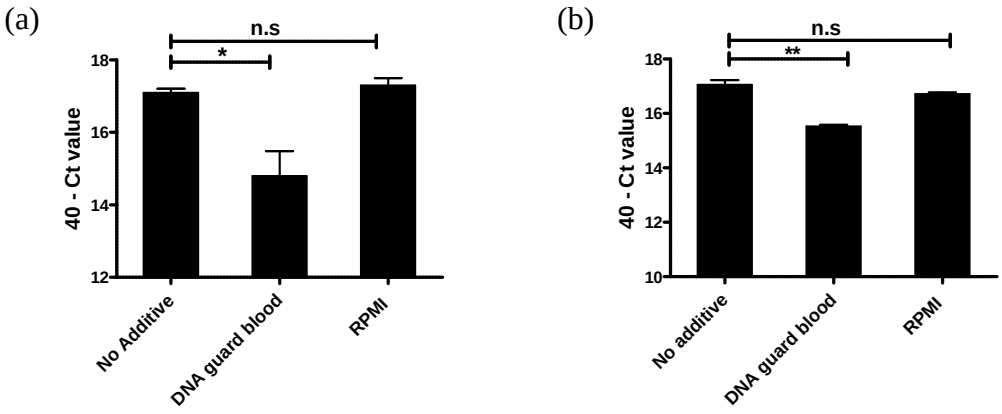

Figure 6-5: Effect of storage and shipping on CSF DNA yield
CSF supernatant from one ALL patient was spiked with *in vitro* cultured SD1 cells and subsequently diluted with RPMI or DNAguard® blood. Samples were incubated at ambient temperature for (a) 7 days or (b) posted to a residential address in Glasgow and posted back to the GBRC. DNA extracted and amplified using PCR with primers specific for a sequence in CXCR7 gene.. Bar graphs of Ct values subtracted from 40 (Ct-40) are presented. Each experimental condition was carried out in triplicates and each replicate analysed in triplicate wells on qPCR. Data were analysed using two-tailed unpaired Student *t* tests. Bars represent mean ± SEM. *p<0.05, **p<0.01

In summary, amplifiable DNA can be extracted from CSF samples left at room temperature for up to 1 week with or without shipping. Use of DNA stabilizer DNAGuard® blood or RPMI does not improve DNA yield in comparison with samples without any preservative.

6.3.4 Optimization of patient specific (ASO) primers and probes

The qPCR method for MRD detection requires a relatively large amount of DNA (50-100 ng/ul). Furthermore, a potential drawback of this method was the risk of false negative results due to clonal evolution or secondary rearrangements in the V(d)J regions in the CSF compartment. For the purpose of bone marrow MRD, at least two different sets of primers are used. However, due to the small quantities of DNA isolated from CSF, this was not always possible. Bone marrow MRD method detects leukaemic cells on a background of normal cells. Furthermore, accurate quantification of residual leukaemia in the bone marrow is of vital importance to clinical decision-making. However, it was anticipated that leukaemic cells in the CSF would not be a minor component of the CSF cell population. Also, the aim was to detect the presence of leukaemic cells and quantification was not necessary. Allele specific oligonucleotides (ASO primers) were designed and qPCR run conditions were optimized at the Glasgow MRD laboratory according to the Biomed-II guidelines. It was aimed to utilize two sets of ASO primers/patient wherever possible.

An arbitrary cut-off value for the CSF qPCR positivity was set. For a CSF sample to be considered positive, the following criteria must be met:

- PCR amplification must be seen before Ct value of 40.
- At least 2/3 wells must show amplification in the qPCR reaction.
- Amplification in the wells should not be more than 1.5 Ct cycles apart.
- MNC or NTC wells should not amplify within 5 Ct cycles of CSF DNA samples.

6.4 Detection of CNS disease by PCR

During the period from July 2011 – July 2014, 66 patients were diagnosed with ALL at Yorkhill. Out of these, 62 were assessed for eligibility. Following assessment on inclusion criteria, 57 patients were enrolled in the study. A study flow chart is present in Figure 6-6.

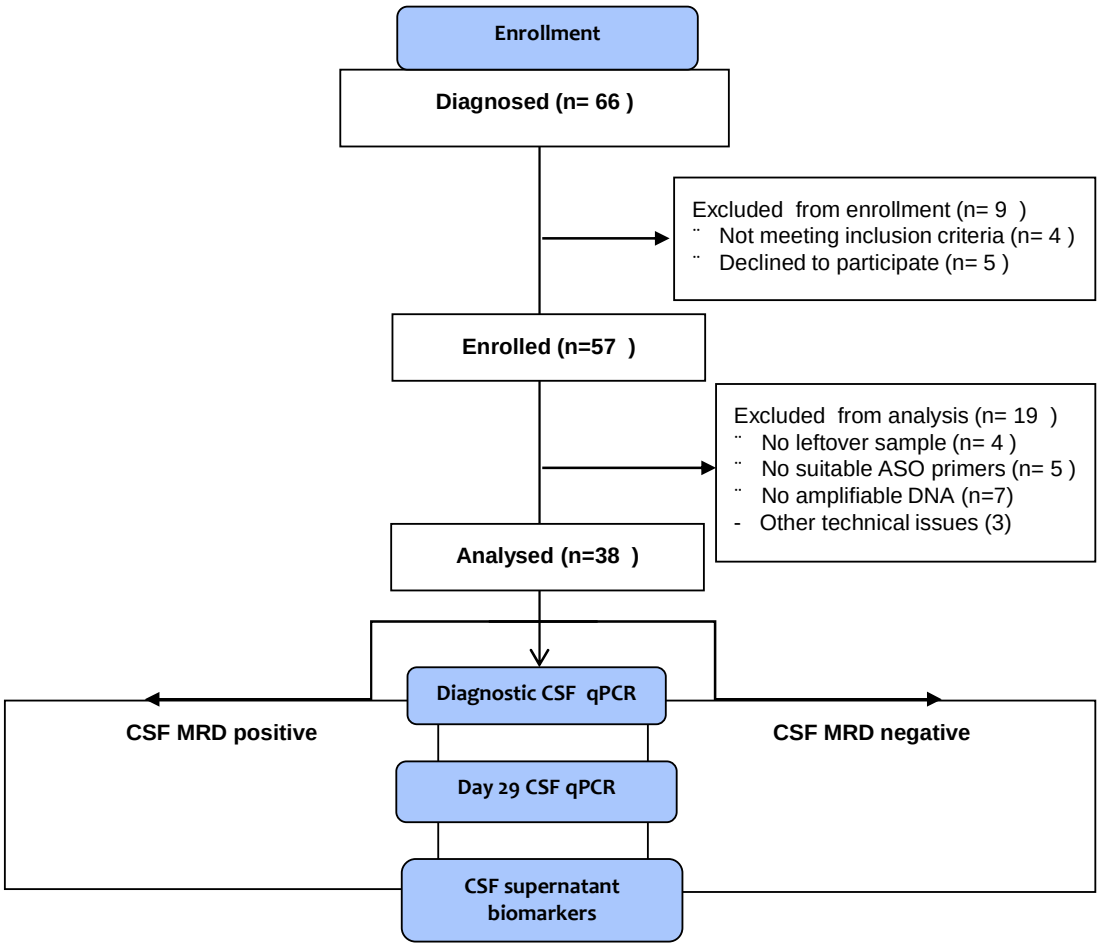

Figure 6-6: Flow chart for patient recruitment and analysis

6.4.1 Clinical and demographic features of recruited patients

The median age of children was 4.7 years (±4.3) with approximately 77% children <10 years of age. The ratio of boys to girls was 2:1. The majority of patients had BCP-ALL (88.9%) and the most common cytogenetic abnormality was High Hyperdiploid (37%) followed by t(12;21) (18.5%). Upon microscopic examination of the CSF cytospins, 50 patients (87%) had CNS-1 disease while traumatic lumbar puncture (TLP) was seen in 7 patients (12.3%). These findings are presented in table 6.1. Clinical features of ALL patients from two large cohorts (SJCRH and BFM) is presented for comparison.

Characteristic		**no.**	**(%)**	**SJCRH***	**BFM****
Age (years)	<10	44	77.1%	74.1%	82.1%
	>10	13	22.9%	25.7%	17.9%
Sex	Male	38	66.7%	56%	57.9%
	Female	19	33.3%	44%	42.1%
Immunophenotype	BCP-ALL	51	89.4%	82.6%	86.5%
	T-ALL	6	10.6%	15.4%	13.5%
Cytogenetics	t(9;22)	1	1.9%	2.4%	2.2%
	MLL-rearranged	3	5.6%	3.0%	2.9%
	t(12;21)	10	18.5%	18.9%	
	High Hyperdiploid	21	36.8%		
WCC	<10	28	49.1%	46.2%	45.9%
(x 10^9/L)	10-50	22	38.5%	29.3%	31.8%
	>50	7	13%	24.5%	22.3%
CNS disease	CNS1	50	87.7%		
	TLP-	3	5.2%		
	TLP+	4	7.0%		
	CNS-3	0	0%	2.7%	2.5%
Anaemia	Hb<8g/dl	30	52.6%	51.8%	53.7%
	Hb>8g/dl	27	47.4%	48.2%	46.3%

Table 6-1 Demographic and clinical features of recruited patients in comparison with SJCRH and BFM trial cohorts
*SJCRH, St. Judes children Research Hospital (1979-2002), **BFM, Berlin-Frankfurt-Munster 90 (1990-95). Adopted from (Liang and Pui, 2005)

6.4.2 Frequency of CSF qPCR positivity at diagnosis

Of 57 patients enrolled in the study, 4 patients had no leftover CSF for analysis and 7 patients samples had poor quality DNA (albumin amplification >38 Ct cycles). In addition, 5 patients were excluded due to lack of suitable primers, 3 qPCR assays had to be excluded for other technical reason. Therefore, diagnostic samples from 38 patients were available for qPCR analysis. A single primer set was utilized in 18 patients and two primer sets each were used for the remaining 20 patients.

Out of the 38 patients analysed for CNS disease by qPCR (CSF qPCR henceforth), 15 (39.5%) tested positive for leukaemic DNA whereas 23 (60.5%) were negative for CSF qPCR. Comparison of clinical and cytogenetic features of CSF qPCR +ve patients with CSF qPCR –ve patients revealed an association with a higher WCC (mean 26.6 x 10^9/l vs 19.4 x10^9/l) and high risk cytogenetics (p=0.04). Interestingly, 2/5 (40%) patients with WCC>50 x 10^9/l tested positive in comparison with 9/14 (64%) patients with WCC 10-50 x 10^9/l. A trend towards male sex was also noted (50% vs 21%), although this was not significant (p= 0.1).

Variable	**Category**	**QPCR+ve**		**QPCR-ve**		
		n	**%**	**n**	**%**	
		15	**39.5%**	**23**	**60.5%**	**p-value***
Age	<10 year	12	39%	19	61%	0.839
	>10 years	3	43%	4	57%	
Sex	Male	12	50%	12	50%	0.101
	Female	3	21%	11	79%	
Immunophenotype	BCP-ALL	12	35%	22	65%	0.280
	T-ALL	3	75%	1	25%	
WCC	<10	4	21%	15	79%	0.043
($x10^9$/L)	10-50	9	64.3%	5	35.7%	
	>50	2	40%	3	60%	
CNS status	CNS-1	11	35%	20	65%	0.084
	TLP+	4	80%	1	20%	
	TLP-	0	0%	2	100%	
Cytogenetic risk✞	Low risk	7	28%	18	72%	0.04
	High risk	3	100%	0	0%	
	Others	5	50%	5	50%	
Day 29 MRD	High risk/ MRD risk	8	50%	8	50%	0.258
	Low risk/standard risk	7	35%	15	65%	

Table 6-2 Comparison between CSF qPCR+ve and qPCR –ve patients
*calculated using Chi square test
✞cytogenetic risk:
Low risk t(12;21), High hyperdiploid
High risk t(9;22), *MLL*-rearranged
Others t(7;9), del 12p, t(9;18), complex cytogenetics of uncertain origin

6.4.2.1 Concordance between cytology and qPCR

In 5 patients with TLP+ve status (traumatic lumbar puncture with blasts) 4 tested positive when assessed using CSF qPCR. One patient (#5) with TLP+ve status tested negative. This patient had a CSF WCC of <0.001/l and on CSF cytospin analysis, the majority of white

cells were normal with occasional blasts. As mentioned above, no CNS-3 cases were available for analysis.

6.4.2.2 Concordance between qPCR targets within individual patients

Two qPCR targets each were used for the 7 patients who tested positive for CNS disease using CSF qPCR. Of these, 4 patients had both targets amplified while target amplification in 1/2 targets was seen in 3 patients. In cases where both targets amplified, similar amplification efficiencies of both the targets were seen. Representative qPCR amplification plots are presented in Figure 6-7.

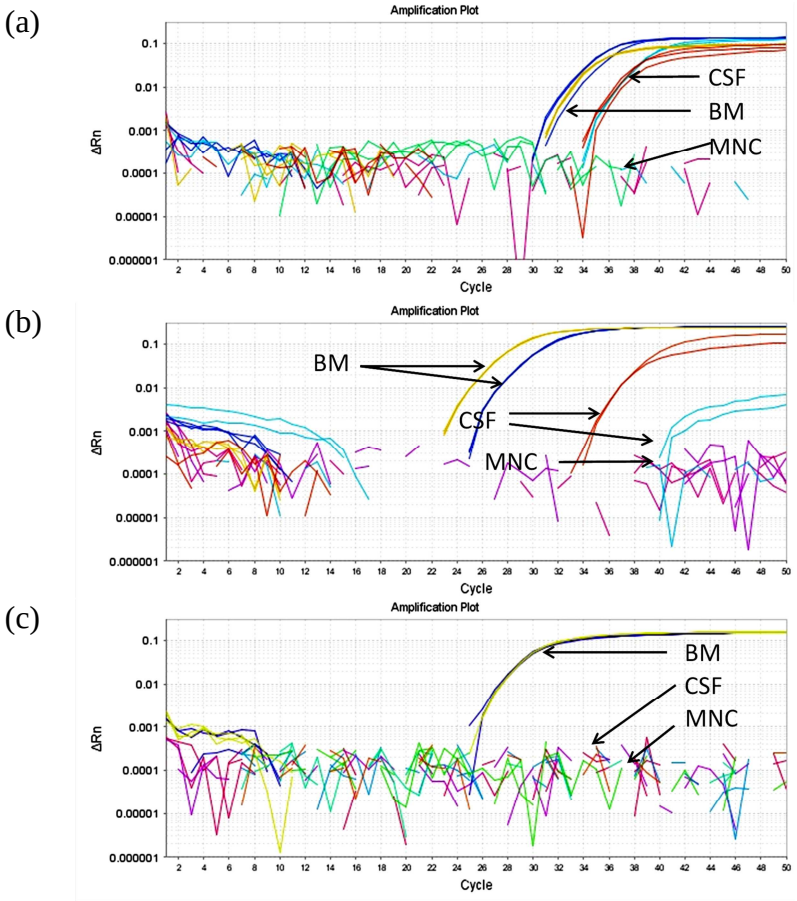

Figure 6-7 CSF qPCR detection by PCR
Real time PCR reactions were performed for 50 thermal cycles using Applied Biosystems 7500 Real Time thermal cycler. Data were analysed using 7500 SDS software v2.0.6. Representative amplification plots of patients with CSF qPCR positivity by (a) 2/2 qPCR ASO targets and (b) 1/2 qPCR ASO targets. (c) CSF qPCR negative case.

In summary, diagnostic CSF DNA samples from 38 patients were analysed for presence of leukaemic DNA. Fifteen (39.5%) tested positive while 23 (60.5%) were negative. High risk cytogenetics and a WCC between 10-50 x 10^9/L were seen in association with qPCR positivity.

6.4.3 Frequency of qPCR positivity during treatment

Following the diagnosis, patients are treated with an intensive induction regimen in the first month. At day 29 of treatment, bone marrow MRD is measured for response to treatment. During this period, patients receive intrathecal therapy along with CSF examination for leukaemic blasts in the CSF. In order to test whether treatment during the induction phase could eliminate submicroscopic levels of disease from the CNS in CSF qPCR positive patients, samples from patients during the induction phase of treatment were analysed. To test this, follow up samples from 10 qPCR negative and 9 qPCR positive patients were tested. All the day 29 samples tested negative for leukaemic DNA. Day 8 and day 15 samples from patient #37 tested positive. Patient #37 had a traumatic lumbar puncture at diagnosis. Notably, the diagnostic sample from this patient was negative by qPCR. In retrospect, this patient was included in the analysis as CSF qPCR positive. Samples from all other (CSF qPCR +ve and –ve) patients tested negative for day 8and day 29 of induction phase. Representative data are presented in Figure 6.2. Overall, these results show that qPCR positive disease is cleared from the CSF during the induction phase of treatment.

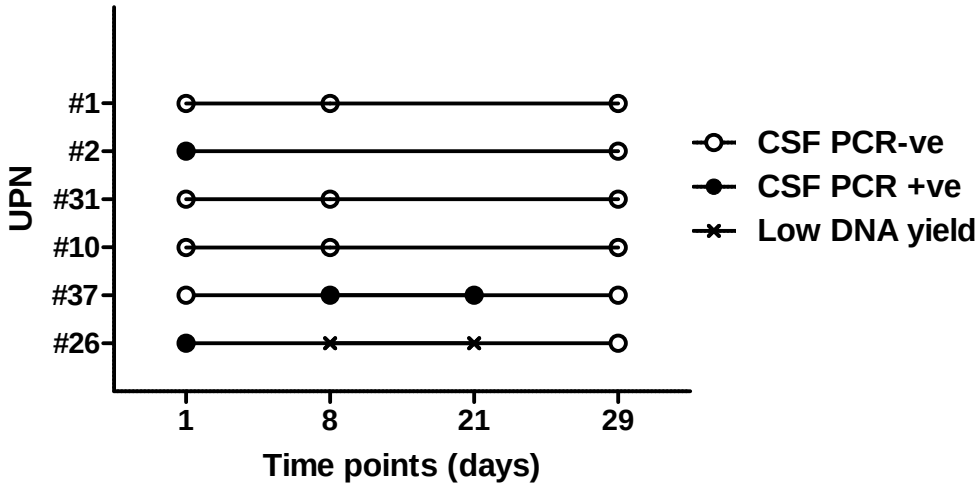

Figure 6-8 CSF qPCR positivity during induction chemotherapy
CSF DNA samples from diagnosis and during the induction period were tested by qPCR. Representative data from 6 patients with and without CSF qPCR positive disease.

In summary, qPCR analysis of diagnostic CSF DNA from 15/38 patients demonstrated amplification of at least one qPCR target. Amplification of two targets was seen in 4/7 patients. Patients with qPCR positive disease at diagnosis became CSF qPCR negative at the end of induction phase.

6.4.4 Analysing chemokines as novel biomarkers for CNS disease

Having established a cohort of patients with CSF qPCR positive disease, it was aimed to test the levels of candidate biomarkers of CNS disease. Although CSF qPCR appears to be a more sensitive tool in detecting and monitoring CNS disease, this method is technically challenging and expensive. Having established that ALL cells possess a repertoire of chemokine receptors on their cell surface it was hypothesised that measurement of their cognate ligands in the CSF may identify patients with leukaemia cells residing in this compartment. Luminex technology allows simultaneous detection of multiple soluble proteins in a small volume of samples. A panel of candidate chemokines (CXCL9, CXCL10, CXCL11, CXCL12, CCL19, CCL21, CCL2, CXCL13 and IL10) was selected to analyse the differences in the levels in CSF qPCR positive and negative patients.

Diagnostic CSF supernatant samples from 15 CSF qPCR+ve and 23 CSF qPCR negative patients were utilized. In addition, CSF supernatant samples from 10 patients with benign intracranial hypertension (BIH) were used as controls. Details of individual patients and controls is presented in Table 6.3.

ID	Age	Sex	Diagnosis	Cytogenetics	CNS status	WCC ($x10^9$/L)	Day 29 MRD	CSF qPCR status	Outcome	Follow up (yr)
#1	7.9	F	BCP-ALL	High hyperdiploid	1	1	High risk	No	CCR	2.4
#2	17.1	M	BCP-ALL	t(9;22)	1	98.49	High risk	yes	CCR**	2.0
#3	11.1	F	BCP-ALL	dic(7;9) Unbalanced transloccation p7 and p9	1	23.8	High risk	No	Refractory disease	2.3
#4	2.8	F	BCP-ALL	High hyperdiploid	1	9.1	Risk	No	CCR	0.4
#5	6.4	M	BCP-ALL	DER (1,16), DER 3,+9, DEL12p	TLP +ve	3.6	Low risk	No	CCR	3.2
#6	15.0	F	BCP-ALL	t(9;18)	TLP -ve	167.5	High risk	No	CCR	2.8
#7	2.7	M	BCP-ALL	High hyperdiploid	1	82	Risk	No	CCR	2.0
#8	6.2	F	BCP-ALL	High hyperdiploid	1	11.7	Risk	No	CCR	0.6
#9	3.9	M	BCP-ALL	High hyperdiploid	1	33.2	Risk	yes	CCR	1.1
#10	14.2	M	T-ALL	Normal Karyotype	1	6.4	High risk	No	CCR	3.3
#11	1.1	M	BCP-ALL	*MLL* rearrangement	1	3.2	Low risk	Yes	CCR	0.7
#12	2.4	M	BCP-ALL	Normal karyotype	1	11.1	Low risk	Yes	CCR	3.0
#13	10.3	M	BCP-ALL	Normal Karyotype	1	1.8	High risk	No	CCR	2.3
#14	2.5	M	BCP-ALL	High hyperdiploid	1	2	Low risk	No	CCR	1.5
#15	3.8	M	BCP-ALL	t(12;21)	1	10.6	Low risk	No	CCR	3.2
#16	6.1	M	BCP-ALL	High hyperdiploid	1	2	Low risk	Yes	CCR	1.3
#17	4.9	M	BCP-ALL	t(12;21)	1	52	Low risk	No	CCR	2.3
#18	9.1	M	T-ALL	Normal Karyotype	1	36.4	High risk	Yes	CCR	2.2
#19	1.1	M	BCP-ALL	High hyperdiploid	1	17.6	Risk	No	CCR	1.9
#20	4.9	M	BCP-ALL	High hyperdiploid	1	6.9	Risk	No	CCR	1.6
#21	1.7	F	BCP-ALL	High hyperdiploid	1	2.7	Risk	Yes	CCR	1.3
#22	2.7	M	BCP-ALL	High hyperdiploid	TLP+ve	10.8	Low risk	Yes	CCR	2.8
#23	3.5	M	BCP-ALL	t(12;21)	TLP+ve	46	Low risk	Yes	CCR	2.8
#24	2.3	F	BCP-ALL	High hyperdiploid	1	3.2	Risk	No	CCR	0.4
#25	5.5	F	BCP-ALL	High hyperdiploid	1	4.2	MRD Risk	No	CCR	2.1
#26	5.4	F	BCP-ALL	Normal Karyotype	1	28	Low risk	Yes	CCR	2.8
#27	6.0	F	BCP-ALL	High hyperdiploid	1	1.1	Low risk	No	CCR	2.1
#38	2.5	F	BCP-ALL	t(12;21)	1	19.1	MRD risk	No	CCR	2.0
#29	3.7	M	BCP-ALL	t(12;21)	1	4.9	MRD Risk	No	CCR	0.5
#30	2.6	F	BCP-ALL	High hyperdiploid	1	6.2	Low risk	Yes	CCR	1.8
#31	5.4	M	BCP-ALL	t(12;21)	1	5.3	Low risk	No	CCR	3.1
#32	2.1	M	T-ALL	Normal Karyotype	1	56.5	Low Risk	Yes	CCR	1.8
#33	3.3	M	BCP-ALL	High hyperdiploid	1	1.7	MRD Risk	No	CCR	1.9
#34	13.9	M	T-ALL	NA	1	28	Risk	Yes	CCR	1.3
#35	3.2	F	BCP-ALL	High hyperdiploid	TLP-ve	3.1	Low risk	No	CCR	0.5
#36	10.8	M	BCP-ALL	High hyperdiploid	TLP +ve	13.6	High risk	Yes	CCR	2.2
#37	2.3	M	BCP-ALL	11q23	TLP+ve	23.4	High risk	Yes	CCR	2.9
#38	3.5	F	BCP-ALL	NA	1	8.1	Low Risk	No	CCR	1.6
Controls										
#39	25.9	F	BIH							
#40	27.3	F	BIH							
#41	65.5	F	BIH							
#42	39.2	F	BIH							
#43	25.6	F	BIH							
#44	30.9	F	BIH							
#45	45.9	F	BIH							
#46	27.7	F	BIH							
#47	35.7	F	BIH							
#48	27.0	F	BIH							

Table 6-3 Raw data of individual patients

CCR= continuous clinical remission, NA= not available, BIH= benign intracranial hypertension

Analysis of CXCR3 ligands (CXCL9, CXCL10 and CXCL11) revealed that there was overall low levels of both CXCL9 (15.8 ± 5.4 pg/ml) and CXCL10 (105.1 ± 24.1 pg/ml) in CSF supernatants. Levels of CXCL11 were negligible (1.04 ± 0.39 pg/ml). Remarkably, levels of CXCL9 and CXCL10 were modestly lower in CSF qPCR+ve group (7.96±2.3 & 88.74±59.36 respectively) compared to CSF qPCR-ve (25.9±10.8 & 94.0 ±30.6 respectively) and control groups (5.1±0.8 & 155.1 ± 28 respectively) (Figure 6-9). Similarly, levels of CXCR4 ligand CXCL12 were lower in the CSF qPCR+ve (18.1±10.9) group in comparison with CSF qPCR-ve (23.1 ± 7.5) and controls (105.8 ±17.8). Analysis of CCR7 ligands CCL19 and CCL21 showed similar trends. Levels of CCL21 were higher than CCL19 (808.3±87.5 vs 4.1± 0.69). Notably, CCL21 levels in the CSF qPCR+ve group (473.5±123.5) were significantly lower than CSF qPCR-ve (690±91.7) and control groups (1582±141.8).

CCL2 (monocyte chemotactic protein 1 or MCP1) is a ligand for CCR2 and CCR4. Levels of CCL2 were found to be significantly lower in CSF qPCR+ve group (60.4±10.1) compared to CSF qPCR-ve group (86.8±7.6). Finally, CXCL13 and IL-10 levels have been shown to be candidate biomarkers of primary CNS lymphoma (Rubenstein et al., 2013). However, in our cohort, the levels of CXCL13 were beyond the quantitative range of the assay whereas IL-10 levels were undetected in any of the CSF samples analysed.

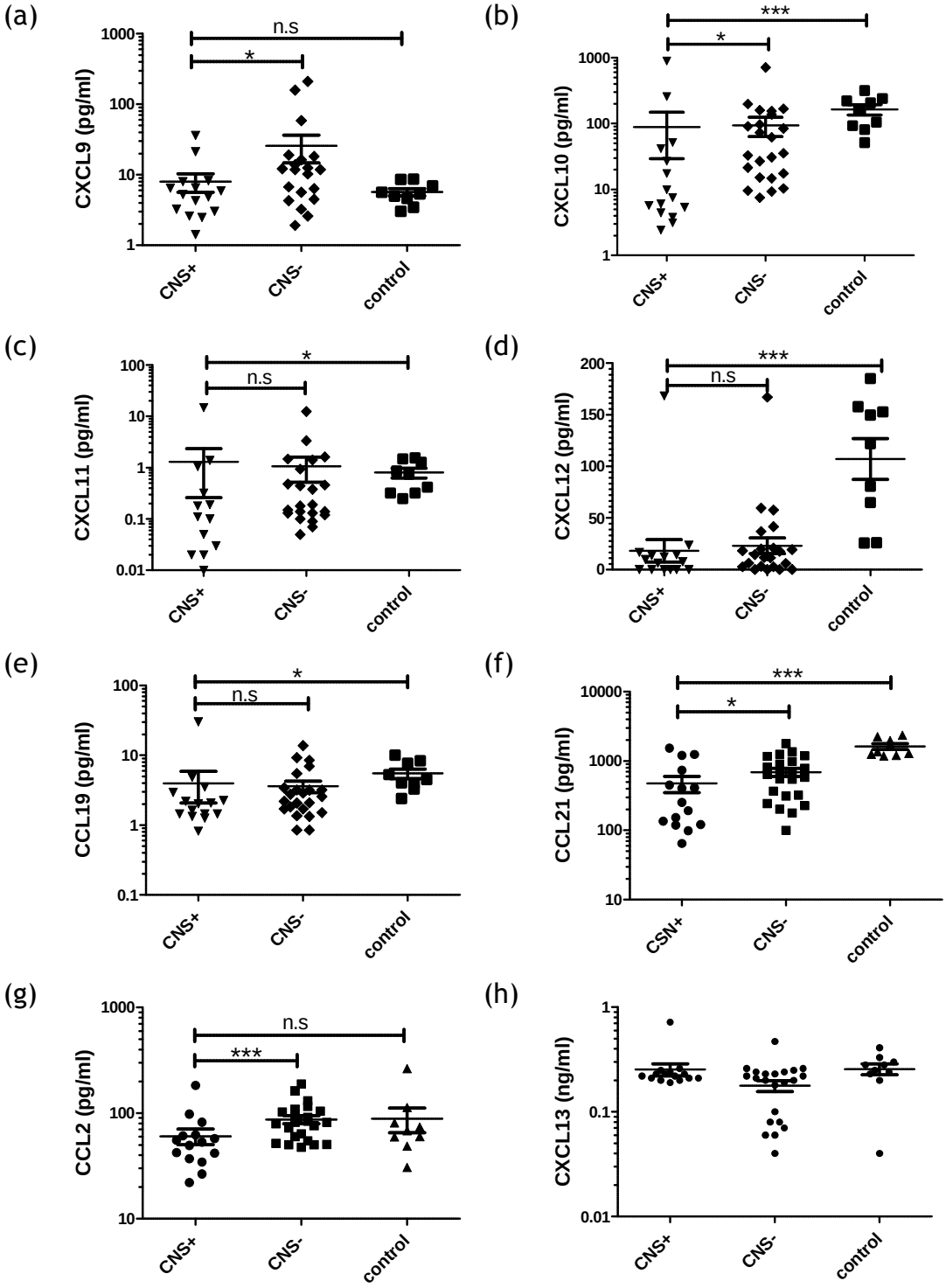

Figure 6-9 Levels of chemokines in CSF qPCR +ve and CSF qPCR –ve patients

CSF supernatants from CSF qPCR +ve (n=15), CSF qPCR –ve (n=23) and the control (n=10) groups were tested for the levels of selected chemokines using Luminex assay. Individual values are presented along with mean ± SEM. Data were analysed on log transformed values using Two-tailed independent samples t- tests. *p<0.05, **p<0.01, ***<0.001. Levels for CXCL13 were not analysed statistically as the majority of values were lower than the quantifiable range.

Due to the small differences in the levels of the selected chemokines between the groups, it was clear that the diagnostic utility of these as biomarkers of CNS disease would be low. To confirm this, receiver operating curve (ROC) analysis was performed. Levels of chemokines in CSF qPCR positive and negative cases were plotted to measure the area under curve (AUC) to evaluate the diagnostic accuracy of measuring chemokines to predict CNS disease. This would identify an optimum cut-off point where the levels of a chemokine can predict CSF qPCR positivity with an optimum sensitivity and specificity. As expected, analysis by ROC revealed poor predictive ability of chemokine levels for CSF qPCR positivity. As can be seen in Figure 6-10a, the plotted values for the chemokines (indicated with colours) illustrate a narrow area above the diagonal line, indicating low sensitivity and specificity. A cut-off point where chemokine levels could predict CSF qPCR positivity with a high sensitivity and specificity could not be identified (Figure 6-10b).

(a)

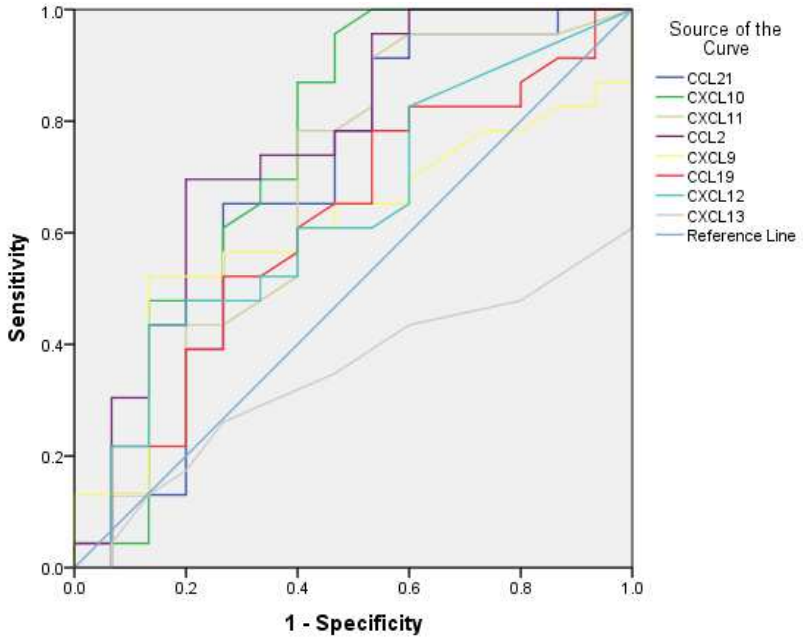

(b)

Chemokine	Cut-off levels (pg/ml)	Sensitivity	Specificity	95% CI
CXCL9	<2.5	82.6%	7%	42.4-79.1
CXCL10	<10.1	87%	60%	56.3-92.7
CXCL11	<1.2	21.7%	87.3%	48.7-86.4
CCL21	<215.0	87%	47%	48.9-86.8
CCL19	<1.4	82.6%	40%	42.9-80.3
CCL2	<50.4	87.3%	46.7%	59.4-92.5
CXCL12	<1.4	42.6%	40%	44.6-81.4

Figure 6-10 ROC analysis for diagnostic accuracy of chemokine levels to predict CSF qPCR positivity

(a) ROC analysis to measure area under curve (AUC) for diagnostic accuracy of the levels of selected chemokines. (b) Selected cut-off values of chemokines to discriminate between CSF qPCR positive and negative cases. Values calculated using chemokine levels from diagnostic samples from 15 CSF qPCR positive and 23 CSF qPCR negative patients. Data were analysed using SPSS (v21) (IBM) software.

In summary, the results from Luminex assay show that the levels of CXCL9, CXCL10, CCL21 and CCL2 in CSF qPCR +ve patients were generally lower than the CSF qPCR -ve patients. However, these levels do not appear to be of any diagnostic utility.

6.5 Discussion

The main aim of this study was to identify the incidence of sub-microscopic levels of leukaemia in the CNS in children with ALL using qPCR and Luminex assays. Preliminary work included: initiating patient recruitment allowing large numbers of data points required for the study, setting up a human tissue biobank to collect and store CSF, blood and bone marrow samples from patients, and optimization of methods required for the aforementioned aims. A cohort of 38 patients was analysed for qPCR detection of leukaemia and 15 patients tested positive for presence of sub-microscopic levels of disease in the CNS by qPCR. Subsequently, to try and identify proteins which could be used as a biomarkers of CNS disease in ALL patients, the concentrations of a panel of candidate chemokines and IL-10 were compared in CSF of CSF qPCR+ve and CSF qPCR-ve patients and that of a control group.

It was shown that amplifiable DNA could be extracted from CSF samples for up to one week without adding any preservative. Pine et al. (2005) reported a similar series of experiments with primary samples and have demonstrated that use of RPMI as an additive considerably improve the otherwise poor DNA yield from primary CSF samples. Results presented in this chapter do not show superiority of RPMI as an additive for DNA stability. This contrast could be due to the use of CSF supernatant spiked with a relatively large number (1×10^6/ml) SD1 cells. Immortalized cell lines in comparison to primary cells may be more resistant to degradation in the CSF. An alternate approach to obtaining patient samples could be that the DNA extraction could be performed at the local centres and purified DNA, which is stable at room temperature, transferred to the core facility.

Real-time qPCR has previously been utilized to detect leukaemic DNA in the CSF (Pine et al., 2005, Scrideli et al., 2004, Biojone et al., 2012). However, consensus primers used in these studies require additional analysis of the qPCR products for specificity of amplification. The leukaemia specific ASO primers for the detection of leukaemic DNA in the CSF offers the advantage of very high specificity for leukaemic DNA. In addition, these primers are routinely designed and optimized for all the patients in the UK. Therefore, CSF analysis for leukaemia can potentially be performed within an already established setup for the bone marrow MRD.

qPCR on CSF DNA identified 39.5% patients as having submicroscopic levels of leukaemia. This percentage of qPCR positivity is consistent with the previously reported 46.8 % (Biojone et al., 2012) and 45.9% (Scrideli et al., 2004) of PCR positivity. However,

Pine et al. (2005) reported only 3/23 samples from CNS-1 patients amplified by qPCR. It is possible that technical issues with sample processing such as the in-house method for DNA extraction might have underestimated the frequency of occult CNS disease. In some cases, only one of the two tested qPCR targets showed amplification. Differences in qPCR amplification efficiency of these primers could account for such discordance. Alternately, evolution of leukaemic clones in the CNS may be responsible. Interestingly, in the study by Scrideli et al. (2004), two patients had clonal rearrangements that differed from bone marrow sequences. If leukaemic cells in the CNS are evolved clones, then using ASO primers may underestimate the true frequency of CNS disease.

The demographic and clinical features of the patients recruited were similar to the global ALL population, suggesting that there was very little sampling bias. CSF qPCR positivity at diagnosis was associated with a high WCC and high risk cytogenetics – a risk factor for CNS relapse. Most patients with TLP tested positive at diagnosis or during the induction period. The question arises whether these patients should have been included in the analysis. TLP status at diagnosis has disputed significance. Patients with a traumatic lumbar traditionally have a worse outcome (Gajjar et al., 2000). However, a link of TLP with increased CNS risk is not well established (te Loo et al., 2006, Burger et al., 2003). TLP may introduce leukaemic blasts in the CNS which might adversely affect outcome. Alternately, TLP at diagnosis may reflect an overall aggressive nature of the disease. For instance coagulopathy or a high WCC increase the risk of TLP (te Loo et al., 2006). Further analysis of larger numbers of patients would be required to establish whether TLP is an independent risk factor for CNS relapse.

Follow up CSF qPCR measurements at day 29 were negative for all the patients analysed, suggesting efficient clearance of CNS disease. In the relatively short duration of follow up (2.0 ±0.9 years median ±SD) no CNS or bone marrow relapses were observed. This raises questions regarding the significance of low level CNS disease at diagnosis. If the majority of the CSF qPCR positive patients achieve clearance of the CNS disease with conventional treatment, will monitoring of low level disease provide useful assessment of risk? The significance of low number of CSF blasts (CNS-2) is debated. Some authors have reported the poor prognostic value of small number of blasts in the CSF at diagnosis. (Mahmoud et al., 1993) However, others have disputed this observation. (Gilchrist et al., 1994, Burger et al., 2003, te Loo et al., 2006) Similar controversy exists about the presence of submicroscopic disease at diagnosis. Earlier studies reported an association between submicroscopic CNS disease the risk of relapse (Scrideli et al., 2004), however more

recent studies have shown no association with the outcome (Martinez-Laperche et al., 2013, Biojone et al., 2012). This improved outcome in the more recent studies appears to be associated with the higher intensity of the more recent treatment regimen. For instance, Biojone et al. (2012) have shown that CSF qPCR positive patients had a significantly higher relapse rate and poor outcome in patients treated with low-intensity treatment protocol. However, when an independent cohort with CSF qPCR positivity was treated with high intensity treatment regimen, no differences in the EFS were observed. Therefore, more intensive protocols eliminate the adverse significance of subclinical CNS disease. However, it may also indicate that high intensity protocols may considerably over treat patients.

The majority of patients in our cohort belonged to MRD low-risk group, with 60% patients in this group testing negative for CNS disease by CSF qPCR. This is an attractive group for dose reduction strategies. Recently, reduction in post-induction maintenance therapy in MRD-low risk patients was carried out successfully without any increase in adverse events (Vora et al., 2013). Similar principles can be applied to this group at a low potential risk of CNS relapse. Although a number of factors may still be considered. For instance, the fact that leukaemic cells primarily reside within the CSF compartment and may not always be detected in the CSF – even with the most sensitive diagnostic methods. In addition, if leukaemic cells in the CNS are clonally evolved then the qPCR primers may show false negative results.

One aim of this chapter was to test soluble biomarkers of CNS disease which could help better risk-stratify patients with CNS disease and inform on biology of CNS disease. Generally, levels of selected chemokines were found to be marginally lower in the CSF qPCR positive patients compared to CSF qPCR negative patients. Such a phenomenon has previously been reported in the bone marrow – a CXCR4 dependent site – where levels of CXCL12 were significantly lower in ALL patients compared to normal controls and rose significantly with treatment (van den Berk et al., 2014). Another case report has shown lower levels of CCL2 in association with CNS disease (Eisenkraft et al., 2006). An intriguing hypothesis is that the leukaemic blasts in the CSF compartment may utilize the chemokines secreted by the CNS micro-environment thus lowering the levels in the CSF. Primary CNS lymphoma cells have been shown to secrete high levels of CXCL13 and IL-10. CSF levels of these biomarkers are not only associated with poor outcome, but also are highly specific for the diagnosis of primary CNS lymphoma (Rubenstein et al., 2013). In my cohort, CSF levels of these candidate biomarkers were found to be very low (CXCL13)

or absent (IL-10) in the CSF. It is not known whether ALL cells express/secrete IL-10 or CXCL13 – these results suggest they do not. Due to unavailability of age matched healthy controls, samples from a considerably older group with benign intracranial hypertension were used.

The results from this chapter present data that may be of relevance to clinical decision-making and may improve our understanding of the biology of CNS disease. However, several limitations must be acknowledged. The data are generated from a relatively small group of patients, and do not include infant ALL – a group at risk of CNS relapse. Furthermore, samples from 7 patients had to be excluded from the analysis due to low DNA yield. Whether this low yield represent lack of leukaemic cells in the CNS compartment, or is merely due to poor sample quality cannot be ascertained. In addition, it is theoretically possible that leukaemic blasts localized to the meningeal surface may not be sampled in the CSF, thus reducing the sensitivity of the CSF qPCR technique. Data presented in chapter 3 lends some support to this hypothesis. A longer follow-up of such CSF qPCR –ve patients will help to analyse this. Diagnostic imaging techniques such as magnetic resonance imaging (MRI) allow identification of localized deposits, however, these are currently not sensitive and only identify advanced disease. Advanced high resolution imaging with 7-t MRI has shown promise in detecting lesions in MS. This can potentially be very useful in detecting CNS lesions in ALL as well (Gaitan et al., 2014).

In summary, it is shown that submicroscopic levels of leukaemia are commonly present in patients without cytological evidence of CNS disease. Follow up of such patients show rapid clearance of disease from the CSF compartment. Using qPCR for the detection of leukaemia appears to be feasible for the diagnosis and monitoring of CNS disease, although the effect of CSF qPCR positivity on the long term outcome remains to be seen. In this chapter, methods for DNA extraction and analysis have been optimized. It is proposed that CSF qPCR monitoring can be incorporated into the routine bone marrow qPCR monitoring. Alternatively, more sensitive and informative genomic strategies using next-generation sequencing (NGS) technology can be utilized to detect CNS disease. Detection of bone marrow MRD by Immunoglobulin gene rearrangement analysis using NGS has shown comparable efficacy with the added advantage of analysis of clonal heterogeneity (Faham et al., 2012). Analysis of paired bone marrow and CNS samples can be more informative than ASO qPCR method. Not only would such an analysis measure precisely the frequency of CNS disease but also will inform on biological questions such as clonal relationship between the bone marrow and CNS blasts.

7 General discussion and conclusions

7.1 Summary of findings

This thesis sets out with the broad aims to investigate the mechanisms underlying central nervous system (CNS) disease in childhood acute lymphoblastic leukaemia and focusses on the frequency, pattern and molecular and cellular determinants that could be associated with CNS disease. The major findings from the previous chapters are summarized below:

1. CNS infiltration is commonly seen in B-cell precursor (BCP)-acute lymphoblastic leukaemia (ALL) cells engrafted in NOD.Cg-*PrkdcscidIl2rgtm1Wjl*/SzJ (NSG) mice. Contrary to the clinical presentation of patients, the majority of mice engrafted with BCP-ALL cells from patients with CNS-1 disease demonstrated heavy CNS infiltration. Histological examination of mice brains clearly showed that the leukaemic cells reside within the cerebrospinal fluid (CSF) compartment, mostly seen as plaques of disease in the leptomeninges. This implies that cells transit across the blood-CSF barrier (BCSFB). CNS parenchyma was sparingly devoid of leukaemia.

2. CNS infiltrating leukaemic cells are common and present in all tested immunophenotypic sub-populations of BCP-ALL and at least 1/10 leukaemic cells possess the ability to infiltrate the CNS.

3. BCP-ALL cells differentially express a variety of leukocyte trafficking molecules at mRNA and surface protein level. The majority of leukaemic samples demonstrate surface expression levels of CXCR3 and CXCR4. However, a molecular ‘address code’ for CNS entry, based on surface expression of selected leukocyte trafficking molecules, is unlikely. No subclonal population based on expression levels of selected leukocyte trafficking molecules could be identified.

4. Dysfunctional expression of CXCR4 in SD1 cells was associated with rapid onset of CNS disease. However, in primary samples, no such association was found. A detailed investigation into the lack of CXCL12 mediated chemotaxis in SD1 cells failed to identify a single mechanism underlying this dysfunction. There was evidence that reduced CXCR4 expression, reduced internalization and constitutively phosphorylated downstream signalling pathways may act synergistically to result in the observed lack of CXCL12 mediated chemotaxis.

5. The majority of primary BCP-ALL samples and cell lines were shown to express

interleukain-15 (IL-15) and IL-15 receptor subunits at mRNA level. Stimulation of SD1 cells with exogenous IL-15 promoted cell growth and upregulated genes associated with trafficking and invasion. The growth promoting effects of IL-15 were more profound in low serum conditions. Unlike IL-15 action on other leukocytes, the increase in cell growth in ALL cells is likely to be accounted by an increased cell proliferation rather than reduced apoptosis. Secreted IL-15 was undetectable in the CSF supernatant samples of patients with overt CNS disease.

6. Methods for DNA extraction from clinical CSF samples were optimized. Using allele specific oligonucleotide (ASO) primers on CSF DNA, 15/38 patients demonstrated positivity for CNS disease. Investigation of selected soluble factors did not reveal a sensitive biomarker of CNS disease. However, levels of CXCL9, CXCL10, CCL2 and CCL21 were found to be lower in patients with CNS disease.

The potential significance of these findings and how they fit into the current body of knowledge on CNS disease in ALL is presented below. How this work can be further investigated, is discussed subsequently.

7.2 How do these finding extend current knowledge on CNS involvement in leukaemia?

These studies aimed to shed light on two main areas: Firstly, the mechanism of CNS disease in ALL and secondly methods to improve diagnosis and CNS-risk stratification of children with ALL. Several aspects of the results identified in this thesis add to knowledge of the biological mechanisms underlying the CNS disease in ALL and may ultimately translate to the clinical aspects of CNS disease diagnosis and risk stratification. A number of clinical and cytogenetic factors are associated with an increased risk of CNS disease. However, to date, very little is known about the biological processes that enable leukaemic cells to enter and proliferate in the CNS. The evidence for CCR7 expressing T-ALL cells in entering the CNS is limited and has not been replicated in primary samples. The studies performed in this project provide evidence for a number of biological and clinical questions in ALL.

7.2.1.1 Xenograft model of CNS disease recapitulates human CNS disease

Engraftment of primary BCP-ALL cells into immunodeficient NSG mice illustrated a pattern of extramedullary disease resembling human leukaemia. Not only did samples from

the majority of low-risk ALL patients engraft but CNS engraftment was also noted in most of these. This model answers a number of questions concerning the pathogenesis of CNS disease in ALL. For instance, it shows that the CSF compartment, rather than the brain parenchyma, is involved in the CNS disease. Parenchymal involvement is only seen late in the disease course following extensive infiltration of the CSF compartment. Furthermore, leukaemic cells are present in the CNS as plaques in the leptomeninges, rather than in a free-floating state, supporting the hypothesis that leukaemic cells may be present in the CNS in patients with CNS-1 disease but missed in the CSF examination. The patterns of infiltration closely resemble the earlier description of human CNS disease presented by Price and Johnson (1973) on a large series of autopsies performed on children with leukaemia. The authors argued that leukaemic cells most commonly enter the CNS via the meningeal veins. From the xenograft model, leukaemic cells were seen in the walls of the meningeal vessels as well as the choroid plexus – both communicate with the CSF compartment. It is difficult to say with confidence whether one route is preferred over the other. What can certainly be said is that the leukaemic cells do not appear to cross the BBB. This has important implications for research. For instance, while investigating CNS disease *in vitro*, BCSFB models are likely to be more representative of trafficking routes than BBB models. This argument goes against findings presented by Holland et al. (2011) who argue that leukaemic cells infiltrate the blood-brain barrier (BBB) in an invasive manner. A number of factors could account for this discrepancy. The observation that SD1 cells but not Sup B15 or REH produce CNS disease in SCID/beige mice (Holland et al., 2011), was not reproducible in NSG mice in our laboratory (Williams et al., 2014). The residual immune system of the SCID/beige mice might have caused selective expansion of invasive sub-clones in SD1 cells only. In addition, there results were based on the observation of leukaemic infiltration of the optic nerve and no direct evidence of invasion across the BBB was presented. Alternately, at the time of cull the disease may have approached to the advanced stage where the expansion of CNS leukaemia may have resulted in physical disruption of the BBB.

Due to the lack of B-, T- and NK cell mediated immunity, NSG mice are the most immunodeficient strain currently available, and therefore represent a more suitable model for investigation of CNS leukaemia in primary ALL samples. However, as with any disease model, is not devoid of drawbacks. A lack of competent immune system in the xenograft mice does not simply equate with leukaemia in an immune-competent patient. As a consequence, human ALL cells may proliferate unchecked in the murine model. Another disadvantage of the xenograft models in the lack of leukaemia-host interactions.

Despite the many known conserved growth factors and cytokines, cross-species differences exist and may affect the cellular behaviour (e.g. receptor/ligand interactions) of the blasts. In addition, the murine microenvironment may be more suited to a particular leukaemia/cell type due to factors not related to leukaemic aggressiveness – the failure of a high-risk leukaemic subtype (11q23) to engraft may be an example of such factors. Despite these various disadvantages, this represents an attractive tool for the study of human disease in mice. This model can be used to investigate biological questions or test novel therapies. The recent report on reduction in CNS disease burden in xenograft mice with the use of MEK inhibitors, provide the proof-of-principle for this argument (Irving et al., 2013).

7.2.1.2 CNS-leukaemia initiating cells are frequent and not related to a distinct phenotype

At diagnosis, only a minority (3-5%) patients present with overt leukaemia; however without CNS prophylaxis, the majority of patients rapidly develop CNS relapse. This forms the basis of risk-stratified CNS prophylaxis. I have provided a scientific basis forthis clinical practice by showing that the majority of samples from patients who are negative for CNS disease at diagnosis, possess the capability to infiltrate the CNS. Currently, all patients without evidence of CNS disease receive some CNS-directed prophylaxis. From clinical studies, it is clear that while patients with CNS-3 disease at diagnosis are at a higher risk for CNS relapse, CNS-1 patients also relapse in the CNS. The fact that samples from CNS-3 patients show a higher proportion of CNS infiltration in mice in comparison with CNS-1 samples supports the current clinical practice.

The question whether all the cells in an individual leukaemia possess the ability to infiltrate the CNS or if it is a property of a subclone that allows leukaemic cells entry into the CNS, is of great scientific interest. If only a subset of leukaemic cells possess the ability to infiltrate the CNS, then comparison of CNS-infiltrating population with that of the bone marrow homing population will lead to identification of novel biomarkers of CNS disease. Data presented in this thesis do not support this hypothesis. Evidence from histological examination of xenograft mice demonstrated that different immunophenotypically sorted ALL subpopulations are able to infiltrate the CNS in mice. Moreover, CNS engraftment was seen in mice transplanted with as low as 10 cells suggesting that CNS engraftment ability is present at a high frequency in ALL. Furthermore, leukaemic populations from the CNS compartment did not appear to be distinct from the bone marrow homing cells in the expression of selected leukocyte trafficking molecules. Still, it cannot be completely

excluded that CNS infiltrating cells are indeed a distinct subpopulation within the bulk of leukaemic cells. CNS infiltrating cells may differ from the cells elsewhere in factors not yet known or investigated in these studies and an unbiased transcriptomic approach may help answer this.

Primary xenografts developed in this thesis represent a snap-shot in the natural history of evolution of CNS-leukaemia. Engraftment kinetics may be a critical factor in identifying the mechanisms underlying the CNS infiltration. In the serial transplant experiments, $REH^{GFP\text{-}Luc}$ cells were retrieved from the CNS and the bone marrow of engrafted mice, and then re-transplanted into a second set of mice. A trend towards early CNS involvement in mice injected with CNS-retrieved cells was observed. It is possible that cells with distinct 'address code' for the CNS gain access and subsequently expand to form a diverse phenotypic population within the CNS compartment. Isolation of cells from the CNS at this point would not allow identification of such a CNS-specific phenotype. When immunophenotypically sorted populations are transplanted in mice, the leukaemic cells reconstitute the diverse phenotypes found in the original patients (le Viseur et al., 2008). In addition, leukaemic cells might have downregulated chemokine receptors required for entry into the CNS once they have entered the CSF compartment.

7.2.1.3 Leukocyte trafficking molecules do not drive CNS entry in BCP-ALL

Although leukaemic cells may require chemokine receptors, selectins and integrins for access to the CNS compartment, they do not appear to play an instructive role in CNS entry of leukaemic cells. Although leukaemic blasts express chemokine receptors at the mRNA and surface level and their ligands are present in the CSF samples of ALL patients, there was no association between chemokine receptor expression and the ability to infiltrate the CNS. Comprehensive analysis of CXCR4-CXCL12 interactions suggested that is not essential for driving CNS entry of leukaemic cells (Williams et al., 2014). Contrary to the argument presented by Crazzolara et al. (2001) that CXCR4 expression can be a biomarker for predicting extramedullary dissemination, the CNS appears to be an exception. In support of this hypothesis, in a murine model of CML, use of CXCR4 inhibitor AMD3100 showed an increase in CNS disease in the mice, suggesting that CNS is a CXCR4-independent niche (Agarwal et al., 2012). The role for CXCR3-CXCL9-11 interaction requires further investigation. Not only do leukaemic cells consistently express high levels of CXCR3, but also the levels of its ligands are lower in patients with CNS-disease. This suggests are CXCR3 expressing leukocytes may utilize CXCL9-11 for homing and retention in the CNS. Whether this plays an essential role in leukaemic entry

or survival remains to be investigated.

7.2.1.4 The CXCR4 surface expression level is insufficient to determine the efficiency of CXCL12 mediated chemotaxis

The characteristic feature of chemokine receptor-ligand interactions is their ability to initiate directional motility of cells. CXCR4-CXCL12 interactions produce potent chemotactic responses. With the CXCR4 receptor implicated in a number of malignant and non-malignant disorders, there a need to focus on the chemokine receptor expression – function relationship. SD1 cells, despite surface expression levels of CXCR4, fail to migrate towards the ligand CXCL12. This observation mirrors several reports of a similar phenomenon seen in normal haematopoiesis (Fedyk et al., 1999, Bleul et al., 1998, Honczarenko et al., 1999) and leukaemia (Bendall et al., 2005). This carries important implications for the use of CXCR4 expression and function as a biomarker of disease. Do CXCR4 surface levels or CXCL12 mediated chemotaxis most adequately represent CXCR4 function? Leukaemic cells expressing surface CXCR4 but lacking CXCL12 mediated migration are still able to home and engraft in the bone marrow (Bendall et al., 2005). It appears that CXCR4 expression, CXCL12 mediated chemotaxis, and *in vivo* migration do not correlate well. Therefore, a combination of *in vitro* and *in vivo* approaches should be utilized when investigating the role of CXCR4 in disease. Analysis of CXCL12- mediated downstream signalling pathways can provide additional clues to disease biology.

7.2.1.5 Blockade of $p190^{BCR\text{-}ABL1}$ tyrosine kinase with Imatinib does not restore CXCL12-mediated migration

In CML, blast crisis is associated with a down-regulation of CXCR4 expression and CXCL12 mediated chemotaxis. In ALL cell lines SD1 and Sup B15, despite a correlation of BCR-ABL1 expression with dysfunctional migration, inhibition of $p190^{BCR\text{-}ABL1}$ tyrosine kinase fails to restore CXCL12 mediated chemotaxis in SD1 cells. This phenomenon has not been previously reported in ALL. Although intriguing, this observation is only limited to BCR-ABL1 positive cell lines. Further work is required to investigate this phenomenon using primary samples.

7.2.1.6 Interleukin-15 promotes proliferation of ALL cells under serum free conditions

IL-15 is a cytokine associated with growth and promotion of various cell types. A role for IL-15 in ALL has been suggested (Lin et al., 2010, Cario et al., 2007, Yang et al., 2009)

but the underlying mechanisms are incompletely understood. Whereas IL-15 is also thought to improve anti-tumour immune response by stimulating T- and NK- cells. IL-15 is currently being used as an adjuvant in AML treatment to enhance anti-leukaemic effect of donor lymphocytes (ClinicalTrials.gov, 2011). The data presented in this thesis provides evidence that such a therapy in ALL may actually enhance tumour growth. IL-15 disease biology is complicated by the fact that both endogenous and exogenous IL-15 production may have pro-survival effects on leukaemic cells. Hypothetically, IL-15 may act in a number of ways: (i) IL-15 complex may stimulate cells in an autocrine manner, (ii) IL-15 secreted by one leukaemic cell may stimulate another leukaemic cell in a paracrine or endocrine manner, (iii) IL-15 production by the tumour microenvironment may result in stimulation of leukaemic blasts, (iv) IL-15 secretion by the tumour microenvironment may stimulate anti-tumour response, or (v) IL-15 secretion by the leukaemic cells may result in stimulation of the anti-tumour response. IL-15 providing a greater growth advantage under serum free conditions may allow leukaemic cells with high IL-15 and IL-15 receptor to survive better in the CNS. In the bone marrow, serum starvation is unlikely to be a selective pressure and other factors such as cytokines, chemokines and growth factors may play a greater role. In addition, IL-15 secretion by leukaemic cells in the bone marrow may stimulate anti-leukaemia immune response which may antagonise IL-15 mediated tumour growth in the bone marrow but not in the CNS where entry of immune cells is more restricted. Preliminary data presented recently at an international conference supports the greater role for IL-15 mediated NK- cell response restricting leukaemic growth in the bone marrow but not in the CNS (Shemesh et al., 2013). IL-15 mediated upregulation of genes associated with dissemination may assist in CNS homing, where together with an increased growth advantage and reduced anti-leukaemia immune surveillance, IL-15 expressing cells may be fit to survive better than the bone marrow microenvironment. This hypothesis is presented in Figure 7.1

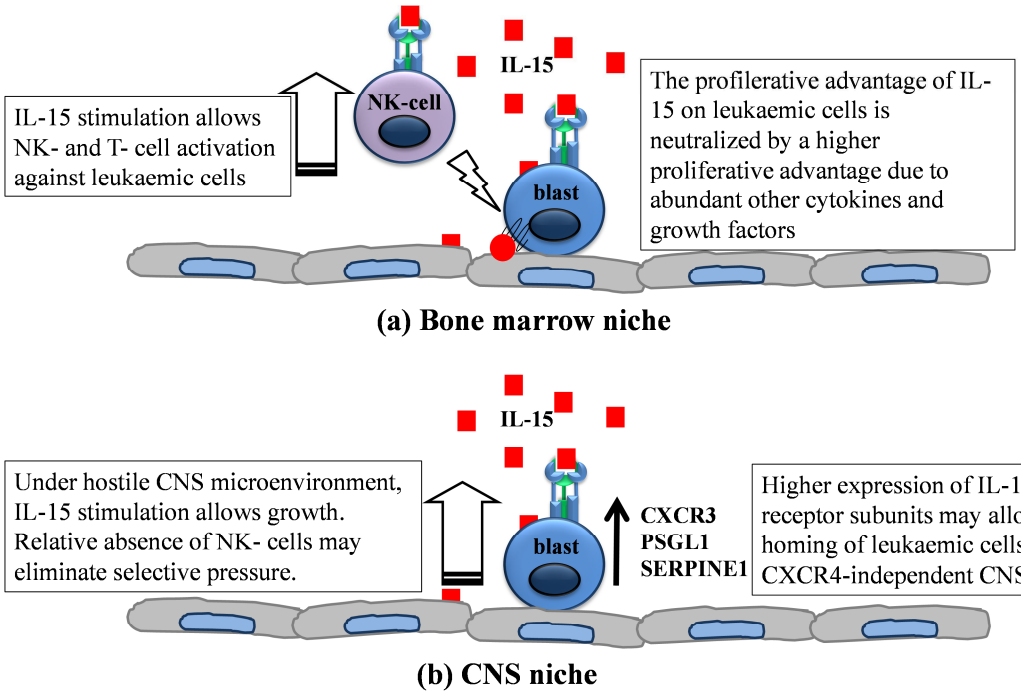

Figure 7-1 IL-15 stimulation may provide survival advantage to leukaemic cells in the CNS but less so in the bone marrow

7.2.2 Clinical implications of the findings

7.2.2.1 CNS disease at diagnosis is significantly more common than currently diagnosed

The observation that patient specific minimal residual disease (MRD) method can be applied and detects leukaemia in approximately 40% diagnostic samples reiterates the need for a more sensitive diagnostic method for the determination of CNS disease. Several authors have used a number of techniques to identify submicroscopic levels of CNS disease in patients. These range from immunohistochemistry to multiparameter flow cytometry and PCR using consensus primers. I utilized the novel patient specific ASO primers and consensus probes to detect CNS disease in patients. MRD determination requires the use of at least two MRD targets. The fact that in some cases only one of the two targets was amplified in the CSF DNA raises important questions. Whether this is due to the differences in sensitivity of the qPCR primers or this phenomenon is due to clonal evolution in the CNS compartment remains to be determined. What is evident is that there may be false negative cases where only one target was analysed. This in theory would underestimate the percentage of qPCR positive cases in the cohort of tested patients. It would be essential to analyse two or more targets for added sensitivity. Alternatively, an unbiased approach using novel techniques such as next generation sequencing (NGS) on DNA isolated from CSF cells may be used. This would eliminate the need for designing and optimizing patient specific reagents. Such an approach is in experimental stage and may be utilized for bone marrow MRD monitoring in future.

The presence of submicroscopic levels of leukaemia in the CNS also raises some important questions. The ultimate aim of determining CNS disease at diagnosis is to determine the true risk for CNS relapse and modification in treatment according to the risk. Whether the patients identified to be negative for CNS disease by qPCR represent truly negative cases? Furthermore, whether patients with CSF qPCR positive disease are at an increased risk for CNS relapse? The improved treatment has enabled excellent prognosis of patients. However, this has made testing new diagnostic and therapeutic measures increasingly difficulty – even more so when relatively rare events such as CNS relapse in low-risk groups are to be investigated. The low incidence of relapse mean that large numbers of patients would be required to follow for long period of times to provide adequate statistical power to draw accurate conclusions. In the set of patients analysed, all but one patient were in CCR during the median follow up of two years. To test whether CSF qPCR predicts CNS relapse, a group of 200 patients would be required to follow up for a period of 3 years

(Michele Robertson and Suzanne Lloyd, The Robertson Centre for Biostatistics, Glasgow – personal communication). Alternatively, the use of post-induction MRD levels is an attractive tool for use as a surrogate marker for predicting outcome. Although a higher percentage of patients with MRD risk were positive for CNS disease by qPCR, this difference was not significant. Bone marrow MRD levels despite being an excellent measure of overall prognosis and the risk of bone marrow relapse, do not predict extramedullary relapse well (Bowman et al., 2011).

Furthermore, are there patients who would not develop CNS relapse? Data from the xenograft model and the qPCR study suggests that in some cases even with heavy bone marrow infiltration, the CNS appears to be free of leukaemia. Nevertheless, bone marrow and CNS relapse are competing events – bone marrow relapse may mask an impending CNS relapse and vice versa. It is very much plausible that all patients may eventually developed CNS disease if they present later in the course of disease.

Another question concerning the origin of CNS relapse is, ‘when do the leukaemic cells enter the CNS?’ At the time of diagnosis, the cells might already be in the CNS. Inadequate clearing of the CNS disease may leave residual leukaemic cells in the CNS which during the post-treatment period will eventually grow to cause overt CNS relapse. Alternately, CNS relapse may be a result of secondary seeding from minimal residual leukaemic cells in the periphery. The fact that adequate systemic treatment without adequate CNS prophylaxis would eventually lead to CNS relapse (Evans et al., 1970) and marked improvement in CNS relapse rates with CNS prophylaxis in CNS-1 patients lead to the general consensus that CNS relapse is indeed a result of CNS-residual leukaemic cells. The data presented in this thesis support this hypothesis. Evidence from the xenograft models show that CNS disease in largely in a non-fluid state and a negative CSF cytospin may not exclude CNS disease. CSF qPCR positivity provides further evidence in support. This may have significance for future research. If this hypothesis were true, the identifying the therapeutically targetable molecules that allow entry to the CNS compartment would be clinically less relevant.

7.2.2.2 Selected soluble molecules are not sensitive biomarkers of submicroscopic CNS disease

Improving the methods of diagnosis of CNS disease is an ongoing effort. An ideal biomarker of CNS disease would be: specific to the disease, secreted in the CSF and specific to the CNS compartment. The successful soluble biomarkers in cancer such as prostate specific antigen (PSA) achieve high accuracy due the high levels secreted in

prostate cancer. Others such as gonadal tumours are characterized by aberrant secretion of α-fetoprotein. Leukaemia, despite possessing aberrant functions, is not known to secrete aberrant soluble molecules. Leukaemic cells in the meninges may secrete molecules which could be detected by analysing the CSF. Alternately, factors secreted by the microenvironment in response to presence of leukaemic cells could also be used as biomarkers. Previous studies have tested several candidate biomarkers without much success. Chemokine levels have not been tested previously in the CSF compartment. A possible reason could be that many of the CNS-disease free patients might have submicroscopic levels of leukaemia. Stratifying patients according to the CSF qPCR presented an opportunity to address this issue. Due to technical limitations in selecting the biomarkers of interest meant that only limited number of molecules could be analysed. As discussed below, the results of the Luminex assay provide promising clues to the biology of CNS disease, the differences in the levels of these do not appear to be useful in identifying CSF qPCR positive patients.

7.3 Future directions

7.3.1 Leukaemia-host microenvironment factors may play a dominant role in determining the risk of CNS relapse disease

Leukaemic entry in the CNS compartment is unlikely to be the selective event determining CNS relapse – instead it may be determined by the ability to survive long term in the CNS micro-environment, or evasion of chemotherapy or immune-surveillance at this site. Once leukaemic cells have entered the meninges they need to adapt to this new microenvoronment. Although B cells not normally present in this compartment in large numbers, there is evidence from MS that B cells can survive for extended periods and clonally expand in the CNS (Owens et al., 2003). In addition evidence for lymphoid neogenesis in the meninges in MS illustrates the role of meninges in lymphoid cell proliferation (Serafini et al., 2004).

Akers et al (2011) have shown that ALL cells can proliferate *in vitro* in contact with meningeal cells and co-culture of meningeal cells with ALL confers protection against chemotherapy. The lower levels of certain chemokines such as CXCL9, CXCL10, CCL21 and CCL2 in CSF qPCR positive patients raise the intriguing question as to whether these molecules are being utilized by leukaemic cells for retention in the CNS. Leukaemic cells are shown to manipulate the levels of chemokines in the bone marrow niche (van den Berk

et al., 2014). If leukaemic cells indeed utilize chemokine receptors such as CXCR3-CXCL9/10 and CCR7-CCL19/21 for retention in the CNS microenvironment, then blocking this interaction is may result in release of cells from leptomeninges and increase the drug penetration by reducing the protective effects of the CNS niche.

In addition to chemotherapy penetration, drug delivery to the meninges might equally affect the susceptibility of cells to therapy. Use of prednisolone is associated with a higher risk of CNS relapse in comparison with Dexamethasone. Rapid clearance of prednisolone from the CSF may limit the duration of leukaemic cell exposure to cytotoxic concentrations of the drug (Balis et al., 1987). Therefore, current trials use Dexamethasone despite the toxicities associated with its use. Strategies to increase the CNS penetration could improve CNS relapse risk without increasing toxicities. It has been suggested that the increased risk of CNS relapse with TLP might be attributed to CSF leakage and the resultant reduction in drug distribution. The incidence of TLP can be reduced by better care such as monitoring of platelet counts and improving skills of the lumbar puncture procedure.

The role of anti-leukaemia immune surveillance in the CNS remains to be investigated. There is some suggestion that graft-versus-leukaemia effect following HSCT is more pronounced in the bone marrow in comparison with the CNS (Ganem et al., 1989, Thompson et al., 1986, Oshima et al., 2008). This implies that the donor lymphocytes do not cross the CNS barriers well. Attempts at improving immune surveillance in the CNS can prove useful in eradicating the disease. As mentioned earlier, cytokine therapy to potentiate the immune surveillance may be counterproductive and benefit leukaemic cells.

7.3.2 Investigating the biomarkers for CNS disease

Improving the methods of diagnosis of CNS disease is an ongoing effort. An ideal biomarker of CNS disease would be: specific to the disease, secreted in the CSF and specific to the CNS compartment. The successful soluble biomarkers in cancer such as prostate specific antigen (PSA) achieve high accuracy due the high levels secreted in prostate cancer. Others such as gonadal tumours are characterized by aberrant secretion of α-fetoprotein. Leukaemia, despite possessing aberrant functions, is not known to secrete aberrant soluble molecules. The search for a soluble biomarker in the CNS may require unbiased screening approaches such as proteomic analysis of the CSF. Nevertheless, certain candidate biomarkers require further investigation. sL-selectin, sCD19 and sCD27 are such molecules of interest. From the CSF Biobank established during the course of this

project, CSF supernatant samples from patients with CSF qPCR positive and negative disease can be utilized to carry out these investigations.

7.3.3 Clonal origins of CNS infiltrating cells

In understanding the origins of CNS disease at diagnosis and relapse, an investigation into the clonal differences between leukaemic cells from the CNS and the bone marrow is likely to provide crucial insights. CSF qPCR detection of CNS disease can be technically challenging and the fact that in a number of samples, only 1 out of 2 targets assessed was identified by qPCR hints towards presence of an evolved clone in the CNS. If this is the case, CSF qPCR is unlikely to be a diagnostically useful or biologically informative. In the recent years, next generation sequencing analysis has emerged as a powerful tool for detection of MRD as well as for the investigation of the clonal hierarchy in leukaemia. Utilizing this technique on the paired bone marrow and CNS samples can simultaneously provide insights into both the avenues. Again, the CSF Biobank will be crucial in providing patient resource material for these studies. In addition, collaboration with national and international centres will ensure sharing of techniques and resources.

7.4 Overall conclusions

Using a range of *in vivo*, *in vitro* and clinical methods, the data presented in this thesis strongly indicate that: CNS disease is present at diagnosis in a higher frequency than clinically diagnosed, CNS entry is frequent and not restricted to a particular CNS risk category and immunophenotypic subtype, and is not determined by a particular set of leukocyte trafficking molecules. In addition, it is suggested that the direct effects of IL-15 on cellular proliferation and gene expression might facilitate leukaemic survival in the CNS. Therefore, attempts at blocking CNS entry of leukaemic cells are unlikely to prevent CNS relapse. The focus of future research should be at exploring the mechanisms that allow long-term survival of leukaemic cells in the CNS is essential preventing CNS relapse.

Appendix: Interleukin-15 enhances cellular proliferation and upregulates CNS homing molecules in pre-B acute lymphoblastic leukaemia

List of References

AGARWAL, A., FLEISCHMAN, A. G., PETERSEN, C. L., MACKENZIE, R., LUTY, S., LORIAUX, M., DRUKER, B. J., WOLTJER, R. L. & DEININGER, M. W. 2012. Effects of plerixafor in combination with BCR-ABL kinase inhibition in a murine model of CML. *Blood,* 120**,** 2658-68.

AGLIANO, A., MARTIN-PADURA, I., MANCUSO, P., MARIGHETTI, P., RABASCIO, C., PRUNERI, G., SHULTZ, L. D. & BERTOLINI, F. 2008. Human acute leukemia cells injected in NOD/LtSz-scid/IL-2R gamma null mice generate a faster and more efficient disease compared to other NOD/scid-related strains. *International Journal of Cancer,* 123**,** 2222-2227.

AKERS, S. M., RELLICK, S. L., FORTNEY, J. E. & GIBSON, L. F. 2011. Cellular elements of the subarachnoid space promote ALL survival during chemotherapy. *Leukemia research,* 35**,** 705-11.

ALKATIB, A., WANG, C. Y., BARDALES, R. & KOZINER, B. 1985. Phenotypic Characterization of Non-T, Non-B Acute Lymphoblastic-Leukemia by a New Panel (Bl) of Monoclonal-Antibodies. *Hematological Oncology,* 3**,** 271-281.

ALLAVENA, P., GIARDINA, G., BIANCHI, G. & MANTOVANI, A. 1997. IL-15 is chemotactic for natural killer cells and stimulates their adhesion to vascular endothelium. *Journal of Leukocyte Biology,* 61**,** 729-735.

ALON, R., KASSNER, P. D., CARR, M. W., FINGER, E. B., HEMLER, M. E. & SPRINGER, T. A. 1995. The integrin VLA-4 supports tethering and rolling in flow on VCAM-1. *The Journal of cell biology,* 128**,** 1243-53.

ANDERSON, K., LUTZ, C., VAN DELFT, F. W., BATEMAN, C. M., GUO, Y., COLMAN, S. M., KEMPSKI, H., MOORMAN, A. V., TITLEY, I., SWANSBURY, J., KEARNEY, L., ENVER, T. & GREAVES, M. 2011. Genetic variegation of clonal architecture and propagating cells in leukaemia. *Nature,* 469**,** 356-61.

ARBONES, M. L., ORD, D. C., LEY, K., RATECH, H., MAYNARDCURRY, C., OTTEN, G., CAPON, D. J. & TEDDER, T. F. 1994. Lymphocyte Homing and Leukocyte Rolling and Migration Are Impaired in L-Selectin-Deficient Mice. *Immunity,* 1**,** 247-260.

ATCC. 2014. *American Type Culture Collection* [Online]. Virginia. Available: http://www.atcc.org/ [Accessed 11/08/14 2014].

ATTARBASCHI, A., MANN, G., KONIG, M., DWORZAK, M. N., TREBO, M. M., MUHLEGGER, N., GADNER, H., HAAS, O. A. & GRP, A. B. C. S. 2004. Incidence and relevance of secondary chromosome abnormalities in childhood TEL/AML1+ acute lymphoblastic leukemia: an interphase FISH analysis. *Leukemia,* 18**,** 1611-1616.

AZZARELLI, B. & ROESSMANN, U. 1977. Pathogenesis of Central Nervous-System Infiltration in Acute-Leukemia. *Archives of Pathology & Laboratory Medicine,* 101**,** 203-205.

BACHELERIE, F., BEN-BARUCH, A., BURKHARDT, A. M., COMBADIERE, C., FARBER, J. M., GRAHAM, G. J., HORUK, R., SPARRE-ULRICH, A. H., LOCATI, M., LUSTER, A. D., MANTOVANI, A., MATSUSHIMA, K., MURPHY, P. M., NIBBS, R., NOMIYAMA, H., POWER, C. A., PROUDFOOT, A. E., ROSENKILDE, M. M., ROT, A., SOZZANI, S., THELEN, M., YOSHIE, O. & ZLOTNIK, A. 2014a. International Union of Pharmacology. LXXXIX.

Update on the extended family of chemokine receptors and introducing a new nomenclature for atypical chemokine receptors. *Pharmacological reviews,* 66**,** 1-79.

BACHELERIE, F., GRAHAM, G. J., LOCATI, M., MANTOVANI, A., MURPHY, P. M., NIBBS, R., ROT, A., SOZZANI, S. & THELEN, M. 2014b. New nomenclature for atypical chemokine receptors. *Nature Immunology,* 15**,** 207-8.

BAHBOUHI, B., BERTHELOT, L., PETTRE, S., MICHEL, L., WIERTLEWSKI, S., WEKSLER, B., ROMERO, I. A., MILLER, F., COURAUD, P. O., BROUARD, S., LAPLAUD, D. A. & SOULILLOU, J. P. 2009. Peripheral blood CD4+ T lymphocytes from multiple sclerosis patients are characterized by higher PSGL-1 expression and transmigration capacity across a human blood-brain barrier-derived endothelial cell line. *Journal of Leukocyte Biology,* 86**,** 1049-63.

BAJETTO, A., BONAVIA, R., BARBERO, S., FLORIO, T. & SCHETTINI, G. 2001. Chemokines and their receptors in the central nervous system. *Frontiers in Neuroendocrinology,* 22**,** 147-184.

BAJOU, K., NOEL, A., GERARD, R. D., MASSON, V., BRUNNER, N., HOLST-HANSEN, C., SKOBE, M., FUSENIG, N. E., CARMELIET, P., COLLEN, D. & FOIDART, J. M. 1998. Absence of host plasminogen activator inhibitor 1 prevents cancer invasion and vascularization. *Nature Medicine,* 4**,** 923-8.

BALABANIAN, K., LAGANE, B., INFANTINO, S., CHOW, K. Y., HARRIAGUE, J., MOEPPS, B., ARENZANA-SEISDEDOS, F., THELEN, M. & BACHELERIE, F. 2005. The chemokine SDF-1/CXCL12 binds to and signals through the orphan receptor RDC1 in T lymphocytes. *The Journal of Biological Chemistry,* 280**,** 35760-6.

BALASHOV, K. E., ROTTMAN, J. B., WEINER, H. L. & HANCOCK, W. W. 1999. CCR5(+) and CXCR3(+) T cells are increased in multiple sclerosis and their ligands MIP-1alpha and IP-10 are expressed in demyelinating brain lesions. *Proceedings of the National Academy of Sciences of the United States of America,* 96**,** 6873-8.

BALIS, F. M., LESTER, C. M., CHROUSOS, G. P., HEIDEMAN, R. L. & POPLACK, D. G. 1987. Differences in cerebrospinal fluid penetration of corticosteroids: possible relationship to the prevention of meningeal leukemia. *Journal of Clinical Oncology,* 5**,** 202-7.

BARATA, J. T., KEENAN, T. D., SILVA, A., NADLER, L. M., BOUSSIOTIS, V. A. & CARDOSO, A. A. 2004. Common gamma chain-signaling cytokines promote proliferation of T-cell acute lymphoblastic leukemia. *Haematologica,* 89**,** 1459-67.

BENDALL, L. J., BARAZ, R., JUAREZ, J., SHEN, W. & BRADSTOCK, K. F. 2005. Defective p38 mitogen-activated protein kinase signaling impairs chemotaxic but not proliferative responses to stromal-derived factor-1alpha in acute lymphoblastic leukemia. *Cancer Research,* 65**,** 3290-8.

BENE, M. C., CASTOLDI, G., KNAPP, W., LUDWIG, W. D., MATUTES, E., ORFAO, A. & VAN'T VEER, M. B. 1995. Proposals for the immunological classification of acute leukemias. European Group for the Immunological Characterization of Leukemias (EGIL). *Leukemia,* 9**,** 1783-6.

BENE, M. C. & KAEDA, J. S. 2009. How and why minimal residual disease studies are necessary in leukemia: a review from WP10 and WP12 of the European LeukaemiaNet. *Haematologica,* 94**,** 1135-1150.

BERAHOVICH, R. D., ZABEL, B. A., PENFOLD, M. E. T., LEWEN, S., WANG, Y.,

MIAO, Z. H., GAN, L., PEREDA, J., DIAS, J., SLUKVIN, I. I., MCGRATH, K. E., JAEN, J. C. & SCHALL, T. J. 2010. CXCR7 Protein Is Not Expressed on Human or Mouse Leukocytes. *Journal of Immunology,* 185**,** 5130-5139.

BERGAMASCHI, C., BEAR, J., ROSATI, M., BEACH, R. K., ALICEA, C., SOWDER, R., CHERTOVA, E., ROSENBERG, S. A., FELBER, B. K. & PAVLAKIS, G. N. 2012. Circulating IL-15 exists as heterodimeric complex with soluble IL-15Ralpha in human and mouse serum. *Blood,* 120**,** e1-8.

BERNARDIN, F., YANG, Y., CLEAVES, R., ZAHURAK, M., CHENG, L., CIVIN, C. I. & FRIEDMAN, A. D. 2002. TEL-AML1, expressed from t(12;21) in human acute lymphocytic leukemia, induces acute leukemia in mice. *Cancer Research,* 62**,** 3904-8.

BHATIA, S., LANDIER, W., SHANGGUAN, M., HAGEMAN, L., SCHAIBLE, A. N., CARTER, A. R., HANBY, C. L., LEISENRING, W., YASUI, Y., KORNEGAY, N. M., MASCARENHAS, L., RITCHEY, A. K., CASILLAS, J. N., DICKENS, D. S., MEZA, J., CARROLL, W. L., RELLING, M. V. & WONG, F. L. 2012. Nonadherence to oral mercaptopurine and risk of relapse in Hispanic and non-Hispanic white children with acute lymphoblastic leukemia: a report from the children's oncology group. *Journal of Clinical Oncology,* 30**,** 2094-101.

BHOJWANI, D., HOWARD, S. C. & PUI, C. H. 2009. High-Risk Childhood Acute Lymphoblastic Leukemia. *Clinical Lymphoma & Myeloma,* 9**,** S222-S230.

BIOJONE, E., QUEIROZ RDE, P., VALERA, E. T., ODASHIMA, N. S., TAKAYANAGUI, O. M., VIANA, M. B., TONE, L. G. & SCRIDELI, C. A. 2012. Minimal residual disease in cerebrospinal fluid at diagnosis: a more intensive treatment protocol was able to eliminate the adverse prognosis in children with acute lymphoblastic leukemia. *Leukemia & lymphoma,* 53**,** 89-95.

BIONDI, A., SCHRAPPE, M., DE LORENZO, P., CASTOR, A., LUCCHINI, G., GANDEMER, V., PIETERS, R., STARY, J., ESCHERICH, G., CAMPBELL, M., LI, C. K., VORA, A., ARICO, M., ROTTGERS, S., SAHA, V. & VALSECCHI, M. G. 2012. Imatinib after induction for treatment of children and adolescents with Philadelphia-chromosome-positive acute lymphoblastic leukaemia (EsPhALL): a randomised, open-label, intergroup study. *The Lancet. Oncology,* 13**,** 936-45.

BLANEY, S. M., POPLACK, D. G., GODWIN, K., MCCULLY, C. L., MURPHY, R. & BALIS, F. M. 1995. Effect of body position on ventricular CSF methotrexate concentration following intralumbar administration. *Journal of Clinical Oncology,* 13**,** 177-9.

BLEUL, C. C., SCHULTZE, J. L. & SPRINGER, T. A. 1998. B lymphocyte chemotaxis regulated in association with microanatomic localization, differentiation state, and B cell receptor engagement. *Journal of Experimental Medicine,* 187**,** 753-62.

BOLDAJIPOUR, B., MAHABALESHWAR, H., KARDASH, E., REICHMAN-FRIED, M., BLASER, H., MININA, S., WILSON, D., XU, Q. & RAZ, E. 2008. Control of chemokine-guided cell migration by ligand sequestration. *Cell,* 132**,** 463-73.

BOMKEN, S., BUECHLER, L., REHE, K., PONTHAN, F., ELDER, A., BLAIR, H., BACON, C. M., VORMOOR, J. & HEIDENREICH, O. 2013. Lentiviral marking of patient-derived acute lymphoblastic leukaemic cells allows in vivo tracking of disease progression. *Leukemia,* 27**,** 718-21.

BOROWITZ, M. J., DEVIDAS, M., HUNGER, S. P., BOWMAN, W. P., CARROLL, A. J., CARROLL, W. L., LINDA, S., MARTIN, P. L., PULLEN, D. J., VISWANATHA, D., WILLMAN, C. L., WINICK, N., CAMITTA, B. M. & GRP,

C. O. 2008. Clinical significance of minimal residual disease in childhood acute lymphoblastic leukemia and its relationship to other prognostic factors: a Children's Oncology Group study. *Blood,* 111**,** 5477-5485.

BOUCHARD, A., RATTHE, C. & GIRARD, D. 2004. Interleukin-15 delays human neutrophil apoptosis by intracellular events and not via extracellular factors: role of Mcl-1 and decreased activity of caspase-3 and caspase-8. *Journal of Leukocyte Biology,* 75**,** 893-900.

BOWMAN, W. P., LARSEN, E. L., DEVIDAS, M., LINDA, S. B., BLACH, L., CARROLL, A. J., CARROLL, W. L., PULLEN, D. J., SHUSTER, J., WILLMAN, C. L., WINICK, N., CAMITTA, B. M., HUNGER, S. P. & BOROWITZ, M. J. 2011. Augmented therapy improves outcome for pediatric high risk acute lymphocytic leukemia: results of Children's Oncology Group trial P9906. *Pediatric Blood & Cancer,* 57**,** 569-77.

BOYERINAS, B., ZAFRIR, M., YESILKANAL, A. E., PRICE, T. T., HYJEK, E. M. & SIPKINS, D. A. 2013. Adhesion to osteopontin in the bone marrow niche regulates lymphoblastic leukemia cell dormancy. *Blood,* 121**,** 4821-31.

BROMBERG, J. E., BREEMS, D. A., KRAAN, J., BIKKER, G., VAN DER HOLT, B., SMITT, P. S., VAN DEN BENT, M. J., VAN'T VEER, M. & GRATAMA, J. W. 2007. CSF flow cytometry greatly improves diagnostic accuracy in CNS hematologic malignancies. *Neurology,* 68**,** 1674-9.

BROXMEYER, H. E., KOHLI, L., KIM, C. H., LEE, Y., MANTEL, C., COOPER, S., HANGOC, G., SHAHEEN, M., LI, X. & CLAPP, D. W. 2003. Stromal cell-derived factor-1/CXCL12 directly enhances survival/antiapoptosis of myeloid progenitor cells through CXCR4 and G(alpha)i proteins and enhances engraftment of competitive, repopulating stem cells. *Journal of Leukocyte Biology,* 73**,** 630-8.

BRUNN, A., MONTESINOS-RONGEN, M., STRACK, A., REIFENBERGER, G., MAWRIN, C., SCHALLER, C. & DECKERT, M. 2007. Expression pattern and cellular sources of chemokines in primary central nervous system lymphoma. *Acta Neuropathologica,* 114**,** 271-276.

BUDAGIAN, V., BULANOVA, E., ORINSKA, Z., LUDWIG, A., ROSE-JOHN, S., SAFTIG, P., BORDEN, E. C. & BULFONE-PAUS, S. 2004. Natural soluble interleukin-15Ralpha is generated by cleavage that involves the tumor necrosis factor-alpha-converting enzyme (TACE/ADAM17). *The Journal of Biological Chemistry,* 279**,** 40368-75.

BUDAGIAN, V., BULANOVA, E., PAUS, R. & BULFONE-PAUS, S. 2006. IL-15/IL-15 receptor biology: A guided tour through an expanding universe. *Cytokine & Growth Factor Reviews,* 17**,** 259-280.

BULFONE-PAUS, S., BULANOVA, E., BUDAGIAN, V. & PAUS, R. 2006. The interieukin-15/interieukin-15 receptor system as a model for juxtacrine and reverse signaling. *Bioessays,* 28**,** 362-377.

BUONAMICI, S., TRIMARCHI, T., RUOCCO, M. G., REAVIE, L., CATHELIN, S., MAR, B. G., KLINAKIS, A., LUKYANOV, Y., TSENG, J. C., SEN, F., GEHRIE, E., LI, M., NEWCOMB, E., ZAVADIL, J., MERUELO, D., LIPP, M., IBRAHIM, S., EFSTRATIADIS, A., ZAGZAG, D., BROMBERG, J. S., DUSTIN, M. L. & AIFANTIS, I. 2009. CCR7 signalling as an essential regulator of CNS infiltration in T-cell leukaemia. *Nature,* 459**,** 1000-4.

BURGER, B., ZIMMERMANN, M., MANN, G., KUHL, J., LONING, L., RIEHM, H., REITER, A. & SCHRAPPE, M. 2003. Diagnostic cerebrospinal fluid examination

in children with acute lymphoblastic leukemia: significance of low leukocyte counts with blasts or traumatic lumbar puncture. *Journal of Clinical Oncology,* 21**,** 184-8.

BURGER, J. A. & BURKLE, A. 2007. The CXCR4 chemokine receptor in acute and chronic leukaemia: a marrow homing receptor and potential therapeutic target. *British Journal of Haematology,* 137**,** 288-96.

BURNS, J. M., SUMMERS, B. C., WANG, Y., MELIKIAN, A., BERAHOVICH, R., MIAO, Z., PENFOLD, M. E., SUNSHINE, M. J., LITTMAN, D. R., KUO, C. J., WEI, K., MCMASTER, B. E., WRIGHT, K., HOWARD, M. C. & SCHALL, T. J. 2006. A novel chemokine receptor for SDF-1 and I-TAC involved in cell survival, cell adhesion, and tumor development. *Journal of Experimental Medicine,* 203**,** 2201-13.

BURTON, J. D., BAMFORD, R. N., PETERS, C., GRANT, A. J., KURYS, G., GOLDMAN, C. K., BRENNAN, J., ROESSLER, E. & WALDMANN, T. A. 1994. A lymphokine, provisionally designated interleukin T and produced by a human adult T-cell leukemia line, stimulates T-cell proliferation and the induction of lymphokine-activated killer cells. *Proceedings of the National Academy of Sciences of the United States of America,* 91**,** 4935-9.

CAMPANA, D. 2003. Determination of minimal residual disease in leukaemia patients. *British Journal of Haematology,* 121**,** 823-38.

CANCELA, C. S. P., MURAO, M., SOUZA, M. E. D. L., BARCELOS, J. M., FURTADO, V. M., SILVA, M. L., VIANA, M. B. & OLIVEIRA, B. M. D. 2013. Central nervous system involvement in acute lymphoblastic leukemia: diagnosis by immunophenotyping. *Jornal Brasileiro de Patologia e Medicina Laboratorial,* 49**,** 260-263.

CANCERRESEARCHUK. 2014. *Childhood cancer mortality statistics* [Online]. London. Available: http://www.cancerresearchuk.org/ [Accessed 11/11 2014].

CARIO, G., IZRAELI, S., TEICHERT, A., RHEIN, P., SKOKOWA, J., MORICKE, A., ZIMMERMANN, M., SCHRAUDER, A., KARAWAJEW, L., LUDWIG, W. D., WELTE, K., SCHUNEMANN, H. J., SCHLEGELBERGER, B., SCHRAPPE, M. & STANULLA, M. 2007. High interleukin-15 expression characterizes childhood acute lymphoblastic leukemia with involvement of the CNS. *Journal of Clinical Oncology,* 25**,** 4813-20.

CARRITHERS, M. D., VISINTIN, I., KANG, S. J. & JANEWAY, C. A., JR. 2000. Differential adhesion molecule requirements for immune surveillance and inflammatory recruitment. *Brain,* 123 (Pt 6)**,** 1092-101.

CARRITHERS, M. D., VISINTIN, I., VIRET, C. & JANEWAY, C. S., JR. 2002. Role of genetic background in P selectin-dependent immune surveillance of the central nervous system. *J Neuroimmunol,* 129**,** 51-7.

CARSON, W. E., FEHNIGER, T. A., HALDAR, S., ECKHERT, K., LINDEMANN, M. J., LAI, C. F., CROCE, C. M., BAUMANN, H. & CALIGIURI, M. A. 1997. A potential role for interleukin-15 in the regulation of human natural killer cell survival. *The Journal of Clinical Investigation,* 99**,** 937-43.

CASTRO, F. V., MCGINN, O. J., KRISHNAN, S., MARINOV, G., LI, J., RUTKOWSKI, A. J., ELKORD, E., BURT, D. J., HOLLAND, M., VAGHJIANI, R., GALLEGO, A., SAHA, V. & STERN, P. L. 2012. 5T4 oncofetal antigen is expressed in high risk of relapse childhood pre-B acute lymphoblastic leukemia and is associated with a more invasive and chemotactic phenotype. *Leukemia,* 26**,** 1487-1498.

CAVALLO, F., FORNI, M., RICCARDI, C., SOLETI, A., DIPIERRO, F. & FORNI, G. 1992. Growth and Spread of Human-Malignant T-Lymphoblasts in Immunosuppressed Nude-Mice - a Model for Meningeal Leukemia. *Blood,* 80**,** 1279-1283.

CAVE, H., TEN BOSCH, J. V., SUCIU, S., GUIDAL, C., WATERKEYN, C., OTTEN, J., BAKKUS, M., THIELEMANS, K., GRANDCHAMP, B., VILMER, E. & LEUKE, E. O. R. T. C. C. 1998. Clinical significance of minimal residual disease in childhood acute lymphoblastic leukemia. *New England Journal of Medicine,* 339**,** 591-598.

CESANO, A., O'CONNOR, R., LANGE, B., FINAN, J., ROVERA, G. & SANTOLI, D. 1991. Homing and progression patterns of childhood acute lymphoblastic leukemias in severe combined immunodeficiency mice. *Blood,* 77**,** 2463-74.

CHARO, I. F. & RANSOHOFF, R. M. 2006. The many roles of chemokines and chemokine receptors in inflammation. *The New England Journal of Medicine,* 354**,** 610-21.

CHASSERIAU, J., RIVET, J., BILAN, F., CHOMEL, J. C., GUILHOT, F., BOURMEYSTER, N. & KITZIS, A. 2004. Characterization of the different BCR-ABL transcripts with a single multiplex RT-PCR. *The Journal of molecular diagnostics,* 6**,** 343-7.

CHEN, I. M., HARVEY, R. C., MULLIGHAN, C. G., GASTIER-FOSTER, J., WHARTON, W., KANG, H., BOROWITZ, M. J., CAMITTA, B. M., CARROLL, A. J., DEVIDAS, M., PULLEN, D. J., PAYNE-TURNER, D., TASIAN, S. K., RESHMI, S., COTTRELL, C. E., REAMAN, G. H., BOWMAN, W. P., CARROLL, W. L., LOH, M. L., WINICK, N. J., HUNGER, S. P. & WILLMAN, C. L. 2012. Outcome modeling with CRLF2, IKZF1, JAK, and minimal residual disease in pediatric acute lymphoblastic leukemia: a Children's Oncology Group study. *Blood,* 119**,** 3512-22.

CHEN, Y. Y., MALIK, M., TOMKOWICZ, B. E., COLLMAN, R. G. & PTASZNIK, A. 2008. BCR-ABL1 alters SDF-1alpha-mediated adhesive responses through the beta2 integrin LFA-1 in leukemia cells. *Blood,* 111**,** 5182-6.

CHESSELLS, J. M., VEYS, P., KEMPSKI, H., HENLEY, P., LEIPER, A., WEBB, D. & HANN, I. M. 2003. Long-term follow-up of relapsed childhood acute lymphoblastic leukaemia. *British Journal of Haematology,* 123**,** 396-405.

CLINICALTRIALS. 2014. *INCB18424 in Treating Young Patients With Relapsed or Refractory Solid Tumor, Leukemia, or Myeloproliferative Disease* [Online]. Available: http://clinicaltrials.gov/show/NCT01164163 [Accessed 13/11 2014].

CLINICALTRIALS.GOV. 2011. *Haploidentical donor natural killer cell infusion with IL-15 in acute myelogenous leukemia (AML)* [Online]. Bethesda (MD): National Library of Medicine (US). US. National Institute of Health. Available: http://clinicaltrials.gov/ct2/show/NCT01385423 [Accessed 08/09 2014].

COBALEDA, C. & SANCHEZ-GARCIA, I. 2009. B-cell acute lymphoblastic leukaemia: towards understanding its cellular origin. *Bioessays,* 31**,** 600-609.

COMERFORD, I. & MCCOLL, S. R. 2011. Mini-review series: focus on chemokines. *Immunology and cell biology,* 89**,** 183-4.

CONTER, V., BARTRAM, C. R., VALSECCHI, M. G., SCHRAUDER, A., PANZER-GRUMAYER, R., MORICKE, A., ARICO, M., ZIMMERMANN, M., MANN, G., DE ROSSI, G., STANULLA, M., LOCATELLI, F., BASSO, G., NIGGLI, F., BARISONE, E., HENZE, G., LUDWIG, W. D., HAAS, O. A., CAZZANIGA, G.,

KOEHLER, R., SILVESTRI, D., BRADTKE, J., PARASOLE, R., BEIER, R., VAN DONGEN, J. J., BIONDI, A. & SCHRAPPE, M. 2010. Molecular response to treatment redefines all prognostic factors in children and adolescents with B-cell precursor acute lymphoblastic leukemia: results in 3184 patients of the AIEOP-BFM ALL 2000 study. *Blood,* 115**,** 3206-14.

CORCIONE, A., ARDUINO, N., FERRETTI, E., PISTORIO, A., SPINELLI, M., OTTONELLO, L., DALLEGRI, F., BASSO, G. & PISTOIA, V. 2006. Chemokine receptor expression and function in childhood acute lymphoblastic leukemia of B-lineage. *Leukemia Research,* 30**,** 365-72.

COUSTAN-SMITH, E., BEHM, F. G., SANCHEZ, J., BOYETT, J. M., HANCOCK, M. L., RAIMONDI, S. C., RUBNITZ, J. E., RIVERA, G. K., SANDLUND, J. T., PUI, C. H. & CAMPANA, D. 1998. Immunological detection of minimal residual disease in children with acute lymphoblastic leukaemia. *Lancet,* 351**,** 550-554.

COUSTAN-SMITH, E., MULLIGHAN, C. G., ONCIU, M., BEHM, F. G., RAIMONDI, S. C., PEI, D., CHENG, C., SU, X., RUBNITZ, J. E., BASSO, G., BIONDI, A., PUI, C. H., DOWNING, J. R. & CAMPANA, D. 2009. Early T-cell precursor leukaemia: a subtype of very high-risk acute lymphoblastic leukaemia. *The Lancet. Oncology,* 10**,** 147-156.

COX, C. V., MARTIN, H. M., KEARNS, P. R., VIRGO, P., EVELY, R. S. & BLAIR, A. 2007. Characterization of a progenitor cell population in childhood T-cell acute lymphoblastic leukemia. *Blood,* 109**,** 674-82.

CRADDOCK, C. F., NAKAMOTO, B., ANDREWS, R. G., PRIESTLEY, G. V. & PAPAYANNOPOULOU, T. 1997. Antibodies to VLA4 integrin mobilize long-term repopulating cells and augment cytokine-induced mobilization in primates and mice. *Blood,* 90**,** 4779-4788.

CRAZZOLARA, R., KRECZY, A., MANN, G., HEITGER, A., EIBL, G., FINK, F. M., MOHLE, R. & MEISTER, B. 2001. High expression of the chemokine receptor CXCR4 predicts extramedullary organ infiltration in childhood acute lymphoblastic leukaemia. *British Journal of Haematology,* 115**,** 545-53.

CRUZ-ORENGO, L., HOLMAN, D. W., DORSEY, D., ZHOU, L., ZHANG, P., WRIGHT, M., MCCANDLESS, E. E., PATEL, J. R., LUKER, G. D., LITTMAN, D. R., RUSSELL, J. H. & KLEIN, R. S. 2011. CXCR7 influences leukocyte entry into the CNS parenchyma by controlling abluminal CXCL12 abundance during autoimmunity. *Journal of Experimental Medicine,* 208**,** 327-339.

DAGDEMIR, A., ERTEM, U., DURU, F. & KIRAZLI, S. 1998. Soluble L-selectin increases in the cerebrospinal fluid prior to meningeal involvement in children with acute lymphoblastic leukemia. *Leukemia & Lymphoma,* 28**,** 391-398.

DE BONT, J. M., HOLT, B., DEKKER, A. W., VAN DER DOES-VAN DEN BERG, A., SONNEVELD, P. & PIETERS, R. 2004. Significant difference in outcome for adolescents with acute lymphoblastic leukemia treated on pediatric vs adult protocols in the Netherlands. *Leukemia,* 18**,** 2032-5.

DE HAAS, V., VET, R. J., VERHAGEN, O. J., KROES, W., VAN DEN BERG, H. & VAN DER SCHOOT, C. E. 2002. Early detection of central nervous system relapse by polymerase chain reaction in children with B-precursor acute lymphoblastic leukemia. *Annals of hematology,* 81**,** 59-61.

DEL PRINCIPE, M. I., BUCCISANO, F., CEFALO, M., MAURILLO, L., DI CAPRIO, L., DI PIAZZA, F., SARLO, C., ANGELIS, G., CONSALVO, M. I., FRABONI, D., DE SANTIS, G., DITTO, C., POSTORINO, M., SCONOCCHIA, G., DEL

POETA, G., AMADORI, S. & VENDITTI, A. 2014. High sensitivity of flow cytometry improves detection of occult leptomeningeal disease in acute lymphoblastic leukemia and lymphoblastic lymphoma. *Annals of Hematology,* 93**,** 1509-1513.

DEN BOER, M. L., VAN SLEGTENHORST, M., DE MENEZES, R. X., CHEOK, M. H., BUIJS-GLADDINES, J. G., PETERS, S. T., VAN ZUTVEN, L. J., BEVERLOO, H. B., VAN DER SPEK, P. J., ESCHERICH, G., HORSTMANN, M. A., JANKA-SCHAUB, G. E., KAMPS, W. A., EVANS, W. E. & PIETERS, R. 2009. A subtype of childhood acute lymphoblastic leukaemia with poor treatment outcome: a genome-wide classification study. *The Lancet. Oncology,* 10**,** 125-34.

DHUT, S., GIBBONS, B., CHAPLIN, T. & YOUNG, B. D. 1991. Establishment of a lymphoblastoid cell line, SD-1, expressing the p190 bcr-abl chimaeric protein. *Leukemia,* 5**,** 49-55.

DIAMANTI, P., COX, C. V. & BLAIR, A. 2012. Comparison of childhood leukemia initiating cell populations in NOD/SCID and NSG mice. *Leukemia,* 26**,** 376-80.

DOBBELING, U., DUMMER, R., LAINE, E., POTOCZNA, N., QIN, J. Z. & BURG, G. 1998. Interleukin-15 is an autocrine/paracrine viability factor for cutaneous T-cell lymphoma cells. *Blood,* 92**,** 252-8.

DOLMANS, M. M., MARINESCU, C., SAUSSOY, P., VAN LANGENDONCKT, A., AMORIM, C. & DONNEZ, J. 2010. Reimplantation of cryopreserved ovarian tissue from patients with acute lymphoblastic leukemia is potentially unsafe. *Blood,* 116**,** 2908-2914.

DREXLER, H. G., DIRKS, W. G., MATSUO, Y. & MACLEOD, R. A. 2003. False leukemia-lymphoma cell lines: an update on over 500 cell lines. *Leukemia,* 17**,** 416-26.

DREXLER, H. G. & UPHOFF, C. C. 2002. Mycoplasma contamination of cell cultures: Incidence, sources, effects, detection, elimination, prevention. *Cytotechnology,* 39**,** 75-90.

DWORZAK, M. N., FROSCHL, G., PRINTZ, D., MANN, G., POTSCHGER, U., MUHLEGGER, N., FRITSCH, G., GADNER, H. & BERLIN-FRANKFURT-MUNSTER, A. 2002. Prognostic significance and modalities of flow cytometric minimal residual disease detection in childhood acute lymphoblastic leukemia. *Blood,* 99**,** 1952-1958.

EBERT, L. M., SCHAERLI, P. & MOSER, B. 2005. Chemokine-mediated control of T cell traffic in lymphoid and peripheral tissues. *Molecular immunology,* 42**,** 799-809.

EDEN, O. B., LILLEYMAN, J. S., RICHARDS, S., SHAW, M. P. & PETO, J. 1991. Results of Medical Research Council Childhood Leukaemia Trial UKALL VIII (report to the Medical Research Council on behalf of the Working Party on Leukaemia in Childhood). *British Journal of Haematology,* 78**,** 187-96.

EINSIEDEL, H. G., VON STACKELBERG, A., HARTMANN, R., FENGLER, R., SCHRAPPE, M., JANKA-SCHAUB, G., MANN, G., HAHLEN, K., GOBEL, U., KLINGEBIEL, T., LUDWIG, W. D. & HENZE, G. 2005. Long-term outcome in children with relapsed ALL by risk-stratified salvage therapy: results of trial acute lymphoblastic leukemia-relapse study of the Berlin-Frankfurt-Munster Group 87. *Journal of Clinical Oncology,* 23**,** 7942-50.

EISENKRAFT, A., KEIDAN, I., BIELORAI, B., KELLER, N., TOREN, A. & PARET, G. 2006. MCP-1 in the cerebrospinal fluid of children with acute lymphoblastic leukemia. *Leukemia Research,* 30**,** 1259-61.

ENSHAEI, A., SCHWAB, C. J., KONN, Z. J., MITCHELL, C. D., KINSEY, S. E., WADE, R., VORA, A., HARRISON, C. J. & MOORMAN, A. V. 2013. Long-term follow-up of ETV6-RUNX1 ALL reveals that NCI risk, rather than secondary genetic abnormalities, is the key risk factor. *Leukemia,* 27**,** 2256-2259.

ESCHERICH, G., HORSTMANN, M. A., ZIMMERMANN, M., JANKA-SCHAUB, G. E. & GROUP, C. S. 2010. Cooperative study group for childhood acute lymphoblastic leukaemia (COALL): long-term results of trials 82,85,89,92 and 97. *Leukemia,* 24**,** 298-308.

EVANS, A. E. & CRAIG, M. 1964. Central Nervous System Involvement in Children with Acute Leukemia - Study of 921 Patients. *Cancer,* 17**,** 256-&.

EVANS, A. E., GILBERT, E. S. & ZANDSTRA, R. 1970. The increasing incidence of central nervous system leukemia in children. (Children's Cancer Study Group A). *Cancer,* 26**,** 404-9.

EXTERMANN, M., BACCHI, M., MONAI, N., FOPP, M., FEY, M., TICHELLI, A., SCHAPIRA, M. & SPERTINI, O. 1998. Relationship between cleaved L-selectin levels and the outcome of acute myeloid leukemia. *Blood,* 92**,** 3115-3122.

FAHAM, M., ZHENG, J. B., MOORHEAD, M., CARLTON, V. E. H., STOW, P., COUSTAN-SMITH, E., PUI, C. H. & CAMPANA, D. 2012. Deep-sequencing approach for minimal residual disease detection in acute lymphoblastic leukemia. *Blood,* 120**,** 5173-5180.

FAZZINA, R., LOMBARDINI, L., MEZZANOTTE, L., RODA, A., HRELIA, P., PESSION, A. & TONELLI, R. 2012. Generation and characterization of bioluminescent xenograft mouse models of MLL-related acute leukemias and in vivo evaluation of luciferase-targeting siRNA nanoparticles. *International Journal of Oncology,* 41**,** 621-628.

FEDYK, E. R., RYYAN, D. H., RITTERMAN, I. & SPRINGER, T. A. 1999. Maturation decreases responsiveness of human bone marrow B lineage cells to stromal-derived factor 1 (SDF-1). *Journal of Leukocyte Biology,* 66**,** 667-73.

FEHNIGER, T. A., SUZUKI, K., PONNAPPAN, A., VANDEUSEN, J. B., COOPER, M. A., FLOREA, S. M., FREUD, A. G., ROBINSON, M. L., DURBIN, J. & CALIGIURI, M. A. 2001. Fatal leukemia in interleukin 15 transgenic mice follows early expansions in natural killer and memory phenotype CD8+ T cells. *Journal of Experimental Medicine,* 193**,** 219-31.

FENG, Y., BRODER, C. C., KENNEDY, P. E. & BERGER, E. A. 1996. HIV-1 entry cofactor: functional cDNA cloning of a seven-transmembrane, G protein-coupled receptor. *Science,* 272**,** 872-7.

FIFE, B. T., KENNEDY, K. J., PANIAGUA, M. C., LUKACS, N. W., KUNKEL, S. L., LUSTER, A. D. & KARPUS, W. J. 2001. CXCL10 (IFN-gamma-inducible protein-10) control of encephalitogenic CD4+ T cell accumulation in the central nervous system during experimental autoimmune encephalomyelitis. *Journal of immunology,* 166**,** 7617-24.

FISCHER, M., SCHWIEGER, M., HORN, S., NIEBUHR, B., FORD, A., ROSCHER, S., BERGHOLZ, U., GREAVES, M., LOHLER, J. & STOCKING, C. 2005. Defining the oncogenic function of the TEL/AML1 (ETV6/RUNX1) fusion protein in a mouse model. *Oncogene,* 24**,** 7579-91.

FLOHR, T., SCHRAUDER, A., CAZZANIGA, G., PANZER-GRUMAYER, R., VAN DER VELDEN, V., FISCHER, S., STANULLA, M., BASSO, G., NIGGLI, F. K., SCHAFER, B. W., SUTTON, R., KOEHLER, R., ZIMMERMANN, M.,

VALSECCHI, M. G., GADNER, H., MASERA, G., SCHRAPPE, M., VAN DONGEN, J. J. M., BIONDI, A., BARTRAM, C. R. & I-BFM-SG 2008. Minimal residual disease-directed risk stratification using real-time quantitative PCR analysis of immunoglobulin and T-cell receptor gene rearrangements in the international multicenter trial AIEOP-BFM ALL 2000 for childhood acute lymphoblastic leukemia. *Leukemia,* 22**,** 771-782.

FORD, A. M., FASCHING, K., PANZER-GRUMAYER, E. R., KOENIG, M., HAAS, O. A. & GREAVES, M. F. 2001. Origins of "late" relapse in childhood acute lymphoblastic leukemia with TEL-AML1 fusion genes. *Blood,* 98**,** 558-64.

FORD, A. M., PALMI, C., BUENO, C., HONG, D., CARDUS, P., KNIGHT, D., CAZZANIGA, G., ENVER, T. & GREAVES, M. 2009. The TEL-AML1 leukemia fusion gene dysregulates the TGF-beta pathway in early B lineage progenitor cells. *Journal of Clinical Investigation,* 119**,** 826-836.

FORONI, L., WILSON, G., GERRARD, G., MASON, J., GRIMWADE, D., WHITE, H. E., DE CASTRO, D. G., AUSTIN, S., AWAN, A., BURT, E., CLENCH, T., FARRUGGIA, J., HANCOCK, J., IRVINE, A. E., KIZILORS, A., LANGABEER, S., MILNER, B. J., NICKLESS, G., SCHUH, A., SPROUL, A., WANG, L., WICKHAM, C. & CROSS, N. C. 2011. Guidelines for the measurement of BCR-ABL1 transcripts in chronic myeloid leukaemia. *British Journal of Haematology,* 153**,** 179-90.

FUKUDA, S., BROXMEYER, H. E. & PELUS, L. M. 2005. Flt3 ligand and the Flt3 receptor regulate hematopoietic cell migration by modulating the SDF-1alpha(CXCL12)/CXCR4 axis. *Blood,* 105**,** 3117-26.

GABERT, J., BEILLARD, E., VAN DER VELDEN, V. H., BI, W., GRIMWADE, D., PALLISGAARD, N., BARBANY, G., CAZZANIGA, G., CAYUELA, J. M., CAVE, H., PANE, F., AERTS, J. L., DE MICHELI, D., THIRION, X., PRADEL, V., GONZALEZ, M., VIEHMANN, S., MALEC, M., SAGLIO, G. & VAN DONGEN, J. J. 2003. Standardization and quality control studies of 'real-time' quantitative reverse transcriptase polymerase chain reaction of fusion gene transcripts for residual disease detection in leukemia - a Europe Against Cancer program. *Leukemia,* 17**,** 2318-57.

GAGGERO, A., AZZARONE, B., ANDREI, C., MISHAL, Z., MEAZZA, R., ZAPPIA, E., RUBARTELLI, A. & FERRINI, S. 1999. Differential intracellular trafficking, secretion and endosomal localization of two IL-15 isoforms. *European journal of immunology,* 29**,** 1265-74.

GAITAN, M. I., MAGGI, P., WOHLER, J., LEIBOVITCH, E., SATI, P., CALANDRI, I. L., MERKLE, H., MASSACESI, L., SILVA, A. C., JACOBSON, S. & REICH, D. S. 2014. Perivenular brain lesions in a primate multiple sclerosis model at 7-tesla magnetic resonance imaging. *Multiple Sclerosis Journal,* 20**,** 64-71.

GAJ, S., EIJSSEN, L., MENSINK, R. P. & EVELO, C. T. 2008. Validating nutrient-related gene expression changes from microarrays using RT(2) PCR-arrays. *Genes and Nutrition,* 3**,** 153-7.

GAJJAR, A., HARRISON, P. L., SANDLUND, J. T., RIVERA, G. K., RIBEIRO, R. C., RUBNITZ, J. E., RAZZOUK, B., RELLING, M. V., EVANS, W. E., BOYETT, J. M. & PUI, C. H. 2000. Traumatic lumbar puncture at diagnosis adversely affects outcome in childhood acute lymphoblastic leukemia. *Blood,* 96**,** 3381-4.

GALOIN, S., DASTE, G., APOIL, P. A., CHOLLET, F., RODA, D., BLANCHER, A., DELSOL, G., CHITTAL, S. & AL SAATI, T. 1997. Polymerase chain reaction on cerebrospinal fluid cells in the detection of leptomeningeal involvement by B-cell

lymphoma and leukaemia: a novel strategy and its implications. *British Journal of Haematology,* 99**,** 122-30.

GANEM, G., KUENTZ, M., BERNAUDIN, F., GHARBI, A., CORDONNIER, C., LEMERLE, S., KARIANAKIS, G., VINCI, G., ROCHANT, H., LEBOURGEOIS, J. P. & ET AL. 1989. Central nervous system relapses after bone marrow transplantation for acute lymphoblastic leukemia in remission. *Cancer,* 64**,** 1796-804.

GAYNON, P. S., ANGIOLILLO, A. L., CARROLL, W. L., NACHMAN, J. B., TRIGG, M. E., SATHER, H. N., HUNGER, S. P., DEVIDAS, M. & CHILDREN'S ONCOLOGY, G. 2010. Long-term results of the children's cancer group studies for childhood acute lymphoblastic leukemia 1983-2002: a Children's Oncology Group Report. *Leukemia,* 24**,** 285-97.

GAYNON, P. S., QU, R. P., CHAPPELL, R. J., WILLOUGHBY, M. L. N., TUBERGEN, D. G., STEINHERZ, P. G. & TRIGG, M. E. 1998. Survival after relapse in childhood acute lymphoblastic leukemia - Impact of site and time to first relapse - the Children's Cancer Group experience. *Cancer,* 82**,** 1387-1395.

GEAY, J. F., BUET, D., ZHANG, Y., FOUDI, A., JARRIER, P., BERTHEBAUD, M., TURHAN, A. G., VAINCHENKER, W. & LOUACHE, F. 2005. p210BCR-ABL inhibits SDF-1 chemotactic response via alteration of CXCR4 signaling and down-regulation of CXCR4 expression. *Cancer Research,* 65**,** 2676-83.

GILCHRIST, G. S., TUBERGEN, D. G., SATHER, H. N., COCCIA, P. F., OBRIEN, R. T., WASKERWITZ, M. J. & HAMMOND, G. D. 1994. Low Numbers of Csf Blasts at Diagnosis Do Not Predict for the Development of Cns Leukemia in Children with Intermediate-Risk Acute Lymphoblastic-Leukemia - a Childrens Cancer Group-Report. *Journal of Clinical Oncology,* 12**,** 2594-2600.

GIRI, J. G., AHDIEH, M., EISENMAN, J., SHANEBECK, K., GRABSTEIN, K., KUMAKI, S., NAMEN, A., PARK, L. S., COSMAN, D. & ANDERSON, D. 1994. Utilization of the beta and gamma chains of the IL-2 receptor by the novel cytokine IL-15. *The EMBO journal,* 13**,** 2822-30.

GIRI, J. G., KUMAKI, S., AHDIEH, M., FRIEND, D. J., LOOMIS, A., SHANEBECK, K., DUBOSE, R., COSMAN, D., PARK, L. S. & ANDERSON, D. M. 1995. Identification and Cloning of a Novel Il-15 Binding-Protein That Is Structurally Related to the Alpha-Chain of the Il-2 Receptor. *The EMBO journal,* 14**,** 3654-3663.

GRABSTEIN, K. H., EISENMAN, J., SHANEBECK, K., RAUCH, C., SRINIVASAN, S., FUNG, V., BEERS, C., RICHARDSON, J., SCHOENBORN, M. A., AHDIEH, M. & ET AL. 1994. Cloning of a T cell growth factor that interacts with the beta chain of the interleukin-2 receptor. *Science,* 264**,** 965-8.

GRAHAM, G. J., LOCATI, M., MANTOVANI, A., ROT, A. & THELEN, M. 2012. The biochemistry and biology of the atypical chemokine receptors. *Immunology letters,* 145**,** 30-8.

GREAVES, M. 2006. Infection, immune responses and the aetiology of childhood leukaemia. *Nature Reviews Cancer,* 6**,** 193-203.

GREAVES, M. & MALEY, C. C. 2012. Clonal evolution in cancer. *Nature,* 481**,** 306-13.

GREAVES, M. F., MAIA, A. T., WIEMELS, J. L. & FORD, A. M. 2003. Leukemia in twins: lessons in natural history. *Blood,* 102**,** 2321-33.

GREAVES, M. F. & WIEMELS, J. 2003. Origins of chromosome translocations in

childhood leukaemia. *Nature reviews. Cancer,* 3**,** 639-49.

GREENWOOD, J., WANG, Y. & CALDER, V. L. 1995. Lymphocyte adhesion and transendothelial migration in the central nervous system: the role of LFA-1, ICAM-1, VLA-4 and VCAM-1. off. *Immunology,* 86**,** 408-15.

GREIL, J., GRAMATZKI, M., BURGER, R., MARSCHALEK, R., PELTNER, M., TRAUTMANN, U., HANSENHAGGE, T. E., BARTRAM, C. R. & FEY, G. H. 1994. The Acute Lymphoblastic-Leukemia Cell-Line Sem with T(411) Chromosomal Rearrangement Is Biphenotypic and Responsive to Interleukin-7. *British Journal of Haematology,* 86**,** 275-283.

GREINER, D. L., SHULTZ, L. D., YATES, J., APPEL, M. C., PERDRIZET, G., HESSELTON, R. M., SCHWEITZER, I., BEAMER, W. G., SHULTZ, K. L., PELSUE, S. C. & ET AL. 1995. Improved engraftment of human spleen cells in NOD/LtSz-scid/scid mice as compared with C.B-17-scid/scid mice. *The American Journal of Pathology,* 146**,** 888-902.

GREVE, T., CLASEN-LINDE, E., ANDERSEN, M. T., ANDERSEN, M. K., SORENSEN, S. D., ROSENDAHL, M., RALFKIAER, E. & ANDERSEN, C. Y. 2012. Cryopreserved ovarian cortex from patients with leukemia in complete remission contains no apparent viable malignant cells. *Blood,* 120**,** 4311-4316.

GREYSTOKE, B. F., HUANG, X., WILKS, D. P., ATKINSON, S. & SOMERVAILLE, T. C. P. 2013. Very high frequencies of leukaemia-initiating cells in precursor T-acute lymphoblastic leukaemia may be obscured by cryopreservation. *British Journal of Haematology,* 163**,** 538-541.

GULINO, A. V., MORATTO, D., SOZZANI, S., CAVADINI, P., OTERO, K., TASSONE, L., IMBERTI, L., PIROVANO, S., NOTARANGELO, L. D., SORESINA, R., MAZZOLARI, E., NELSON, D. L., NOTARANGELO, L. D. & BADOLATO, R. 2004. Altered leukocyte response to CXCL12 in patients with warts hypogammaglobulinemia, infections, myelokathexis (WHIM) syndrome. *Blood,* 104**,** 444-452.

GUNTHER, R., CHELSTROM, L. M., TUEL-AHLGREN, L., SIMON, J., MYERS, D. E. & UCKUN, F. M. 1995. Biotherapy for xenografted human central nervous system leukemia in mice with severe combined immunodeficiency using B43 (anti-CD19)-pokeweed antiviral protein immunotoxin. *Blood,* 85**,** 2537-45.

HAGEDORN, N., ACQUAVIVA, C., FRONKOVA, E., VON STACKELBERG, A., BARTH, A., ZUR STADT, U., SCHRAUDER, A., TRKA, J., GASPAR, N., SEEGER, K., HENZE, G., CAVE, H., ECKERT, C. & RESISTANT DISEASE COMMITTEE OF THE INTERNATIONAL, B. F. M. S. G. 2007. Submicroscopic bone marrow involvement in isolated extramedullary relapses in childhood acute lymphoblastic leukemia: a more precise definition of "isolated" and its possible clinical implications, a collaborative study of the Resistant Disease Committee of the International BFM study group. *Blood,* 110**,** 4022-9.

HALSEY, C., BUCK, G., RICHARDS, S., VARGHA-KHADEM, F., HILL, F. & GIBSON, B. 2011. The impact of therapy for childhood acute lymphoblastic leukaemia on intelligence quotients; results of the risk-stratified randomized central nervous system treatment trial MRC UKALL XI. *Journal of Hematology & Oncology,* 4**,** 42.

HANTSCHEL, O., RIX, U. & SUPERTI-FURGA, G. 2008. Target spectrum of the BCR-ABL inhibitors imatinib, nilotinib and dasatinib. *Leukemia & lymphoma,* 49**,** 615-9.

HARMS, D. 1974. Changes of the protein composition of the cerebrospinal fluid in

childhood acute leukemia. *Z Kinderheilkd,* 118**,** 97-105.

HARRISON, C. J., MOORMAN, A. V., BARBER, K. E., BROADFIELD, Z. J., CHEUNG, K. L., HARRIS, R. L., JALALI, G. R., ROBINSON, H. M., STREFFORD, J. C., STEWART, A., WRIGHT, S., GRIFFITHS, M., ROSS, F. M., HAREWOOD, L. & MARTINEAU, M. 2005. Interphase molecular cytogenetic screening for chromosomal abnormalities of prognostic significance in childhood acute lymphoblastic leukaemia: a UK Cancer Cytogenetics Group Study. *British Journal of Haematology,* 129**,** 520-530.

HARTMANN, T. N., GRABOVSKY, V., PASVOLSKY, R., SHULMAN, Z., BUSS, E. C., SPIEGEL, A., NAGLER, A., LAPIDOT, T., THELEN, M. & ALON, R. 2008. A crosstalk between intracellular CXCR7 and CXCR4 involved in rapid CXCL12-triggered integrin activation but not in chemokine-triggered motility of human T lymphocytes and CD34+ cells. *Journal of Leukocyte Biology,* 84**,** 1130-40.

HAWKINS, B. T. & DAVIS, T. P. 2005. The blood-brain barrier/neurovascular unit in health and disease. *Pharmacological reviews,* 57**,** 173-85.

HEROLD, R., STIBENZ, D., HARTMANN, R., HENZE, G. & BUHRER, C. 2002. Soluble l-selectin (sCD62L) in relapsed childhood acute lymphoblastic leukaemia. *British Journal of Haematology,* 119**,** 677-84.

HICKEY, W. F. & KIMURA, H. 1988. Perivascular microglial cells of the CNS are bone marrow-derived and present antigen in vivo. *Science,* 239**,** 290-2.

HIJIYA, N., LIU, W., SANDLUND, J. T., JEHA, S., RAZZOUK, B. I., RIBEIRO, R. C., RUBNITZ, J. E., HOWARD, S. C., KYZER, E. P., REDD, D., CHENG, C., RIVERA, G. K., HUDSON, M. M., RELLING, M. V. & PUI, C. H. 2005. Overt testicular disease at diagnosis of childhood acute lymphoblastic leukemia: lack of therapeutic role of local irradiation. *Leukemia,* 19**,** 1399-1403.

HODGE, D. L., YANG, J., BUSCHMAN, M. D., SCHAUGHENCY, P. M., DANG, H., BERE, W., YANG, Y., SAVAN, R., SUBLESKI, J. J., YIN, X. M., LOUGHRAN, T. P., JR. & YOUNG, H. A. 2009. Interleukin-15 enhances proteasomal degradation of bid in normal lymphocytes: implications for large granular lymphocyte leukemias. *Cancer Research,* 69**,** 3986-94.

HOLLAND, M., CASTRO, F. V., ALEXANDER, S., SMITH, D., LIU, J., WALKER, M., BITTON, D., MULRYAN, K., ASHTON, G., BLAYLOCK, M., BAGLEY, S., CONNOLLY, Y., BRIDGEMAN, J., MILLER, C., KRISHNAN, S., DEMPSEY, C., MASUREKAR, A., STERN, P., WHETTON, A. & SAHA, V. 2011. RAC2, AEP, and ICAM1 expression are associated with CNS disease in a mouse model of pre-B childhood acute lymphoblastic leukemia. *Blood,* 118**,** 638-49.

HOLMFELDT, L., WEI, L., DIAZ-FLORES, E., WALSH, M., ZHANG, J., DING, L., PAYNE-TURNER, D., CHURCHMAN, M., ANDERSSON, A., CHEN, S. C., MCCASTLAIN, K., BECKSFORT, J., MA, J., WU, G., PATEL, S. N., HEATLEY, S. L., PHILLIPS, L. A., SONG, G., EASTON, J., PARKER, M., CHEN, X., RUSCH, M., BOGGS, K., VADODARIA, B., HEDLUND, E., DRENBERG, C., BAKER, S., PEI, D., CHENG, C., HUETHER, R., LU, C., FULTON, R. S., FULTON, L. L., TABIB, Y., DOOLING, D. J., OCHOA, K., MINDEN, M., LEWIS, I. D., TO, L. B., MARLTON, P., ROBERTS, A. W., RACA, G., STOCK, W., NEALE, G., DREXLER, H. G., DICKINS, R. A., ELLISON, D. W., SHURTLEFF, S. A., PUI, C. H., RIBEIRO, R. C., DEVIDAS, M., CARROLL, A. J., HEEREMA, N. A., WOOD, B., BOROWITZ, M. J., GASTIER-FOSTER, J. M., RAIMONDI, S. C., MARDIS, E. R., WILSON, R. K., DOWNING, J. R., HUNGER, S. P., LOH, M. L. & MULLIGHAN, C. G. 2013.

The genomic landscape of hypodiploid acute lymphoblastic leukemia. *Nature Genetics,* 45**,** 242-52.

HOMANS, A. C., BARKER, B. E., FORMAN, E. N., CORNELL, C. J., JR., DICKERMAN, J. D. & TRUMAN, J. T. 1990. Immunophenotypic characteristics of cerebrospinal fluid cells in children with acute lymphoblastic leukemia at diagnosis. *Blood,* 76**,** 1807-11.

HONCZARENKO, M., DOUGLAS, R. S., MATHIAS, C., LEE, B., RATAJCZAK, M. Z. & SILBERSTEIN, L. E. 1999. SDF-1 responsiveness does not correlate with CXCR4 expression levels of developing human bone marrow B cells. *Blood,* 94**,** 2990-2998.

HOOIJKAAS, H., HAHLEN, K., ADRIAANSEN, H. J., DEKKER, I., VAN ZANEN, G. E. & VAN DONGEN, J. J. 1989. Terminal deoxynucleotidyl transferase (TdT)-positive cells in cerebrospinal fluid and development of overt CNS leukemia: a 5-year follow-up study in 113 children with a TdT-positive leukemia or non-Hodgkin's lymphoma. *Blood,* 74**,** 416-22.

HUHMER, A. F., BIRINGER, R. G., AMATO, H., FONTEH, A. N. & HARRINGTON, M. G. 2006. Protein analysis in human cerebrospinal fluid: Physiological aspects, current progress and future challenges. *Disease Markers,* 22**,** 3-26.

HUMPERT, M. L., TZOUROS, M., THELEN, S., BIGNON, A., LEVOYE, A., ARENZANA-SEISDEDOS, F., BALABANIAN, K., BACHELERIE, F., LANGEN, H. & THELEN, M. 2012. Complementary methods provide evidence for the expression of CXCR7 on human B cells. *Proteomics,* 12**,** 1938-1948.

HUNGER, S. P., LU, X. M., DEVIDAS, M., CAMITTA, B. M., GAYNON, P. S., WINICK, N. J., REAMAN, G. H. & CARROLL, W. L. 2012. Improved Survival for Children and Adolescents With Acute Lymphoblastic Leukemia Between 1990 and 2005: A Report From the Children's Oncology Group. *Journal of Clinical Oncology,* 30**,** 1663-1669.

HUSTU, H. O., AUR, R. J. A., VERZOSA, M. S., SIMONE, J. V. & PINKEL, D. 1973. Prevention of Central Nervous-System Leukemia by Irradiation. *Cancer,* 32**,** 585-597.

HYNES, R. O. 2002. Integrins: bidirectional, allosteric signaling machines. *Cell,* 110**,** 673-87.

İNCESOY-ÖZDEMIR, S., ŞAHIN, G., BOZKURT, C., ÖREN, A. C., BALKAYA, E. & ERTEM, U. 2013. The relationship between cerebrospinal fluid osteopontin level and central nervous system involvement in childhood acute leukemia. *Turkish Journal of Pediatrics,* 55**,** 42-49.

INFANTINO, S., MOEPPS, B. & THELEN, M. 2006. Expression and regulation of the orphan receptor RDC1 and its putative ligand in human dendritic and B cells. *Journal of Immunology,* 176**,** 2197-207.

IRVING, J., JESSON, J., VIRGO, P., CASE, M., MINTO, L., EYRE, L., NOEL, N., JOHANSSON, U., MACEY, M., KNOTTS, L., HELLIWELL, M., DAVIES, P., WHITBY, L., BARNETT, D., HANCOCK, J., GOULDEN, N., LAWSON, S., GRP, U. F. M. & GRP, U. M. S. 2009. Establishment and validation of a standard protocol for the detection of minimal residual disease in B lineage childhood acute lymphoblastic leukemia by flow cytometry in a multi-center setting. *Haematologica,* 94**,** 870-874.

IRVING, J., MATHESON, E. C., MINTO, L., BLAIR, H., CASE, M., HALSEY, C., SWIDENBANK, I., PONTHAN, F., KIRSCHNER-SCHWABE, R.,

GROENEVELD-KRENTZ, S., HOF, J., ALLAN, J., HARRISON, C. J., VORMOOR, J., STACKELBERG, A. & ECKERT, C. 2013. RAS Pathway Mutations Are Highly Prevalent In Relapsed Childhood Acute Lymphoblastic Leukaemia, Are Frequently Relapse-Drivers and Confer Sensitivity To MEK Inhibition. *Blood,* 122.

ITO, M., HIRAMATSU, H., KOBAYASHI, K., SUZUE, K., KAWAHATA, M., HIOKI, K., UEYAMA, Y., KOYANAGI, Y., SUGAMURA, K., TSUJI, K., HEIKE, T. & NAKAHATA, T. 2002. NOD/SCID/gamma(null)(c) mouse: an excellent recipient mouse model for engraftment of human cells. *Blood,* 100**,** 3175-3182.

IWAMOTO, S., MIHARA, K., DOWNING, J. R., PUI, C. H. & CAMPANA, D. 2007. Mesenchymal cells regulate the response of acute lymphoblastic leukemia cells to asparaginase. *The Journal of Clinical Investigation,* 117**,** 1049-57.

JALILI, A., SHIRVAIKAR, N., MIRZA, I., ILNITSKY, S., PENFOLD, M., SCHALL, T. J. & JANOWSKA-WIECZOREK, A. 2008. CXCR7 Is Expressed in B Acute Lymphoblastic Leukemia (ALL) Cells and Mediates Their Transendothelial Migration. *ASH Annual Meeting Abstracts,* 112**,** 1916-.

JEHA, S., COUSTAN-SMITH, E., PEI, D., SANDLUND, J. T., RUBNITZ, J. E., HOWARD, S. C., INABA, H., BHOJWANI, D., METZGER, M. L., CHENG, C., CHOI, J. K., JACOBSEN, J., SHURTLEFF, S. A., RAIMONDI, S., RIBEIRO, R. C., PUI, C. H. & CAMPANA, D. 2014. Impact of tyrosine kinase inhibitors on minimal residual disease and outcome in childhood Philadelphia chromosome-positive acute lymphoblastic leukemia. *Cancer,* 120**,** 1514-9.

JUAREZ, J., BRADSTOCK, K. F., GOTTLIEB, D. J. & BENDALL, L. J. 2003. Effects of inhibitors of the chemokine receptor CXCR4 on acute lymphoblastic leukemia cells in vitro. *Leukemia,* 17**,** 1294-300.

JUAREZ, J., DELA PENA, A., BARAZ, R., HEWSON, J., KHOO, M., CISTERNE, A., FRICKER, S., FUJII, N., BRADSTOCK, K. F. & BENDALL, L. J. 2007. CXCR4 antagonists mobilize childhood acute lymphoblastic leukemia cells into the peripheral blood and inhibit engraftment. *Leukemia,* 21**,** 1249-57.

JUAREZ, J. G., THIEN, M., DELA PENA, A., BARAZ, R., BRADSTOCK, K. F. & BENDALL, L. J. 2009. CXCR4 mediates the homing of B cell progenitor acute lymphoblastic leukaemia cells to the bone marrow via activation of p38MAPK. *British Journal of Haematology,* 145**,** 491-9.

KAKINUMA, T. & HWANG, S. T. 2006. Chemokines, chemokine receptors, and cancer metastasis. *Journal of Leukocyte Biology,* 79**,** 639-51.

KALATSKAYA, I., BERCHICHE, Y. A., GRAVEL, S., LIMBERG, B. J., ROSENBAUM, J. S. & HEVEKER, N. 2009. AMD3100 Is a CXCR7 Ligand with Allosteric Agonist Properties. *Molecular Pharmacology,* 75**,** 1240-1247.

KAMIYAMA, R. & FUNATA, N. 1976. A study of leukemic cell infiltration in the testis and ovary. *The Bulletin of Tokyo Medical and Dental University,* 23**,** 203-10.

KANG, Y., SIEGEL, P. M., SHU, W., DROBNJAK, M., KAKONEN, S. M., CORDON-CARDO, C., GUISE, T. A. & MASSAGUE, J. 2003. A multigenic program mediating breast cancer metastasis to bone. *Cancer Cell,* 3**,** 537-49.

KANTARJIAN, H. M., TALPAZ, M., DHINGRA, K., ESTEY, E., KEATING, M. J., KU, S., TRUJILLO, J., HUH, Y., STASS, S. & KURZROCK, R. 1991. Significance of the P210 versus P190 molecular abnormalities in adults with Philadelphia chromosome-positive acute leukemia. *Blood,* 78**,** 2411-8.

KATO, I., NIWA, A., HEIKE, T., FUJINO, H., SAITO, M. K., UMEDA, K., HIRAMATSU, H., ITO, M., MORITA, M., NISHINAKA, Y., ADACHI, S., ISHIKAWA, F. & NAKAHATA, T. 2011. Identification of hepatic niche harboring human acute lymphoblastic leukemic cells via the SDF-1/CXCR4 axis. *PLoS One,* 6**,** e27042.

KERFOOT, S. M. & KUBES, P. 2002. Overlapping roles of P-selectin and alpha 4 integrin to recruit leukocytes to the central nervous system in experimental autoimmune encephalomyelitis. *Journal of immunology,* 169**,** 1000-6.

KERSTEN, M. J., EVERS, L. M., DELLEMIJN, P. L., VAN DEN BERG, H., PORTEGIES, P., HINTZEN, R. Q., VAN LIER, R. A., VON DEM BORNE, A. E. & VAN OERS, R. H. 1996. Elevation of cerebrospinal fluid soluble CD27 levels in patients with meningeal localization of lymphoid malignancies. *Blood,* 87**,** 1985-9.

KESTENBAUM, L. A., EBBERSON, J., ZORC, J. J., HODINKA, R. L. & SHAH, S. S. 2010. Defining cerebrospinal fluid white blood cell count reference values in neonates and young infants. *Pediatrics,* 125**,** 257-64.

KINDLER, T., CORNEJO, M. G., SCHOLL, C., LIU, J., LEEMAN, D. S., HAYDU, J. E., FROHLING, S., LEE, B. H. & GILLILAND, D. G. 2008. K-RasG12D-induced T-cell lymphoblastic lymphoma/leukemias harbor Notch1 mutations and are sensitive to gamma-secretase inhibitors. *Blood,* 112**,** 3373-82.

KINLEN, L. 1988. Evidence for an infective cause of childhood leukaemia: comparison of a Scottish new town with nuclear reprocessing sites in Britain. *Lancet,* 2**,** 1323-7.

KINLEN, L. J. 1995. Epidemiological evidence for an infective basis in childhood leukaemia. *British Journal of Cancer,* 71**,** 1-5.

KIVISAKK, P., MAHAD, D. J., CALLAHAN, M. K., TREBST, C., TUCKY, B., WEI, T., WU, L., BAEKKEVOLD, E. S., LASSMANN, H., STAUGAITIS, S. M., CAMPBELL, J. J. & RANSOHOFF, R. M. 2003. Human cerebrospinal fluid central memory CD4+ T cells: evidence for trafficking through choroid plexus and meninges via P-selectin. *Proceedings of the National Academy of Sciences of the United States of America,* 100**,** 8389-94.

KLEIN, R. M., BERNSTEIN, D., HIGGINS, S. P., HIGGINS, C. E. & HIGGINS, P. J. 2012. SERPINE1 expression discriminates site-specific metastasis in human melanoma. *Experimental Dermatology,* 21**,** 551-4.

KONG, G., DU, J., LIU, Y., MELINE, B., CHANG, Y. I., RANHEIM, E. A., WANG, J. & ZHANG, J. 2013. Notch1 gene mutations target KRAS G12D-expressing CD8+ cells and contribute to their leukemogenic transformation. *The Journal of Biological Chemistry,* 288**,** 18219-27.

KONOPLEV, S., LU, H., FIEGL, M. A., ZENG, Z., CHEN, W., ANDREEFF, M. & KONOPLEVA, M. 2008. Expression and Function of the CXCR7 Chemokine Receptor in Leukemias. *ASH Annual Meeting Abstracts,* 112**,** 2423-.

KONRAD, M., METZLER, M., PANZER, S., OSTREICHER, I., PEHAM, M., REPP, R., HAAS, O. A., GADNER, H. & PANZER-GRUMAYER, E. R. 2003. Late relapses evolve from slow-responding subclones in t(12;21)-positive acute lymphoblastic leukemia: evidence for the persistence of a preleukemic clone. *Blood,* 101**,** 3635-40.

KRENTZ, S., HOF, J., MENDIOROZ, A., VAGGOPOULOU, R., DORGE, P., LOTTAZ, C., ENGELMANN, J. C., GROENEVELD, T. W. L., KORNER, G., SEEGER, K., HAGEMEIER, C., HENZE, G., ECKERT, C., VON STACKELBERG, A. & KIRSCHNER-SCHWABE, R. 2013. Prognostic value of genetic alterations in

children with first bone marrow relapse of childhood B-cell precursor acute lymphoblastic leukemia. *Leukemia,* 27**,** 295-304.

KRISHNAN, S., WADE, R., MOORMAN, A. V., MITCHELL, C., KINSEY, S. E., EDEN, T. O., PARKER, C., VORA, A., RICHARDS, S. & SAHA, V. 2010. Temporal changes in the incidence and pattern of central nervous system relapses in children with acute lymphoblastic leukaemia treated on four consecutive Medical Research Council trials, 1985-2001. *Leukemia,* 24**,** 450-9.

KRUMBHOLZ, M., THEIL, D., STEINMEYER, F., CEPOK, S., HEMMER, B., HOFBAUER, M., FARINA, C., DERFUSS, T., JUNKER, A., ARZBERGER, T., SINICINA, I., HARTLE, C., NEWCOMBE, J., HOHLFELD, R. & MEINL, E. 2007. CCL19 is constitutively expressed in the CNS, up-regulated in neuroinflammation, active and also inactive multiple sclerosis lesions. *Journal of Neuroimmunology,* 190**,** 72-79.

KUCIA, M., JANKOWSKI, K., RECA, R., WYSOCZYNSKI, M., BANDURA, L., ALLENDORF, D. J., ZHANG, J., RATAJCZAK, J. & RATAJCZAK, M. Z. 2004. CXCR4-SDF-1 signalling, locomotion, chemotaxis and adhesion. *Journal of Molecular Histology,* 35**,** 233-45.

KUKITA, T., ARIMA, N., MATSUSHITA, K., ARIMURA, K., OHTSUBO, H., SAKAKI, Y., FUJIWARA, H., OZAKI, A., MATSUMOTO, T. & TEI, C. 2002. Autocrine and/or paracrine growth of adult T-cell leukaemia tumour cells by interleukin 15. *British Journal of Haematology,* 119**,** 467-74.

KWAN, J. & KILLEEN, N. 2004. CCR7 directs the migration of thymocytes into the thymic medulla. *Journal of Immunology,* 172**,** 3999-4007.

LASZIK, Z., JANSEN, P. J., CUMMINGS, R. D., TEDDER, T. F., MCEVER, R. P. & MOORE, K. L. 1996. P-selectin glycoprotein ligand-1 is broadly expressed in cells of myeloid, lymphoid, and dendritic lineage and in some nonhematopoietic cells. *Blood,* 88**,** 3010-3021.

LE VISEUR, C., HOTFILDER, M., BOMKEN, S., WILSON, K., ROTTGERS, S., SCHRAUDER, A., ROSEMANN, A., IRVING, J., STAM, R. W., SHULTZ, L. D., HARBOTT, J., JURGENS, H., SCHRAPPE, M., PIETERS, R. & VORMOOR, J. 2008. In childhood acute lymphoblastic leukemia, blasts at different stages of immunophenotypic maturation have stem cell properties. *Cancer Cell,* 14**,** 47-58.

LEE, W., KIM, S. J., LEE, S., KIM, J., KIM, M., LIM, J., KIM, Y., CHO, B., LEE, E. J. & HAN, K. 2005. Significance of cerebrospinal fluid sIL-2R level as a marker of CNS involvement in acute lymphoblastic leukemia. *Annals of Clinical and Laboratory Science,* 35**,** 407-12.

LEPPERT, D., WAUBANT, E., GALARDY, R., BUNNETT, N. W. & HAUSER, S. L. 1995. T cell gelatinases mediate basement membrane transmigration in vitro. *Journal of Immunology,* 154**,** 4379-89.

LEPUS, C. M., GIBSON, T. F., GERBER, S. A., KAWIKOVA, I., SZCZEPANIK, M., HOSSAIN, J., ABLAMUNITS, V., KIRKILES-SMITH, N., HEROLD, K. C., DONIS, R. O., BOTHWELL, A. L., POBER, J. S. & HARDING, M. J. 2009. Comparison of human fetal liver, umbilical cord blood, and adult blood hematopoietic stem cell engraftment in NOD-scid/gammac-/-, Balb/c-Rag1-/-gammac-/-, and C.B-17-scid/bg immunodeficient mice. *Human Immunology,* 70**,** 790-802.

LEVINSEN, M., TASKINEN, M., ABRAHAMSSON, J., FORESTIER, E., FRANDSEN, T. L., HARILA-SAARI, A., HEYMAN, M., JONSSON, O. G., LÄHTEENMÄKI,

P. M., LAUSEN, B., VAITKEVIČIENĖ, G., ÅSBERG, A., SCHMIEGELOW, K., ON BEHALF OF THE NORDIC SOCIETY OF PAEDIATRIC, H. & ONCOLOGY 2014. Clinical features and early treatment response of central nervous system involvement in childhood acute lymphoblastic leukemia. *Pediatric Blood & Cancer***,** n/a-n/a.

LEVOYE, A., BALABANIAN, K., BALEUX, F., BACHELERIE, F. & LAGANE, B. 2009. CXCR7 heterodimerizes with CXCR4 and regulates CXCL12-mediated G protein signaling. *Blood,* 113**,** 6085-93.

LEY, K. 2003. The role of selectins in inflammation and disease. *Trends Mol Med,* 9**,** 263-8.

LEY, K., LAUDANNA, C., CYBULSKY, M. I. & NOURSHARGH, S. 2007. Getting to the site of inflammation: the leukocyte adhesion cascade updated. *Nature reviews. Immunology,* 7**,** 678-89.

LI, S., ILARIA, R. L., JR., MILLION, R. P., DALEY, G. Q. & VAN ETTEN, R. A. 1999. The P190, P210, and P230 forms of the BCR/ABL oncogene induce a similar chronic myeloid leukemia-like syndrome in mice but have different lymphoid leukemogenic activity. *Journal of Experimental Medicine,* 189**,** 1399-412.

LI, Y. M., PAN, Y., WEI, Y. K., CHENG, X. Y., ZHOU, B. H. P., TAN, M., ZHOU, X. Y., XIA, W. Y., HORTOBAGYI, G. N., YU, D. H. & HUNG, M. C. 2004. Upregulation of CXCR4 is essential for HER2-mediated tumor metastasis. *Cancer Cell,* 6**,** 459-469.

LIANG, D. C. & PUI, C. H. 2005. Childhood Acute Lymphoblastic Leukaemia. *In:* HOFFBRAND, A. V., CATOVSKY, D. & TUDDENHAM, E. G. D. (eds.) *Postgraduate Haematology.* 5 ed. Oxford: Blackwell Publishing.

LIANG, Y., CA, Q., ZHAI, Z. M. & WANG, N. L. 2013. A Practical Strategy of Monitoring Minimal Residue Disease and Intervention for Central Nervous System Relapse of Childhood Acute Lymphoblastic Leukemia: A Single Chinese Center's Experience. *Journal of Pediatric Hematology Oncology,* 35**,** 388-393.

LIANG, Z., BROOKS, J., WILLARD, M., LIANG, K., YOON, Y., KANG, S. & SHIM, H. 2007. CXCR4/CXCL12 axis promotes VEGF-mediated tumor angiogenesis through Akt signaling pathway. *Biochemical and Biophysical Research Communications,* 359**,** 716-22.

LICHTY, B. D., KEATING, A., CALLUM, J., YEE, K., CROXFORD, R., CORPUS, G., NWACHUKWU, B., KIM, P., GUO, J. & KAMEL-REID, S. 1998. Expression of p210 and p190 BCR-ABL due to alternative splicing in chronic myelogenous leukaemia. *British Journal of Haematology,* 103**,** 711-5.

LIN, D., LIU, C., XUE, M., LIU, R., JIANG, L., YU, X., BAO, G., DENG, F., YU, M., AO, J., ZHOU, Y., WU, D. & LIU, H. 2010. The role of interleukin-15 polymorphisms in adult acute lymphoblastic leukemia. *PLoS One,* 5**,** e13626.

LIU, L., HUANG, D., MATSUI, M., HE, T. T., HU, T., DEMARTINO, J., LU, B., GERARD, C. & RANSOHOFF, R. M. 2006. Severe disease, unaltered leukocyte migration, and reduced IFN-gamma production in CXCR3-/- mice with experimental autoimmune encephalomyelitis. *Journal of immunology,* 176**,** 4399-409.

LOCK, R. B., LIEM, N., FARNSWORTH, M. L., MILROSS, C. G., XUE, C., TAJBAKHSH, M., HABER, M., NORRIS, M. D., MARSHALL, G. M. & RICE, A. M. 2002. The nonobese diabetic/severe combined immunodeficient (NOD/SCID) mouse model of childhood acute lymphoblastic leukemia reveals

intrinsic differences in biologic characteristics at diagnosis and relapse. *Blood,* 99**,** 4100-8.

LODOLCE, J. P., BOONE, D. L., CHAI, S., SWAIN, R. E., DASSOPOULOS, T., TRETTIN, S. & MA, A. 1998. IL-15 receptor maintains lymphoid homeostasis by supporting lymphocyte homing and proliferation. *Immunity,* 9**,** 669-76.

LOH, M. L., GOLDWASSER, M. A., SILVERMAN, L. B., POON, W. M., VATTIKUTI, S., CARDOSO, A., NEUBERG, D. S., SHANNON, K. M., SALLAN, S. E. & GILLILAND, D. G. 2006. Prospective analysis of TEL/AML1-positive patients treated on Dana-Farber Cancer Institute consortium protocol 95-01. *Blood,* 107**,** 4508-4513.

LU, Y., KHAM, S. K., ARIFFIN, H., OEI, A. M., LIN, H. P., TAN, A. M., QUAH, T. C. & YEOH, A. E. 2014. Host genetic variants of ABCB1 and IL15 influence treatment outcome in paediatric acute lymphoblastic leukaemia. *British Journal of Cancer,* 110**,** 1673-80.

LUGO, T. G., PENDERGAST, A. M., MULLER, A. J. & WITTE, O. N. 1990. Tyrosine kinase activity and transformation potency of bcr-abl oncogene products. *Science,* 247**,** 1079-82.

LUSTER, A. D., ALON, R. & VON ANDRIAN, U. H. 2005. Immune cell migration in inflammation: present and future therapeutic targets. *Nature immunology,* 6**,** 1182-90.

MAHMOUD, H. H., RIVERA, G. K., HANCOCK, M. L., KRANCE, R. A., KUN, L. E., BEHM, F. G., RIBEIRO, R. C., SANDLUND, J. T., CRIST, W. M. & PUI, C. H. 1993. Low leukocyte counts with blast cells in cerebrospinal fluid of children with newly diagnosed acute lymphoblastic leukemia. *The New England Journal of Medicine,* 329**,** 314-9.

MAKSYM, R. B., TARNOWSKI, M., GRYMULA, K., TARNOWSKA, J., WYSOCZYNSKI, M., LIU, R., CZERNY, B., RATAJCZAK, J., KUCIA, M. & RATAJCZAK, M. Z. 2009. The role of stromal-derived factor-1-CXCR7 axis in development and cancer. *European Journal of Pharmacology,* 625**,** 31-40.

MAN, S., UBOGU, E. E. & RANSOHOFF, R. M. 2007. Inflammatory cell migration into the central nervous system: a few new twists on an old tale. *Brain Pathology,* 17**,** 243-50.

MARCHESI, F., LOCATELLI, M., SOLINAS, G., ERRENI, M., ALLAVENA, P. & MANTOVANI, A. 2010. Role of CX3CR1/CX3CL1 axis in primary and secondary involvement of the nervous system by cancer. *Journal of neuroimmunology,* 224**,** 39-44.

MARCHESI, F., MONTI, P., LEONE, B. E., ZERBI, A., VECCHI, A., PIEMONTI, L., MANTOVANI, A. & ALLAVENA, P. 2004. Increased survival, proliferation, and migration in metastatic human pancreatic tumor cells expressing functional CXCR4. *Cancer Research,* 64**,** 8420-7.

MARTINEZ-LAPERCHE, C., GOMEZ-GARCIA, A. M., LASSALETTA, A., MOSCARDO, C., VIVANCO, J. L., MOLINA, J., FUSTER, J. L., COUSELO, J. M., DE TOLEDO, J. S., BUREO, E., MADERO, L. & RAMIREZ, M. 2013. Detection of occult cerebrospinal fluid involvement during maintenance therapy identifies a group of children with acute lymphoblastic leukemia at high risk for relapse. *American journal of hematology,* 88**,** 359-64.

MARWAHA, R. K., KULKARNI, K. P., BANSAL, D. & TREHAN, A. 2010. Central nervous system involvement at presentation in childhood acute lymphoblastic

leukemia: management experience and lessons. *Leukemia & Lymphoma,* 51**,** 261-268.

MASUREKAR, A. N., PARKER, C. A., SHANYINDE, M., MOORMAN, A. V., HANCOCK, J. P., SUTTON, R., ANCLIFF, P. J., MORGAN, M., GOULDEN, N. J., FRASER, C., HOOGERBRUGGE, P. M., REVESZ, T., DARBYSHIRE, P. J., KRISHNAN, S., LOVE, S. B. & SAHA, V. 2014. Outcome of Central Nervous System Relapses In Childhood Acute Lymphoblastic Leukaemia - Prospective Open Cohort Analyses of the ALLR3 Trial. *PLoS One,* 9**,** e108107.

MAVLIGHT, G. M., STUCKEY, S. E., CABANILLAS, F. F., KEATING, M. J., TOURTELLOTTE, W. W., SCHOLD, S. C. & FREIREICH, E. J. 1980. Diagnosis of leukemia or lymphoma in the central nervous system by beta 2-microglobulin determination. *The New England Journal of Medicine,* 303**,** 718-22.

MAZURIER, F., DOEDENS, M., GAN, O. I. & DICK, J. E. 2003. Rapid myeloerythroid repopulation after intrafemoral transplantation of NOD-SCID mice reveals a new class of human stem cells. *Nature Medicine,* 9**,** 959-63.

MCCANDLESS, E. E., WANG, Q., WOERNER, B. M., HARPER, J. M. & KLEIN, R. S. 2006. CXCL12 Limits Inflammation by Localizing Mononuclear Infiltrates to the Perivascular Space during Experimental Autoimmune Encephalomyelitis. *J Immunol,* 177**,** 8053-8064.

MCDERMOTT, D. H., LIU, Q., VELEZ, D., LOPEZ, L., ANAYA-O'BRIEN, S., ULRICK, J., KWATEMAA, N., STARLING, J., FLEISHER, T. A., PRIEL, D. A., MERIDETH, M. A., GIUNTOLI, R. L., EVBUOMWAN, M. O., LITTEL, P., MARQUESEN, M. M., HILLIGOSS, D., DECASTRO, R., GRIMES, G. J., HWANG, S. T., PITTALUGA, S., CALVO, K. R., STRATTON, P., COWEN, E. W., KUHNS, D. B., MALECH, H. L. & MURPHY, P. M. 2014. A phase 1 clinical trial of long-term, low-dose treatment of WHIM syndrome with the CXCR4 antagonist plerixafor. *Blood,* 123**,** 2308-16.

MCEVER, R. P. & CUMMINGS, R. D. 1997. Role of PSGL-1 binding to selectins in leukocyte recruitment. *The Journal of Clinical Investigation,* 100**,** S97-103.

MELO, R. C. C., LONGHINI, A. L., BIGARELLA, C. L., BARATTI, M. O. & TRAINA, F. 2014. CXCR7 Is Highly Expressed in Acute Lymphoblastic Leukemia and Potentiates CXCR4 Response to CXCL12 (vol 9, e85926, 2014). *Plos One,* 9.

MEYER, L. H., ECKHOFF, S. M., QUEUDEVILLE, M., KRAUS, J. M., GIORDAN, M., STURSBERG, J., ZANGRANDO, A., VENDRAMINI, E., MORICKE, A., ZIMMERMANN, M., SCHRAUDER, A., LAHR, G., HOLZMANN, K., SCHRAPPE, M., BASSO, G., STAHNKE, K., KESTLER, H. A., KRONNIE, G. T. & DEBATIN, K. M. 2011. Early Relapse in ALL Is Identified by Time to Leukemia in NOD/SCID Mice and Is Characterized by a Gene Signature Involving Survival Pathways. *Cancer Cell,* 19**,** 206-217.

MIAO, Z., LUKER, K. E., SUMMERS, B. C., BERAHOVICH, R., BHOJANI, M. S., REHEMTULLA, A., KLEER, C. G., ESSNER, J. J., NASEVICIUS, A., LUKER, G. D., HOWARD, M. C. & SCHALL, T. J. 2007. CXCR7 (RDC1) promotes breast and lung tumor growth in vivo and is expressed on tumor-associated vasculature. *Proceedings of the National Academy of Sciences of the United States of America,* 104**,** 15735-15740.

MINN, A. J., GUPTA, G. P., SIEGEL, P. M., BOS, P. D., SHU, W. P., GIRI, D. D., VIALE, A., OLSHEN, A. B., GERALD, W. L. & MASSAGUE, J. 2005. Genes that mediate breast cancer metastasis to lung. *Nature,* 436**,** 518-524.

MITCHELL, C., RICHARDS, S., HARRISON, C. J. & EDEN, T. 2010. Long-term follow-up of the United Kingdom medical research council protocols for childhood acute lymphoblastic leukaemia, 1980-2001. *Leukemia,* 24**,** 406-418.

MOGHRABI, A., LEVY, D. E., ASSELIN, B., BARR, R., CLAVELL, L., HURWITZ, C., SAMSON, Y., SCHORIN, M., DALTON, V. K., LIPSHULTZ, S. E., NEUBERG, D. S., GELBER, R. D., COHEN, H. J., SALLAN, S. E. & SILVERMAN, L. B. 2007. Results of the Dana-Farber Cancer Institute ALL Consortium Protocol 95-01 for children with acute lymphoblastic leukemia. *Blood,* 109**,** 896-904.

MOMBAERTS, P., IACOMINI, J., JOHNSON, R. S., HERRUP, K., TONEGAWA, S. & PAPAIOANNOU, V. E. 1992. Rag-1-Deficient Mice Have No Mature Lymphocytes-B and Lymphocytes-T. *Cell,* 68**,** 869-877.

MORI, H., COLMAN, S. M., XIAO, Z. J., FORD, A. M., HEALY, L. E., DONALDSON, C., HOWS, J. M., NAVARRETE, C. & GREAVES, M. 2002. Chromosome translocations and covert leukemic clones are generated during normal fetal development. *Proceedings of the National Academy of Sciences of the United States of America,* 99**,** 8242-8247.

MORICKE, A., REITER, A., ZIMMERMANN, M., GADNER, H., STANULLA, M., DORDELMANN, M., LONING, L., BEIER, R., LUDWIG, W. D., RATEI, R., HARBOTT, J., BOOS, J., MANN, G., NIGGLI, F., FELDGES, A., HENZE, G., WELTE, K., BECK, J. D., KLINGEBIEL, T., NIEMEYER, C., ZINTL, F., BODE, U., URBAN, C., WEHINGER, H., NIETHAMMER, D., RIEHM, H., SCHRAPPE, M. & STU, G. A. S. A. B. 2008. Risk-adjusted therapy of acute lymphoblastic leukemia can decrease treatment burden and improve survival: treatment results of 2169 unselected pediatric and adolescent patients enrolled in the trial ALL-BFM 95. *Blood,* 111**,** 4477-4489.

MULHERN, R. K., FAIRCLOUGH, D. & OCHS, J. 1991. A prospective comparison of neuropsychologic performance of children surviving leukemia who received 18-Gy, 24-Gy, or no cranial irradiation. *Journal of Clinical Oncology,* 9**,** 1348-56.

MULLER, A., HOMEY, B., SOTO, H., GE, N., CATRON, D., BUCHANAN, M. E., MCCLANAHAN, T., MURPHY, E., YUAN, W., WAGNER, S. N., BARRERA, J. L., MOHAR, A., VERASTEGUI, E. & ZLOTNIK, A. 2001. Involvement of chemokine receptors in breast cancer metastasis. *Nature,* 410**,** 50-6.

MULLIGHAN, C. G. 2012. Molecular genetics of B-precursor acute lymphoblastic leukemia. *Journal of Clinical Investigation,* 122**,** 3407-3415.

MULLIGHAN, C. G., COLLINS-UNDERWOOD, J. R., PHILLIPS, L. A., LOUDIN, M. G., LIU, W., ZHANG, J., MA, J., COUSTAN-SMITH, E., HARVEY, R. C., WILLMAN, C. L., MIKHAIL, F. M., MEYER, J., CARROLL, A. J., WILLIAMS, R. T., CHENG, J., HEEREMA, N. A., BASSO, G., PESSION, A., PUI, C. H., RAIMONDI, S. C., HUNGER, S. P., DOWNING, J. R., CARROLL, W. L. & RABIN, K. R. 2009a. Rearrangement of CRLF2 in B-progenitor- and Down syndrome-associated acute lymphoblastic leukemia. *Nature Genetics,* 41**,** 1243-6.

MULLIGHAN, C. G., GOORHA, S., RADTKE, I., MILLER, C. B., COUSTAN-SMITH, E., DALTON, J. D., GIRTMAN, K., MATHEW, S., MA, J., POUNDS, S. B., SU, X., PUI, C. H., RELLING, M. V., EVANS, W. E., SHURTLEFF, S. A. & DOWNING, J. R. 2007. Genome-wide analysis of genetic alterations in acute lymphoblastic leukaemia. *Nature,* 446**,** 758-64.

MULLIGHAN, C. G., MILLER, C. B., RADTKE, I., PHILLIPS, L. A., DALTON, J., MA, J., WHITE, D., HUGHES, T. P., LE BEAU, M. M., PUI, C. H., RELLING, M. V., SHURTLEFF, S. A. & DOWNING, J. R. 2008a. BCR-ABL1 lymphoblastic

leukaemia is characterized by the deletion of Ikaros. *Nature,* 453**,** 110-4.

MULLIGHAN, C. G., PHILLIPS, L. A., SU, X., MA, J., MILLER, C. B., SHURTLEFF, S. A. & DOWNING, J. R. 2008b. Genomic analysis of the clonal origins of relapsed acute lymphoblastic leukemia. *Science,* 322**,** 1377-80.

MULLIGHAN, C. G., SU, X., ZHANG, J., RADTKE, I., PHILLIPS, L. A., MILLER, C. B., MA, J., LIU, W., CHENG, C., SCHULMAN, B. A., HARVEY, R. C., CHEN, I. M., CLIFFORD, R. J., CARROLL, W. L., REAMAN, G., BOWMAN, W. P., DEVIDAS, M., GERHARD, D. S., YANG, W., RELLING, M. V., SHURTLEFF, S. A., CAMPANA, D., BOROWITZ, M. J., PUI, C. H., SMITH, M., HUNGER, S. P., WILLMAN, C. L., DOWNING, J. R. & CHILDREN'S ONCOLOGY, G. 2009b. Deletion of IKZF1 and prognosis in acute lymphoblastic leukemia. *The New England Journal of Medicine,* 360**,** 470-80.

MUNIZ, C., MARTIN-MARTIN, L., LOPEZ, A., SANCHEZ-GONZALEZ, B., SALAR, A., ALMEIDA, J., SANCHO, J. M., RIBERA, J. M., HERAS, C., PENALVER, F., GOMEZ, M., GONZALEZ-BARCA, E., ALONSO, N., NAVARRO, B., OLAVE, T., SALA, F., CONDE, E., MARQUEZ, J. A., CABEZUDO, E., CLADERA, A., GARCIA-MALO, M., CABALLERO, M. D. & ORFAO, A. 2014. Contribution of cerebrospinal fluid sCD19 levels to the detection of CNS lymphoma and its impact on disease outcome. *Blood,* 123**,** 6.

MURAKAMI, T., MAKI, W., CARDONES, A. R., FANG, H., TUN KYI, A., NESTLE, F. O. & HWANG, S. T. 2002. Expression of CXC chemokine receptor-4 enhances the pulmonary metastatic potential of murine B16 melanoma cells. *Cancer Research,* 62**,** 7328-34.

MURPHY, P. M., BAGGIOLINI, M., CHARO, I. F., HEBERT, C. A., HORUK, R., MATSUSHIMA, K., MILLER, L. H., OPPENHEIM, J. J. & POWER, C. A. 2000. International union of pharmacology. XXII. Nomenclature for chemokine receptors. *Pharmacological reviews,* 52**,** 145-76.

NAGASAWA, T., HIROTA, S., TACHIBANA, K., TAKAKURA, N., NISHIKAWA, S., KITAMURA, Y., YOSHIDA, N., KIKUTANI, H. & KISHIMOTO, T. 1996. Defects of B-cell lymphopoiesis and bone-marrow myelopoiesis in mice lacking the CXC chemokine PBSF/SDF-1. *Nature,* 382**,** 635-8.

NAKADA, D., OGURO, H., LEVI, B. P., RYAN, N., KITANO, A., SAITOH, Y., TAKEICHI, M., WENDT, G. R. & MORRISON, S. J. 2014. Oestrogen increases haematopoietic stem-cell self-renewal in females and during pregnancy. *Nature,* 505**,** 555-8.

NATIONALCANCERINSTITUTE. 2014. *SEER Cancer Statistics Review (CSR) 1975-2011* [Online]. Bethesda. Available: http://seer.cancer.gov/csr/1975_2011/ [Accessed 11/11 2014].

NAUMANN, U., CAMERONI, E., PRUENSTER, M., MAHABALESHWAR, H., RAZ, E., ZERWES, H. G., ROT, A. & THELEN, M. 2010. CXCR7 functions as a scavenger for CXCL12 and CXCL11. *PLoS One,* 5**,** e9175.

NAUMOVSKI, L., MORGAN, R., HECHT, F., LINK, M. P., GLADER, B. E. & SMITH, S. D. 1988. Philadelphia Chromosome-Positive Acute Lymphoblastic-Leukemia Cell-Lines without Classical Breakpoint Cluster Region Rearrangement. *Cancer Research,* 48**,** 2876-2879.

NEEL, N. F., SCHUTYSER, E., SAI, J., FAN, G. H. & RICHMOND, A. 2005. Chemokine receptor internalization and intracellular trafficking. *Cytokine & Growth Factor Reviews,* 16**,** 637-58.

NGUYEN, K., DEVIDAS, M., CHENG, S. C., LA, M., RAETZ, E. A., CARROLL, W. L., WINICK, N. J., HUNGER, S. P., GAYNON, P. S., LOH, M. L. & GRP, C. O. 2008. Factors influencing survival after relapse from acute lymphoblastic leukemia: a Children's Oncology Group study. *Leukemia,* 22**,** 2142-2150.

NIETO, M., DEL POZO, M. A. & SANCHEZ-MADRID, F. 1996. Interleukin-15 induces adhesion receptor redistribution in T lymphocytes. *European journal of immunology,* 26**,** 1302-7.

NIGROVIC, L. E., KIMIA, A. A., SHAH, S. S. & NEUMAN, M. I. 2012. Relationship between Cerebrospinal Fluid Glucose and Serum Glucose. *New England Journal of Medicine,* 366**,** 576-578.

NOTTA, F., DOULATOV, S. & DICK, J. E. 2010. Engraftment of human hematopoietic stem cells is more efficient in female NOD/SCID/IL-2Rg(c)-null recipients. *Blood,* 115**,** 3704-3707.

NOWELL, P. C. 1976. The clonal evolution of tumor cell populations. *Science,* 194**,** 23-8.

NOWELL, P. C. & HUNGERFORD, D. A. 1960. A minute chromosome in chronic granulocytic leukemia. *Science,* 132.

ONU, A., POHL, T., KRAUSE, H. & BULFONEPAUS, S. 1997. Regulation of IL-15 secretion via the leader peptide of two IL-15 isoforms. *Journal of Immunology,* 158**,** 255-262.

OSHIMA, K., KANDA, Y., YAMASHITA, T., TAKAHASHI, S., MORI, T., NAKASEKO, C., FUJIMAKI, K., YOKOTA, A., FUJISAWA, S., MATSUSHIMA, T., FUJITA, H., SAKURA, T., OKAMOTO, S., MARUTA, A., SAKAMAKI, H. & KANTO STUDY GROUP FOR CELL, T. 2008. Central nervous system relapse of leukemia after allogeneic hematopoietic stem cell transplantation. *Biol Blood Marrow Transplant,* 14**,** 1100-7.

OWENS, G. P., RITCHIE, A. M., BURGOON, M. P., WILLIAMSON, R. A., CORBOY, J. R. & GILDEN, D. H. 2003. Single-cell repertoire analysis demonstrates that clonal expansion is a prominent feature of the B cell response in multiple sclerosis cerebrospinal fluid. *Journal of Immunology,* 171**,** 2725-2733.

PALMESINO, E., MOEPPS, B., GIERSCHIK, P. & THELEN, M. 2006. Differences in CXCR4-mediated signaling in B cells. *Immunobiology,* 211**,** 377-89.

PARKER, C., WATERS, R., LEIGHTON, C., HANCOCK, J., SUTTON, R., MOORMAN, A. V., ANCLIFF, P., MORGAN, M., MASUREKAR, A., GOULDEN, N., GREEN, N., REVESZ, T., DARBYSHIRE, P., LOVE, S. & SAHA, V. 2010. Effect of mitoxantrone on outcome of children with first relapse of acute lymphoblastic leukaemia (ALL R3): an open-label randomised trial. *Lancet,* 376**,** 2009-17.

PATEL, K. D., CUVELIER, S. L. & WIEHLER, S. 2002. Selectins: critical mediators of leukocyte recruitment. *Seminars in Immunology,* 14**,** 73-81.

PILLER, G. 2001. Leukaemia - a brief historical review from ancient times to 1950. *British Journal of Haematology,* 112**,** 282-92.

PINE, S. R., YIN, C., MATLOUB, Y. H., SABAAWY, H. E., SANDOVAL, C., LEVENDOGLU-TUGAL, O., OZKAYNAK, M. F. & JAYABOSE, S. 2005. Detection of central nervous system leukemia in children with acute lymphoblastic leukemia by real-time polymerase chain reaction. *The Journal of molecular diagnostics,* 7**,** 127-32.

PORTNOY, J. M. & OLSON, L. C. 1985. Normal Cerebrospinal-Fluid Values in Children

- Another Look. *Pediatrics,* 75**,** 484-487.

PRICE, R. A. & JOHNSON, W. W. 1973. The central nervous system in childhood leukemia. I. The arachnoid. *Cancer,* 31**,** 520-33.

PROPP, S. & LIZZI, F. A. 1970. Philadelphia chromosome in acute lymphocytic leukemia. *Blood,* 36**,** 353-60.

PTASZNIK, A., URBANOWSKA, E., CHINTA, S., COSTA, M. A., KATZ, B. A., STANISLAUS, M. A., DEMIR, G., LINNEKIN, D., PAN, Z. K. & GEWIRTZ, A. M. 2002. Crosstalk between BCR/ABL oncoprotein and CXCR4 signaling through a Src family kinase in human leukemia cells. *Journal of Experimental Medicine,* 196**,** 667-678.

PUI, C. H. 2006. Central nervous system disease in acute lymphoblastic leukemia: prophylaxis and treatment. *Hematology / the Education Program of the American Society of Hematology. American Society of Hematology. Education Program***,** 142-6.

PUI, C. H. & CAMPANA, D. 2000. New definition of remission in childhood acute lymphoblastic leukemia. *Leukemia,* 14**,** 783-785.

PUI, C. H., CHENG, C., LEUNG, W., RAI, S. N., RIVERA, G. K., SANDLUND, J. T., RIBEIRO, R. C., RELLING, M. V., KUN, L. E., EVANS, W. E. & HUDSON, M. M. 2003. Extended follow-up of long-term survivors of childhood acute lymphoblastic leukemia. *The New England Journal of Medicine,* 349**,** 640-9.

PUI, C. H. & HOWARD, S. C. 2008. Current management and challenges of malignant disease in the CNS in paediatric leukaemia. *The Lancet. Oncology,* 9**,** 257-68.

PUI, C. H., ROBISON, L. L. & LOOK, A. T. 2008. Acute lymphoblastic leukaemia. *Lancet,* 371**,** 1030-43.

QUACKENBUSH, R. C., REUTHER, G. W., MILLER, J. P., COURTNEY, K. D., PEAR, W. S. & PENDERGAST, A. M. 2000. Analysis of the biologic properties of p230 Bcr-Abl reveals unique and overlapping properties with the oncogenic p185 and p210 Bcr-Abl tyrosine kinases. *Blood,* 95**,** 2913-21.

QUAH, B. J. & PARISH, C. R. 2012. New and improved methods for measuring lymphocyte proliferation in vitro and in vivo using CFSE-like fluorescent dyes. *Journal of immunological methods,* 379**,** 1-14.

RAETZ 2008. Reinduction platform for children with first marrow relapse of acute lymphoblastic leukemia: A children's oncology group study (vol 26, pg 3971, 2008). *Journal of Clinical Oncology,* 26**,** 4697-4697.

RAGHAVENDRA, P. & NAVEEN, K. 2006. Congenital leukemia in a 2-month old boy. *The internet journal of Paediatrics and Neonatology,* 6.

RAIMONDI, S. C., PUI, C. H., HEAD, D. R., RIVERA, G. K. & BEHM, F. G. 1993. Cytogenetically different leukemic clones at relapse of childhood acute lymphoblastic leukemia. *Blood,* 82**,** 576-80.

RAIMONDI, S. C., ZHOU, Y. M., SHURTLEFF, S. A., RUBNITZ, J. E., PUI, C. H. & BEHM, F. G. 2006. Near-triploidy and near-tetraploidy in childhood acute lymphoblastic leukemia: association with B-lineage blast cells carrying the ETV6-RUNXI fusion, T-lineage immunophenotype, and favorable outcome. *Cancer Genetics and Cytogenetics,* 169**,** 50-57.

RAJAGOPAL, S., KIM, J., AHN, S., CRAIG, S., LAM, C. M., GERARD, N. P., GERARD, C. & LEFKOWITZ, R. J. 2010. beta-arrestin- but not G protein-mediated signaling by the "decoy" receptor CXCR7. *Proceedings of the National*

Academy of Sciences of the United States of America, 107**,** 628-632.

RAJANTIE, J., KOSKINIEMIA, M. L., SIIMES, M. A., SALONEN, E. M. & VAHERE, A. I. 1989. CSF fibronectin in Burkitt's lymphoma: an early marker for CNS involvement. *European Journal of Haematology,* 42**,** 313-4.

RAMANUJACHAR, R., RICHARDS, S., HANN, I. & WEBB, D. 2006. Adolescents with acute lymphoblastic leukaemia: emerging from the shadow of paediatric and adult treatment protocols. *Pediatric Blood & Cancer,* 47**,** 748-56.

RANSOHOFF, R. M. & ENGELHARDT, B. 2012. The anatomical and cellular basis of immune surveillance in the central nervous system. *Nature reviews. Immunology,* 12**,** 623-35.

REBOLDI, A., COISNE, C., BAUMJOHANN, D., BENVENUTO, F., BOTTINELLI, D., LIRA, S., UCCELLI, A., LANZAVECCHIA, A., ENGELHARDT, B. & SALLUSTO, F. 2009. C-C chemokine receptor 6-regulated entry of TH-17 cells into the CNS through the choroid plexus is required for the initiation of EAE. *Nature immunology,* 10**,** 514-23.

REEVES, J. D., HUTTER, J. J. & FAVARA, B. E. 1978. Spinal-Fluid Ldh Activity in Children with Acute-Leukemia. *American Journal of Diseases of Children,* 132**,** 635-635.

REHE, K., WILSON, K., BOMKEN, S., WILLIAMSON, D., IRVING, J., DEN BOER, M. L., STANULLA, M., SCHRAPPE, M., HALL, A. G., HEIDENREICH, O. & VORMOOR, J. 2013. Acute B lymphoblastic leukaemia-propagating cells are present at high frequency in diverse lymphoblast populations. *Embo Molecular Medicine,* 5**,** 38-51.

REICHMAN-FRIED, M., MININA, S. & RAZ, E. 2004. Autonomous modes of behavior in primordial germ cell migration. *Developmental Cell,* 6**,** 589-96.

REISS, Y., PROUDFOOT, A. E., POWER, C. A., CAMPBELL, J. J. & BUTCHER, E. C. 2001. CC chemokine receptor (CCR)4 and the CCR10 ligand cutaneous T cell-attracting chemokine (CTACK) in lymphocyte trafficking to inflamed skin. *Journal of Experimental Medicine,* 194**,** 1541-7.

REITER, A., SCHRAPPE, M., LUDWIG, W. D., HIDDEMANN, W., SAUTER, S., HENZE, G., ZIMMERMANN, M., LAMPERT, F., HAVERS, W., NIETHAMMER, D. & ET AL. 1994. Chemotherapy in 998 unselected childhood acute lymphoblastic leukemia patients. Results and conclusions of the multicenter trial ALL-BFM 86. *Blood,* 84**,** 3122-33.

RELLING, M. V., HANCOCK, M. L., RIVERA, G. K., SANDLUND, J. T., RIBEIRO, R. C., KRYNETSKI, E. Y., PUI, C. H. & EVANS, W. E. 1999. Mercaptopurine therapy intolerance and heterozygosity at the thiopurine S-methyltransferase gene locus. *Journal of the National Cancer Institute,* 91**,** 2001-8.

RIBEIRO, R. C., ABROMOWITCH, M., RAIMONDI, S. C., MURPHY, S. B., BEHM, F. & WILLIAMS, D. L. 1987. Clinical and biologic hallmarks of the Philadelphia chromosome in childhood acute lymphoblastic leukemia. *Blood,* 70**,** 948-53.

RICHARDS, S., PUI, C. H., GAYON, P. & CHILDHOOD ACUTE LYMPHOBLASTIC LEUKEMIA COLLABORATIVE, G. 2013. Systematic review and meta-analysis of randomized trials of central nervous system directed therapy for childhood acute lymphoblastic leukemia. *Pediatric Blood & Cancer,* 60**,** 185-95.

RITCHEY, A. K., POLLOCK, B. H., LAUER, S. J., ANDEJESKI, Y., BARREDO, J. & BUCHANAN, G. R. 1999. Improved survival of children with isolated CNS

relapse of acute lymphoblastic leukemia: a pediatric oncology group study. *Journal of Clinical Oncology,* 17**,** 3745-52.

ROMO-GONZALEZ, T., CHAVARRIA, A. & PEREZ-H, J. 2012. Central nervous system: A modified immune surveillance circuit? *Brain Behavior and Immunity,* 26**,** 823-829.

ROSENBERG, G. A. 2002. Matrix metalloproteinases in neuroinflammation. *Glia,* 39**,** 279-91.

ROY, A., CARGILL, A., LOVE, S., MOORMAN, A. V., STONEHAM, S., LIM, A., DARBYSHIRE, P. J., LANCASTER, D., HANN, I., EDEN, T. & SAHA, V. 2005. Outcome after first relapse in childhood acute lymphoblastic leukaemia - lessons from the United Kingdom R2 trial. *British Journal of Haematology,* 130**,** 67-75.

ROYCHOWDHURY, S., MAY, K. F., JR., TZOU, K. S., LIN, T., BHATT, D., FREUD, A. G., GUIMOND, M., FERKETICH, A. K., LIU, Y. & CALIGIURI, M. A. 2004. Failed adoptive immunotherapy with tumor-specific T cells: reversal with low-dose interleukin 15 but not low-dose interleukin 2. *Cancer Research,* 64**,** 8062-7.

RUBENSTEIN, J. L., WONG, V. S., KADOCH, C., GAO, H. X., BARAJAS, R., CHEN, L., JOSEPHSON, S. A., SCOTT, B., DOUGLAS, V., MAITI, M., KAPLAN, L. D., TRESELER, P. A., CHA, S., HWANG, J. H., CINQUE, P., CYSTER, J. G. & LOWELL, C. 2013. CXCL13 plus interleukin 10 is highly specific for the diagnosis of CNS lymphoma. *Blood,* 121**,** 4740-8.

SALGIA, R., QUACKENBUSH, E., LIN, J., SOUCHKOVA, N., SATTLER, M., EWANIUK, D. S., KLUCHER, K. M., DALEY, G. Q., KRAEFT, S. K., SACKSTEIN, R., ALYEA, E. P., VON ANDRIAN, U. H., CHEN, L. B., GUTIERREZ-RAMOS, J. C., PENDERGAST, A. M. & GRIFFIN, J. D. 1999. The BCR/ABL oncogene alters the chemotactic response to stromal-derived factor-1alpha. *Blood,* 94**,** 4233-46.

SALZER, W. L., DEVIDAS, M., CARROLL, W. L., WINICK, N., PULLEN, J., HUNGER, S. P. & CAMITTA, B. A. 2010. Long-term results of the pediatric oncology group studies for childhood acute lymphoblastic leukemia 1984-2001: a report from the children's oncology group. *Leukemia,* 24**,** 355-70.

SANCHEZ-MARTIN, L., SANCHEZ-MATEOS, P. & CABANAS, C. 2013. CXCR7 impact on CXCL12 biology and disease. *Trends in Molecular Medicine,* 19**,** 12-22.

SATHIYANADAN, K., COISNE, C., ENZMANN, G., DEUTSCH, U. & ENGELHARDT, B. 2014. PSGL-1 and E/P-selectins are essential for T-cell rolling in inflamed CNS microvessels but dispensable for initiation of EAE. *European journal of immunology,* 44**,** 2287-94.

SAYED, D., BADRAWY, H., ALI, A. M. & SHAKER, S. 2009. Immunophenotyping and immunoglobulin heavy chain gene rearrangement analysis in cerebrospinal fluid of pediatric patients with acute lymphoblastic leukemia. *Leukemia research,* 33**,** 655-61.

SCHIOPPA, T., URANCHIMEG, B., SACCANI, A., BISWAS, S. K., DONI, A., RAPISARDA, A., BERNASCONI, S., SACCANI, S., NEBULONI, M., VAGO, L., MANTOVANI, A., MELILLO, G. & SICA, A. 2003. Regulation of the chemokine receptor CXCR4 by hypoxia. *Journal of Experimental Medicine,* 198**,** 1391-402.

SCHMIEGELOW, K., FORESTIER, E., HELLEBOSTAD, M., HEYMAN, M., KRISTINSSON, J., SODERHALL, S., TASKINEN, M., NORDIC SOCIETY OF PAEDIATRIC, H. & ONCOLOGY 2010. Long-term results of NOPHO ALL-92

and ALL-2000 studies of childhood acute lymphoblastic leukemia. *Leukemia,* 24**,** 345-54.

SCHNEIDER, P., VASSE, M., AL BAYATI, A., LENORMAND, B. & VANNIER, J. P. 2002. Is high expression of the chemokine receptor CXCR-4 of predictive value for early relapse in childhood acute lymphoblastic leukaemia? *British Journal of Haematology,* 119**,** 579-80.

SCHRAPPE, M., REITER, A., LUDWIG, W. D., HARBOTT, J., ZIMMERMANN, M., HIDDEMANN, W., NIEMEYER, C., HENZE, G., FELDGES, A., ZINTL, F., KORNHUBER, B., RITTER, J., WELTE, K., GADNER, H. & RIEHM, H. 2000. Improved outcome in childhood acute lymphoblastic leukemia despite reduced use of anthracyclines and cranial radiotherapy: results of trial ALL-BFM 90. German-Austrian-Swiss ALL-BFM Study Group. *Blood,* 95**,** 3310-22.

SCHRAPPE, M., VALSECCHI, M. G., BARTRAM, C. R., SCHRAUDER, A., PANZER-GRUMAYER, R., MORICKE, A., PARASOLE, R., ZIMMERMANN, M., DWORZAK, M., BULDINI, B., REITER, A., BASSO, G., KLINGEBIEL, T., MESSINA, C., RATEI, R., CAZZANIGA, G., KOEHLER, R., LOCATELLI, F., SCHAFER, B. W., ARICO, M., WELTE, K., VAN DONGEN, J. J. M., GADNER, H., BIONDI, A. & CONTER, V. 2011. Late MRD response determines relapse risk overall and in subsets of childhood T-cell ALL: results of the AIEOP-BFM-ALL 2000 study. *Blood,* 118**,** 2077-2084.

SCHULTZ, K. R., BOWMAN, W. P., ALEDO, A., SLAYTON, W. B., SATHER, H., DEVIDAS, M., WANG, C., DAVIES, S. M., GAYNON, P. S., TRIGG, M., RUTLEDGE, R., BURDEN, L., JORSTAD, D., CARROLL, A., HEEREMA, N. A., WINICK, N., BOROWITZ, M. J., HUNGER, S. P., CARROLL, W. L. & CAMITTA, B. 2009. Improved early event-free survival with imatinib in Philadelphia chromosome-positive acute lymphoblastic leukemia: a children's oncology group study. *Journal of Clinical Oncology,* 27**,** 5175-81.

SCRIDELI, C. A., QUEIROZ, R. P., TAKAYANAGUI, O. M., BERNARDES, J. E., MELO, E. V. & TONE, L. G. 2004. Molecular diagnosis of leukemic cerebrospinal fluid cells in children with newly diagnosed acute lymphoblastic leukemia. *Haematologica,* 89**,** 1013-5.

SCRIDELI, C. A., QUEIROZ, R. P., TAKAYANAGUI, O. M., BERNARDES, J. E. & TONE, L. G. 2003. Polymerase chain reaction on cerebrospinal fluid cells in suspected leptomeningeal involvement in childhood acute lymphoblastic leukemia: comparison to cytomorphological analysis. *Diagnostic Molecular Pathology,* 12**,** 124-7.

SEEHUSEN, D. A., REEVES, M. M. & FOMIN, D. A. 2003. Cerebrospinal fluid analysis. *American Family Physician,* 68**,** 1103-8.

SERAFINI, B., COLUMBA-CABEZAS, S., DI ROSA, F. & ALOISI, F. 2000. Intracerebral recruitment and maturation of dendritic cells in the onset and progression of experimental autoimmune encephalomyelitis. *Am J Pathol,* 157**,** 1991-2002.

SERAFINI, B., ROSICARELLI, B., MAGLIOZZI, R., STIGLIANO, E. & ALOISI, F. 2004. Detection of ectopic B-cell follicles with germinal centers in the meninges of patients with secondary progressive multiple sclerosis. *Brain Pathology,* 14**,** 164-174.

SHEMESH, A., FRENKEL, S., BAR-SINAI, A., NI, Z., KAUFMAN, D. S., MEYER, L. H., CARIO, G., HOCHMAN, J., PROGADOR, A. & IZRAELI, S. 2013. *The Regulation Of Central Nervous System Acute Lymphoblastic Leukemia By Natural*

Killer Cells.

SHEN, H., CHENG, T., OLSZAK, I., GARCIA-ZEPEDA, E., LU, Z., HERRMANN, S., FALLON, R., LUSTER, A. D. & SCADDEN, D. T. 2001. CXCR-4 desensitization is associated with tissue localization of hemopoietic progenitor cells. *Journal of immunology,* 166**,** 5027-33.

SHINKAI, Y., RATHBUN, G., LAM, K. P., OLTZ, E. M., STEWART, V., MENDELSOHN, M., CHARRON, J., DATTA, M., YOUNG, F., STALL, A. M. & ALT, F. W. 1992. Rag-2-Deficient Mice Lack Mature Lymphocytes Owing to Inability to Initiate V(D)J Rearrangement. *Cell,* 68**,** 855-867.

SHULMAN, Z., SHINDER, V., KLEIN, E., GRABOVSKY, V., YEGER, O., GERON, E., MONTRESOR, A., BOLOMINI-VITTORI, M., FEIGELSON, S. W., KIRCHHAUSEN, T., LAUDANNA, C., SHAKHAR, G. & ALON, R. 2009. Lymphocyte crawling and transendothelial migration require chemokine triggering of high-affinity LFA-1 integrin. *Immunity,* 30**,** 384-96.

SHULTZ, L. D., LANG, P. A., CHRISTIANSON, S. W., GOTT, B., LYONS, B., UMEDA, S., LEITER, E., HESSELTON, R., WAGAR, E. J., LEIF, J. H., KOLLET, O., LAPIDOT, T. & GREINER, D. L. 2000. NOD/LtSz-Rag1null mice: an immunodeficient and radioresistant model for engraftment of human hematolymphoid cells, HIV infection, and adoptive transfer of NOD mouse diabetogenic T cells. *Journal of Immunology,* 164**,** 2496-507.

SINGH, S., SINGH, U. P., GRIZZLE, W. E. & LILLARD, J. W., JR. 2004. CXCL12-CXCR4 interactions modulate prostate cancer cell migration, metalloproteinase expression and invasion. *Laboratory Investigation; A Journal of Technical Methods and Pathology,* 84**,** 1666-76.

SIPKINS, D. A., WEI, X., WU, J. W., RUNNELS, J. M., COTE, D., MEANS, T. K., LUSTER, A. D., SCADDEN, D. T. & LIN, C. P. 2005. In vivo imaging of specialized bone marrow endothelial microdomains for tumour engraftment. *Nature,* 435**,** 969-73.

SIRVENT, N., SUCIU, S., BERTRAND, Y., UYTTEBROECK, A., LESCOEUR, B. & OTTEN, J. 2007. Overt testicular disease (OTD) at diagnosis is not associated with a poor prognosis in childhood acute lymphoblastic leukemia: results of the EORTC CLG Study 58881. *Pediatric Blood & Cancer,* 49**,** 344-8.

SISIRAK, V., VEY, N., VANBERVLIET, B., DUHEN, T., PUISIEUX, I., HOMEY, B., BOWMAN, E. P., TRINCHIERI, G., DUBOIS, B., KAISERLIAN, D., LIRA, S. A., PUISIEUX, A., BLAY, J. Y., CAUX, C. & BENDRISS-VERMARE, N. 2011. CCR6/CCR10-mediated plasmacytoid dendritic cell recruitment to inflamed epithelia after instruction in lymphoid tissues. *Blood,* 118**,** 5130-40.

SMITH, J. R., BRAZIEL, R. M., PAOLETTI, S., LIPP, M., UGUCCIONI, M. & ROSENBAUM, J. T. 2003. Expression of B-cell-attracting chemokine 1 (CXCL13) by malignant lymphocytes and vascular endothelium in primary central nervous system lymphoma. *Blood,* 101**,** 815-21.

SMITH, M., ARTHUR, D., CAMITTA, B., CARROLL, A. J., CRIST, W., GAYNON, P., GELBER, R., HEEREMA, N., KORN, E. L., LINK, M., MURPHY, S., PUI, C. H., PULLEN, J., REAMAN, G., SALLAN, S. E., SATHER, H., SHUSTER, J., SIMON, R., TRIGG, M., TUBERGEN, D., UCKUN, F. & UNGERLEIDER, R. 1996. Uniform approach to risk classification and treatment assignment for children with acute lymphoblastic leukemia. *Journal of Clinical Oncology,* 14**,** 18-24.

SPERTINI, O., CALLEGARI, P., CORDEY, A. S., HAUERT, J., JOGGI, J., VON

FLIEDNER, V. & SCHAPIRA, M. 1994. High levels of the shed form of L-selectin are present in patients with acute leukemia and inhibit blast cell adhesion to activated endothelium. *Blood,* 84**,** 1249-56.

SPERTINI, O., FREEDMAN, A. S., BELVIN, M. P., PENTA, A. C., GRIFFIN, J. D. & TEDDER, T. F. 1991. Regulation of leukocyte adhesion molecule-1 (TQ1, Leu-8) expression and shedding by normal and malignant cells. *Leukemia,* 5**,** 300-8.

SPIEGEL, A., KOLLET, O., PELED, A., ABEL, L., NAGLER, A., BIELORAI, B., RECHAVI, G., VORMOOR, J. & LAPIDOT, T. 2004. Unique SDF-1-induced activation of human precursor-B ALL cells as a result of altered CXCR4 expression and signaling. *Blood,* 103**,** 2900-7.

SPORICI, R. & ISSEKUTZ, T. B. 2010. CXCR3 blockade inhibits T-cell migration into the CNS during EAE and prevents development of adoptively transferred, but not actively induced, disease. *European journal of immunology,* 40**,** 2751-61.

SRICHAI, M. B. & ZENT, R. 2010. Integrin Structure and Function. *Cell-Extracellular Matrix Interactions in Cancer***,** 19-41.

SRIDHARAN, S. M., I. MARQUEZ-CURTIS, LA. TURNER, AR. LARRAT, L. SHIRVAIKAR, N. SURMAWALA, A. JANOWSKA-WIECZOREK, A. 2012. CXCR7 protein is strongly expressed in B-acute lymphoblastic leukemia (ALL) but not in T-ALL or acute myelogenous leukemia. *In: Proceedings of the 103rd Annual Meeting of the American Association for Cancer Research;*. Chicago, IL.

STEINHERZ, P. G., GAYNON, P. S., BRENEMAN, J. C., CHERLOW, J. M., GROSSMAN, N. J., KERSEY, J. H., JOHNSTONE, H. S., SATHER, H. N., TRIGG, M. E., UCKUN, F. M. & BLEYER, W. A. 1998. Treatment of patients with acute lymphoblastic leukemia with bulky extramedullary disease and T-cell phenotype or other poor prognostic features: randomized controlled trial from the Children's Cancer Group. *Cancer,* 82**,** 600-12.

STOCK, W., LA, M., SANFORD, B., BLOOMFIELD, C. D., VARDIMAN, J. W., GAYNON, P., LARSON, R. A. & NACHMAN, J. 2008. What determines the outcomes for adolescents and young adults with acute lymphoblastic leukemia treated on cooperative group protocols? A comparison of Children's Cancer Group and Cancer and Leukemia Group B studies. *Blood,* 112**,** 1646-1654.

STUCKI, A., CORDEY, A. S., MONAI, N., DEFLAUGERGUES, J. C., SCHAPIRA, H. & SPERTINI, O. 1995. Cleaved L-Selectin Concentrations in Meningeal Leukemia. *Lancet,* 345**,** 286-289.

SVENNINGSSON, A., ANDERSEN, O., EDSBAGGE, M. & STEMME, S. 1995. Lymphocyte phenotype and subset distribution in normal cerebrospinal fluid. *Journal of neuroimmunology,* 63**,** 39-46.

SWERDLOW, H., CAMPO, E., HARRIS, N., JAFFE, E., PILERI, S., STEIN, H., THIELE, J., VARDIMAN, J. & EDS 2008. *WHO Classification of Tumours of Haematopoietic and Lymphoid Tissues,* Lyon, International agency for research on Cancer (IARC).

SYNOLD, T. W., RELLING, M. V., BOYETT, J. M., RIVERA, G. K., SANDLUND, J. T., MAHMOUD, H., CRIST, W. M., PUI, C. H. & EVANS, W. E. 1994. Blast cell methotrexate-polyglutamate accumulation in vivo differs by lineage, ploidy, and methotrexate dose in acute lymphoblastic leukemia. *Journal of Clinical Investigation,* 94**,** 1996-2001.

TAGAYA, Y., BAMFORD, R. N., DEFILIPPIS, A. P. & WALDMANN, T. A. 1996. IL-15: a pleiotropic cytokine with diverse receptor/signaling pathways whose

expression is controlled at multiple levels. *Immunity,* 4**,** 329-36.

TAGAYA, Y., KURYS, G., THIES, T. A., LOSI, J. M., AZIMI, N., HANOVER, J. A., BAMFORD, R. N. & WALDMANN, T. A. 1997. Generation of secretable and nonsecretable interleukin 15 isoforms through alternate usage of signal peptides. *Proceedings of the National Academy of Sciences of the United States of America,* 94**,** 14444-9.

TAKESHITA, Y. & RANSOHOFF, R. M. 2012. Inflammatory cell trafficking across the blood-brain barrier: chemokine regulation and in vitro models. *Immunological reviews,* 248**,** 228-39.

TANG, Y. T., JIANG, F., GUO, L., SI, M. Y. & JIAO, X. Y. 2013. The soluble VEGF receptor 1 and 2 expression in cerebral spinal fluid as an indicator for leukemia central nervous system metastasis. *Journal of Neuro-oncology,* 112**,** 329-38.

TARNOWSKI, M., LIU, R., WYSOCZYNSKI, M., RATAJCZAK, J., KUCIA, M. & RATAJCZAK, M. Z. 2010. CXCR7: a new SDF-1-binding receptor in contrast to normal CD34(+) progenitors is functional and is expressed at higher level in human malignant hematopoietic cells. *European Journal of Haematology,* 85**,** 472-83.

TE LOO, D. M., KAMPS, W. A., VAN DER DOES-VAN DEN BERG, A., VAN WERING, E. R. & DE GRAAF, S. S. 2006. Prognostic significance of blasts in the cerebrospinal fluid without pleiocytosis or a traumatic lumbar puncture in children with acute lymphoblastic leukemia: experience of the Dutch Childhood Oncology Group. *Journal of Clinical Oncology,* 24**,** 2332-6.

TEDDER, T. F., STEEBER, D. A. & PIZCUETA, P. 1995. L-Selectin-Deficient Mice Have Impaired Leukocyte Recruitment into Inflammatory Sites. *Journal of Experimental Medicine,* 181**,** 2259-2264.

TENENBAUM, T., STEINMANN, U., FRIEDRICH, C., BERGER, J., SCHWERK, C. & SCHROTEN, H. 2013. Culture models to study leukocyte trafficking across the choroid plexus. *Fluids and Barriers of the CNS,* 10**,** 1.

THOMAS, L. B. 1965. Pathology of leukemia in the brain and meninges: postmortem studies of patients with acute leukemia and of mice given inoculations of L1210 leukemia. *Cancer Research,* 25**,** 1555-71.

THOMPSON, C. B., SANDERS, J. E., FLOURNOY, N., BUCKNER, C. D. & THOMAS, E. D. 1986. The risks of central nervous system relapse and leukoencephalopathy in patients receiving marrow transplants for acute leukemia. *Blood,* 67**,** 195-9.

TINHOFER, I., MARSCHITZ, I., HENN, T., EGLE, A. & GREIL, R. 2000. Expression of functional interleukin-15 receptor and autocrine production of interleukin-15 as mechanisms of tumor propagation in multiple myeloma. *Blood,* 95**,** 610-8.

TONEGAWA, S. 1983. Somatic Generation of Antibody Diversity. *Nature,* 302**,** 575-581.

TRENTIN, L., CERUTTI, A., ZAMBELLO, R., SANCRETTA, R., TASSINARI, C., FACCO, M., ADAMI, F., RODEGHIERO, F., AGOSTINI, C. & SEMENZATO, G. 1996. Interleukin-15 promotes the growth of leukemic cells of patients with B-cell chronic lymphoproliferative disorders. *Blood,* 87**,** 3327-35.

TREVINO, L. R., YANG, W., FRENCH, D., HUNGER, S. P., CARROLL, W. L., DEVIDAS, M., WILLMAN, C., NEALE, G., DOWNING, J., RAIMONDI, S. C., PUI, C. H., EVANS, W. E. & RELLING, M. V. 2009. Germline genomic variants associated with childhood acute lymphoblastic leukemia. *Nature Genetics,* 41**,** 1001-5.

TSUZUKI, S., SETO, M., GREAVES, M. & ENVER, T. 2004. Modeling first-hit

functions of the t(12;21) TEL-AML1 translocation in mice. *Proceedings of the National Academy of Sciences of the United States of America,* 101**,** 8443-8448.

UCKUN, F. M., SATHER, H., REAMAN, G., SHUSTER, J., LAND, V., TRIGG, M., GUNTHER, R., CHELSTROM, L., BLEYER, A., GAYNON, P. & CRIST, W. 1995. Leukemic-Cell Growth in Scid Mice as a Predictor of Relapse in High-Risk B-Lineage Acute Lymphoblastic-Leukemia. *Blood,* 85**,** 873-878.

UCKUN, F. M., SATHER, H. N., WAURZYNIAK, B. J., SENSEL, M. G., CHELSTROM, L., EK, O., SARQUIS, M. B., NACHMAN, J., BOSTROM, B., REAMAN, G. H. & GAYNON, P. S. 1998. Prognostic significance of B-lineage leukemic cell growth in SCID mice: a Children's Cancer Group Study. *Leukemia & lymphoma,* 30**,** 503-14.

VAGACE, J. M. & GERVASINI, G. 2011. *Chemotherapy Toxicity in Patients with Acute Leukemia*.

VAITKEVICIENE, G., FORESTIER, E., HELLEBOSTAD, M., HEYMAN, M., JONSSON, O. G., LAHTEENMAKI, P. M., ROSTHOEJ, S., SODERHALL, S., SCHMIEGELOW, K. & HAEMATOLOGY, N. S. P. 2011. High white blood cell count at diagnosis of childhood acute lymphoblastic leukaemia: biological background and prognostic impact. Results from the NOPHO ALL-92 and ALL-2000 studies. *European Journal of Haematology,* 86**,** 38-46.

VAN DEN BERK, L. C., VAN DER VEER, A., WILLEMSE, M. E., THEEUWES, M. J., LUIJENDIJK, M. W., TONG, W. H., VAN DER SLUIS, I. M., PIETERS, R. & DEN BOER, M. L. 2014. Disturbed CXCR4/CXCL12 axis in paediatric precursor B-cell acute lymphoblastic leukaemia. *British Journal of Haematology*.

VAN DER LINDEN, M. H., VALSECCHI, M. G., DE LORENZO, P., MORICKE, A., JANKA, G., LEBLANC, T. M., FELICE, M., BIONDI, A., CAMPBELL, M., HANN, I., RUBNITZ, J. E., STARY, J., SZCZEPANSKI, T., VORA, A., FERSTER, A., HOVI, L., SILVERMAN, L. B. & PIETERS, R. 2009. Outcome of congenital acute lymphoblastic leukemia treated on the Interfant-99 protocol. *Blood,* 114**,** 3764-8.

VAN DER VEER, A., WAANDERS, E., PIETERS, R., WILLEMSE, M. E., VAN REIJMERSDAL, S. V., RUSSELL, L. J., HARRISON, C. J., EVANS, W. E., VAN DER VELDEN, V. H. J., HOOGERBRUGGE, P. M., VAN LEEUWEN, F., ESCHERICH, G., HORSTMANN, M. A., KHANKAHDANI, L. M., RIZOPOULOS, D., DE GROOT-KRUSEMAN, H. A., SONNEVELD, E., KUIPER, R. P. & DEN BOER, M. L. 2013. Independent prognostic value of BCR-ABL1-like signature and IKZF1 deletion, but not high CRLF2 expression, in children with B-cell precursor ALL. *Blood,* 122**,** 2622-2629.

VAN DER VELDEN, V. H., CAZZANIGA, G., SCHRAUDER, A., HANCOCK, J., BADER, P., PANZER-GRUMAYER, E. R., FLOHR, T., SUTTON, R., CAVE, H., MADSEN, H. O., CAYUELA, J. M., TRKA, J., ECKERT, C., FORONI, L., ZUR STADT, U., BELDJORD, K., RAFF, T., VAN DER SCHOOT, C. E., VAN DONGEN, J. J. & EUROPEAN STUDY GROUP ON, M. R. D. D. I. A. L. L. 2007. Analysis of minimal residual disease by Ig/TCR gene rearrangements: guidelines for interpretation of real-time quantitative PCR data. *Leukemia,* 21**,** 604-11.

VAN DER VELDEN, V. H. J., HOCHHAUS, A., CAZZANIGA, G., SZCZEPANSKI, T., GABERT, J. & VAN DONGEN, J. J. M. 2003. Detection of minimal residual disease in hematologic malignancies by real-time quantitative PCR: principles, approaches, and laboratory aspects. *Leukemia,* 17**,** 1013-1034.

VAN DONGEN, J. J., MACINTYRE, E. A., GABERT, J. A., DELABESSE, E., ROSSI, V., SAGLIO, G., GOTTARDI, E., RAMBALDI, A., DOTTI, G., GRIESINGER, F., PARREIRA, A., GAMEIRO, P., DIAZ, M. G., MALEC, M., LANGERAK, A. W., SAN MIGUEL, J. F. & BIONDI, A. 1999. Standardized RT-PCR analysis of fusion gene transcripts from chromosome aberrations in acute leukemia for detection of minimal residual disease. Report of the BIOMED-1 Concerted Action: investigation of minimal residual disease in acute leukemia. *Leukemia,* 13**,** 1901-28.

VAN DONGEN, J. J. M., SERIU, T., PANZER-GRUMAYER, E. R., BIONDI, A., PONGERS-WILLEMSE, M. J., CORRAL, L., STOLZ, F., SCHRAPPE, M., MASERA, G., KAMPS, W. A., GADNER, H., VAN WERING, E. R., LUDWIG, W. D., BASSO, G., DE BRUIJN, M. A. C., CAZZANIGA, G., HETTINGER, A., VAN DER DOES-VAN DEN BERG, A., HOP, W. C. J., RIEHM, H. & BARTRAM, C. R. 1998. Prognostic value of minimal residual disease in acute lymphoblastic leukaemia in childhood. *Lancet,* 352**,** 1731-1738.

VENKATESAN, S., ROSE, J. J., LODGE, R., MURPHY, P. M. & FOLEY, J. F. 2003. Distinct mechanisms of agonist-induced endocytosis for human chemokine receptors CCR5 and CXCR4. *Molecular Biology of the Cell,* 14**,** 3305-24.

VIRELY, C., MOULIN, S., COBALEDA, C., LASGI, C., ALBERDI, A., SOULIER, J., SIGAUX, F., CHAN, S., KASTNER, P. & GHYSDAEL, J. 2010. Haploinsufficiency of the IKZF1 (IKAROS) tumor suppressor gene cooperates with BCR-ABL in a transgenic model of acute lymphoblastic leukemia. *Leukemia,* 24**,** 1200-4.

VONCKEN, J. W., KAARTINEN, V., PATTENGALE, P. K., GERMERAAD, W. T., GROFFEN, J. & HEISTERKAMP, N. 1995. BCR/ABL P210 and P190 cause distinct leukemia in transgenic mice. *Blood,* 86**,** 4603-11.

VORA, A., GOULDEN, N., WADE, R., MITCHELL, C., HANCOCK, J., HOUGH, R., ROWNTREE, C. & RICHARDS, S. 2013. Treatment reduction for children and young adults with low-risk acute lymphoblastic leukaemia defined by minimal residual disease (UKALL 2003): a randomised controlled trial. *The Lancet. Oncology,* 14**,** 199-209.

WANG, H. S., BEATY, N., CHEN, S., QI, C. F., MASIUK, M., SHIN, D. M. & MORSE, H. C. 2012. The CXCR7 chemokine receptor promotes B-cell retention in the splenic marginal zone and serves as a sink for CXCL12. *Blood,* 119**,** 465-468.

WANG, J. H., SHIOZAWA, Y. S., WANG, J. C., WANG, Y., JUNG, Y. H., PIENTA, K. J., MEHRA, R., LOBERG, R. & TAICHMAN, R. S. 2008. The role of CXCR7/RDC1 as a chemokine receptor for CXCL12/SDF-1 in prostate cancer. *Journal of Biological Chemistry,* 283**,** 4283-4294.

WEIR, E. G., COWAN, K., LEBEAU, P. & BOROWITZ, M. J. 1999. A limited antibody panel can distinguish B-precursor acute lymphoblastic leukemia from normal B precursors with four color flow cytometry: implications for residual disease detection. *Leukemia,* 13**,** 558-567.

WELSCHINGER, R., LIEDTKE, F., BASNETT, J., DELA PENA, A., JUAREZ, J. G., BRADSTOCK, K. F. & BENDALL, L. J. 2013. Plerixafor (AMD3100) induces prolonged mobilization of acute lymphoblastic leukemia cells and increases the proportion of cycling cells in the blood in mice. *Experimental Hematology,* 41**,** 293-302 e1.

WILLIAMS, M. T., YOUSAFZAI, Y., COX, C., BLAIR, A., CARMODY, R., SAI, S., CHAPMAN, K. E., MCANDREW, R., THOMAS, A., SPENCE, A., GIBSON, B.,

GRAHAM, G. J. & HALSEY, C. 2014. Interleukin-15 enhances cellular proliferation and upregulates CNS homing molecules in pre-B acute lymphoblastic leukemia. *Blood,* 123**,** 3116-27.

WILSON, E. H., WENINGER, W. & HUNTER, C. A. 2010. Trafficking of immune cells in the central nervous system. *The Journal of Clinical Investigation,* 120**,** 1368-79.

WONG, S. & FULCHER, D. 2004. Chemokine receptor expression in B-cell lymphoproliferative disorders. *Leukemia & lymphoma,* 45**,** 2491-6.

WU, S., FISCHER, L., GOKBUGET, N., SCHWARTZ, S., BURMEISTER, T., NOTTER, M., HOELZER, D., FUCHS, H., BLAU, I. W., HOFMANN, W. K. & THIEL, E. 2010. Expression of interleukin 15 in primary adult acute lymphoblastic leukemia. *Cancer,* 116**,** 387-92.

WU, S., GESSNER, R., TAUBE, T., KORTE, A., VON STACKELBERG, A., KIRCHNER, R., HENZE, G. & SEEGER, K. 2006. Chemokine IL-8 and chemokine receptor CXCR3 and CXCR4 gene expression in childhood acute lymphoblastic leukemia at first relapse. *Journal of Pediatric Hematology and Oncology,* 28**,** 216-20.

YAMASAKI, S., MAEDA, M., OHSHIMA, K., KIKUCHI, M., OTSUKA, T. & HARADA, M. 2004. Growth and apoptosis of human natural killer cell neoplasms: role of interleukin-2/15 signaling. *Leukemia research,* 28**,** 1023-31.

YANG, J. J., CHENG, C., YANG, W., PEI, D., CAO, X., FAN, Y., POUNDS, S. B., NEALE, G., TREVINO, L. R., FRENCH, D., CAMPANA, D., DOWNING, J. R., EVANS, W. E., PUI, C. H., DEVIDAS, M., BOWMAN, W. P., CAMITTA, B. M., WILLMAN, C. L., DAVIES, S. M., BOROWITZ, M. J., CARROLL, W. L., HUNGER, S. P. & RELLING, M. V. 2009. Genome-wide interrogation of germline genetic variation associated with treatment response in childhood acute lymphoblastic leukemia. *The Journal of the American Medical Association,* 301**,** 393-403.

YEDNOCK, T. A., CANNON, C., FRITZ, L. C., SANCHEZ-MADRID, F., STEINMAN, L. & KARIN, N. 1992. Prevention of experimental autoimmune encephalomyelitis by antibodies against alpha 4 beta 1 integrin. *Nature,* 356**,** 63-6.

ZABEL, B. A., LEWEN, S., BERAHOVICH, R. D., JAEN, J. C. & SCHALL, T. J. 2011. The novel chemokine receptor CXCR7 regulates trans-endothelial migration of cancer cells. *Molecular Cancer,* 10.

ZETTERBERG, E. & RICHTER, J. 1993. Correlation between serum level of soluble L-selectin and leukocyte count in chronic myeloid and lymphocytic leukemia and during bone marrow transplantation. *European Journal of Haematology,* 51**,** 113-9.

ZHANG, J., DING, L., HOLMFELDT, L., WU, G., HEATLEY, S. L., PAYNE-TURNER, D., EASTON, J., CHEN, X., WANG, J., RUSCH, M., LU, C., CHEN, S. C., WEI, L., COLLINS-UNDERWOOD, J. R., MA, J., ROBERTS, K. G., POUNDS, S. B., ULYANOV, A., BECKSFORT, J., GUPTA, P., HUETHER, R., KRIWACKI, R. W., PARKER, M., MCGOLDRICK, D. J., ZHAO, D., ALFORD, D., ESPY, S., BOBBA, K. C., SONG, G., PEI, D., CHENG, C., ROBERTS, S., BARBATO, M. I., CAMPANA, D., COUSTAN-SMITH, E., SHURTLEFF, S. A., RAIMONDI, S. C., KLEPPE, M., COOLS, J., SHIMANO, K. A., HERMISTON, M. L., DOULATOV, S., EPPERT, K., LAURENTI, E., NOTTA, F., DICK, J. E., BASSO, G., HUNGER, S. P., LOH, M. L., DEVIDAS, M., WOOD, B., WINTER, S., DUNSMORE, K. P., FULTON, R. S., FULTON, L. L., HONG, X., HARRIS, C. C., DOOLING, D. J., OCHOA, K., JOHNSON, K. J., OBENAUER, J. C., EVANS, W. E., PUI, C. H., NAEVE, C. W., LEY, T. J., MARDIS, E. R.,

WILSON, R. K., DOWNING, J. R. & MULLIGHAN, C. G. 2012. The genetic basis of early T-cell precursor acute lymphoblastic leukaemia. *Nature,* 481**,** 157-63.

ZHANG, Y., YANG, C. Q., GAO, Y., WANG, C., ZHANG, C. L. & ZHOU, X. H. 2014. Knockdown of CXCR7 inhibits proliferation and invasion of osteosarcoma cells through inhibition of the PI3K/Akt and beta-arrestin pathways. *Oncology Reports*.

ZHOU, J. B., GOIDWASSER, M. A., LI, A. H., DAHLBERG, S. E., NEUBERG, D., WANG, H. J., DALTON, V., MCBRIDE, K. D., SALLAN, S. E., SILVERMAN, L. B., GRIBBEN, J. G. & INSTITUTE, D.-F. C. 2007. Quantitative analysis of minimal residual disease predicts relapse in children with B-lineage acute lymphoblastic leukemia in DFCI ALL Consortium Protocol 95-01. *Blood,* 110**,** 1607-1611.

ZLOTNIK, A., BURKHARDT, A. M. & HOMEY, B. 2011. Homeostatic chemokine receptors and organ-specific metastasis. *Nature Reviews Immunology,* 11**,** 597-606.

ZLOTNIK, A. & YOSHIE, O. 2000. Chemokines: a new classification system and their role in immunity. *Immunity,* 12**,** 121-7.

ZLOTOFF, D. A., SAMBANDAM, A., LOGAN, T. D., BELL, J. J., SCHWARZ, B. A. & BHANDOOLA, A. 2010. CCR7 and CCR9 together recruit hematopoietic progenitors to the adult thymus. *Blood,* 115**,** 1897-905.

ZOU, Y. R., KOTTMANN, A. H., KURODA, M., TANIUCHI, I. & LITTMAN, D. R. 1998. Function of the chemokine receptor CXCR4 in haematopoiesis and in cerebellar development. *Nature,* 393**,** 595-9.

ZWEEMER, A. J., TORASKAR, J., HEITMAN, L. H. & AP, I. J. 2014. Bias in chemokine receptor signalling. *Trends in immunology,* 35**,** 243-252.